

22232

22232

000

IMPACT OF NONOPERATING PERIODS ON EQUIPMENT RELIABILITY

David W. Coit
Mary G. Priore

September 1984

Prepared for:

Rome Air Development Center
Air Force Systems Command
Griffiss Air Force Base, NY 13441

Prepared by:

IIT Research Institute
Turin Road, North
P.O. Box 180
Rome, NY 13440

SECURITY CLASSIFICATION OF THIS PAGE (When Data Entered)

REPORT DOCUMENTATION PAGE		READ INSTRUCTIONS BEFORE COMPLETING FORM
1. REPORT NUMBER RADC-TR-	2. GOVT ACCESSION NO.	3. RECIPIENT'S CATALOG NUMBER
4. TITLE (and Subtitle) Impact of Nonoperating Periods on Equipment Reliability		5. TYPE OF REPORT & PERIOD COVERED Final Technical Report Feb 83 - Sept 84
		6. PERFORMING ORG. REPORT NUMBER N/A
7. AUTHOR(s) David W. Coit Mary G. Priore		8. CONTRACT OR GRANT NUMBER(s) F30602-83-C-0056
9. PERFORMING ORGANIZATION NAME AND ADDRESS IIT Research Institute Turin Road, North, P.O. Box 180, Rome, NY 13440		10. PROGRAM ELEMENT, PROJECT, TASK AREA & WORK UNIT NUMBERS
11. CONTROLLING OFFICE NAME AND ADDRESS Rome Air Development Center (RBE-2) Griffiss AFB, NY 13441		12. REPORT DATE September 1984
		13. NUMBER OF PAGES
14. MONITORING AGENCY NAME & ADDRESS (if different from Controlling Office) Same		15. SECURITY CLASS. (of this report) UNCLASSIFIED
		15a. DECLASSIFICATION/DOWNGRADING SCHEDULE N/A
16. DISTRIBUTION STATEMENT (of this Report) Approved for public release; distribution unlimited.		
17. DISTRIBUTION STATEMENT (of the abstract entered in Block 20, if different from Report) Same		
18. SUPPLEMENTARY NOTES RADC Project Engineer: Preston MacDiarmid		
19. KEY WORDS (Continue on reverse side if necessary and identify by block number) Reliability Storage Failure Rate Power On-Off Cycling Nonoperating MIL-HDBK-217 Dormancy		
20. ABSTRACT (Continue on reverse side if necessary and identify by block number) Nonoperating failure rate prediction models were developed for all part types in MIL-HDBK-217. Observed field failure rate data were collected and analyzed to develop the proposed models. Additionally, a discussion is included concerning comprehensive reliability prediction for both operating and nonoperating periods.		

PREFACE

This Final Report was prepared by IIT Research Institute, Rome, New York, for the Rome Air Development Center, Griffiss AFB, New York, under Contract F30602-83-C-0056. The RADC laboratory contract manager for this program was Mr. Preston MacDiarmid (RBE-2). The study originator and initial RADC laboratory contract manager was Mr. Lester Gubbins. This report covers the work performed from February 1983 to September 1984.

The principal investigator for this project was David W. Coit. Valuable assistance was provided by Mary Priore, Donald Fulton, Donald Rymer, James Carey, Kieron Dey, Thomas Ballou, Bernard Radigan, Harold Lauffenburger, William Denson, Michael Rossi, Donald Rash and David Dylis. Report production was coordinated by Pamela Coe and Virginia Dwyer.

MANAGEMENT SUMMARY

The objective of this study was to develop a procedure to predict the quantitative effects of nonoperating periods on electronic equipment reliability. A series of nonoperating failure rate prediction models were developed at the component level. The models are capable of evaluating component nonoperating failure rate for any anticipated environment with the exception of a satellite environment.

The proposed nonoperating failure rate prediction methodology is intended to provide the ability to predict the component nonoperating failure rate and reliability as a function of the characteristics of the devices, technology employed in producing the device, and external factors such as environmental stresses which have a significant effect on device nonoperating reliability. The prediction methodology is presented in a form compatible with MIL-HDBK-217 as an Appendix to the technical report.

Observed nonoperating failure rate data were collected from a variety of sources. The following criteria were established for an acceptable source of data:

- o Data available to the part level
- o Primary failures can be separated from total maintenance actions
- o Nonoperating failures can be separated from operating failures
- o Sufficient detail can be identified for components
- o Sufficient equipment nonoperating hours to expect failures

A summary of the collected data is presented in Table MS-1.

The model development approach was based primarily on empirical data analysis. Thus, the proposed models include variables which can be shown to significantly affect nonoperating failure rate. A model development matrix is presented in Table MS-2. The model development matrix indicates the part class, data sources, empirical model factors, assumed/theoretical model factors and also provides a discussion.

A clear and concise procedure was also developed to apply the component nonoperating failure rate prediction models to assess the impact of nonoperating periods at the equipment level. Additionally, a comprehensive reliability prediction methodology was presented which describes the use of the proposed nonoperating failure rate prediction models together with the documented operating failure rate assessment techniques (i.e. MIL-HDBK-217D).

It is recommended that the proposed nonoperating failure rate prediction models developed during this study be incorporated into MIL-HDBK-217. Additionally, it is recommended that the nonoperating failure rate prediction models be updated periodically to reflect changes in technology or other factors which temporarily result in an inaccurate or missing model.

TABLE MS-1: NONOPERATING FAILURE RATE DATA SUMMARY

Part Class	Model Development			Model Evaluation		
	Data Records	Failures	Part Hrs. (x10 ⁶)	Data Records	Failures	Part Hrs. (x10 ⁶)
Monolithic Micro-circuits	644	353	25862	11	50	1947
Hybrid Microcircuits	27	2082	50050	0	0	0
Transistors	106	121	21983	16	23	8422
Diodes	139	57	22181	28	77	25468
Inductive Devices	73	87	49833	0	0	0
Resistors	413	34	113119	21	17	16390
Capacitors	324	48	41841	22	14	5004
Tubes	47	364	795	0	0	0
Rotating Mechanisms	8	20	149	0	0	0
Relays	13	36	1360	0	0	0
Switches	16	35	408	0	0	0
Connectors	6	1	82444	0	0	0
Interconnection Assemblies	8	3	2977	0	0	0
Misc. Parts	8	5	129	0	0	0

TABLE MS-2: MODEL DEVELOPMENT MATRIX

Part Class	Data Sources	Empirical Factors	Assumed/Theoretical Factors	Discussion
Monolithic ICs	MICOM Martin Marietta F-16 HUD/RIW Sandia PRC RAC ERADCOM	complexity (1) temperature logic screening : enclosure type power cycling (2)	environment	The proposed models were based on diverse data sets. The model for memory devices should be further investigated because it was based primarily on high temperature storage life test data.
Hybrid ICs	MICOM F-16 HUD/RIW	# ICs # transistors # diodes	environment quality	Several of the potential variables were correlated making independent analysis of all variables impossible. The data were primarily for low complexity hybrids.
Bubble Memories	none	none	# gates # loops temperature environment logic	No nonoperating failure data were available. The failure rate for bubble memories should be further investigated.

TABLE MS-2: MODEL DEVELOPMENT MATRIX (CONT'D)

Part Class	Data Sources	Empirical Factors	Assumed/Theoretical Factors	Discussion
Transistors	MICOM Martin Marietta F-16 HUD/RIW AFCIQ (3) PRC ERADCOM	device style temperature quality power cycling	environment	Model was based on a large and varied data set.
Diodes	MICOM Martin Marietta F-16 HUD/RIW PRC	device style quality power cycling	environment temperature	An appropriate temperature factor was assumed based on the observed transistor temperature relationship.
Opto-electronics	none	none	device style quality environment	No nonoperating failure data were available. This part class should be further investigated.
Resistors	MICOM Martin Marietta F-16 HUD/RIW PRC	device style quality power cycling	environment	Model was based on a large and varied data set.

TABLE MS-2: MODEL DEVELOPMENT MATRIX (CONT'D)

Part Class	Data Sources	Empirical Factors	Assumed/Theoretical Factors	Discussion
Capacitors	MICOM Martin Marietta F-16 HUD/RIW PRC	device style quality power cycling	environment	The nonoperating failure rate of A10 and nonsolid Ta capacitors is anticipated to increase with time. Thus, the proposed model is an average failure rate. This issue should be further studied.
Inductive Devices	MICOM Martin Marietta F-16 HUD/RIW AFCIQ Southern Tech.	device style quality power cycling	environment	Data were available on a variety of coils and transformers.
Lasers	none	none	environment device style # optical surfaces	No nonoperating failure rate data were available. The proposed model should be evaluated when data becomes available.

TABLE MS-2: MODEL DEVELOPMENT MATRIX (CONT'D)

	Part Class	Data Sources	Empirical Factors	Assumed/Theoretical Factors	Discussion
	Lasers (continued)				Specific attention should be addressed to the effects of equipment power cycling.
	Tubes	MICOM	device style	environment	The effect of equipment power cycling and non-constant tube failure rates are two areas where additional research should be directed.
x.	Rotating Mechanisms	MICOM Martin Marietta	device style	none	Periodic equipment power cycling can prolong the nonoperating life of rotating mechanisms. There were insufficient data to analyze this effect.

TABLE MS-2: MODEL DEVELOPMENT MATRIX (CONT'D)

Part Class	Data Sources	Empirical Factors	Assumed/Theoretical Factors	Discussion
Relays	MICOM Martin Marietta Hughes AFCIQ	quality	enclosure type contact rating environment	Surface films will form on the contacts of non-hermetic relays and switches during nonoperating periods. These films may or may not result in a failure depending on the contact actuation frequency and the applied voltage during operation. The effect of actuation and power cycling frequency should be further investigated.
Switches	MICOM Martin Marietta	none	enclosure type contact rating environment quality	
Connectors	MICOM Martin Marietta	none	device style environment	Only a limited supply of nonoperating data were available for connectors.
P.W. Assemblies	MICOM AFCIQ	technology # circuit planes	# PTHs environment	Only a limited supply of nonoperating data were available for interconnection assemblies.

x

TABLE MS-2: MODEL DEVELOPMENT MATRIX (CONT'D)

Part Class	Data Sources	Empirical Factors	Assumed/Theoretical Factors	Discussion
Connections	none	none	type	The nonoperating reliability of solder connections and other connections should be further investigated.
Misc. Parts	MICOM Martin Marietta	device type	none	Data were available for crystals, fuses, incandescent lamps and neon lamps.

- NOTES: (1) The effect of complexity was determined empirically for random logic and linear/interface microcircuits. No significant effect could be determined for the complexity of memory devices.
- (2) The effect of equipment power cycling was determined empirically for linear/interface microcircuits. A power cycling factor was hypothesized for digital microcircuits.
- (3) High temperature storage life test data from AFCIQ were used for model development of transistors. The transistor field data from AFCIQ were used for model evaluation.

TABLE OF CONTENTS

	Page
PREFACE.....	ii
MANAGEMENT SUMMARY.....	iii
1.0 INTRODUCTION.....	1-1
1.1 Objective.....	1-1
1.2 Background.....	1-1
1.3 Definitions.....	1-4
2.0 DATA/INFORMATION COLLECTION.....	2-1
2.1 Literature Search.....	2-1
2.2 Data Collection Approach.....	2-4
2.3 Data Summary.....	2-7
3.0 DATA ANALYSIS OVERVIEW.....	3-1
3.1 Data Deficiencies.....	3-1
3.2 Statistical Methods.....	3-3
3.3 Zero Failure Data.....	3-8
3.4 Effect of Nonoperating Failures on Operating Models...	3-11
4.0 NONOPERATING FAILURE RATE MODELING CONCEPTS.....	4-1
4.1 Failure Rate Modeling Approach.....	4-1
4.2 Theoretical Model Development.....	4-6
4.3 Equipment Power Cycling Effects.....	4-7
4.3.1 Dormancy and Power On-Off Cycling Effects on Electronic Equipment and Part Reliability (RADC-TR-73-248)	4-8
4.3.2 Planning Research Corporation Studies.....	4-9
4.3.3 ARINC Study.....	4-10
4.3.4 Hughes Presentations.....	4-11
4.3.5 Equipment Power Cycling Conclusions.....	4-11
4.3.6 Equipment Power Cycling Analysis.....	4-12
4.4 Temperature Effects.....	4-16
4.5 Environmental Factor Analysis.....	4-22
4.6 Screening Effectiveness.....	4-44
5.0 NONOPERATING FAILURE RATE MODEL DEVELOPMENT.....	5-1
5.1 Microcircuits.....	5-4

TABLE OF CONTENTS (CONT'D)

	Page
5.1.1 Monolithic Microcircuit Nonoperating Failure. Rate Prediction Models	5-4
5.1.2 Digital Microcircuit Model Development.....	5-9
5.1.3 Linear/Interface Microcircuits.....	5-38
5.1.4 Memory Device Model Development.....	5-50
5.1.5 Monolithic Microcircuit Model Validation.....	5-52
5.1.6 Hybrid Microcircuit Nonoperating Failure..... Rate Model	5-57
5.1.7 Hybrid Model Development.....	5-58
5.1.8 Proposed Magnetic Bubble Memory Nonoperating.. Failure Rate Prediction Model	5-74
5.1.9 Magnetic Bubble Memory Model Development.....	5-76
5.2 Discrete Semiconductors.....	5-79
5.2.1 Discrete Semiconductor Nonoperating Failure... Rate Prediction Models	5-79
5.2.2 Transistor Model Development.....	5-86
5.2.3 Diode Model Development.....	5-101
5.2.4 Opto-electronic Semiconductor Model..... Development	5-116
5.2.5 Model Validation.....	5-120
5.3 Resistors.....	5-125
5.3.1 Proposed Resistor Nonoperating Failure Rate... Prediction Model	5-125
5.3.2 Model Development.....	5-127
5.3.3 Model Validation.....	5-148
5.4 Capacitors.....	5-152
5.4.1 Proposed Capacitor Nonoperating Failure Rate.. Prediction Model	5-152
5.4.2 Model Development.....	5-153
5.4.3 Model Validation.....	5-173

TABLE OF CONTENTS (CONT'D)

	Page
5.5 Inductive Devices.....	5-176
5.5.1 Proposed Inductor Nonoperating Failure Rate... Prediction Model	5-176
5.5.2 Inductor Model Development.....	5-178
5.6 Lasers.....	5-191
5.6.1 Proposed Laser Nonoperating Failure Rate..... Prediction Models	5-191
5.6.2 Laser Model Development.....	5-194
5.7 Tubes.....	5-199
5.7.1 Proposed Tube Nonoperating Failure Rate..... Prediction Model	5-196
5.7.2 Tube Model Development.....	5-197
5.8 Mechanical/Electromechanical Devices.....	5-208
5.8.1 Proposed Mechanical/Electromechanical Device.. Nonoperating Failure Rate Prediction Models	5-208
5.8.2 Rotating Mechanisms.....	5-212
5.8.3 Contact Device Model Development.....	5-215
5.8.4 Connectors.....	5-227
5.9 Interconnection Assemblies.....	5-232
5.9.1 Proposed Interconnection Assembly Nonoper-.... ating Failure Rate Prediction Model	5-232
5.9.2 Interconnection Assembly Model Development....	5-233
5.10 Connections.....	5-240
5.10.1 Proposed Connections Nonoperating Failure..... Rate Prediction Model	5-240
5.10.2 Model Development.....	5-241
5.11 Miscellaneous Parts.....	5-244
5.11.1 Proposed Miscellaneous Parts Nonoperating..... Failure Rates	5-244
5.11.2 Model Development.....	5-245

TABLE OF CONTENTS (CONT'D)

	Page
6.0 APPLICATION OF NONOPERATING RELIABILITY MODELS.....	6-1
6.1 Comprehensive Reliability Models.....	6-1
6.2 Proposed Comprehensive Reliability Prediction Method...	6-3
7.0 COMPARISON OF OPERATING AND NONOPERATING FAILURE RATES.....	7-1
8.0 CONCLUSIONS.....	8-1
9.0 RECOMMENDATIONS.....	9-1
REFERENCES.....	R-1
Appendix A: Proposed Nonoperating Failure Rate Prediction Models..	A-1

LIST OF FIGURES

	Page
FIGURE 3.3-1: CONCEPTUAL FAILURE RATE DISTRIBUTION.....	3-10
FIGURE 4.1-1: MODEL DEVELOPMENT FLOW CHART.....	4-2
FIGURE 4.4-1: LINEAR MICROCIRCUIT STORAGE FAILURE RATE VS.....	4-19
TEMPERATURE	
FIGURE 4.5-1: FAILURE MECHANISM DISTRIBUTION, ACCELERATED BY.....	4-36
ENVIRONMENTAL STRESS (CASE I)	
FIGURE 4.5-2: FAILURE MECHANISM DISTRIBUTION, ACCELERATED BY.....	4-36
OPERATIONAL STRESS (CASE II)	
FIGURE 4.5-3: FAILURE MECHANISM DISTRIBUTION, ACCELERATED BY.....	4-38
COMBINED OPERATIONAL/ENVIRONMENTAL STRESS (CASE III)	
FIGURE 4.6-1: CONCEPTUAL SCREENING EFFECTIVENESS COMPARISON.....	4-46
FIGURE 5.1.2-1: FAILURE RATE VS. TEMPERATURE.....	5-24

LIST OF TABLES

	Page
TABLE 2.1-1: LITERATURE SEARCH RESOURCES.....	2-3
TABLE 2.2-1: NONOPERATING FAILURE RATE DATA SOURCES.....	2-7
TABLE 2.3-1: SUMMARIZED NONOPERATING FAILURE RATE DATA.....	2-8
TABLE 3.2-1: EXAMPLE OF QUALITATIVE REGRESSION ANALYSIS.....	3-5
TABLE 4.5-1: ENVIRONMENT CATEGORIES.....	4-25
TABLE 4.5-2: MIL-HDBK-217D ENVIRONMENTAL FACTOR CLASSIFICATION....	4-32
TABLE 4.5-3: ENVIRONMENTAL FACTOR ANALYSIS (CASE II) -.....	4-41
SIMULTANEOUS EQUATIONS	
TABLE 5.0-1: PART CLASS CATEGORIZATION.....	5-1
TABLE 5.0-2: MODEL DEVELOPMENT OVERVIEW.....	5-2
TABLE 5.1.1-1: DIGITAL MICROCIRCUIT NONOPERATING TEMPERATURE.....	5-6
FACTOR CONSTANTS	
TABLE 5.1.1-2: MICROCIRCUIT NONOPERATING ENVIRONMENTAL FACTORS.....	5-6
TABLE 5.1.1-3: MICROCIRCUIT NONOPERATING ENVIRONMENTAL FACTORS.....	5-7
(π _{NE})	
TABLE 5.1.2-1: DIGITAL MICROCIRCUIT CHARACTERIZATION VARIABLES.....	5-11
TABLE 5.1.2-2: DIGITAL MICROCIRCUIT NONOPERATING FAILURE RATE DATA..	5-12
TABLE 5.1.2-3: DIGITAL MICROCIRCUIT TEMPERATURE MATRIX.....	5-16
TABLE 5.1.2-4: DIGITAL MICROCIRCUIT QUALITY VARIABLE MATRIX.....	5-18
TABLE 5.1.2-5: DIGITAL MICROCIRCUIT REGRESSION RESULTS.....	5-19
TABLE 5.1.2-6: DIGITAL MICROCIRCUIT NONOPERATING QUALITY FACTOR.....	5-21
TABLE 5.1.2-7: MICROCIRCUIT NONOPERATING TEMPERATURE FACTOR.....	5-23
COEFFICIENTS	
TABLE 5.1.2-8: MOS DIGITAL SSI/MSI FAILURE MECHANISM DISTRIBUTION...	5-32
TABLE 5.1.2-9: BIPOLAR DIGITAL SSI/MSI FAILURE MECHANISM.....	5-33
DISTRIBUTION	
TABLE 5.1.2-10: RANDOM LOGIC LSI FAILURE MECHANISM DISTRIBUTION.....	5-34
TABLE 5.1.2-11: K ₃ and K ₄ TEMPERATURE FACTOR CONSTANTS FOR.....	5-37
DIGITAL MICROCIRCUITS	
TABLE 5.1.3-1: LINEAR/INTERFACE MICROCIRCUIT CHARACTERIZATION.....	5-39
VARIABLES	

LIST OF TABLES

	Page
TABLE 5.1.3-2: LINEAR/INTERFACE MICROCIRCUIT NONOPERATING FAILURE... RATE DATA	5-40
TABLE 5.1.3-3: LINEAR/INTERFACE INITIAL REGRESSION RESULTS.....	5-43
TABLE 5.1.3-4: LINEAR/INTERFACE FINAL REGRESSION RESULTS.....	5-45
TABLE 5.1.4-1: MEMORY DEVICE NONOPERATING FAILURE RATE DATA.....	5-49
TABLE 5.1.5-1: MONOLITHIC MICROCIRCUIT MODEL VALIDATION DATA.....	5-56
TABLE 5.1.6-1: HYBRID NONOPERATING ENVIRONMENT FACTORS (π_{NE}).....	5-59
TABLE 5.1.7-1: HYBRID PART CHARACTERIZATION.....	5-60
TABLE 5.1.7-2: SUMMARIZED HYBRID NONOPERATING RELIABILITY DATA.....	5-62
TABLE 5.1.7-3: HYBRID VARIABLE CORRELATION COEFFICIENT MATRIX.....	5-64
TABLE 5.1.7-4: HYBRID REGRESSION RESULTS (I).....	5-68
TABLE 5.1.7-5: HYBRID REGRESSION RESULTS (II).....	5-68
TABLE 5.1.7-6: HYBRID COEFFICIENT CONFIDENCE INTERVALS.....	5-71
TABLE 5.1.7-7: HYBRID NONOPERATING QUALITY FACTORS.....	5-72
TABLE 5.2.1-1: DISCRETE SEMICONDUCTOR NONOPERATING TEMPERATURE..... FACTOR PARAMETERS	5-80
TABLE 5.2.1-2: TRANSISTOR NONOPERATING ENVIRONMENTAL FACTORS (π_{NE})...	5-82
TABLE 5.2.1-3: DIODE NONOPERATING ENVIRONMENTAL FACTORS (π_{NE}).....	5-84
TABLE 5.2.1-4: OPTO-ELECTRONIC SEMICONDUCTOR NONOPERATING..... ENVIRONMENTAL FACTORS (π_{NE})	5-85
TABLE 5.2.2-1: TRANSISTOR PART CHARACTERIZATION.....	5-87
TABLE 5.2.2-2: TRANSISTOR NONOPERATING FAILURE RATE DATA.....	5-89
TABLE 5.2.2-3: TRANSISTOR STYLE VARIABLE MATRIX.....	5-90
TABLE 5.2.2-4: TRANSISTOR REGRESSION RESULTS II.....	5-92
TABLE 5.2.2-5: SIGNAL AND POWER TRANSISTOR FAILURE MECHANISM..... DISTRIBUTION	5-95
TABLE 5.2.2-6: FET FAILURE MECHANISM DISTRIBUTION.....	5-96
TABLE 5.2.2-7: HIGH TEMPERATURE STORAGE LIFE TEST DATA.....	5-99
TABLE 5.2.3-1: DIODE CHARACTERIZATION VARIABLES.....	5-103
TABLE 5.2.3-2: DIODE NONOPERATING FAILURE RATE DATA.....	5-104
TABLE 5.2.3-3: DIODE STYLE VARIABLE MATRIX.....	5-106
TABLE 5.2.3-4: DIODE INITIAL REGRESSION RESULTS.....	5-107

LIST OF TABLES

	Page
TABLE 5.2.3-5: DIODE FINAL REGRESSION RESULTS.....	5-110
TABLE 5.2.3-6: DIODE NONOPERATING QUALITY FACTORS.....	5-111
TABLE 5.2.3-7: ZENER DIODE FAILURE MODE/MECHANISM DISTRIBUTIONS.....	5-112
TABLE 5.2.3-8: SMALL SIGNAL DIODE FAILURE MODE/MECHANISM.....	5-113
DISTRIBUTIONS	
TABLE 5.2.3-9: DIODE NONOPERATING BASE FAILURE RATES.....	5-115
TABLE 5.2.4-1: OPTO-ELECTRONIC DEVICE CHARACTERIZATION VARIABLES....	5-117
TABLE 5.2.4-2: OPTO-ELECTRONIC NONOPERATING BASE FAILURE RATES.....	5-120
TABLE 5.2.5-1: TRANSISTOR MODEL VALIDATION DATA.....	5-122
TABLE 5.2.5-2: DIODE MODEL VALIDATION DATA.....	5-123
TABLE 5.3.1-1: RESISTOR NONOPERATING ENVIRONMENTAL FACTORS (π_{NE})...	5-126
TABLE 5.3.2-1: RESISTOR PART CHARACTERIZATION.....	5-128
TABLE 5.3.2-2: RESISTOR NONOPERATING FAILURE RATE DATA.....	5-130
TABLE 5.3.2-3: RESISTOR STYLE VARIABLE MATRIX.....	5-134
TABLE 5.3.2-4: RESISTOR INITIAL REGRESSION RESULTS.....	5-136
TABLE 5.3.2-5: RESISTOR NONOPERATING QUALITY FACTORS.....	5-140
TABLE 5.3.2-6: COMPOSITION RESISTOR FAILURE MECHANISM DISTRIBUTION.	5-142
TABLE 5.3.2-7: FILM RESISTOR FAILURE MECHANISM DISTRIBUTION.....	5-142
TABLE 5.3.2-8: WIREWOUND RESISTOR FAILURE MECHANISM DISTRIBUTION...	5-143
TABLE 5.3.2-9: VARIABLE WIREWOUND RESISTOR FAILURE MECHANISM.....	5-143
DISTRIBUTION	
TABLE 5.3.2-10: VARIABLE COMPOSITION RESISTOR FAILURE MECHANISM.....	5-144
DISTRIBUTION	
TABLE 5.3.2-11: THERMISTOR FAILURE MECHANISM DISTRIBUTION.....	5-144
TABLE 5.3.2-12: RESISTOR NONOPERATING BASE FAILURE RATES.....	5-146
TABLE 5.3.3-1: RESISTOR MODEL VALIDATION DATA.....	5-151
TABLE 5.4.1-1: CAPACITOR NONOPERATING ENVIRONMENTAL FACTORS.....	5-154
TABLE 5.4.2-1: CAPACITOR PART CHARACTERIZATION.....	5-155
TABLE 5.4.2-2: CAPACITOR NONOPERATING FAILURE RATE DATA TABLE.....	5-157
TABLE 5.4.2-3: CAPACITOR DEVICE STYLE VARIABLE MATRIX.....	5-159
TABLE 5.4.2-4: CAPACITOR INITIAL REGRESSION RESULTS.....	5-162
TABLE 5.4.2-5: CAPACITOR NONOPERATING QUALITY FACTORS.....	5-167

LIST OF TABLES

	Page
TABLE 5.4.2-6: PAPER AND PLASTIC CAPACITOR FAILURE MECHANISM..... DISTRIBUTION	5-168
TABLE 5.4.2-7: CERAMIC CAPACITOR FAILURE MECHANISM DISTRIBUTION....	5-168
TABLE 5.4.2-8: MICA CAPACITOR FAILURE MECHANISM DISTRIBUTION.....	5-169
TABLE 5.4.2-9: GLASS CAPACITOR FAILURE MECHANISM DISTRIBUTION.....	5-169
TABLE 5.4.2-10: WET FOIL CAPACITOR FAILURE MECHANISM DISTRIBUTION...	5-170
TABLE 5.4.2-11: SOLID TANTULUM CAPACITOR FAILURE MECHANISM..... DISTRIBUTION	5-170
TABLE 5.4.2-12: ALUMINUM ELECTROLYTIC CAPACITOR FAILURE MECHANISM.. DISTRIBUTION	5-171
TABLE 5.4.2-13: VARIABLE CAPACITOR FAILURE MECHANISM DISTRIBUTION...	5-171
TABLE 5.4.2-14: CAPACITOR NONOPERATING BASE FAILURE RATES.....	5-172
TABLE 5.4.3-1: CAPACITOR MODEL VALIDATION DATA.....	5-174
TABLE 5.5.1-1: INDUCTOR NONOPERATING ENVIRONMENTAL FACTORS.....	5-177
TABLE 5.5.2-1: INDUCTOR PART CHARACTERIZATION.....	5-179
TABLE 5.5.2-2: INDUCTOR NONOPERATING FAILURE RATE DATA.....	5-180
TABLE 5.5.2-3: DEVICE QUALITY VARIABLE MATRIX.....	5-183
TABLE 5.5.2-4: INDUCTOR INITIAL REGRESSION RESULTS.....	5-184
TABLE 5.5.2-5: INDUCTOR NONOPERATING QUALITY FACTORS.....	5-188
TABLE 5.5.2-6: RF COIL FAILURE MECHANISM DISTRIBUTION.....	5-190
TABLE 5.5.2-7: TRANSFORMER FAILURE MECHANISM DISTRIBUTION.....	5-190
TABLE 5.6.1-1: LASER NONOPERATING ENVIRONMENTAL FACTORS.....	5-193
TABLE 5.7.1-1: TUBE NONOPERATING ENVIRONMENTAL FACTORS.....	5-197
TABLE 5.7.2-1: TUBE PART CLASSIFICATION.....	5-198
TABLE 5.7.2-2: TUBE NONOPERATING FAILURE RATE DATA.....	5-201
TABLE 5.7.2-3: DEVICE STYLE VARIABLE MATRIX.....	5-202
TABLE 5.7.2-4: TUBE REGRESSION RESULTS.....	5-203
TABLE 5.7.2-5: TUBE OPERATING AND NONOPERATING FAILURE RATE..... COMPARISON	5-207
TABLE 5.8.1-1: ROTATING DEVICE AVERAGE NONOPERATING FAILURE RATES..	5-209
TABLE 5.8.1-2: RELAY NONOPERATING ENVIRONMENTAL FACTORS.....	5-210
TABLE 5.8.1-3: SWITCH NONOPERATING ENVIRONMENTAL FACTORS.....	5-211

LIST OF TABLES

	Page
TABLE 5.8.1-4: CONNECTOR NONOPERATING ENVIRONMENTAL FACTORS.....	5-212
TABLE 5.8.2-1: ROTATING MECHANISM NONOPERATING FAILURE RATE DATA...	5-214
TABLE 5.8.3-1: RELAY PART CHARACTERIZATION.....	5-217
TABLE 5.8.3-2: SWITCH PART CHARACTERIZATION.....	5-218
TABLE 5.8.3-3: RELAY NONOPERATING FAILURE RATE DATA.....	5-220
TABLE 5.8.3-4: RELAY NONOPERATING QUALITY FACTORS.....	5-222
TABLE 5.8.3-5: ARMATURE RELAY FAILURE MECHANISM DISTRIBUTION.....	5-223
TABLE 5.8.3-6: TOGGLE SWITCH MECHANISM COMPARISONS.....	5-225
TABLE 5.8.3-7: SWITCH NONOPERATING FAILURE RATE DATA.....	5-226
TABLE 5.8.4-1: CONNECTOR NONOPERATING FAILURE RATE DATA.....	5-229
TABLE 5.9.1-1: INTERCONNECTION ASSEMBLY NONOPERATING ENVIRONMENTAL FACTORS	5-233
TABLE 5.9.2-1: INTERCONNECTION ASSEMBLY CHARACTERIZATION.....	5-235
TABLE 5.9.2-2: INTERCONNECTION ASSEMBLY NONOPERATING FAILURE RATE.. DATA	5-236
TABLE 5.10.1-1: CONNECTIONS NONOPERATING ENVIRONMENTAL FACTORS.....	5-241
TABLE 5.11.1-1: NONOPERATING FAILURE RATES FOR MISCELLANEOUS PARTS..	5-244
TABLE 5.11.2-1: MISCELLANEOUS PART NONOPERATING FAILURE RATE DATA...	5-245
TABLE 6.2-1: COMPREHENSIVE RELIABILITY PREDICTION TASKS.....	6-3
TABLE 7.0-1: SAMPLE CALCULATIONS COMPARING NONOPERATING AND..... MIL-HDBK-217D MODELS	7-2
TABLE 7.0-2: RATIOS OF MIL-HDBK-217D TO NONOPERATING FAILURE..... RATES	7-6
TABLE 7.0-3: DISCRETE SEMICONDUCTOR OPERATING TO NONOPERATING.... FAILURE RATE RATIOS	7-8

1.0 INTRODUCTION

1.1 Objective

The objective of this study was to develop a procedure to predict the quantitative effects of nonoperating periods on electronic equipment reliability. A series of nonoperating failure rate prediction models were developed at the component level. The models are capable of evaluating component nonoperating failure rate for any anticipated environment with the exception of a satellite environment. A clear and concise procedure was also developed to apply the component nonoperating failure rate prediction models to assess the impact of nonoperating periods at the equipment level. Additionally, a comprehensive reliability prediction methodology was presented which describes the use of the proposed nonoperating failure rate prediction models together with the documented operating failure rate assessment techniques (i.e. MIL-HDBK-217D).

The proposed nonoperating failure rate prediction methodology was intended to provide the ability to predict the component nonoperating failure rate and reliability as a function of the characteristics of the devices, technology employed in producing the device, and external factors such as environmental stresses which have a significant effect on device nonoperating reliability. An analytical approach using observed data was taken for model development where possible. Thus, the proposed models only include variables which can be shown to significantly affect nonoperating failure rate. The prediction methodology is presented in a form compatible with MIL-HDBK-217 in Appendix A.

1.2 Background

Failure rate and reliability prediction capabilities are essential tools in the development and maintenance of reliable electronic equipments. Predictions performed during the design phase yield early estimates of the anticipated equipment reliability and provide a quantitative basis for performing proposal evaluations, design trade-off

analyses, reliability growth monitoring and life-cycle cost studies. This is particularly important when an electronic equipment is in a nonoperating state for a prolonged period of time. Equipment nonoperating reliability cannot be determined until power is applied. If no test schedule has been established, an equipment in a nonoperating state has an unknown reliability until the point in time when it is required. Unexpected poor performance can have disastrous results. Therefore, it is essential that nonoperating reliability assessment techniques are implemented on the same scale as operating reliability assessment.

Manufacturers and government customers for missiles have long recognized the need for nonoperating reliability assessment. Conversely, U.S. Air Force airborne electronic equipments have often been assumed to possess a nonoperating failure rate of zero. This has been an oversight, particularly when it is considered that a typical fighter aircraft is exposed to over twenty times more nonoperating time than operating time. Even if the nonoperating failure rate is a small fraction of the corresponding operating failure rate, the total number of nonoperating failures may be equivalent to the number of operating failures. Two studies sponsored by RADC (References 1 and 2) identified this oversight as a possible reason that operating failure rate predictions differ from observed field data (where it is generally assumed that all failures are operating failures).

Previous attempts (References 3, 4, 5 and 6) to predict nonoperating reliability have generally been in one of two categories. Either (1) an equipment level multiplicative "K" factor has been applied to an equipment operating failure rate, or (2) operating failure rate relationships have been extrapolated to zero stress. The first method has merit under controlled circumstances. The second method has little or no merit. As a general nonoperating failure rate prediction methodology which can be applied for any equipment in any environment, neither of these previous methods are acceptable.

Use of a multiplicative "K" factor has merit under certain circumstances. The "K" factor can be accurately used to predict nonoperating failure rate if it was based on equipment level data from the same contractor on a similar equipment type with similar derating and screening. In any other circumstances, the use of a "K" factor is a very approximate method at best. Additionally, it is intuitively wrong to assume that operating and nonoperating failure rates are directly proportional. Many application and design variables would be anticipated to have a pronounced effect on operating failure rate, yet negligible effect on nonoperating failure rate. Derating is one example. It has been observed that derating results in a significant decrease in operating failure rate, but a similar decrease would not be expected with no power applied. Additionally, the stresses on parts are different in the nonoperating state, and therefore, there is no reason to believe that the operating factors for temperature, environment, quality and application would also be applicable for nonoperating reliability prediction purposes.

An invalid approach for nonoperating failure rate assessment has been to extrapolate operating failure rate relationships to zero electrical stress. All factors in MIL-HDBK-217D, whether for electrical stress, temperature or another factor, represent empirical relationships (as opposed to theoretical relationships). An empirical relationship is based on observed data, and proposed because of the supposedly good fit to the data. However, empirical relationships may not be valid beyond the range of parameters found in the data and this range does not include zero electrical stress for MIL-HDBK-217D operating reliability relationships. Extrapolation of empirical relationships beyond the range found in the data can be particularly dangerous when the variable is part of an exponential relationship. A relatively small error in the exponent can correspond to a large error in the resultant predicted failure rate. Additionally, there are many intuitive or qualitative reasons why small amounts of applied power can be preferable to pure storage conditions. For nonhermetic microcircuits, the effect of humidity is the primary failure accelerating stress. A small current will result in a temperature rise, burning off moisture, and probably decreasing device failure rate.

Also, the detrimental effects of equipment power on-off cycling would be expected to be less for any electronic part when a small current is applied to the part. Another example where nonoperating failure rates could be expected to be higher than low stress operating failure rates is for storage degradation components such as electrolytic capacitors, motors and electromechanical devices. These part types benefit from periodic operation.

One of the assumptions which dominated these two approaches was also necessary in this study. No empirical nonoperating failure rate data were available for other than ground based environments. Nonoperating environmental factor values were, therefore, determined based on an in-depth study and comparison of operating and nonoperating failure mechanisms and failure causing stresses. However, for the most part, the factors and models presented in this report represent empirical nonoperating relationships determined from observed nonoperating failure rate data.

1.3 Definitions

Many terms have been used during previous studies of nonoperating reliability. Unfortunately, the definitions given in the literature are hardly standardized, and in many cases conflicting. It was not considered desirable to develop unique definitions for this study. This would only further confuse the issue. Therefore, the appropriate definitions, which were used for this study, were based on a review of the available literature, and were adopted from Reference 7.

Operating - Operating is defined as the state of a subsystem, assembly or component when it is activated (as designed) by electrical or mechanical means at any level of stress. At the subsystem level, if any portion of the subsystem is operating, then the entire subsystem is considered to be operating.

Nonoperating - A subsystem, assembly, or component is considered to be nonoperating when it is experiencing none of the electrical or mechanical stresses inherent in the (designed) activation of that subsystem, assembly, or component. It may however be experiencing stress caused by the environment, transportation and handling, such as captive carry G-forces, etc.

Storage - Storage is defined as the state in which a system, subsystem, assembly, or component is zero percent activated, and is in its normal configuration in a storage area.

Dormancy - Dormancy is defined as those states wherein an equipment is in its normal operation configuration and is not operating, or is maintained in operationally ready storage. Dormancy includes the nonoperating portions of alert, captive carry, transportation and handling, and launcher carriage. The operationally ready storage mode is predominant in that this state is where "long periods" of dormancy occur. The ability of a system to withstand these "long periods" may be influenced by relatively short periods of test time or the stress inherent in other states such as transportation, captive carry, or launcher carriage.

Shelf Life - According to AFR 136-1, "Nonnuclear Munitions Product Assurance Program," September 1979, shelf life is defined as: the length of time an item may remain in storage under prescribed packaging and storage conditions, and operate satisfactorily when removed from storage.

Equipment Power On-Off Cycle - An equipment power on-off cycle is defined as that state during which an electronic system goes from the zero electrical activation level to its normal design system activation level plus that state during which it returns to zero.

Equipment Power On-Off Cycling Frequency - Power cycling frequency is defined as the number of equipment power on-off cycles for a given time interval (1000 nonoperating hours was used for this study).

It should be noted that the definition of dormancy can vary considerably. According to Reference 5, dormancy is equal to any condition where the electrical activation level is less than or equal to 10% of the normal design level. The dormancy definition adopted for this study was consistent with information defined in the RADC statement of work explicitly defining nonoperating.

2.0 DATA/INFORMATION COLLECTION

The proposed nonoperating failure rate prediction model development approach involved the analysis of large amounts of empirical data. Therefore, the data collection task was a prerequisite for numerical analyses and an integral part of the overall process. Additionally, the proposed models were scrutinized with a theoretical evaluation. Thus, a thorough literature search was required to locate pertinent information. This section describes the literature search, the data collection approach and the available data.

2.1 Literature Search

The literature search was an essential part of the study approach. Information obtained through the literature search was used to develop theoretical models, evaluate the proposed models and complement the analyses for part families without sufficient data. To insure an efficient and successful literature search, a concise methodology was developed to locate applicable nonoperating reliability information.

Two major information sources were used. The first source consisted of libraries and other data resources covering open technical literature. The second source consisted of contacts established in past and present electronic systems reliability projects. This included contacts whose work has not yet been published in the open literature. Use of these diverse sources ensured that a comprehensive review of the field was achieved. Four technical areas which were extensively researched are:

- o Actual equipment level environmental stresses (environmental profiles).
- o Component susceptibility to environmental stresses.
- o Equipment level operating scenarios (percentage of on/off time per mission and distribution of mission types).
- o Theoretical nonoperating reliability relationships for temperature, environment, and equipment power on-off cycling.

The information gathered for the first two areas listed was used in the development of nonoperating environmental factors. The information gathered for the third area was sought for all equipment environments. The information was occasionally required for the derivation of the number of nonoperating hours. This information was necessary to develop a nonoperating failure rate from data collected on equipments which did not contain elapsed time meters or where the time numeric recorded was flight hours. The information in the fourth area was used to aid in the development of theoretical models and to complement the data analysis task.

In order to efficiently conduct a comprehensive literature search it was necessary to define and implement a methodology, whose critical elements included the following:

- o Problem/goal definition

In this step, the key concepts of the search were defined and also any related areas that could potentially yield any information were identified. Other factors that were considered at this stage included the time span of the search, and its general scope.

- o Identification of information resources

The main activity in this area consisted of identifying the relevant abstracts, indexes, reference works and technical journals for the problems defined in the previous step.

- o Search strategy formulation

A search strategy was devised which identified those information resources which could most effectively yield the information defined in the first step of the process.

- o Literature Survey

Using the search strategy as a roadmap, the information specialist surveyed the information resources for potentially relevant information. Both manual and automated search methods were used.

- o Evaluation

This was the most important step. The results of the search were reviewed and search strategy was redefined as required.

o Literature Search

An in-depth search was then conducted. Close contact was maintained between the project engineer and information specialist to insure the goals of the search were met.

A variety of information resources were used. Table 2.1-1 presents a brief description the more useful resources.

TABLE 2.1-1: LITERATURE SEARCH RESOURCES

<u>Resource</u>	<u>Description</u>
Defense Technical Information Center (DTIC)	DTIC maintains a large computerized database of technical documents produced by government sponsored efforts.
Reliability Analysis Center (RAC)	RAC is a DoD information analysis center primarily concerned with electronics component and system reliability. The center has an automated library and data base with numerous hardware reliability references.
IITRI Computer Search Center (CSC)	This service located at the IITRI Chicago office is staffed by professional information specialists who are experts in searching computerized bibliographic data bases. The Center has access to approximately 150 individual data bases.
Government Industry Data Exchange Program (GIDEP)	The GIDEP data base contains four separate data banks. Of these the Engineering Data Bank, the Reliability-Maintainability Data Bank, and the Failure Experience Data Bank were most relevant to this study.

The literature search task was very successful. The most relevant documents and technical articles are listed in the References section of this report.

2.2 Data Collection Approach

The development of nonoperating failure rate prediction methodologies should be derived from field failure rate data representing a large range of application and construction variables. A general data collection approach was developed to efficiently collect a large data base.

The Reliability Analysis Center (RAC) operated by the IIT Research Institute at Griffiss Air Force Base was solicited to aid in the data collection process. Numerous contacts in both government and industry have been established at RAC as part of the regular data collection process. Additionally, high temperature storage life test data for microcircuits were available as part of the RAC microcircuit data base.

Two key conditions caused data collection to be particularly difficult for this study. First, the objective of the study was to develop nonoperating failure rate prediction models for all part classes in MIL-HDBK-217D. The range and variety of the part types included in MIL-HDBK-217D is extremely large. Data collection could not be concentrated on one generic part family at the expense of other part types. The other condition which made data collection difficult was the inherently low failure rate which many part types exhibit in storage or dormant applications, and the further fact that many of the part types fall in the category of low population parts. Many potential data sources could not be used simply because insufficient nonoperating time had accumulated to expect any failures.

To insure an efficient and effective data collection process, five criteria were established for an acceptable data source. Each potential data source was evaluated with these criteria before proceeding with data summarization. These five criteria were:

1. Data available to the part level.
2. Primary failures can be separated from total maintenance actions.

3. Nonoperating failures can be separated from operating failures.
4. Sufficient detail can be identified for components.
5. Sufficient equipment nonoperating hours to expect failures.

These five attributes were used as a guide to determine suitable candidate equipments. Information collection trips were made to (1) U.S. Army MICOM (Missile Command), Redstone Arsenal, (2) U.S. Army ARRADCOM (Armament Research and Development Command), (3) U.S. Navy Sea Systems Command, (4) U.S. Department of Commerce, and (4) Tobyhanna Army Depot to evaluate potential sources of data. These organizations were chosen based on information provided in initial telephone contacts. In person contact was required to emphasize the importance of this study, get acquainted with additional reliability data bases, retrieve raw data and/or inspect raw data more closely. Many sources of information could be accessed by telephone or written requests and did not require on-site visits. Telephone contact was made with numerous other industrial and government organizations including the Product Performance Agreement Center at Wright-Patterson Air Force Base. The conclusion was reached after evaluation of the potential sources to concentrate data collection efforts on large, preferably automated data bases which had already been summarized (i.e. nonoperating failures identified, part characterization performed, part hours computed) and pertained only to nonoperating reliability. The separation of nonoperating and operating failures proved to be difficult and prevented the inclusion of many possible data sources.

The Product Performance Agreement Center at Wright-Patterson Air Force Base provided information regarding U.S. Air Force equipments purchased under Reliability Improvement Warranty (RIW) contracts. In general, RIW failure reporting is preferable to that of large automated military reliability data bases. The reporting allows for decisions to be made regarding primary versus secondary failures, and is generally more complete. As with other data sources, the issue of separating nonoperating failures from total failures was difficult. The F-16 heads-

up-display (HUD) was selected from the list of RIW contracts to summarize for nonoperating reliability data. The F-16 HUD met each of five requirements for an acceptable data source. Additionally, there were a relatively wide range of component styles included in the design. Decisions for operating versus nonoperating failures were made using the on-equipment maintenance action "when discovered" code.

The Storage Reliability of Missile Materiel Program maintained by U.S. Army MICOM, Redstone Arsenal provided the best source of nonoperating failure rate data. Nonoperating failure rate data were available for a wide range of part types for a number of missile programs. A summary of this data is presented in Reference 3. Time and budget constraints would have prevented independent summarization of a data base as large as the MICOM data base. MICOM has periodically issued a set of documents presenting the data in various formats, describing data analyses, and presenting nonoperating failure rate prediction models for missile electronics. A 1982 revision of these documents was issued and then recalled. This action was not indicative of poor or inaccurate data, but was necessary because of errors in presentation of the data and prediction models, and clerical errors. In fact, the same sources of data were used in the 1982 documents as in the previous revisions (which did not include errors). Therefore, the use of this data and the problems encountered by MICOM do not adversely affect in any manner the validity or accuracy of the analyses or proposed nonoperating failure rate prediction models presented in this technical report. The successful completion of this study relied heavily on the use of large summarized data from sources such as MICOM.

Another organization which contributed data was the French group Association Francaise pour le Controle Industriel et la Qualite (AFCIQ). This group produced a document (Reference 8) which includes a summary of the MICOM data, as well as additional data from European sources. This data were used for model validation for microcircuits, discrete

semiconductors, resistors and capacitors, and for model development for the remaining part styles with data.

Many other data sources were identified and evaluated as part of the data collection approach. Table 2.2-1 presents a list of the organizations and/or equipments which supplied data in sufficient quality and quantity for numerical analysis.

TABLE 2.2-1: NONOPERATING FAILURE RATE DATA SOURCES

<u>Source</u>	<u>Equipment</u>	<u>Data Type</u>
MICOM	Missile electronics	field/test
F-16 HUD/RIW	HUD	field (RIW)
RAC	N/A	high temperature testing
Sandia National Labs	nuclear weapon electronics	field
U.S. Army ERADCOM	N/A	high humidity testing
U.S. Army TSARCOM	generator sets	field
Planning Research Corp.	satellite	field
Martin Marietta	various	field
AFCIQ	various	field

2.3 Data Summary

A summary of the collected nonoperating failure rate data by device style is presented in Table 2.3-1. Table 2.3-1 presents the sum total of observed failures and part hours. A more detailed list of the data, including data sources, is included in the individual model development sections.

TABLE 2.3-1: SUMMARIZED NONOPERATING FAILURE RATE DATA

Part Class	Failures	Part Hours (X10 ⁶)
Random Logic Microcircuits	155	21441.1
Linear/Interface Microcircuits	76	3605.8
Memory Microcircuits	122	814.6
Hybrid Microcircuits	2082	50049.9
Transistors	121	21983.1
Diodes	57	22180.6
Resistors	34	113118.9
Capacitors	48	41840.6
Inductive Devices	87	49833.0
Tubes	364	794.8
Rotating Devices	20	149.0
Relays	36	1360.4
Switches	35	408.3
Connectors	1	82444.0

3.0 DATA ANALYSIS OVERVIEW

The nonoperating failure rate prediction models presented in this study are primarily based on numerical analysis of observed data. This section presents a brief overview of the applicable data analysis techniques. Additionally, inherent problems with the available data are discussed, and the treatment of zero failure data records is described.

3.1 Data Deficiencies

Analytical evaluation of the nonoperating failure rate for electronic or electromechanical components requires a large data base. Development of nonoperating failure rate data bases which have sufficient quantity and detail is difficult, if not impossible. This section presents a brief overview of inherent problems with the available data and data quality control measures implemented to minimize error. A more detailed description of data deficiencies and data quality control is presented in Reference 9.

Available sources of nonoperating failure rate data were generally either high temperature storage life test data or equipment level field experience data. Each type of data has several inherent difficulties.

Life test data generally are of a high statistical quality because there is very little uncertainty with regard to recorded failures, number of parts on test, test time and environmental conditions. The major deficiencies with life test data are (1) the data often consists of many parts on test for a relatively short time each, and (2) the test conditions are usually not representative of the actual usage environment.

Field experience data are the more desirable type of data. This type of nonoperating failure rate data represents what actually occurred in the field, which is what the proposed model attempts to predict. The inherent difficulties with field experience data are related to the accuracy with which a failure can be defined, the precision with which the number of

nonoperating part hours can be measured, and the ability to determine the environmental stresses applied to a part.

Several classes of parts degrade during nonoperating periods and would be anticipated to have a time dependent failure rate. A problem associated with available sources of field experience data was that individual nonoperating times to failure could not be determined. Data were only available in the form of X failures observed in Y part hours. The nonoperating part hours are a cumulative count of nonoperating hours from individual components. The result of this data deficiency is that the exponential reliability function (i.e., constant failure rate) must be assumed for all part types. For most electronic parts, it was not believed that this assumption introduced significant error. However, for electromechanical parts, electrolytic capacitors, tubes and other part types where degradation failure mechanisms are significant, the constant failure rate calculated by dividing the observed failures by the nonoperating part hours may not be meaningful. This is particularly true when the data consists of many parts on test (or fielded) for a relatively short time each. To minimize error, data sources were sought with long storage times per equipment. In these instances, the calculated constant nonoperating failure rate represents an average failure rate value for the data collection interval. The average failure rate is equal to the failure rate due to random stresses plus an average failure rate contribution due to wearout or degradation stresses.

Field nonoperating failure data samples for most electronic and electromechanical parts are necessarily restricted because the average mean time to failure (approximately 10^6 to 10^{10} part hours) is longer than the technology has been available. However good the failure rate data, it can only cover the first few percentiles of the probability density function. One result of these relatively high mean time to failures for most part types during nonoperating periods is data records with zero observed failures. The presence of zero failure data records weakens the analysis. There exists no accurate method for determining a nonoperating failure rate without observed failures. However, these entries could not

be neglected. In some instances, a large percentage of the collected data is zero failure records. In other instances, the zero failure data records indicate that the predicted failure rate should be lower than what the data records containing failures indicates. The treatment of zero failure data records is discussed in Section 3.3.

Another data deficiency was related to the data collection approach. Data were collected from any and all sources. This was a necessary approach because of the anticipated lack of data. However, the resulting data bases often contained variables, (i.e. part types, screen level, application environment, etc.) which were correlated. Statistical analysis can not be correctly applied if the variables are not reasonably independent. Error was minimized in these instances by carefully choosing independent variables, and by complementing the data analysis task with theoretical or empirical relationships located during the literature search.

3.2 Statistical Methods

This section presents a very brief discussion of statistical methods used in this study. References are provided which include much greater detail.

Stepwise Multiple Linear Regression Analysis. Regression analysis is an important statistical tool and was used to develop the nonoperating failure rate prediction models for the majority of the devices. A more thorough discussion of stepwise multiple linear regression analysis is given in Reference 10. A brief description follows.

The stepwise multiple linear regression analysis technique assumes a preliminary model of the form

$$Y = b_0 + b_1X_1 + b_2X_2 + \dots + b_iX_i$$

where Y is the resultant dependent variable, X_1, X_2, \dots, X_i are the independent variables which are thought to influence the value of Y , and $b_0, b_1, b_2, \dots, b_i$ are the coefficients which are to be found by the regression.

To perform a regression, a number of data points, each consisting of a known Y and its corresponding X variables are required. A proper regression requires that the X variables are independent and that there are many more data points than X variables. Estimates of the b_i coefficients are then made by minimizing the sum of the squared residuals.

The significance of independent variables can be analyzed by comparing the F -ratio to the critical F numeric for a specified confidence level. In this manner, different regression solutions can be found depending on the specified confidence level. Only independent variables with a F -ratio greater than the critical F are included in the solution.

Nonoperating failure rate prediction models are rarely assumed to be in the additive form of the regression solution. However, by using transformations, many possible model forms can assume the additive form. An example can best illustrate this point. The equivalent Arrhenius relationship was determined to be applicable to the nonoperating failure rate of microcircuits, and takes the following form,

$$\lambda = A \exp(-B/T)$$

where T is the independent variable, λ is the dependent variable and A and B are constants. By taking the natural logarithm of each side, the equation becomes,

$$\ln \lambda = \ln A - \frac{B}{T}$$

which can be solved by regression analysis with $1/T$ the independent variable and $\ln \lambda$ the dependent variable. Other transformations are

available such that stepwise multiple linear regression can be used to quantify a variety of failure rate model forms.

The previous paragraphs have discussed how regression analysis can be useful in developing nonoperating failure rate prediction models in which failure rate is a function of quantitative variables such as temperature or number of gates. However, there are often significant variables which can not be measured on a continuous quantitative scale. Application environment and quality level are examples of variables which are qualitative. To determine numerical quantities for qualitative factors in a regression analysis, a matrix of "dummy variables" (0 or 1) is used as the independent variables. The regression solution by least squares computes numerical values of the coefficients which can be used to determine numerical factors.

An example can best illustrate qualitative regression. Consider a part type which is represented by a multiplicative model and has four clearly defined quality levels based on the amount of screening. The four quality levels are signified as L_1 , L_2 , L_3 and L_4 . The following matrix given in Table 3.2-1 presents quality level as a function of three qualitative "dummy variables" (Q_1 , Q_2 , Q_3).

TABLE 3.2-1: EXAMPLE OF QUALITATIVE REGRESSION ANALYSIS

Quality Level	Q_1	Q_2	Q_3
L_1	0	0	0
L_2	1	0	0
L_3	0	1	0
L_4	0	0	1

Nonoperating failure rate data would be introduced into the analysis for L_1 parts by setting $(Q_1, Q_2, Q_3) = (0, 0, 0)$. Data would be similarly entered into the analysis for L_2 , L_3 and L_4 parts. Determination of coefficients for Q_1 , Q_2 and Q_3 allows for computation of quality factor

values by use of the following equations. These equations assume that the dependent variable was the natural logarithm of nonoperating failure rate.

$$\begin{aligned}\pi_{NQ} &= \exp(b_1Q_1 + b_2Q_2 + b_3Q_3) \\ \pi_{NQ1} &= \exp(0 + 0 + 0) = 1 \\ \pi_{NQ2} &= \exp(b_1 + 0 + 0) = \exp(b_1) \\ \pi_{NQ3} &= \exp(0 + b_2 + 0) = \exp(b_2) \\ \pi_{NQ4} &= \exp(0 + 0 + b_3) = \exp(b_3)\end{aligned}$$

This example was constructed such that a level L_1 nonoperating quality factor was equal to one. Any of the other nonoperating quality levels could have been set equal to one without changing the overall results. The relative differences caused by changing which factor was set equal to one would be compensated for by a change in the base failure rate.

It often happens in reliability analyses that some of the data records used in a regression analysis are less precise than others. For example, a data entry with 100 observed failures would be expected to be relatively more precise than a similar data entry with only one failure. To accommodate this difference, it is sometimes advantageous to "weight" the data records. A suitable weighting factor is the reciprocal of the variance. However, this information was not available for empirical nonoperating failure rate data. As an approximate weighting factor, the number of observed failures could be used. Several weighted regressions were performed in this study to assess the effects of equipment power on-off cycling.

F-Ratio and Critical F. The F-ratio and critical F are parameters which are used in conjunction with regression analysis to determine significance of independent variables. The critical F value corresponds to the degrees of freedom of the model (equal to the number of data points minus the number of b_j coefficients minus one) and a specified confidence limit. This number may be used to test the significance of each variable as it is considered for addition to or deletion from the model. The F-ratio value for a regression is the quotient of the mean square due to

regression and the mean square due to residual variation. If the F-ratio value for any independent variable is greater than the critical F value, then it was considered a significant factor influencing nonoperating failure rate and was included in the regression solution.

R-Squared Coefficient. The R^2 coefficient or multiple coefficient of determination is equal to the ratio of the sum of squares of the variance explained by the regression to the sum of the squares of the variance of the observed data. The R^2 value is often used as a means to determine the accuracy of a regression model. The coefficient ranges from 0 to 1.0. A coefficient value of 1.0 indicates a perfect fit between the model and observed data.

The Correlation Coefficient. The correlation coefficient is a measure of the relation between any two variables. It varies between -1 and 1 (from perfect negative to perfect positive correlation). A correlation coefficient of zero indicates that two variables have no correlation.

Standard Error of Estimate. The standard error of estimate allows for computation of a confidence interval for an individual b_i regression coefficient. The standard error is equal to the square root of the residual mean square (the estimate of the variance about the regression). Upper and lower confidence limits of the regression coefficients can be determined from the standard error for a predetermined confidence (α) by,

$$b_i \pm t_{n-2}(S.E.)$$

where

b_i = regression coefficient

t_{n-2} = $1 - \frac{1}{2}\alpha$ percentage point of a t - distribution with n-2 degrees of freedom

n = number of observations

S.E. = standard error of estimate

When the assumed failure rate model form is a multiplicative model, the upper and lower confidence limit values are not exact, but are approximate due to the transformation. Values for the t - distribution are given in Reference 10.

Chi-squared Confidence Intervals. The chi-squared statistic is used to compute a confidence interval around the nonoperating failure rate point estimate for an exponentially distributed reliability function. It is possible to define a 90% confidence interval such that 90% of all possible intervals (of which ours is just one) will contain the true failure rate point estimate. Assumptions concerning data censoring are made to calculate the confidence interval values. These values are calculated as follows:

$$\text{Upper Confidence Limit} = \frac{\chi^2(2(r + 1), \alpha/2)}{2T}$$

$$\text{Point estimate} = \frac{r}{T}$$

$$\text{Lower Confidence Limit} = \frac{\chi^2(2r, 1 - \alpha/2)}{2T}$$

where

r = number of observed failures

T = part hours

$\chi^2(a,b)$ = chi-squared statistic with "a" degrees of freedom at the bth percentile

1- α = confidence (100 x (1- α) is the confidence expressed as a percentage)

3.3 Zero Failure Data

For "zero failure" data records, the standard method of dividing the number of observed failures by the part hours results in a failure rate value of zero. This value was considered to be intuitively

unsatisfactory. Zero observed failures can be a result of a very low inherent nonoperating part failure rate, but it can also be a result of insufficient collected part hours. Any potential data record will exhibit zero failures if the data collection time period is short enough. In many instances, the nonoperating failure rates studied were extremely low, and there were many zero failure data records as a result. This section presents a discussion of zero failure data and how it was treated in this study.

Zero failure data could not be ignored or discarded for several reasons, including,

- o For some part types, zero failure data records represented a substantial percentage of all data.
- o A data sample with only failure data would include failure rates higher than the mean more often than corresponding lower failure rates.

The second item warranted further discussion. Given an infinite sample of data, some of the calculated failure rates would be higher than the "true" mean failure rate, and the rest would be less. However, given a time-truncated data sample for inherently reliable components (as was the case in this study), the failed items will more likely come from the sub-population with failure rates above the "true" mean. Indeed, high failure rates are characterized by observed failures. For the corresponding low failure rates, no failures would be expected because of the number of available part hours. This is especially true when the nonoperating part hours fall into a certain range due to practical constraints. Extremely high part hours are unattainable due to physical constraints, and sources with very low part hours are avoided during data collection. A conceptual illustration of this behavior is presented in Figure 3.3-1. The distribution estimated from the failure data has a higher estimated mean failure rate than the true, unknown distribution. Given large sample sizes, the true and the estimated means would be expected to align themselves. However, this may not necessarily be true

for small sample sizes. This was considered to be one reason that zero failure data could not be ignored.

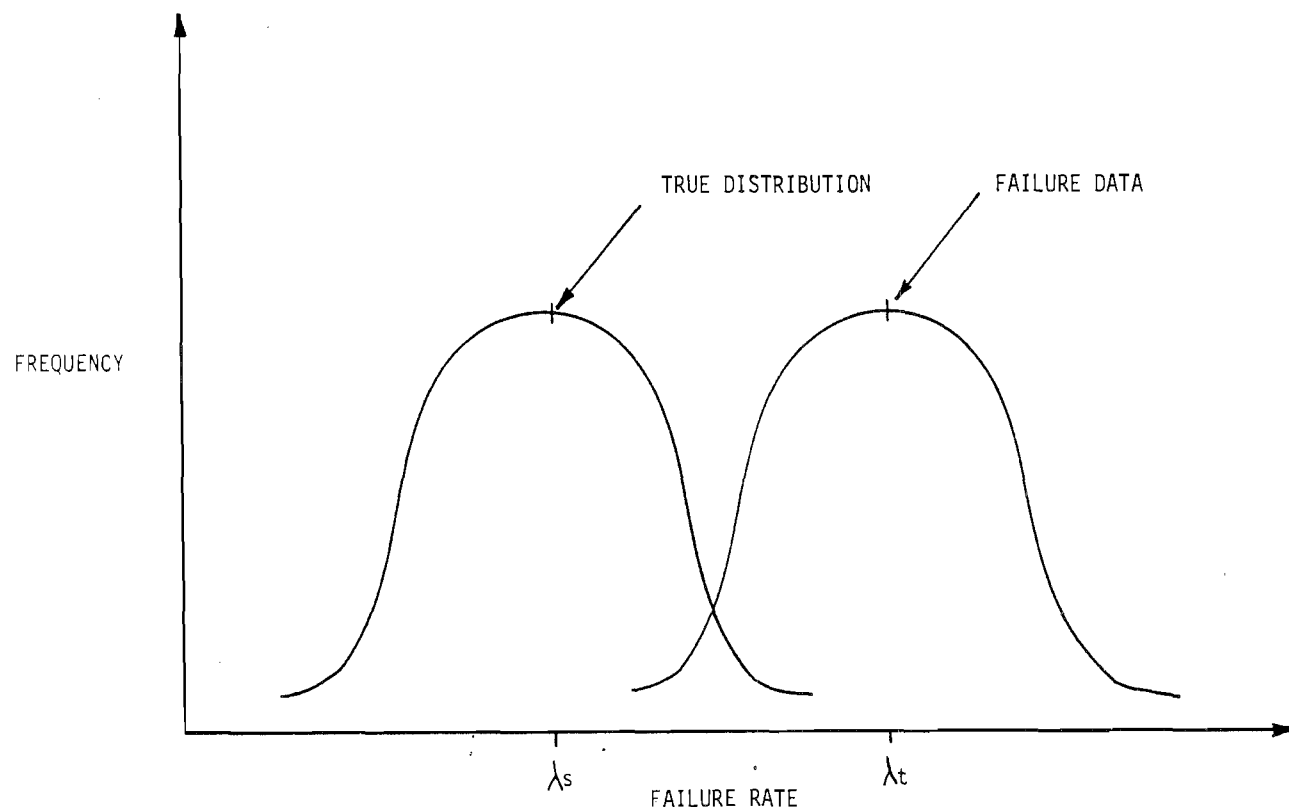


FIGURE 3.3-1: CONCEPTUAL FAILURE RATE DISTRIBUTION

Zero failure data hypothetically could be segregated into two categories; (1) data records indicative of a very low failure rate, and (2) data records indicative of insufficient part hours. Practically, it was impossible to divide the zero failure data into one category or another. However, a largely intuitive method was developed to ascertain which data had sufficient part hours to estimate a failure rate without observed failures.

A preliminary analysis was performed using only failure data to determine which zero failure data records had sufficient part hours to estimate a failure rate. This method was used for data records on similar part types in similar applications. If the number of part hours for each of the zero failure data records were larger than the mean-time-to-failure for the data with failures, then it was assumed that the data entry had

sufficient part hours. An approximate nonoperating failure rate was determined by calculating an upper, single-sided 60% confidence limit. This value represents an upper bound on failure rate. If an individual zero failure data record had less part hours than the mean-time-to-failure, then it was assumed that there were insufficient part hours to expect a failure, and the data record was discarded. This method was intuitively satisfactory for two reasons. First, a zero failure data record with more part hours than the mean-time-to-failure could be used as an argument that the failure rate (computed from failure data) was too high, and thus, required additional data. The second reason was that by including the failure rates computed without failures, the estimated failure rate mean (depicted in Figure 3.3-1) would move closer to the true, unknown value.

It was concluded during this study that zero failure data could neither be arbitrarily discarded nor arbitrarily used. An intuitive approach was developed and subsequently implemented to decide which zero failure data records had sufficient part hours to estimate a failure rate.

3.4 Effect of Nonoperating Failures on Operating Models

The failure rate models which appear in the current version of MIL-HDBK-217 may, or may not, include a contribution due to nonoperating failures. For example; if the failure rate model is based primarily upon life test, physics or failure data or verified operating failures, then the model would exclude nonoperating failures. In contrast, if the failure rate model were based primarily upon field experience utilizing military aircraft where all failures were assumed to be operating failures, then the model may include nonoperating failures mixed within the operating failures.

The difference between the MIL-HDBK-217D failure rate and the actual operating failure rate is dependent on,

- o the extent which nonoperating failures were separated from operating failures
- o the ratio of operating to nonoperating failure rate
- o the ratio of operating to nonoperating time

If no attempt was made to eliminate nonoperating failures from the total number of failures, then the following set of equations represent the relationship of MIL-HDBK-217 failure rate, inherent operating failure rate and nonoperating failure rate.

$$\begin{aligned}
 \lambda_{217} &= \frac{f_o + f_n}{T_o} \\
 &= \frac{f_o}{T_o} + \frac{f_n}{T_o} \\
 &= \frac{f_o}{T_o} + \frac{f_n}{T_n} \frac{T_n}{T_o} \\
 &= \lambda_o + \lambda_n \frac{T_n}{T_o}
 \end{aligned}$$

where

λ_{217} = MIL-HDBK-217 failure rate (if nonoperating failures were not separated)

f_o = operating failures

f_n = nonoperating failures

T_o = operating hours

T_n = nonoperating hours

λ_o = operating failure rate

λ_n = nonoperating failure rate

An applicable multiplicative correction factor would then be equal to the ratio of λ_0 to λ_{217} , or,

correction factor = λ_0/λ_{217}

$$= 1 - \frac{\lambda_n}{\lambda_{217}} \frac{T_n}{T_0}$$

To fully investigate the influence of nonoperating failures on MIL-HDBK-217D models, the ratio of nonoperating time to operating time would have to be determined for all data sources used in the model development process. The RADC technical reports describing each model development effort were located to determine this information. Unfortunately, the extent to which nonoperating failures were considered and the duty cycles for each data source were generally not presented in the technical reports. Additionally, the data sources often were not identified, thereby preventing further investigations. As a result, correction factors could not be determined to eliminate the effect of nonoperating failures on the MIL-HDBK-217D models. However, based on the information which was available, it was concluded that much of the data used to determine the MIL-HDBK-217D models were either from life testing or from equipments which experience significant operating times. Therefore, the correction factor would generally be close to one.

4.0 NONOPERATING FAILURE RATE MODELING CONCEPTS

This section presents an overview of the general nonoperating failure rate modeling approach developed for this study. In addition, the effects of equipment power on-off cycling, temperature, environment and screening are discussed in detail.

4.1 Failure Rate Modeling Approach

This study involved the development of a large number of nonoperating failure rate prediction models. A general failure rate modeling approach was established and applied to all generic part classes. Use of a similar modeling approach for all part classes resulted in nonoperating failure rate prediction models which were consistent and complementary.

The basic nonoperating failure rate modeling approach is presented in Figure 4.1-1. This approach was used for all generic part categories. Deviation from the general approach was occasionally required because of imbalanced data sets, inconsistent results or other reasons. Detailed descriptions of the model development process for each part category are included in the appropriate subsection of Section 5 of this report. The following paragraphs provide a discussion of the techniques referred to in Figure 4.1-1.

The initial phase of the nonoperating failure rate modeling process was to identify potential variables. For each generic part category, of part construction and application variables were identified to properly characterize the subject part in a nonoperating environment. Emphasis during the variable identification task was directed towards identification of variables which would be accessible to the prediction model users. These variables represent possible prediction model input parameters. In addition, the identification of potential variables was a prerequisite for both the data collection and theoretical model development tasks.

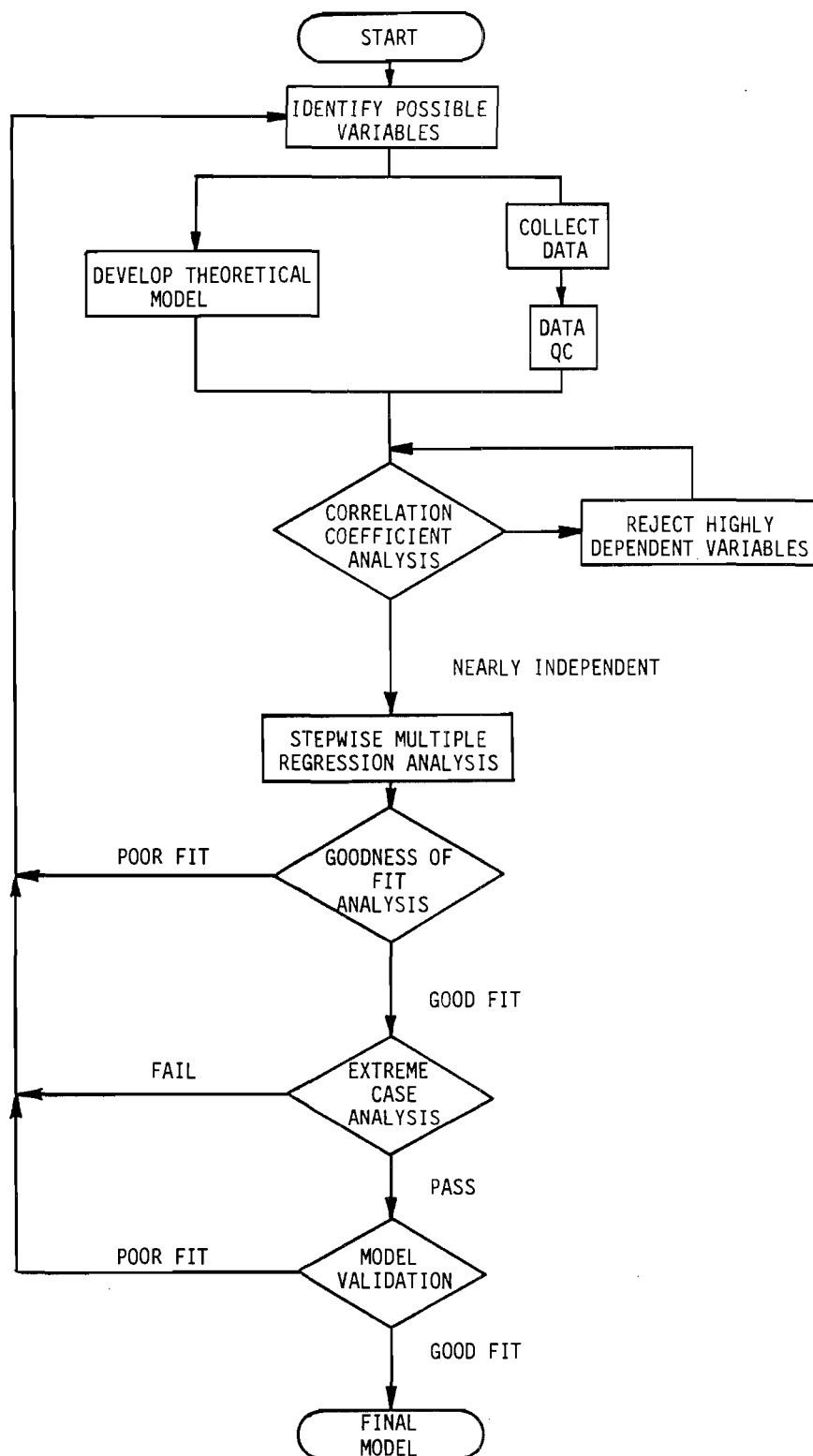


FIGURE 4.1-1: MODEL DEVELOPMENT FLOW CHART

Development of a theoretical nonoperating failure rate prediction model was an integral part of the overall model development process. It was recognized early in this study that limited data resources might prevent the identification of all significant variables using purely statistical techniques. Unbalanced data sets or correlated variables could result in inconsistent or incorrect conclusions. Additionally, decisions regarding the optimal model form (i.e. multiplicative, additive, etc.) were enhanced by a fundamentally sound theoretical model. Also, the theoretical model proved to be useful for interpreting or explaining observed analysis results.

An extensive data collection effort was performed concurrent with the theoretical model development. The data collection approach and a summary of the collected data is described in great detail in Section 2.0 of this report.

Following the data collection activities, a data quality control task was performed. All data items received during the data collection efforts were reviewed for completeness and examined for any inherent biases. Any data submitted which displayed obvious bias was not considered in subsequent analyses. Those data records lacking sufficient detail were not considered until the necessary additional information was acquired. Additionally, the number of observed nonoperating failures and the corresponding failure definition were scrutinized.

The objective of the correlation coefficient analysis was to identify highly correlated variables. Definition of correlation coefficient and a brief explanation is presented in Section 3.2. During the analysis, correlation coefficients were computed for each pair of independent variables. Regression analysis requires that all independent variables are uncorrelated. Therefore, the effects of correlated variables could not be simultaneously quantified. If the variables were correlated inherently (e.g. number of pins and number of gates for SSI/MSI devices), then a decision was made to include only the most significant variable in the regression analysis. If the variables were correlated due to chance

(e.g. quality vs. temperature), then several options were considered. If a valid theoretical or empirical relationship was found for one of the correlated variables, then the effect of that variable was removed from the data by assuming the relationship to be correct. If this assumption was correct, then the effect of the remaining correlated variable could be accurately assessed by data analysis.

The next step in the model development process was to apply stepwise multiple regression analysis. Regression analysis is defined and briefly described in Section 3.2 of this report. This technique was used to compute the coefficients of an assumed model form in a least squares fit to the data. Regression solutions were found for decreasing confidence limits beginning with 90%. In addition, F-ratios and standard error statistics were computed for each significant variable to obtain an indication of the degree of significance and the accuracy of coefficient estimates. Additionally, upper and lower 90% confidence interval values were determined for each coefficient. In general, variables were not included in the proposed model if they did not significantly effect nonoperating failure rate with at least 70% confidence. However, if a variable such as device screening was known to influence nonoperating failure rate, then coefficients were computed with less than 70% confidence and a corresponding factor proposed. In these instances, the resultant factor was considered approximate. This was necessary only occasionally, and no factors were proposed with less than 50% confidence.

The goodness of fit of the regression solution was then tested using the R-squared statistic. No absolute acceptable limit was defined to determine what constituted a "good fit" because of the relative variability between part classes and because of different sample sizes. For example, the acceptable R-squared value computed for hybrid microcircuits would have been unacceptable for monolithic microcircuits. The inherent variability of hybrid nonoperating failure rate and the large number of potential variables (vs. a smaller number of data records) prevented a highly accurate model for hybrid devices. Nevertheless, an R-squared value was computed and the proposed model evaluated for each part

class. If the proposed model was determined to be unacceptable, then the model development process returned to the variable identification task to identify missing variables.

The next phase of the general model development process was to perform an extreme case analysis. Predictions were made using the proposed model for parameters beyond the ranges found in the data. The intent of the extreme case analysis was two-fold. The first objective was to identify any set of conditions which cause the proposed model to numerically "blow up". The other objective of the extreme case analysis was to identify any set of conditions which predict a nonoperating failure rate which is intuitively incorrect. For instance, a model that predicted an unscreened device with a lower failure rate than a similar screened device, or predicted a negative failure rate would be examples of an intuitively incorrect model. Reasons for failing the extreme case analysis primarily involve an incorrect choice of model form. If the extreme case analysis indicated that the proposed model was unacceptable, then the entire model development process was begun again.

The final phase of the general model development process was a model validation task. Data which had been withheld from the model development process were used to evaluate the accuracy of the proposed models. Data obtained from the European organization AFCIQ were used for this purpose for microcircuits, diodes, transistors, resistors and capacitors. In each case, the AFCIQ data indicated that the proposed models provided accurate predictions. If this had not been the case, then the model development process would have been started again with the AFCIQ data as part of the data base. For other part types, scarcity of data required that all data were included in the model development process.

Establishing a general nonoperating failure rate model development process allowed for efficient data analyses, and consistent proposed models. The following sections include more detailed discussions of the - theoretical model development process, and the effects on nonoperating

failure rate of equipment power on-off cycling, temperature, application environment and screening.

4.2 Theoretical Model Development

A series of theoretical nonoperating failure rate prediction models was hypothesized to provide direction to the model development process and to provide the resultant models with a theoretical foundation. Information obtained through the literature search was evaluated and reviewed to aid in development of the theoretical model. Both theoretical and intuitive nonoperating reliability relationships located in the literature proved to be extremely relevant in the later stages of model development.

In general, the theoretical model development consisted of evaluation of the hypothetical effect on nonoperating failure rate of the following factors.

- o Function
- o Technology
 - Fabrication Techniques
 - Fabrication Process Maturity
 - Failure Mode/Mechanism Experience
- o Complexity
- o Packaging Techniques
- o Effectiveness of Process Controls
- o Effectiveness of Screening and Test Techniques
- o Nonoperating Environment and Temperature
- o Frequency of Equipment Power Cycles

In addition, different model forms were investigated and an optimal model form hypothesized. For example, assumed relationships between nonoperating failure rate and equipment power on-off cycling had been referenced in many sources (References 5, 11 - 17). The proposed equipment power on-off cycling factors were based on the general agreement between

several of these references. It was doubtful that a similar factor would have been developed using only analytical methods.

Specifically, three major advantages were gained by the theoretical model development process. (1) Selection of significant variables was not always possible by purely statistical techniques. For example, application environment was believed to be a significant variable, but could not be evaluated empirically because all data were from a ground based environment. The theoretical model complemented the data analysis in these instances. (2) Another benefit from the theoretical model was the selection of an appropriate model form. Many of the model forms presented in this study were based on conclusions made in the theoretical model development. The form of proposed factors for temperature, quality and equipment power on-off cycling were assumed based on the theoretical model, and then quantified with the available data. (3) A final advantage of the theoretical model development was to identify existing relationships in the literature. These relationships were often valuable for the analysis of correlated variables.

4.3 Equipment Power Cycling Effects

Equipments in long term storage are often energized periodically in an attempt to increase the reliability and availability of the inventory. It has generally been assumed that the majority of observed failures were storage related and thus, the testing was justified as a means to increase availability. However, if the majority of failures were related to the test procedure itself, then the testing may be unnecessary and excessively costly. One of the major objectives of this study was to investigate the effects of equipment power on-off cycling on electronic and electromechanical components. For the purpose of this study, an equipment power on-off cycle was defined as the state during which an electronic equipment goes from zero electrical activation level to the normal design activation level and then returns to zero.

A proper investigation of nonoperating reliability must also include a study of the effects of equipment power on-off cycling. Storage related failures and failures induced by the power on-off cycle are the result of quite different causal factors. However, both types of failures can generally only be detected when power is applied to the equipment and are subsequently grouped together in the available data. As a result, failures due to storage can not be distinguished from failures due to the power on-off cycling. A two phase approach was taken to properly assess the effects of power on-off cycling. The first phase was to investigate previous work done in this area and to reach conclusions based on the available information. The second phase of the power cycling investigation consisted of treating equipment power on-off cycling frequency as a quantitative variable in a nonlinear regression analysis. Nonoperating failure rate data were collected for a wide range of cycling frequencies. If cycling frequency was not identified as a significant variable, then it could be concluded that the observed failures were dominated by storage related failures. Conversely, if the regression solution indicated that nonoperating failure rate (in units of failures per 10^6 nonoperating hours) was approximately proportional to cycling frequency, then it could be concluded that the observed failures were primarily induced by the power cycling.

4.3.1 Dormancy and Power On-Off Cycling Effects on Electronic Equipment and Part Reliability (RADC-TR-73-248)

The issue of equipment power on-off cycling was addressed in RADC-TR-73-248, "Dormancy and Power On-off Cycling Effects on Electronic Equipment and Part Reliability" (Reference 5) performed by Martin Marietta Aerospace. Included in this study was a mathematical analysis of failure rate versus equipment power cycling. Equation 1.1.2-9 in Reference 5 presents a mathematical relationship for service life failure rate for systems which undergo long term storage and dormancy. The service life failure rate was presented as a function of dormant failure rate and average equipment power cycling rate. The mathematical expression was

developed based on intuitive reliability relationships. This expression is given by the following equation.

$$\lambda_{SL} = (1 + K_{C/D}(N_C)) \lambda_D$$

where

λ_{SL} = service life failure rate

$K_{C/D}$ = ratio of cyclic failure rate to dormancy failure rate (in hours of dormancy per cycle)

N_C = average cycling rate expected during the service life of an electronic system (in cycles per total unit time of service life)

λ_D = dormant failure rate

This equation was then extended to component nonoperating failure rates and estimates of the $K_{C/D}$ term were made. It was noted that the $K_{C/D}$ term ideally should vary with part type, part quality, cyclic rate, temperature effects, transient suppression protection and environmental application. However, the $K_{C/D}$ estimates were only made based on part types because of practical restraints.

4.3.2 Planning Research Corporation Studies

The effects of equipment power on-off cycling have been investigated by Planning Research Corporation (PRC) during several studies performed for the Navy Space Systems Activity, and Goddard Space Flight Center (References 11, 12, 13 and 14). Equipment and component level observed data were collected and compared for continuous operation, standby operation, intermittent operation, cyclical operation, dormancy and storage. The subject equipments were spacecraft electronic systems. No significant difference was identified during the studies between cyclical operation and steady state operation. This was due primarily to data limitations rather than a definitive conclusion concerning cyclical vs. steady state failure rate. Nevertheless, it was stated in Reference 13,

"It is rather clear, however, that cycled components in general do not have order of magnitude worse failure rates than their non-cycled counterparts."

4.3.3 ARINC Study

Cited in the PRC reports was a ARINC study (Reference 15) concerned with the effect of equipment power cycling on shipboard electronic equipment. A summary of the conclusions from this study are as follows.

- o The expected number of equipment malfunctions per hour of operation, b_t , is given by,

$$b_t = b_0(1 + 8N)$$

where

b_0 = expected number of malfunctions per hour of continuous operation

N = the number of cycles per hour of continuous operation

- o More severe environments would be expected to increase the cycling factor and more benign environments to reduce it.
- o The study revealed a substantially higher level of equipment malfunctions during a short period of time after each power turn-on than during any other operating time interval. It could not be determined which of these failures occurred in dormancy and which were due to turn-on transients.
- o On/off cycling was not observed to introduce any specific type of failure.

The cycling equation constant of 8 was empirically determined from a broad class of shipboard electronic equipments, primarily of the vacuum - tube variety. Similarities in form were noted between this equation and the previously presented mathematical expression for service life failure rate from the Martin Marietta report. In both instances, the equipment power cycling frequency was multiplied by a constant term and then added to one.

4.3.4 Hughes Presentations

Missile storage test data compiled by Hughes Aircraft Co. (Reference 16 and 17) indicates that missile testing is the dominant variable affecting the performance of missile electronics in storage. Equipment level test data were collected for the Maverick and TOW missiles. The data indicates that a similar percentage of missiles fail regardless of the storage interval. It was concluded by Hughes that this observation was because the testing process had induced a large majority of the observed failures. Extended to the component level, this observation would result in nonoperating failure rate prediction models (measured in units of failures per 10^6 nonoperating hours) directly proportional to the testing frequency. The data appears to strongly support the conclusion, although no trend analysis or statistical tests were described in the references to help validate the conclusion.

It should also be noted that failures caused by operator or maintenance error would tend to be concentrated during the test interval as opposed to being evenly distributed throughout the storage period. Therefore, if the data were not accurately recorded, screened and characterized, then other factors could be partially responsible for the relatively constant percentage of "failed" missiles observed by Hughes.

4.3.5 Equipment Power Cycling Conclusions

Two major conclusions were made based on the literature review. The first conclusion was that equipment power cycling must be considered as part of any effort to investigate or predict nonoperating failure rates. The second conclusion was that the effects of equipment power on-off cycling can be predicted by a multiplicative model of the following form.

$$\pi_{cyc} = 1 + K_1(N_c)$$

where

π_{cyc} = equipment power on-off cycling factor

K_1 = constant

N_c = number of power on-off cycles per 10^3 nonoperating hours

The form of this cycling factor was based on the agreement between the Martin Marietta and ARINC results. In addition, a factor of this form is intuitively appealing. At extremely low cycling rates, the predicted nonoperating failure rate would become independent of cycling rate and equal to the dormant/storage failure rate. At high cycling rates, a predicted nonoperating failure rate would be proportional to the cycling rate.

A cycling rate factor of this form would not be applicable when the power cycles interfere with one another (i.e. the equipment has not yet cooled down from the previous cycle when a new one is initiated). However, this restriction was not believed to limit the utility of the results of this study.

The units for equipment power cycling rate were chosen to be number of equipment power on-off cycles per 10^3 nonoperating hours. This decision was made for convenience. Storage intervals as long as ten years ($.011$ cycles/ 10^3 hrs.) and as short as one day (41.67 cycles/ 10^3 hrs.) could be expressed easily.

4.3.6 Equipment Power Cycling Analysis

The second phase of the equipment power cycling analysis was to quantify the effects of power cycling by application of appropriate statistical techniques. As a prerequisite to data analysis, it was required that the cycling rate must be identified for each data source described in Section 2.3. This task proved to be more difficult than anticipated. For some cases, the test schedule information was proprietary. In other instances, the testing frequency was unknown or

variable. Nevertheless, average cycling rates were obtained or calculated for the majority of data sources. For data sources where the testing frequency was variable (e.g. Hawk, Maverick and TOW missiles) an average cycling rate was computed for the data collection interval.

A multiplicative model with the assumed equipment power cycling factor was nonlinear. Thus, linear regression analysis could not be directly applied. An iterative approach was taken to solve the nonlinear equation. Specifically, the iterative process began by defining three distinct cycling rate categories. Then, the effects of all significant variables were quantified including computation of unique regression coefficients for each of the three cycling rate categories. In effect, equipment power cycling was initially treated as a qualitative variable. Conceptually, this first step can be represented by the following equations.

The first equation depicts an example nonlinear nonoperating failure rate prediction model. The model is nonlinear due to the effect of power cycling, and is also a function of device style, quality and temperature.

$$\lambda_p = \lambda_{nb} \pi_{NQ} \pi_{NT} (1 + K_1(N_C))$$

where

λ_p = part nonoperating failure rate

λ_{nb} = base failure rate, based on device style

π_{NQ} = nonoperating quality factor

π_{NT} = temperature factor

K_1 = cycling factor constant

N_C = number of equipment power on-off cycles per 10^3 nonoperating hours

Three distinct cycling rate categories were defined to enable the computation of unique regression coefficients for each category. The resultant model then becomes linear (with a logarithm transformation) and

regression analysis can be applied to quantify each variable. The model then takes the following form.

$$\lambda_p = \lambda_{nb} \pi_{NQ} \pi_{NT} A_i$$

where

A_i = multiplicative cycling rate constant

A_1 = constant for $N_1 \geq N_c > N_2$, cycling rate category one

A_2 = constant for $N_2 \geq N_c > N_3$, cycling rate category two

A_3 = constant for $N_3 \geq N_c > N_4$, cycling rate category three

The preliminary cycling rate factor could then be computed by performing a two-dimensional regression (A_i vs. average cycling rate) to obtain estimates for the cycling factor constant (K_1). The following equation depicts this relationship.

$$A_i = K_2(1 + K_1(\bar{N}_i))$$

where \bar{N}_i is the mean cycling rate for each cycling rate category, and K_2 is a normalization constant.

The iterative process was required unless A_i correlated exactly with N_i (correlation coefficient = 1). Practically, it is doubtful that a correlation coefficient of exactly one will be observed, and the iterative process was required in all cases for this study.

As the iterative process continues, the preliminary equipment power cycling factor would then be assumed exact, and the coefficients for all other variables recalculated. Generally, the observed change in coefficient values was small. Then, those coefficients would be assumed to be exact and the equipment cycling factor recalculated. The iterative process continued until observed changes in coefficient estimates were negligible. In practice, it was found that less than three iterations were generally required. For example, the coefficients stabilized after

one iteration for resistors and three iterations for capacitors. However, six iterations were required for linear/interface microcircuits.

K_1 constant values were computed for each generic part category where it was determined that equipment power on-off cycling was a significant variable. Ideally, unique K_1 values should be determined for every conceivable combination of part class, quality, temperature and environment. However, an extremely large amount of nonoperating failure rate data would have been needed to quantify an equipment power cycling factor as a function of each of those variables. Since the available data was limited, the equipment power cycling factors determined in this study represent the best possible values. When additional nonoperating reliability data becomes available, these factors should be investigated to determine their validity. The equipment power cycling factors for specific part classes are presented in the respective model development section of this report.

Whether or not equipment power cycling significantly increases the reliability and availability of an inventory of stored equipments, it must be recognized that the testing process accelerates the frequency of electronic component failure. Conversely, the opposite can be assumed to be true for certain electromechanical components. Long periods of storage for switches, relays, electric motors, servomechanisms and connectors can result in severe degradation. Effects of the degradation process can often be minimized by periodic actuation of contact devices or periodic turn on for motors and servomechanisms. Similarly, certain styles of capacitors are known to degrade in storage and require reforming of the dielectric at certain time intervals.

Switches and relays designed to control low voltage digital circuits are particularly susceptible to storage degradation. A resistive surface film will form on normally open contacts depending on package type, contact material and environment. Periodic actuation of the contacts can break thru the resistive surface film to provide electrical contact. If the time interval between actuations is too long, the resistive film

becomes relatively thick and thereby, results in poor contact. Unfortunately there were insufficient data to quantify the effects of equipment power on-off cycling on contact devices.

For motors and servomechanisms, periodic turn-on is essential to maintain the integrity of the lubrication. As was the case with switches and relays, there were insufficient data to accurately ascertain the effects of equipment power on-off cycling for these rotating mechanisms. It is recommended that future studies addressing the issue of equipment power cycling investigate the effects of cycling on these mechanical and electromechanical part types.

4.4 Temperature Effects

An investigation into the effects of temperature on nonoperating failure rate was a crucial part of this study effort. Electronic assemblies in a ground storage environment can be exposed to a relatively wide range of temperatures depending on the applicable mission profile, geographic location, and availability of environment controlled storage facilities. To investigate temperature effects, high temperature storage life test data were collected for microcircuits and discrete semiconductors. Data were available for test temperatures ranging up to 350°C. As a result, unique nonoperating temperature factors were determined for microcircuits, transistors and diodes.

The impact of storage temperature was believed to be one of the most significant variables effecting microcircuit nonoperating failure rate. Most microcircuit failure mechanisms involve one or more physical or chemical processes which occur at a rate which is dependent on temperature. It was assumed that the Arrhenius model applies to the reaction rate of microcircuit storage failure mechanisms. The Arrhenius model was based on empirical data and predicts that the rate of a given physical or chemical reaction will be exponential with the inverse of temperature. Conceptually, the Arrhenius model is given by the following equation.

$$\text{Reaction Rate} \propto \exp(-\epsilon_{ea}/KT)$$

where

ϵ_{ea} = activation energy (eV)

K = Boltzman's constant

$$= 8.63 \times 10^{-5} \text{ (eV/}^{\circ}\text{K)}$$

T = temperature ($^{\circ}\text{K}$)

Every chemical and physical reaction has a unique activation energy associated with it. During the storage life of an electronic component there are several such reactions proceeding simultaneously, each capable of causing a part failure. Individual consideration of each of these different reactions would result in very complex nonoperating failure rate prediction models which are not in accordance with the simple form of the Arrhenius model. Consideration of each physical and chemical failure mechanism separately (and assuming each mechanism is independent) would result in a nonoperating failure rate prediction model similar to,

$$\lambda_p \propto \sum_{i=1}^n (-\epsilon_{eai}/KT)$$

where

λ_p = nonoperating failure rate

n = number of failure mechanisms

ϵ_{eai} = activation energy of the i^{th} failure mechanism

This relationship was determined to be much too complex to be quantified with the available data. Therefore, alternate mathematical expressions for device nonoperating failure rate vs. temperature were explored. The activation energy Arrhenius relationship concept has been applied to microcircuit failure rates (instead of failure mechanism reaction rates) often enough (References 18 and 19) to warrant further investigation. It has been found for general classes of components with similar failure mechanism distributions, the cumulative effects of the

various reactions can be approximated by an Arrhenius model for a specified temperature range. This relationship was designated as the "equivalent Arrhenius relationship." Because of the documented accuracy of this approximation, it was decided to investigate the effects of temperature using the equivalent Arrhenius relationship. It should be emphasized that at extreme high and low temperatures, this relationship will no longer be applicable. Use of the Arrhenius model to predict failure rate can be a very useful and accurate tool. However, the limitations of this assumption must be fully understood.

The storage failure rate of linear microcircuits has been observed to approximate the equivalent Arrhenius model over a wide range of storage temperatures. Figure 4.4-1, taken from Reference 20, presents the logarithm of observed storage failure rates for linear devices as a function of the inverse of temperature (which is equivalent to the Arrhenius relationship). The information depicted in Figure 4.4-1 is for a range of temperatures of 150°C to 350°C. The relationship appears linear at least until 300°C. In addition, the microcircuit nonoperating data collected in support of this study included application temperatures from 18°C for field data to 350°C for high temperature storage life test data.

A preliminary multiplicative temperature factor for microcircuits was determined to be the following equation.

$$\pi_{t,p} = \exp(-A_n(1/T))$$

where

$\pi_{t,p}$ = preliminary temperature factor

T = temperature (°K)

A_n = constant = (equivalent activation energy)/(Boltzman's constant)

- It was decided to add a reference temperature term to improve the utility of the proposed nonoperating microcircuit models. A reference

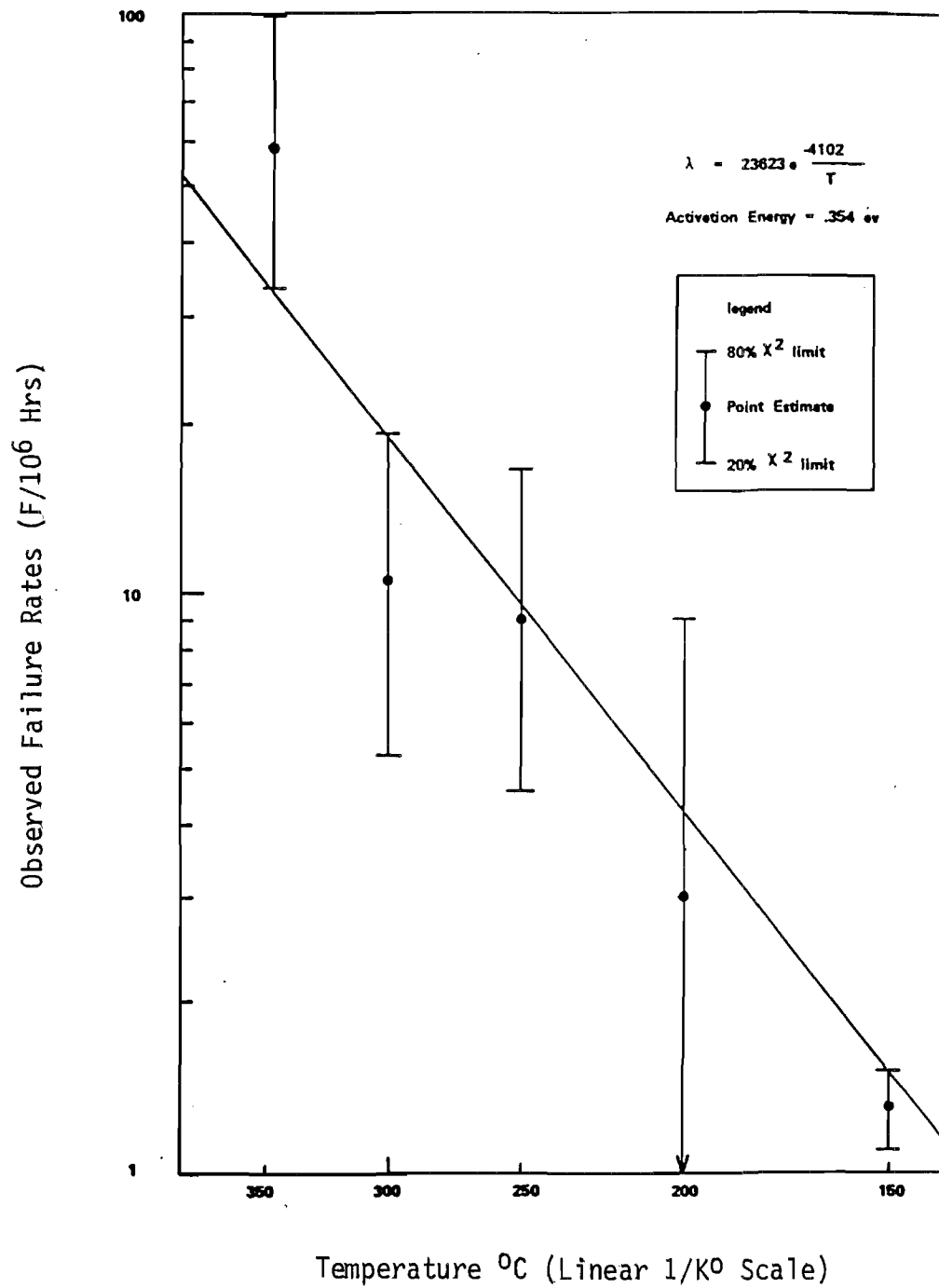


FIGURE 4.4-1: LINEAR MICROCIRCUIT STORAGE FAILURE RATE VS. TEMPERATURE

temperature of 298°K (i.e. 25°C) was selected to be consistent with MIL-HDBK-217D. The preliminary temperature factor with a reference temperature term is therefore, given by,

$$\pi_{t,p} = \exp(-A_n(\frac{1}{T} - \frac{1}{T_r}))$$

where

$\pi_{t,p}$ = temperature factor

A_n = constant

T = temperature (°K)

T_r = reference temperature (°K) = 298°K

Mathematically, adding the reference temperature term to the proposed model has no effect on the resultant nonoperating failure rate prediction. Relative differences caused by selection of the reference temperature are compensated by corresponding changes in the proposed base failure rate. The following series of mathematical expressions depict this relationship.

$$\begin{aligned}\lambda_1 &= \lambda_2 \exp(-A_n(\frac{1}{T})) \\ &= \lambda_2 \exp(-A_n(\frac{1}{T} - \frac{1}{T_r} + \frac{1}{T_r})) \\ &= \lambda_2 \exp(-A_n(\frac{1}{T_r})) \exp(-A_n(\frac{1}{T} - \frac{1}{T_r})) \\ &= \lambda_3 \exp(-A_n(\frac{1}{T} - \frac{1}{T_r}))\end{aligned}$$

where

λ_1 = nonoperating failure rate

λ_2 = preliminary base failure rate

λ_3 = base failure rate = $\lambda_2 \exp(-A_n(\frac{1}{T_r}))$

Initially, introduction of the reference temperature term seemed to needlessly complicate the proposed model. However, it was decided to include the reference temperature for two reasons:

- 1) A proposed model with the reference temperature term provides more information. The base failure rate would be equal to the device failure rate at the reference temperature. Thus, inspection of the base failure rate value provides meaningful information for quick analyses. Without the reference temperature term, the base failure rate would correspond to when $(1/T)$ approaches zero, and would thus be meaningless by itself.
- 2) A proposed model with the reference temperature term would minimize the need for exponential numbers (e.g. 7×10^{34}) and would therefore result in models which are easier to use. The temperature factor would be equal to one when the ambient temperature equals the reference temperature, and would generally be below 100 for even the highest possible ambient temperatures found in nonoperating applications.

A modification was then made to the preliminary temperature factor so the predicted nonoperating failure rates would approach constant values at low temperatures and become asymptotic to the operating failure rate at high temperatures. The need for this modification was identified during the microcircuit model validation stage. The proposed microcircuit nonoperating temperature factor was, therefore, given by the following expression.

$$\pi_t = K_3 + K_4 \exp(-A_n(\frac{1}{T} - \frac{1}{T_r}))$$

where

K_3, K_4 = constants

It was concluded after evaluating all the available information that microcircuit nonoperating failure rates could be predicted by use of this temperature relationship for the range of nonoperating temperatures found during normal usage (-55°C to 125°C , maximum). Unique Arrhenius

relationship constants were determined as a function of logic type for digital, linear and memory devices.

High temperature storage life test data was also collected for discrete semiconductors with temperatures ranging from 150°C to 200°C. It could not be verified whether the equivalent Arrhenius relationship was linear for the total range of temperature values found in the data; 18°C to 200°C. Therefore, an additional term was added to the general form of the temperature factor expression to allow for a nonlinear relationship for the logarithm of failure rate versus the inverse of temperature. The multiplicative temperature factor expression for discrete semiconductors was assumed to be the described by following equation.

$$\pi_T = \exp(-A_n(\frac{1}{T} - \frac{1}{T_r}) + (\frac{T}{T_m})^P)$$

where

T_m , P = shaping parameters

If the equivalent Arrhenius relationship was determined to be applicable for the entire range of temperature values, then the second term would become negligible.

The derivation of appropriate temperature factors for microcircuits and discrete semiconductors was an essential part of the methodology developed to assess the effects of nonoperating periods on equipment reliability. Appropriate temperature factors were determined empirically and are included in the respective nonoperating failure rate prediction models. Temperature factors for less temperature dependent part types could not be developed due to data limitations.

4.5 Environmental Factor Analysis

The primary objective of this study was to develop a nonoperating failure rate prediction methodology which can be applied to any

conceivable mission profile with nonoperating periods. Therefore, it was essential that any proposed prediction models account for the apparent differences in nonoperating failure rate caused by environmental stresses such as temperature cycling, vibration, humidity, mechanical shock, electromagnetic interference and many other stresses. There is a wide variety of environmental stresses that electronic equipments can be exposed to while in the nonoperating condition. For example, at one extreme, missile guidance systems in a captive-carry application are exposed to the extreme vibration and temperature cycling stresses associated with an airborne uninhabited environment. Conversely, missile electronics stored in a sealed container are subjected to significantly lower levels of environmental stress. In the development of theoretical nonoperating failure rate prediction models, it was determined that environment would indeed have a significant effect on nonoperating failure rate for each major part category (i.e., microcircuits, discrete semiconductors, resistors, etc.)

The early stages of this study effort included plans to derive nonoperating failure rate prediction models as a function of specific environmental stress values (i.e. relative humidity, g-force, etc.). A model of this form would provide maximum prediction accuracy and proper discrimination against known failure mechanism accelerating factors. However, after careful consideration, this approach was rejected for the following reasons.

- o The nonoperating reliability data available for analysis for this study generally did not include specific values for all environmental stresses. In fact, the ambient temperature was usually the only environment variable which could be precisely determined. Therefore, assumptions would have to be made to assess the quantitative effect on device nonoperating failure rate. This would clearly diminish the significance of analysis results.
- o One of the more important objectives of this study was to develop failure rate prediction models which are relatively easy to use. In the design phase of an equipment, specific values for all environment related variables may not be available. Therefore, the benefits afforded by including specific environmental stress

variables would be negated by a decreased ability to use the models.

- o It would be difficult for the government costumer to verify or document the environmental stress input parameters. This would introduce additional uncertainties regarding equipment reliability predictions.

As an alternative to the analysis of specific environmental stresses, the approach was taken to consider well defined environment categories which experience similar levels of environmental stress. This is consistent with the methods used in MIL-HDBK-217D. Benefits offered by this approach are that the models would be easy to use while still discriminating against variables known to increase failure rate. The only variable analyzed apart from the generic environment categories was ambient temperature. This was for three reasons. The first, ambient temperature is the most significant of individual environmental stresses for many part types. The second reason was that the ambient temperature for electronic assemblies in a ground storage environment can vary substantially depending on the geographic location and the availability of environment controlled storage facilities. The last reason was that ambient temperature was generally available from the data sources used for this study. Therefore, statistical techniques including regression analysis were used to determine the effect of failure rate versus ambient temperature for microcircuits, transistors and diodes.

The number of application environments included in MIL-HDBK-217D, Notice 1 has been expanded to 26 as a result of the work presented in References 4 and 21. The environment categories are presented in Table 4.5-1 with a brief description and the appropriate abbreviation. Electronic equipments can hypothetically experience nonoperating periods in any of these environments. Therefore, these same environment categories, with the exception of the space flight environment, were considered for nonoperating failure rate prediction purposes. In addition to these categories it was anticipated that reliability differences between storage, dormant and captive-carry missile applications would be considered as part of the environmental factor.

TABLE 4.5-1: ENVIRONMENT CATEGORIES

ENVIRONMENT	SYMBOL	DESCRIPTION
Ground, Benign	G _B	Nonmobile, laboratory environment readily accessible to maintenance; includes laboratory instruments and test equipment, medical electronic equipment, business and scientific computer complexes.
Ground, Fixed	G _F	Conditions less than ideal such as installation in permanent racks with adequate cooling air and possible installation in unheated buildings; includes permanent installation of air traffic control, radar and communications facilities.
Ground, Mobile	G _M	Equipment installed on wheeled or tracked vehicles; includes tactical missile ground support equipment, mobile communication equipment, and tactical fire direction systems.
Space, Flight	S _F	Earth orbital. Approaches benign ground conditions. Vehicle neither under powered flight nor in atmospheric reentry; includes satellites and shuttles.
Manpack	M _p	Portable electronic equipment being manually transported while in operation; includes portable field communications equipment and laser designations and range finders.
Naval, Sheltered	N _S	Sheltered or below deck conditions, protected from weather; includes surface ships communication, computer, and sonar equipment.
Naval, Unsheltered	N _U	Nonprotected surface shipborne equipment exposed to weather conditions; includes most mounted equipments and missile/projectile fire control equipment.
Naval, Undersea, Unsheltered	N _{UU}	Equipment immersed in salt water; includes sonar sensors and special purpose anti-submarine warfare equipment.
Naval, Submarine	N _{SB}	Equipment installed in submarines; includes navigation and launch control systems.

TABLE 4.5-1: ENVIRONMENT CATEGORIES (CONT'D)

ENVIRONMENT	SYMBOL	DESCRIPTION
Naval, Hydrofoil	NH	Equipment installed in a hydrofoil vessel.
Airborne, Inhabited, Cargo	AIC	Typical conditions in cargo compartments occupied by aircrew without environment extremes of pressure, temperature, shock and vibration and installed on long mission cargo aircraft.
Airborne, Inhabited, Trainer	AIT	Same as AIC but installed on high performance aircraft such as trainer aircraft.
Airborne, Inhabited, Bomber	AIB	Typical conditions in bomber compartments occupied by aircrew without environment extremes of pressure, temperature, shock and vibration and installed on long mission bomber aircraft.
Airborne, Inhabited, Attack	AIA	Same as AIC but installed on high performance aircraft such as used for ground support.
Airborne, Inhabited, Fighter	AIF	Same as AIC but installed on high performance aircraft such as fighters and interceptors.
Airborne, Uninhabited, Cargo	AUC	Bomb bay, equipment bay, tail or where extreme pressure, vibration and temperature cycling may be aggravated by contamination from oil, hydraulic fluid and engine exhaust. Installed on long mission transport aircraft.
Airborne, Uninhabited, Trainer	AUT	Same as AUC but installed on high performance aircraft such as used for trainer aircraft.
Airborne, Uninhabited, Bomber	AUB	Bomb bay, equipment bay, tail or where extreme pressure, vibration and temperature cycling may be aggravated by contamination from oil, hydraulic fluid and engine exhaust. Installed on long mission bomber aircraft.
Airborne, Uninhabited Attack	AUA	Same as AUC but installed on high performance aircraft such as used for ground support.
Airborne, Uninhabited Fighter	AUF	Same as AUC but installed on high performance aircraft such as fighters and interceptors.

TABLE 4.5-1: ENVIRONMENT CATEGORIES (CONT'D)

ENVIRONMENT	SYMBOL	DESCRIPTION
Airborne, Rotary Winged	A _{RW}	Equipment installed on helicopters, includes laser designators and fire control systems.
Missile, Launch	M _L	Severe conditions related to missile launch (air and ground), and space vehicle boost into orbit, vehicle re-entry and landing by parachute. Conditions may also apply to rocket propulsion powered flight.
Cannon, Launch	C _L	Extremely severe conditions related to cannon launching of 155 mm and 5 inch guided projectiles. Conditions apply from launch to target impact.
Undersea, Launch	U _{SL}	Conditions related to undersea torpedo mission and missile launch.
Missile, Free Flight	M _{FF}	Missiles in non-powered free flight.
Airbreathing Missile, Flight	M _{FA}	Conditions related to powered flight of air breathing missile; includes cruise missiles.

The optimal approach to determine nonoperating environmental factors would have been to analyze observed nonoperating field data for all 26 environment categories presented in Table 4.5-1. However, this method was not feasible due to severe data restrictions. In fact, all collected data were for ground based environments despite considerable efforts expended to collect data for other environments. There were several major reasons why nonoperating data were not available for the more stressful environments. Several of these reasons are presented in the following paragraphs.

One of the primary reasons that nonoperating data were not available for airborne environments was that aircraft mission profiles include a composite of environments. Many airborne equipments (i.e. heads-up-display, radar) are powered up prior to take-off and remain on throughout the flight, and therefore do not experience any nonoperating airborne stresses. Data of this nature was available, and subsequently summarized for the F-16 heads-up-display. However, the data is not representative of an airborne nonoperating environment. Equipments which are nonoperating while airborne, such as laser target designators, captive-carry missiles or countermeasures sets, experience a variety of nonoperating environments and corresponding stresses. The equipments are exposed to a nonoperating ground fixed environment between flights, a nonoperating ground mobile environment during ground taxi time, and a nonoperating airborne environment during flights. Unfortunately, nonoperating failures can only be detected when the equipment is powered up. Therefore, observed nonoperating failures could not be accurately designated as ground fixed, ground mobile or airborne. Additional problems, including depot data recording practices and airborne "when discovered" code definitions, also prevented summarization of nonoperating data for composite environment applications.

Another reason that data was unavailable for stressful nonoperating environments was the common misconception in the electronics industry that all failures are attributable to operating stresses. With the exception of missile storage applications, no attempt generally has been made to identify nonoperating failures. Therefore, no centralized database has been established which includes nonoperating reliability for airborne environments. In fact, the Missile Materiel Storage Reliability Program managed by U.S. Army MICOM, Redstone Arsenal, AL represents the only centralized reliability database which includes nonoperating data.

Another major reason that nonoperating data for airborne and other non-ground environments were not available was the general lack of accurate piece part data for any operating or nonoperating application. The additional requirement that the data include only primary failures, correspond to a nonoperating state, and correspond to a non-ground environment further compounds an already difficult problem. Data from large automated data bases like the U.S. Air Force D056, U.S. Navy 3M and U.S. Army Sample Data Collection Program could not meet the requirements of this study. Specifically, the D056 and 3M data bases are incomplete at the piece part level (i.e. not all depot level repair actions are reported into the system). In addition, the task of separating primary (or inherent) part failures from secondary (or induced) failures is very difficult. These observations are documented for the U.S. Air Force data collection system in Reference 22. The Sample Data Collection program is operated by the Cobro Corporation and managed by U.S. Army TSARCOM, St. Louis, MO. This program offered several distinct advantages in regard to separating operating from nonoperating failures, and primary from secondary failures. However, the Sample Data Collection program was also inadequate for tracking failures to the piece part level.

The lack of traceability between on-equipment maintenance actions and depot part replacements was another reason that collection of nonoperating data for airborne environments was unsuccessful. On-equipment maintenance actions can often be designated as operating or nonoperating failures by use of a "when discovered" code. It can be assumed that failures observed

when the equipment was energized are due to the effects of nonoperating period or the result of the power on-off cycle. However, this information is of no use unless depot level part replacements can be accurately traced back to the on-equipment action. Unfortunately, traceability is usually poor due to time and location differences between on-equipment and depot maintenance, and incomplete data recording practices.

An alternate nonoperating environmental factor development method was determined to compensate for the lack of available data. The alternate method was based on the hypothesis that a series of nonoperating environmental factors could be developed from the documented operating environmental factors. Two recent studies (References 4 and 21) evaluated and proposed operating environmental factors for every environment category presented in Table 4.5-1. It was assumed that these numerical values properly characterize the effects of environmental stress for the operating applications. It was also assumed that nonoperating environmental factors could be generated from the operating environmental factors by comparing differences in failure mechanism accelerating factors and average application temperatures.

Specifically, the nonoperating environmental factor development process took place in four phases. The first phase consisted of an analysis of the operating environmental factor in the context of the MIL-HDBK-217D failure rate prediction model. Several factors, including the presence of a separate temperature factor, influence the definition of the environmental factor. The second phase of the nonoperating environmental factor development process was to compare typical temperature differences between the operating and nonoperating state. If both operating and proposed nonoperating models do not include separate temperature factors, then an adjustment was possibly required to the operating environmental factors. The third phase of this method was to compare the differences between operating and nonoperating failure mechanism accelerating factors (i.e. environmental or operational stresses which accelerate the occurrence of failure mechanisms). Decisions were made regarding whether the magnitude of nonoperating environmental factors would be greater than,

less than, or approximately the same as the MIL-HDBK-217D operating environmental factors. The final phase of the environmental factor development process was to determine numerically the magnitude of environmental factor differences, if any. Theoretical methods and failure simulations based on assumed distributions were utilized to aid in the process. The following paragraphs present a general discussion of the environmental factor determination method. Results for specific part types are included in the respective model development sections of this report.

The relationship of the operating environmental factor to the MIL-HDBK-217D failure rate prediction model was identified in the first phase of the nonoperating environmental factor development process. It was found that the MIL-HDBK-217D failure rate prediction models incorporated the environmental factor four separate ways, which are,

- 1) multiplicative environmental factor without a separate temperature dependent factor.
- 2) multiplicative environmental factor with a separate temperature dependent factor.
- 3) environmental factor part of the non-linear microcircuit model.
- 4) no environmental factor.

Table 4.5-2 presents the distribution of part types in MIL-HDBK-217D into these categories. The distinction between multiplicative environmental factors without a separate temperature dependent factor (category 1) and factors with a separate temperature dependent factor (category 2) was very important. If a model does not include a separate temperature dependent factor, then the environmental factor accounts for all environmental stresses including temperature. If the model does include a separate temperature dependent factor, then the environmental factor accounts for all environmental stresses except changes in temperature. The temperature factor (or base failure rate as a function of temperature) predicts the effect of changes in temperature due to both ambient temperature and internal heat generation. In effect, the

environmental factor alone, for category 2 models, predicts the failure rate difference due to environmental stress given that the temperature is constant.

TABLE 4.5-2: MIL-HDBK-217D ENVIRONMENTAL FACTOR CLASSIFICATION

Category 1 (1)	Category 2 (2)	Category 3 (3)	Category 4 (4)
Tubes	Transistors	Microcircuits	Motors
Lasers	Diodes	Hybrids	Misc. Parts
Thermistors	Opto-electronics	Bubble Memories	
Switches	Resistors		
P.W. Assemblies	Capacitors		
Connection	Transformers		
Crystals (5)	Coils		
Fuses (5)	Synchros		
Inc. Lamps (5)	Resolvers		
Meters (5)	Relays		
Circuit Breakers (5)	Connectors		

- Notes: 1) Type 1 environmental factors predict the effects of all environmental stresses.
- 2) Type 2 environmental factors predict the effects of all environmental stresses except temperature
- 3) Type 3 environmental factors are part of a non-linear microcircuit model.
- 4) Type 4 part type models have no environmental factors.
- 5) An updated model for these part types is presented in Reference 43.

The second phase of the nonoperating environmental factor development process was to determine numerical adjustment factors to account for differences in operating and nonoperating temperatures. If both operating and proposed nonoperating failure rate prediction models include separate temperature and environmental factors, then no temperature adjustment was required. Failure rate differences due to internal heat generation are predicted by the respective temperature factors of the operating and proposed nonoperating models. This was the case for transistors, diodes and microcircuits.

If neither the operating or proposed nonoperating model included a temperature factor, then (as a minimum) the operating factors would have to be adjusted to account for the relatively lower temperatures found in the nonoperating condition. The difference in operating and nonoperating temperature is greater for the more stressful environments. There are several reasons for this observation including better ventilation and environmental control available for ground based environments. Determination of the anticipated temperature difference between operating and nonoperating environments was difficult. The range of possible missions, applications and locations for electronic equipments is so great that determination of an average temperature difference based on a sample of mission profiles was not deemed feasible. In addition, the available literature concerning ambient temperatures for different application environments was inconclusive at best. However, many technical documents were reviewed including the documented temperature relationships in MIL-HDBK-217D. Table 5.2-17 "Ambient Temperature for all Parts" and Table 5.1.2.5-4 Note 2 "Microcircuit Case Temperatures" from MIL-HDBK-217D, Notice 1 were utilized to estimate the relative difference between operating and nonoperating applications. Those tables indicated that the temperature difference between operating and nonoperating is approximately 20°C more for airborne uninhabited environments than for the ground benign environment. This value was used to compute environmental factor temperature adjustment factors for tubes, lasers, thermistors, switches, printed wiring assemblies, connections, crystals, fuses, incandescent lamps, meters and circuit breakers.

A third case was identified where the operating failure rate prediction model included a separate temperature factor and the proposed nonoperating failure rate prediction model did not. No nonoperating temperature factors were determined in this case because of data deficiencies. For these part types, the increase in temperature due to the applied power is accounted for by the operating temperature dependent factor and not the environmental factor. Therefore no large temperature adjustment was required as in the previous case. A study of environmental profiles (Reference 4 and 24) revealed that temperature cycling and

temperature extremes varied radically for more stressful nonoperating environments such as airborne uninhabited fighter. However, the typical change in average temperature was much less for the nonoperating environment than the operating environment. It was determined that appropriate temperature adjustment factors would be small in magnitude. The relatively smaller temperature adjustment for these part types would be less than the inherent variability involved with failure rate estimation, and thus were not warranted. Therefore, no temperature adjustment was made for opto-electronic semiconductors, resistors, capacitors, transformers, coils, synchros, resolvers, relays and connectors.

The third phase of the environmental factor analysis task was to compare operating and nonoperating failure mechanism accelerating factors. Decisions were made as to whether the magnitude of proposed nonoperating environmental factors would be greater than, less than, or approximately the same as operating environmental factors. A literature search was performed to identify documented sources of operating and nonoperating failure mechanism distributions. In addition, the microcircuit failure mode/mechanism data base at the RAC was available for analysis. After completion of the literature search and preliminary analyses, it was concluded that there was severe absence of substantial, documented failure mechanism distribution information. Much of the available information was incomplete and/or conflicting. This deficiency was particularly acute for nonoperating applications. However, the available information provided a good boundary for the failure mechanism distributions and average failure mechanism and failure mechanism accelerating factor distributions were estimated for each major part class after evaluating all available information. These failure mechanism distributions are presented in the appropriate subsections of Section 5.0 of this technical report.

Each failure mechanism for the specific part types was categorized as either (1) primarily accelerated by environmental stresses, (2) primarily accelerated by operational stresses, (e.g., applied voltage or current, mechanical actuations, etc.) or (3) accelerated by simultaneous exposure

to environmental and operational stresses. Conceptually, the implications of these three types of failure mechanisms are presented in Figures 4.5-1, 4.5-2 and 4.5-3. Each figure presents a hypothetical distribution of failure mechanism accelerating factors for ground and airborne environments, and for operating and nonoperating applications. The failure rate due only to operational stress (e.g. electrical current) is shown to be constant with regard to environment. The failure rates due to environmental stress and combined environmental/operational stress are shown to increase with the amount of environmental stress. Additionally, all nonoperating failure rates are shown to be accelerated only by environmental stress. The relative increase in failures due to environmental stress is shown to be the same for operating and nonoperating. These conceptual examples assume that temperature differences have been numerically compensated for.

Figure 4.5-1 represents the failure behavior of a specific part type which has operating failure mechanisms primarily accelerated by environmental stresses. The difference in operating and nonoperating failure rate is relatively small, and the ratio of airborne to ground failure rate is slightly greater for nonoperating than operating applications. Proposed nonoperating environmental factors would be slightly greater than operating factors for part types with failure behavior similar to that depicted in Figure 4.5-1. The contribution of the constant operational stress term causes this phenomenon. There is no operational stress contribution for the nonoperating case and therefore the increase in environmental stress failure rate is a larger percentage of the total failure rate. Multiplicative environmental factors predict the relative increase in total failure rate. Thus, the nonoperating environmental factors would be slightly larger. It must be emphasized that this does not mean that the nonoperating failure rate would be slightly larger, but that the rate of change of failure rate is greater in the nonoperating mode.

Figure 4.5-2 represents the failure behavior of a specific part type which has operating failure mechanisms primarily accelerated by

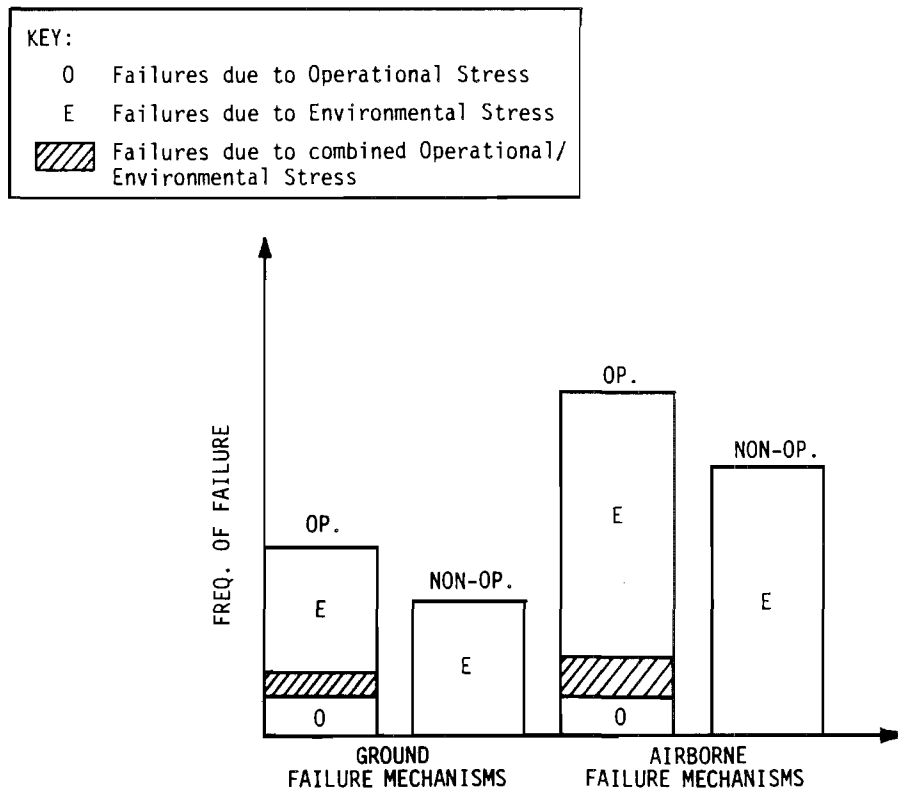


FIGURE 4.5-1: FAILURE MECHANISM DISTRIBUTION, ACCELERATED BY ENVIRONMENTAL STRESS (CASE I)

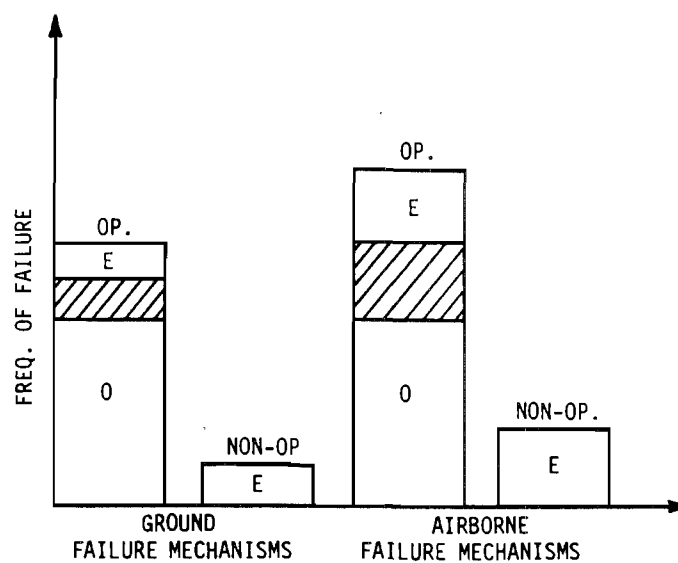


FIGURE 4.5-2: FAILURE MECHANISM DISTRIBUTION, ACCELERATED BY OPERATIONAL STRESS (CASE II)

"operational" stresses. The difference in operating and nonoperating failure rate is relatively large, and the ratio of airborne to ground failure rate is significantly larger for nonoperating than operating applications. As the environment changes from ground to airborne for this class, the number of failures would be expected to increase for both operating and nonoperating applications. This expected increase would be relatively less for the nonoperating condition because of the smaller probability of failures due to combined environmental/operational stress. However, the expected failure rate increase for the nonoperating environment would be a much greater percentage of the overall failure rate. This is because the nonoperating failure rate is relatively low in the ground based environments. Therefore, the magnitude of proposed nonoperating environmental factors would need to be greater than the multiplicative operating MIL-HDBK-217D environmental factors. This can be observed in Figure 4.5-2.

Figure 4.5-3 represents the failure behavior of a specific part type in which operating failure mechanisms are primarily accelerated by the simultaneous exposure to environmental and operational stresses. This case represents perhaps the most common and also the most complex. The example depicted in Figure 4.5-3 shows the ratio of airborne to ground failure rate to be greater for operating than nonoperating applications. The example was constructed with the rate of increase for the combined stress failure mechanisms greater than the rate of increase for the environmental stress failure mechanisms. This seemed logical because the expected number of failures for mechanisms accelerated by the combined stresses. However, necessarily the case, and additionally, the relative rates of increase had important implications for development. To further investigate, were performed assuming a rate of increase. The failure mechanisms was seen. Results of the failure mechanisms accelerated

Switch
Pages 4-37
and 4-38
the three tables so
4.5-1, 4.5-2 and 4.5-3

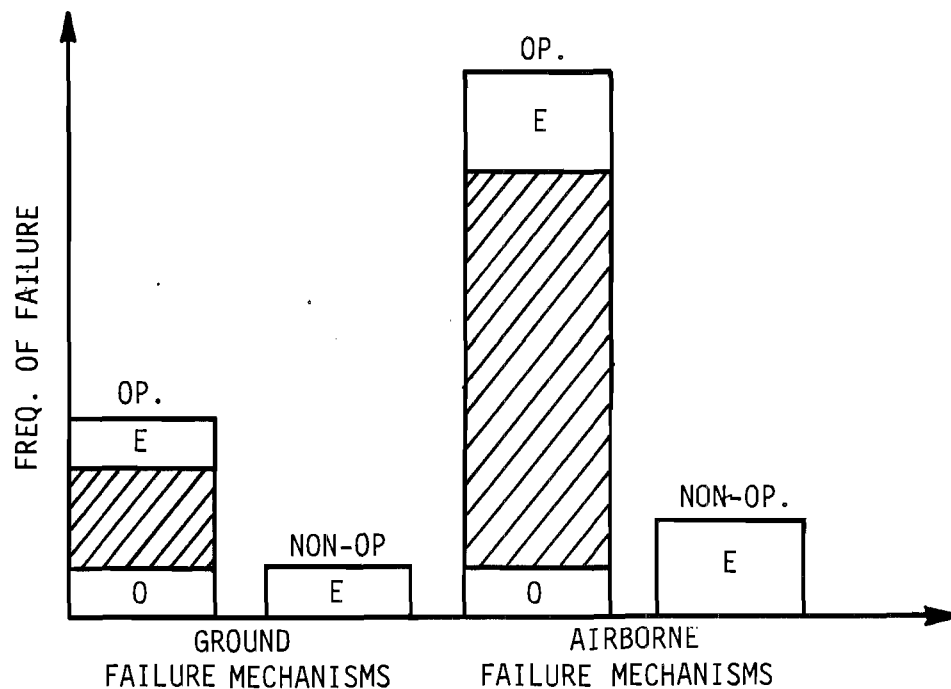
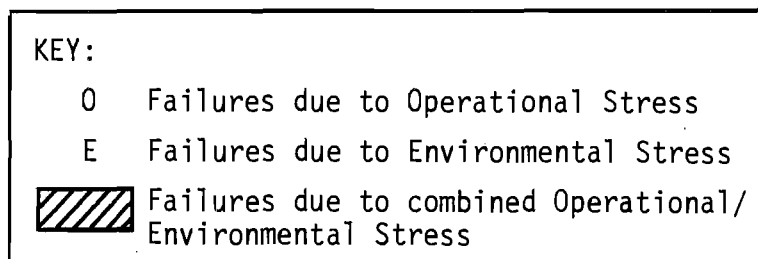


FIGURE 4.5-3: FAILURE MECHANISM DISTRIBUTION,
ACCELERATED BY COMBINED OPERATIONAL/ENVIRONMENTAL STRESS
(CASE III)

magnitude of multiplicative nonoperating environmental factors were slightly less than the operating factors, and (2) as the percentage of failure mechanisms due to only operational, or only environmental stresses increase, the magnitude of the nonoperating environmental factors approach and possibly surpass the operational environmental factors. It must again be emphasized that this does not infer that the nonoperating failure rates are higher. The operating and nonoperating environmental factors are in separate ranges. Therefore the nonoperating environmental factors can be higher, but the resultant nonoperating failure rates lower.

The failure mechanism distributions estimated previously for specific part types were further investigated to determine which of the examples depicted in Figures 4.5-1, 4.5-2, and 4.5-3 more closely approximated the respective failure mechanism distributions. It was found for most part types that the operating failure mechanisms were accelerated primarily by the combination of operational/environmental stress, or by environmental stress alone. In either case, the expected difference between operating and nonoperating environmental factors was anticipated to be small. Therefore, for these cases, it was proposed that the operating environmental factors could be applied for nonoperating failure rate prediction purposes. The inexact nature of the nonoperating environmental factor determination process and the imprecision involved with estimating failure mechanism distributions precluded the use of adjustment factors which were much smaller than the inherent noise included in part level reliability data or the variability involved in failure rate prediction.

The failure mechanisms for several part types were primarily accelerated by operational stress, and therefore the operating environmental factors could not be applied to nonoperating failure rate prediction. For these part types, the range of nonoperating environmental factors were anticipated to be significantly larger than the range of temperature adjusted (if required) operating environmental factors. Incandescent lamps, lasers and microwave tubes were included in this category.

A general nonoperating environment factor expression was derived for these parts by solving simultaneous equations to determine nonoperating environmental factor as a function of operating environmental factor, R_1 , R_2 and R_3 . R_1 was defined as the fraction of operating failures due to only environmental stress. R_2 was defined as the fraction of operating failures due to simultaneous exposure to environmental and operational stress. R_3 was defined as the fraction of operating failures due to only operational related stress. The equations which were solved simultaneously are presented in Table 4.5-3. There were six unknowns (i.e., π_{NE} , λ_{ei} , λ_{ef} , λ_{eoi} , λ_{eof} , λ_o) and six independent equations. Equation 5 in Table 4.5-3 is not independent. π_{OE} (the MIL-HDBK-217 environmental factor) is a known quantity. This method presupposes that estimates of R_1 , R_2 and R_3 could be found from the available literature. The nonoperating environmental factor expression was determined to be the following expression.

$$\pi_{NE} = \frac{\pi_{OE}}{R_1 + R_2} - \frac{R_3}{R_1 + R_2}$$

where

π_{NE} = nonoperating environmental factor

π_{OE} = operating environmental factor

R_1 = fraction of operating failures due to only environmental stress
($0 < R_1 < 1$)

R_2 = fraction of operating failures due to simultaneous exposure to environmental and operational stress ($0 < R_2 < 1$)

R_3 = fraction of operating failures due to only operational related stress ($0 < R_3 < 1$)

It was noted that the expression only applies when $(R_1 + R_2)$ is greater than 0.20. Also, it should be noted that $R_1 + R_2 + R_3 = 1$. Estimates of R_1 , R_2 and R_3 values were determined from the available literature. R_1 , R_2 and R_3 values used for lamps, lasers, and microwave tubes are presented in the respective model development section.

TABLE 4.5-3: ENVIRONMENTAL FACTOR ANALYSIS (CASE
II) - SIMULTANEOUS EQUATIONS

NO.	EQUATION	BASIS
1	$\pi_{NE} = \lambda_{ei}/\lambda_{ef}$	Definition
2	$\pi_{OE} = \frac{\lambda_{ei} + \lambda_{eoi} + \lambda_o}{\lambda_{ef} + \lambda_{eof} + \lambda_o}$	Definition
3	$R_1 = \frac{\lambda_{ef}}{\lambda_{ef} + \lambda_{eof} + \lambda_o}$	Definition
4	$R_2 = \frac{\lambda_{eof}}{\lambda_{ef} + \lambda_{eof} + \lambda_o}$	Definition
5	$R_3 = \frac{\lambda_o}{\lambda_{ef} + \lambda_{eof} + \lambda_o}$	Definition
6	$R_1 + R_2 + R_3 = 1$	Equations 3, 4 and 5
7	$\frac{\lambda_{ei}}{\lambda_{eoi}} = \frac{\lambda_{ef}}{\lambda_{eof}}$	Assumption

NOTES:	π_{NE}	=	nonoperating environmental factor
	π_{OE}	=	operating environmental factor
	λ_{ei}	=	failure rate due to environmental stress in the i^{th} environment
	λ_{ef}	=	failure rate due to environmental stress in a fixed environment
	λ_{eoi}	=	failure rate due to combined operational/environmental stress in the i^{th} environment
	λ_{eof}	=	failure rate due to combined operational/environmental stress in a fixed environment
	λ_o	=	failure rate due to only operational stress (independent of environment)

The fourth phase of the nonoperating environmental factor development process was to consolidate the findings from the first three phases and propose numerical adjustment factors. **Eleven generic part categories required environmental factor adjustments.** For the remaining part types, it was determined that the effects of environmental stress were sufficiently similar to propose the same numerical values for nonoperating environmental factors as the documented MIL-HDBK-217D operating environmental factors. For thermistors, switches, printed wiring assemblies, connections, crystals, fuses, meters and circuit breakers, the nonoperating environmental factor was determined to be given by the following equation.

$$\pi_{NE} = A_T \pi_{OE}$$

where

π_{NE} = nonoperating environmental factor

A_T = temperature adjustment factor

= f(environment, part type)

π_{OE} = MIL-HDBK-217D operating environmental factor

For tubes, lasers and incandescent lamps, the nonoperating environmental factor is given by the following equation.

$$\pi_{NE} = \frac{A_T \pi_{OE}}{R_1 + R_2} - \frac{R_3}{R_1 + R_2}$$

where all variables have been previously defined.

An additional modification was required for microcircuit nonoperating environmental factor development for two reasons. First, the operating environmental factor is part of a complex, nonlinear model form. Conversely, the proposed nonoperating failure rate prediction model is a multiplicative model with one nonlinear term. The second reason was that the nonoperating failure mechanism distribution for hermetic and nonhermetic devices varies considerably. Specifically, nonhermetic

devices were determined to be significantly more sensitive to environmental stresses, particularly humidity and contaminated environments. The microcircuit environmental factor derivation was determined to be.

$$\pi_{NE} = A_1 \pi_{OE} + B_1$$

where

A_1 and B_1 = normalization constants for hermetic devices

A_2 and B_2 = normalization constants for nonhermetic devices

Numerical values for A_1 and B_1 were estimated to be 0.66 and 0.75 respectively. These values were based on the typical model parameters presented in MIL-HDBK-217D, Notice 1, Table 5.2-18, "Model Parameters for Random Logic and Memory Microelectronic Semiconductor Devices". Additionally, the equation was normalized so that the nonoperating environmental factor for a ground benign environment was equal to one. Estimates for A_2 and B_2 for nonhermetic devices were determined to be 1.4 and 0.46. The higher environmental factor values for nonhermetic devices were hypothesized using the results of the Panama nonhermetic microcircuit life test data (described in Section 2.3) as a foundation.

Determination of nonoperating environmental factors allows for analysis of the reliability for any proposed mission profile. Many specific mission profiles consist of a composite of environments. For example, missile mission profiles may consist of storage, dormancy, transportation and captive carry environments. Definition of the appropriate mission profile is required including specific time periods in individual environments and a detailed description of the test plan. This information can be used with the methods described in Section 6.0, "Equipment Nonoperating Reliability Prediction Procedure" to assess the reliability of any conceivable mission profile. For example, a comparison of storage and dormant applications can be performed by defining the respective environmental profiles and test plans, and then applying the

methods developed in this study. This approach is preferable to previous attempts to compare storage failure rates to dormant failure rates directly. For example, missile electronics storage applications can range from very benign environment controlled facilities to more stressful uncontrolled storage. Dormant applications can also vary but generally are in a ground fixed environment. Therefore, a comparison of storage versus dormant missile applications is virtually meaningless without proper environmental characterization.

In conclusion, it would have been preferable to analyze observed nonoperating failure rate data in all 26 environment categories. However, inherent difficulties of collecting nonoperating reliability data prevented the collection of data for any non-ground environments. A viable approach was developed to compare temperatures and failure mechanisms, and to generate nonoperating environmental factors from the documented MIL-HDBK-217D operating environmental factors. This method was used to derive nonoperating environmental factors for eleven part types. For the remaining part types, it was determined that no adjustment was required and that the operating environmental factors also approximate the effects of environmental stress on nonoperating failure rate.

4.6 Screening Effectiveness

During the nonoperating failure rate model development process, it was observed that the magnitude of the nonoperating quality factors were generally small in comparison to the corresponding MIL-HDBK-217D operating quality factors. Initially, this observation seemed unusual because the devices are screened before entering into either an operating or nonoperating state, and it was unclear why screening would effect the nonoperating failure rate any differently than the operating failure rate. The observation would probably have been attributed to variability in the data if not for the consistency of the results. The same trend was noticed for microcircuits, transistors, diodes, resistors, capacitors and inductors. In each case, the empirically determined nonoperating quality factors were small in comparison with the corresponding operating values.

To evaluate this apparent trend, a separate study was initiated concerning the effectiveness of screening on nonoperating failure rates. The argument presented in the following paragraphs is offered not as a rationale to propose assumed nonoperating quality factors but as a possible explanation for the observed trend.

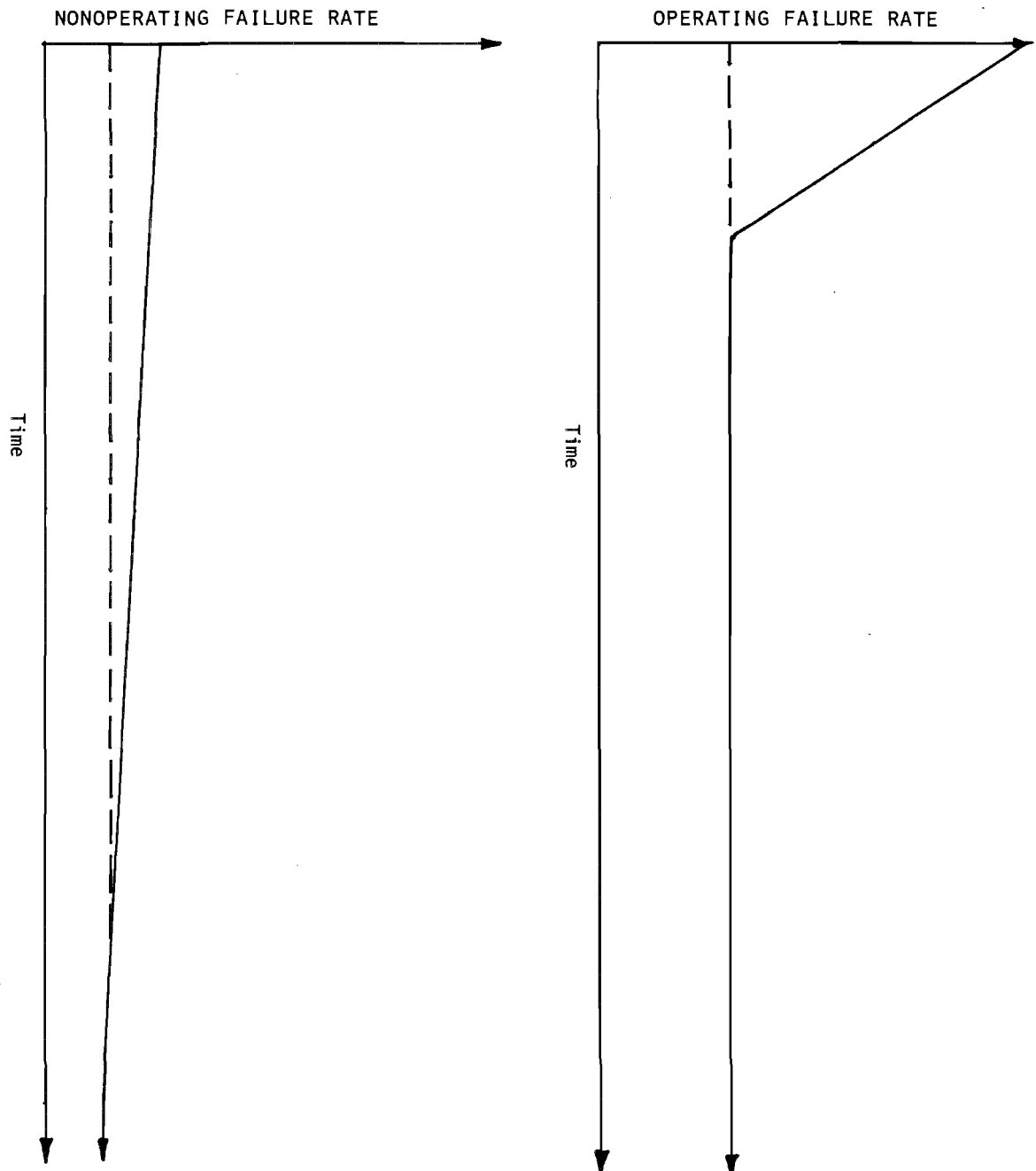
The intention of device screening is to lower the field failure rate of a component lot by eliminating inherently weak devices. The fact that the failure rate decreases as screening level increases is evidence that the instantaneous failure rate is not constant with time, but is decreasing. Since the number of weak devices is independent of operational mode, the rate at which the hazard rate decreases following the screen is the important parameter for quality factor comparisons.

Whether a sample of parts is intended for long term storage or immediate operation, the percentage of inherently weak devices surviving an identical screen is relatively constant. However, the rate at which the surviving weak components fail is what indicates the relative effect on operating or nonoperating failure rate. Weak devices will clearly fail more quickly in an operating mode. This is why devices are "burned-in" with the power applied.

The operating quality factors have generally been determined from empirical data and represent the ratio of the failure rate for unscreened, and various levels of screened parts. The MIL-HDBK-217D failure rates are constant with time and therefore represent some average failure rate over an unknown data collection interval. Since the weak devices surviving the screen fail more quickly during operation, the computed operating quality factors appear to be more sensitive to screening. However, given infinite time, the same number of inherently weak devices for a similar screen would fail in either operating or nonoperating applications.

An example is provided to illustrate that the observed nonoperating failure rate screening effectiveness was probably also the expected result. Figure 4.6-1 presents two graphs of failure rate versus time for

FIGURE 4.6-1: CONCEPTUAL SCREENING EFFECTIVENESS COMPARISON



similar samples of parts screened to similar specifications. In the upper graph, the devices are operating. The operating failure rate is shown to be decreasing and asymptotic to some constant failure rate. In the lower graph, the devices are nonoperating and the failure rate is asymptotic to some lower constant failure rate. In each case, the number of weak devices surviving the screening process is constant and represented by the area between the failure rate curve and the dotted line. The time at which virtually all the devices have failed is much shorter for the operating case. Applying the concepts of geometry, it can be concluded that the differential between the instantaneous failure rate and the constant failure rate must be smaller in the nonoperating state if the number of weak devices (i.e. area between the solid and dotted lines) is the same.

Additionally, both operating and proposed nonoperating quality factors correspond to some unknown data collection interval near the beginning of the devices life. As the data collection interval becomes shorter and closer to time zero, the expected difference between operating and nonoperating quality factors would be maximized. As the data collection interval approaches infinity, the ratio of operating to nonoperating quality factors would theoretically become unity. Therefore, the numerical quality factor values, both operating and nonoperating, are an indication of screening effectiveness, data collection interval length and operational mode.

To further investigate the issue, a literature search was performed to identify any sources which address the relative effects of screening on operating and nonoperating failure rate. One document was located (Reference 25) which concluded on the basis of a theoretical analysis that dormant and operating failure rates for electronic parts tend to equality as part quality improves. This conclusion was equivalent to stating that as part quality worsens, the difference between dormant and operating failure rates would increase. Thus, MIL-HDBK-217D style quality factors would have to be numerically larger in the operating state to reflect the increasing difference in failure rate.

This discussion represents a brief comparison of operating and nonoperating instantaneous failure rates and screening effectiveness. The concepts presented here were not used to develop or assume any of the nonoperating quality factors presented in this report. The nonoperating quality factors were all determined empirically where data allowed and extrapolated for quality levels without data. This discussion was presented simply as a possible explanation for an observed trend which consistently occurred during the electronic component nonoperating failure rate modeling efforts performed in this study.

5.0 NONOPERATING FAILURE RATE MODEL DEVELOPMENT

Nonoperating failure rate prediction models were developed for each part type in MIL-HDBK-217D. The integrity of the proposed models is related to the diversity and quantity of the available nonoperating failure rate data. Table 5.0-1 presents an overview of the amount of data available for analysis and the basis for model development. Each part class is divided into a category of either "sufficient data", "some data" or "assumptions" depending on the basis for model development. Categorization decisions were subjective. Consideration was given to the number of data records, number of failures, part hours and number of potential variables.

TABLE 5.0-1: PART CLASS CATEGORIZATION

SUFFICIENT DATA	SOME DATA	ASSUMPTIONS
Digital ICs (1)	Memory ICs	Bubble Memories
Linear/Interface ICs	Hybrid ICs	Opto-Electronics
Transistors	Tubes	Lasers
Diodes	Rotating Mechanisms	Connections
Resistors	Relays	
Capacitors	Switches	
Inductors	Connectors	
	P.W. Assemblies	
	Miscellaneous Parts	

NOTES (1): Digital ICs refers to digital SSI/MSI, random logic LSI and microprocessor devices.

The general model development approach described in Section 4.1 was followed to the extent possible. For part classes without empirical data, the proposed models were based on theoretical considerations and hypothetical reliability relationships. Required assumptions are clearly stated in each model development section. Table 5.0-2 presents an overview of the model development process.

TABLE 5.0-2: MODEL DEVELOPMENT OVERVIEW

PART CLASS	DATA SOURCES	EMPIRICAL FACTORS	ASSUMED/THEORETICAL FACTORS
Monolithic ICs	MICOM Martin Marietta F-16 HUD/RIW Sandia PRC RAC ERADCOM	complexity temperature logic screening enclosure type power cycling	environment
Hybrid ICs	MICOM F-16 HUD/RIW	# ICs # transistors # diodes	environment quality
Bubble Memories	none	none	# gates # loops temperature environment logic
Transistors	MICOM Martin Marietta F-16 HUD/RIW AFCIQ PRC ERADCOM	device style temperature quality power cycling	environment
Diodes	MICOM Martin Marietta F-16 HUD/RIW PRC	device style quality power cycling	environment temperature
Opto-electronics	none	none	device style quality environment
Resistors	MICOM Martin Marietta F-16 HUD/RIW PRC	device style quality power cycling	environment

TABLE 5.0-2: MODEL DEVELOPMENT OVERVIEW (CONT'D)

PART CLASS	DATA SOURCES	EMPIRICAL FACTORS	ASSUMED/THEORETICAL FACTORS
Capacitors	MICOM Martin Marietta F-16 HUD/RIW	device style quality power cycling	environment
Inductive Devices	MICOM Martin Marietta F-16 HUD/RIW AFCIQ Southern Tech.	device style quality power cycling	environment
Lasers	none	none	environment device style
Tubes	MICOM	device style	environment
Rotating Mechanisms	MICOM Martin Marietta	device style	none
Relays	MICOM Martin Marietta Hughes AFCIQ	quality	enclosure type contact rating environment
Switches	MICOM Martin Marietta	none	enclosure type contact rating environment quality
Connectors	MICOM Martin Marietta	none	device style environment
P.W. Assemblies	MICOM AFCIQ	technology # circuit planes	# PTHs environment
Connections	none	none	type
Misc. Parts	MICOM Martin Marietta	device type	none

5.1 Microcircuits

The generic category of microcircuits includes an overwhelming number of devices with diverse characteristics. Failure rate model development could not be attempted at the "microcircuit level" without making gross generalities and oversimplifications. Therefore the nonoperating failure rate model development process (and the collected data) needed to be divided into a workable number of categories which would provide sufficient data per category, while properly categorizing the microcircuit family. It was decided to divide the microcircuit model development process into five distinct sections. The five sections were (1) digital SSI/MSI, random logic, and microprocessors, (2) linear/interface, (3) memory, (4) hybrid, and (5) bubble memories. Data was segregated into these categories, and the reliability attributes were studied individually. Ideally it would have been advantageous to divide the model development process to even finer subcategories. However, practical restraints, most notably data limitations, prevented any finer division beyond these categories.

5.1.1 Monolithic Microcircuit Nonoperating Failure Rate Prediction Models

This section presents the proposed nonoperating failure rate prediction models for monolithic microcircuits. Separate models were developed for (1) digital SSI/MSI, random logic and microprocessor devices, (2) linear/interface devices, and (3) memory devices. The models are presented in Appendix A in a form compatible with MIL-HDBK-217D.

Digital SSI/MSI, Random Logic Devices and Microprocessors

The proposed model for digital SSI/MSI, random logic and microprocessors is represented by the following equation.

$$\lambda_p = \lambda_{nb} \pi_{NT} \pi_{NQ} \pi_{NE} \pi_{cyc}$$

where

λ_p = digital SSI/MSI, random logic LSI and microprocessor
nonoperating failure rate

λ_{nb} = nonoperating base failure rate (failures/ 10^6 hours)
= $.00029(N_g)^{.477}$, $N_g \leq 3100$ gates
= $.014$, $N_g > 3100$ gates

where

N_g = number of gates

π_{NT} = nonoperating temperature factor
= $K_3 + K_4 \exp(-A_n(\frac{1}{T} - \frac{1}{298}))$
 $-.58 \quad .42 \quad 7059$

where

T = nonoperating temperature (°K)

K_3, K_4, A_n = temperature coefficients (See Table 5.1.1-1)

π_{NQ} = nonoperating quality factor (see Table 5.1.1-2)

π_{NE} = nonoperating environmental factor (see Table 5.1.1-3)

π_{cyc} = equipment power on-off cycling factor

= $1 + .02(N_c)$

where

N_c = number of equipment power on-off cycles per 10^3 nonoperating
hours

TABLE 5.1.1-1: DIGITAL MICROCIRCUIT NONOPERATING TEMPERATURE
FACTOR CONSTANTS

Technology	K ₃	K ₄	A _n
TTL, HTTL, DTL, ECL	.91	.09	4813
LTTL, STTL	.90	.10	5261
LSTTL	.89	.11	5711
IIL	.86	.14	6607
MNOS	.61	.39	6607
PMOS	.68	.32	5711
NMOS, CCD	.65	.35	6159
CMOS, CMOS/SOS	.58	.42	7059

TABLE 5.1.1-2: MICROCIRCUIT NONOPERATING QUALITY FACTORS

Quality Level	πNQ
S	0.53
B	1.0
B-1	1.4
B-2	2.0
C	2.3
C-1	2.4
D	2.5
D-1	8.7

TABLE 5.1.1-3: MICROCIRCUIT NONOPERATING ENVIRONMENTAL FACTORS (π NE)

Environment	Hermetic Devices	Nonhermetic Devices
G _B	1	1
G _F	2.4	4.0
G _M	3.5	6.5
M _P	3.2	5.9
N _{SB}	3.4	6.2
N _S	3.4	6.2
N _U	4.5	8.6
N _H	4.6	8.9
N _{UU}	4.9	9.5
A _{RW}	6.3	13
A _{IC}	2.4	4.0
A _{IT}	2.7	4.7
A _{IB}	4.0	7.6
A _{IA}	3.4	6.2
A _{IF}	4.7	9.0
A _{UC}	2.7	2.7
A _{UT}	3.4	3.4
A _{UB}	5.7	11
A _{UA}	4.7	9.0
A _{UF}	6.7	13
S _F	(1)	(1)
M _{FF}	3.3	6.0
M _{FA}	4.3	8.2
U _{SL}	8.0	16
M _L	9.3	19
C _L	150	310

Notes: (1) Space flight environment was not addressed in this study.

Linear and Interface Devices

The proposed model for linear and interface devices is the following equation.

$$\lambda_p = \lambda_{nb} \pi_{NT} \pi_{NQ} \pi_{NE} \pi_{cyc}$$

where

$$\begin{aligned} \lambda_p &= \text{linear/interface device nonoperating failure rate} \\ \lambda_{nb} &= \text{nonoperating base failure rate (failures/10}^6 \text{ nonoperating} \\ &\quad \text{hours)} \\ &= 0.00024(N_t)^{.887} \end{aligned}$$

where

$$\begin{aligned} N_t &= \text{number of transistors} \\ \pi_{NT} &= \text{nonoperating temperature factor} \\ &= \exp(-4748(\frac{1}{T} - \frac{1}{298})) \\ \pi_{NQ} &= \text{nonoperating quality factor (see Table 5.1.1-2)} \\ \pi_{NE} &= \text{nonoperating environmental factor (See Table 5.1.1-3)} \\ \pi_{cyc} &= \text{equipment power on-off cycling factor} \\ &= 1 + .031(N_c) \end{aligned}$$

where

$$N_c = \text{number of equipment power on-off cycles per } 10^3 \text{ nonoperating hours}$$

Memory Devices

The proposed nonoperating failure rate prediction model is for RAM, ROM, PROM and CCD memory devices, and is given by the following equation.

$$\lambda_p = \lambda_{nb} \pi_{NT} \pi_{NQ} \pi_{NE} \pi_{cyc}$$

where

$$\begin{aligned}\lambda_p &= \text{memory device nonoperating failure rate} \\ \lambda_{nb} &= \text{nonoperating base failure rate (failures/10}^6 \text{ nonoperating} \\ &\quad \text{hours)} \\ &= 0.0034, \text{ bipolar memory devices} \\ &= 0.0017, \text{ MOS memory devices} \\ \pi_{NT} &= \text{nonoperating temperature factor} \\ &= K_3 + K_4 \exp(-A_n(\frac{1}{T} - \frac{1}{298}))\end{aligned}$$

where

$$\begin{aligned}K_3, K_4, A_n &= \text{temperature coefficients (See Table 5.1.1-1)} \\ \pi_{NQ} &= \text{nonoperating quality factor (see Table 5.1.1-2)} \\ \pi_{NE} &= \text{nonoperating environmental factor (see Table 5.1.1-3)} \\ \pi_{cyc} &= \text{equipment power on-off cycling factor} \\ &= 1 + .02(N_c)\end{aligned}$$

where

$$N_c = \text{number of equipment power on-off cycles per } 10^3 \text{ nonoperating hours}$$

The proposed models for monolithic microcircuit are also presented in Appendix A. The following sections describe the model development processes.

5.1.2 Digital Microcircuit Model Development

The failure rate modeling approach described in Section 4.1 was successfully implemented to develop a model for digital SSI/MSI, random logic devices and microprocessors. Model development for memory devices is presented in Section 5.1.4. A theoretical nonoperating failure rate model was hypothesized based on known failure mechanisms and physics of failure information (References 3, 26 and 27). The theoretical model was

evaluated and quantified with the available data. Failure rate prediction model parameters for complexity, screening and temperature were determined empirically from the data. Modifying factors for equipment power cycling and application environment were determined by alternate methods.

Application and construction variables which characterize digital microcircuits in a nonoperating environment are presented in Table 5.1.2-1. These factors were determined whenever possible for all summarized data. The variables presented in Table 5.1.2-1 represent possible failure rate model parameters.

Development of a theoretical model for digital microcircuits was conducted in two phases. The initial phase consisted of identifying variables which hypothetically have the greatest impact on reliability. It was determined that nonoperating ambient temperature theoretically has the most significant influence on nonoperating reliability for hermetic digital microcircuits. Other factors which have been identified in the literature (References 3, 26, 27, 28 and 29) are humidity, complexity, equipment power cycling and screening. The second phase of the theoretical model development process consisted of a study of various model forms to determine which would be applicable to microcircuit nonoperating failure rate prediction. Model forms which were studied include multiplicative models, additive models and nonlinear model forms.

The MIL-HDBK-217D operating failure rate prediction model for microcircuits is a combination of an additive and multiplicative model form (Reference 19). The application stresses during nonoperating periods are sufficiently different to preclude an assumption, without additional justification, that the nonoperating model form is the same or similar to the operating model form. Nevertheless, a model form similar to the MIL-HDBK-217D microcircuit model was considered for nonoperating failure rate model development. The mathematically attractive purely additive and purely multiplicative models were also considered. After evaluating the advantages and disadvantages of the various model forms, the decision was

TABLE 5.1.2-1: DIGITAL MICROCIRCUIT CHARACTERIZATION VARIABLES

- I. Technology
 - A. DTL E. ECL I. IIL M. CCD
 - B. TTL F. LTTL J. MNOS N. CMOS
 - C. HTTL G. STTL K. PMOS O. CMOS/SOS
 - D. DTL H. LSTTL L. NMOS P. HMOS
- II. Number of Gates
- III. Construction
 - A. Dip E. Chip Carrier
 - B. Can F. Quad In-Line (staggered leads)
 - C. Flatpack G. In-Line
 - D. Square
- IV. Enclosure
 - A. Hermetic
 - B. Non-Hermetic
- V. Package Material
 - A. Metal E. Glass I. Metal/Epoxy
 - B. Ceramic F. Plastic/Ceramic J. Silicon
 - C. Metal/Ceramic G. Epoxy K. Phenolic
 - D. Metal/Glass H. Ceramic/Plastic/Window
- VI. Number of Pins
- VII. Number of Interconnects
- VIII. Die Bond
 - A. Eutectic
 - B. Epoxy
 - C. Glass
- IX. Quality Level
 - A. S C. B-1 E. C G. D
 - B. B D. B-2 F. C-1 H. D-1
- X. Application Environment
- XI. Temperature
 - A. Rated
 - B. Actual
- XII. Number of Power On/Off Cycles per 10^3 Nonoperating Hours

made to initially proceed with the general theoretical model form developed for this study. This model form is a multiplicative model with the exception of the equipment power cycling contribution.

The summarized digital microcircuit data collected in support of this study effort is presented in Table 5.1.2-2. The nonoperating failure rate data collectively consists of 155 failures, 21441.1×10^6 part hours and 399 individual data records. Data was available for parts screened to S, B, C, D and D-1 quality levels as defined in MIL-HDBK-217D.

TABLE 5.1.2-2: DIGITAL MICROCIRCUIT NONOPERATING
FAILURE RATE DATA

No.	Equipment/Source	Data Records	Complexity	Tech.	Failures	Part Hours ($\times 10^6$)
1	Hawk/MICOM	6	SSI	bipolar	1	768.9
2	Maverick/MICOM	3	SSI	bipolar	1	432.4
3	Maverick/MICOM	2	MSI	bipolar	1	308.9
4	F-16 HUD/RIW	36	SSI	bipolar	10	4320.7
5	F-16 HUD/RIW	50	MSI	bipolar	7	3398.2
6	F-16 HUD/RIW	2	LSI	bipolar	0	129.8
7	F-16 HUD/RIW	2	LSI	MOS	0	26.0
8	Martin Marietta	3	SSI/MSI	bipolar	18	9550.8
9	Sandia	1	LSI	MOS	1	46.7
10	Sandia	1	SSI	bipolar	0	2432.1
11	PRC	2	SSI/MSI	bipolar	0	3.8
12	RAC (1)	120	SSI	bipolar	17	6.9
13	RAC (1)	14	SSI	MOS	43	0.4
14	RAC (1)	130	MSI	bipolar	20	4.3
15	RAC (1)	2	LSI	bipolar	0	0.1
16	RAC (1)	1	VLSI (2)	bipolar	1	0.1
17	ERADCOM (3)	17	SSI	bipolar	18	7.7
18	ERADCOM (3)	7	SSI	MOS	17	3.3
TOTALS		399			155	21441.1

- 1) High temperature storage life test data. Storage temperatures range from 150°C to 350°C.
- 2) VLSI parts defined as having greater than 3000 gates.
- 3) Panama life test data for nonhermetic devices. Ambient temperature = 30°C, relative humidity = 90%.

Early in the model development process, the issue of device complexity was addressed. The terms "complexity" and "complexity factor" are convenient, yet ambiguous. Complexity is a relative term. A device may be relatively complex in a number of ways; process, function, size, etc. It was considered desirable to investigate the effects of nonoperating failure rate versus a quantitative measure of complexity. Possible measures of complexity were evaluated for digital microcircuits. Several of the possible complexity measures which were given consideration are the following:

- o Number of gates
- o Number of transistors
- o Number of package pins
- o Number of package I/O functions
- o Die area

In addition, the possibilities were considered that more than one complexity measure should be included in the optimal model form for digital microcircuits, or that perhaps complexity had only a negligible effect on nonoperating failure rate.

After evaluating the different measures of complexity, it was determined that the number of gates and the number of package pins were the two best complexity measures. These two complexity measures would be further investigated by analysis of the available data. Both parameters represent information which is readily available, and theoretically have an effect on failure rate. For VLSI digital devices, the gate count may not be available. This potential problem is analyzed at a later stage of the model development process. Die area was initially thought to have merit as a measure of complexity. However, it was found that die area information is often vendor proprietary, and thus would not be suitable for failure rate prediction purposes.

The digital microcircuit data were initially analyzed without merging data records. Point estimate failure rates were calculated for data

entries with observed failures. The methods described in Section 3.3 were used to determine which zero failure data entries had sufficient part hours to estimate a failure rate without failures. Correlation coefficients were computed for every pair of independent variables. In addition, the available data was evaluated to identify weaknesses in the data set. Results from these initial analyses are given below.

- 1) All collected data were from a ground based environment or from storage life testing. Therefore there was a insufficient range of environmental stresses represented in the data to develop environmental factors based on data analysis.
- 2) All data were for digital microcircuits with one of the following logic types; DTL, TTL, LSTTL, ECL, CMOS, or CMOS/SOS.
- 3) 88% of all MOS data records were for high temperature or high humidity applications.
- 4) 86% of all field data records were for 14 or 16 pin devices.
- 5) The correlation coefficient for number of gates vs. number of pins was 0.52.
- 6) 100% of all data on nonhermetic devices were from high temperature or high humidity testing.

It had been desired to analyze the effect that both number of pins and number of gates had on nonoperating failure rate. However, characteristics of the data base and conclusions from the preliminary data analysis made it very difficult to properly address the effect of package pins on failure rate. Proper application of regression analysis required that all independent variables were uncorrelated (i.e. correlation coefficient not significantly different from zero) and that there was a large range of variable values represented in the data.

The observation that gate count and pin count were correlated was further investigated. A recent study (Reference 30) regarding VLSI device reliability indicated that there was little or no correlation between gate count and pin count. After further studying the issue, it was determined that there is theoretically an intermediate amount of correlation between

pin count and gate count for SSI and MSI devices. Then, as device complexity enters into the LSI and VLSI ranges, the correlation decreases. Field data was not available for the most current state-of-the-art LSI and VLSI devices. The long nonoperating times required to observe failures precludes the existence of such data. As a result, the field data available for analysis were concentrated in the SSI and MSI ranges. This explains the observed correlation. The implications of the observed correlation are two-fold. First, regression analysis could not be correctly applied to quantify the effects of both variables. Second, a regression analysis for failure rate versus gate count implicitly includes the effects of pin count for SSI and MSI devices. That is, a regression analysis for failure rate against either one of the two variables includes the effects of both because the number of pins and the number of gates increase together for the lower complexities. Therefore it was decided to include only gate count as a measure of complexity. The natural logarithm of the complexity was designated as C_1 .

It was determined in the theoretical model development process that ambient temperature was the most significant variable influencing nonoperating failure rate for digital microcircuits. It was also assumed that the effects of temperature would be different depending on the logic type of the device. In addition, the equivalent Arrhenius relationship (described in Section 4.4) was determined to be applicable to nonoperating failure rate prediction. The preliminary form of the nonoperating temperature factor was determined to be:

$$\pi_{NT} = \exp\left(\frac{-eV}{K} \left(\frac{1}{T} - \frac{1}{T_r}\right)\right)$$

where

π_{NT} = nonoperating temperature factor

eV = equivalent activation energy

K = Boltzman's constant = 8.63×10^{-5} eV/°K

T = temperature (°K)

T_r = reference temperature = 298 °K

The addition of the reference temperature term was for convenience. The temperature factor was defined to be equal to unity when the ambient temperature is equal to the reference temperature. The value of 298⁰K was selected to be consistent with the reference temperature term used for failure rate prediction in MIL-HDBK-217D.

It was assumed that the equivalent activation energy would vary with logic type. Data was available for DTL, TTL, LSTTL, ECL, CMOS and CMOS/SOS. Introducing temperature (or inverse of temperature) into a regression by itself would result in only one temperature coefficient. Therefore, a temperature matrix with two temperature variables was defined to derive a temperature factor of the desired form. Introducing the temperature matrix as independent variables in a regression analysis allowed for computation of unique activation energies. The logic types were grouped into the categories of (1) bipolar or (2) MOS technology. The temperature matrix is presented in Table 5.1.2-3.

TABLE 5.1.2-3: DIGITAL MICROCIRCUIT TEMPERATURE MATRIX

Technology	1/T1	1/T2
bipolar	1/T	0
MOS	0	1/T

The following equations depict the relationship of nonoperating failure rate versus 1/T1 and 1/T2. These equations are conceptual in nature, and temporarily ignore all variables except temperature.

$$\ln(\lambda) = b_0 + b_1(1/T1) + b_2(1/T2) + \epsilon$$

$$\lambda = f(1/T1, 1/T2) = \exp(b_0)\exp(b_1(1/T1) + b_2(1/T2))$$

$$\begin{aligned}\lambda_1 &= f(1/T, 0) = \exp(b_0)\exp(b_1(1/T1) + b_2(0)), \text{ bipolar} \\ &= \exp(b_0)\exp(b_1(1/T1)), \text{ bipolar}\end{aligned}$$

$$\begin{aligned}\lambda_2 &= f(0,1/T) = \exp(b_0)\exp(b_1(0) + b_2(1/T^2)), \text{ MOS} \\ &= \exp(b_0)\exp(b_2(1/T^2)), \text{ MOS}\end{aligned}$$

b_0 , b_1 and b_2 are regression coefficients and ϵ is the residual. The equivalent activation energy for the logic types in the bipolar category was equal to the b_1 coefficient multiplied by Boltzman's constant. Similarly, the equivalent activation energy for the MOS logic types was equal to the b_2 coefficient multiplied by Boltzman's constant.

The theoretical model for digital microcircuits was determined to include an equipment power cycling factor. The factor was assumed to be of the following form.

$$\text{Cycling Factor} = 1 + K(\text{cycles}/10^3 \text{ hr})$$

where K is a constant. The other factors in the theoretical model were multiplicative. Development of an equipment power cycling factor of this form resulted in a proposed model which is neither linear nor can be transformed into linear form. Therefore, application of regression analysis was more difficult. This problem and a proposed solution is described in-depth in Section 4.3. As recommended in Section 4.3, equipment cycling rate was temporarily treated as a qualitative variable and three "dummy variables" were defined (cyc1, cyc2, and cyc3).

A matrix of "dummy variables" (0 or 1) was defined to accommodate quality level in quantitative analyses. The quality level matrix is presented in Table 5.1.2-4. In addition, a technology qualitative variable was designated TECH. The TECH variable was assigned a value of zero for bipolar devices and one for MOS devices.

TABLE 5.1.2-4: DIGITAL MICROCIRCUIT QUALITY VARIABLE MATRIX

Quality Level	Q ₁	Q ₂	Q ₃	Q ₄
S	1	0	0	0
B	0	0	0	0
C	0	1	0	0
D	0	0	1	0
D-1	0	0	0	1

The data were then merged according to equipment, technology, temperature, quality level and gate count. The data were merged by summing failures and part hours. To maximize the number of failures and part hours per data record, data within complexity categories of 10 gate intervals were merged. For example, all data for devices which were similar in regard to equipment, technology, temperature and quality level, and which have between 21 and 30 gates were merged. The average number of gates for the category was used as the measure of complexity for each merged data record. There were a total of 33 merged data records available for further analyses.

At this stage in the model development process, the data were in a format suitable for application of regression analysis. All of the available data were utilized except the Panama life test data. This testing was performed for nonhermetic devices found in the Panama jungle. The observed failure rates from the Panama testing were not representative of nonhermetic microcircuits in a ground fixed environment. Additionally, there was neither an accurate method to extrapolate the observed failure rates to typical ground fixed conditions nor sufficient detail in all data sources to develop a unique humidity factor. Therefore, this data were not included in the regression analysis.

Results of the regression analysis are given in Table 5.1.2-5. The dependent variable was $\ln(\text{failure rate})$ and the independent variables were TECH, $1/T_1$, $1/T_2$, Q_1 , Q_2 , Q_3 , Q_4 , C_1 , cyc1, cyc2, and cyc3. The R-squared value computed for the analysis was 0.98. However, this value was misleading. The absence of temperature values between 20°C and 150°C

together with the dominant effect of temperature resulted in a much higher R-squared value than would have been observed if the temperatures were evenly distributed.

TABLE 5.1.2-5: DIGITAL MICROCIRCUIT REGRESSION RESULTS

variable	coefficient	standard error	f-ratio	confidence limit
TECH	7.524	1.368	30.26	0.90
1/T1	-4812.803	205.468	548.67	0.90
1/T2	-7056.722	550.861	164.10	0.90
Q1	-0.637	0.698	0.83	0.60
Q2	0.836	0.698	1.44	0.70
Q3	0.882	0.279	9.99	0.90
Q4	2.158	0.520	17.20	0.90
C1	0.477	0.086	30.88	0.90
b ₀	9.368	--	--	--

The coefficients given in Table 5.1.2-5 were the results of a regression with the dependent variable equal to the natural logarithm of failure rate. Transforming the regression solution into an equation where failure rate (as opposed to log of failure rate) is the dependent variable results in the following preliminary multiplicative model.

$$\lambda_d = A'_b (\# \text{ gates})^{.477} \exp(-A_n/T) \pi_{NQ}$$

where

λ_d = predicted digital microcircuit nonoperating failure rate
(failures/10⁶ hours)

A'_b = preliminary base failure rate constant
= $\exp(7.524 + 9.368(\text{TECH}))$
= 1.852×10^3 , bipolar
= 2.168×10^7 , MOS

A_n = temperature coefficient

= 4813, bipolar

= 7057, MOS

T = temperature ($^{\circ}\text{K}$)

π_{NQ} = nonoperating quality factor

= $\exp(-0.637(Q_1) + 0.836(Q_2) + 0.882(Q_3) + 2.158(Q_4))$

= 0.53, S

= 1.0, B

= 2.3, C

= 2.4, D

= 8.7, D-1

The variables TECH, Q_1 , Q_2 , Q_3 , and Q_4 have been previously defined. It is emphasized that the above equation represents a preliminary model, which is only applicable to ground based environment.

Conclusions and observations were made based on the regression results. These conclusions and observations are given in the following paragraphs.

The nonoperating failure rate of D and D-1 quality devices was significantly different, with 90% confidence, from devices screened to the B quality level. The nonoperating failure rate difference between devices screened to C and B levels was significant at a 70% confidence, and the difference between S and B quality level parts was significant at a 60% confidence. It was considered very encouraging that the ranking of quality factor values was precisely as expected based on the screening specifications and screening effectiveness characteristics. Generally, separate factors were not proposed in this study when the confidence limit was lower than 0.70. However there are strong theoretical reasons why the failure rate for S quality devices is lower than B quality devices. It was assumed that the failure rate difference between S quality and B quality microcircuits (less than two to one) was approximately the same magnitude as the statistical noise inherent in the data. This would explain the low confidence.

The standard error statistic allows for the computation of confidence intervals around the nonoperating quality factor estimates. Table 5.1.2-6 presents point estimate quality factor values, as well as lower and upper 90% confidence interval values. Confidence limit values could not be computed for B quality because all factors are in comparison to the B level. In addition, Table 5.1.2-6 presents interpolated quality factor values for quality levels where no data was available.

TABLE 5.1.2-6: DIGITAL MICROCIRCUIT NONOPERATING QUALITY FACTOR

Quality Level	$\pi_{NQ,.05}$	$\pi_{NQ1}(1)$	$\pi_{NQ,.95}$	$\pi_{NQ2}(2)$
S	0.16	0.53	1.7	0.53
B	--	1.0	--	1.0
B-1	--	--	--	1.4
B-2	--	--	--	2.0
C	0.70	2.3	7.6	2.3
C-1	--	--	--	2.4
D	1.5	2.4	3.9	2.4
D-1	3.6	8.7	21.1	8.7

Notes: 1) π_{NQ1} is the point estimate quality factor.

2) π_{NQ2} is the point estimate quality factor supplemented by interpolated values for B-1, B-2 and C-1 quality levels.

It was noticed that the range of the nonoperating quality factors (0.53, 8.7) was much less than the range of microcircuit operating quality factors (0.50, 35) found in Table 5.1.2.5-1 of MIL-HDBK-217D. This was believed to be indicative of a significantly slower rate for "infant mortality" failure occurrence during periods of nonoperation. Therefore, the effects of screening are less evident. This same trend was noticed for practically all electronic component types, and is discussed in Section 4.6 of this report. Conversely, package type appeared to have a more severe effect on nonoperating failure rate. The best indication of the failure rate difference between hermetic and nonhermetic devices is the ratio of the D-1 quality factor to the D quality factor. The ratio is 2:1 for operating failure rate based on the information provided in MIL-HDBK-217D. The ratio is 3.6:1 for nonoperating failure rate based on the

nonoperating quality factors presented in Table 5.1.2-6. Therefore, it was concluded that the difference in failure rate between hermetic and nonhermetic digital microcircuits is larger for nonoperating failure rate than operating failure rate.

As expected, device nonoperating temperature was a significant variable with 90% confidence. Unique temperature factors were computed for bipolar (i.e. DTL, TTL, ECL) and MOS (i.e. CMOS, CMOS/SOS) technologies. The temperature coefficient for bipolar devices was determined to be -4813. This is equivalent to an activation energy of 0.42 eV. The standard error statistic allowed for computation of a 90% confidence interval around the coefficient. The upper and lower 90% confidence interval values for bipolar devices were determined to be -4461 and -5164 respectively. The point estimate temperature coefficient for MOS devices was found to be -7057. This is equivalent to an activation energy of 0.61 eV. Upper and lower 90% confidence interval values were computed for MOS device temperature coefficient and found to be -6114 and -7999 respectively.

The temperature coefficients computed from the available data correspond to five logic types. For other logic types, appropriate temperature coefficients were interpolated by assuming a similar ranking as that found in Table 5.1.2.5-4, MIL-HDBK-217D. The preliminary digital microcircuit nonoperating temperature factor was therefore determined to be the following equation. The temperature factor expression was defined to include a reference temperature term for convenience. The preliminary temperature factor assumes a value of one for any logic type at the reference temperature of 298°K.

$$\pi_{NT,p} = \exp(-A_n(\frac{1}{T} - \frac{1}{298}))$$

where

$\pi_{NT,p}$ = preliminary nonoperating temperature factor
 A_n = temperature coefficient (given in Table 5.1.2-7)
 T = nonoperating temperature ($^{\circ}\text{K}$)

TABLE 5.1.2-7: MICROCIRCUIT NONOPERATING TEMPERATURE FACTOR COEFFICIENTS

Technology	A_n
TTL, HTTL, DTL, ECL	4,813
LTTL, STTL	5,261
LSTTL	5,711
IIL, MNOS	6,607
PMOS	5,711
NMOS, CCD	6,159
CMOS, CMOS/SOS	7,057

No distinction was made during the nonoperating temperature factor development process between hermetic and nonhermetic digital devices. This was done for several reasons. All available data for nonhermetic devices was life test data with a test temperature of 150°C . Therefore separate temperature coefficients for nonhermetic devices could not be determined empirically. A wide range of temperatures would have been required to determine an empirical relationship. A second reason was that the nonoperating failure rate difference between hermetic and nonhermetic devices was accounted for by both the nonoperating quality factor and environmental factor. It was determined that failure rate effects caused by humidity and moisture intrusion are the major differences between hermetic and nonhermetic devices. These factors were better predicted by use of the environmental factors. A third reason was that an assumption of a more temperature dependent relationship for nonhermetic devices could result in optimistic failure rate predictions (i.e. predicts too low a failure rate) for temperatures less than the 150°C test temperature. An example which illustrates this relationship is presented in the following paragraph.

The relationship of failure rate versus temperature is shown for two different equivalent activation energies in Figure 5.1.2-1. If it is assumed that nonhermetic devices exhibit a more temperature dependent failure rate, then the example depicted in Figure 5.1.2-1 is analogous to the study of activation energies for nonhermetic devices. The activation energy (E_{a1}) for the more temperature dependent failure rate is greater than the activation energy (E_{a2}) for the less temperature dependent failure rate, as would be expected. However, the failure rate is lower for the more temperature dependent relationship for all points to the right of the intersection point. It should also be noted that as temperature decreases, the $(1/KT)$ term increases. Therefore in the example depicted in Figure 5.1.2-1, the failure rate is less for the E_{a1} activation energy relationship for all temperatures less than T_0 (i.e. to the right of the intersection point). The E_{a2} activation energy is equivalent to the observed values for hermetic devices. The E_{a1} activation energy would be equivalent to an assumed higher A_n value for nonhermetic devices.

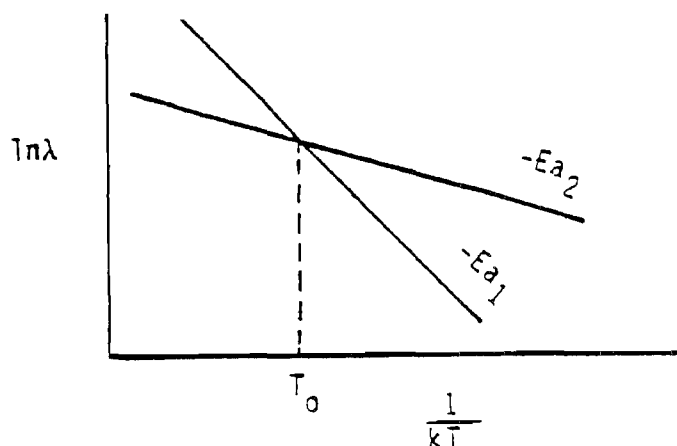


FIGURE 5.1.2-1: FAILURE RATE VS. TEMPERATURE

The temperature intersection point was 150°C for nonhermetic digital devices. Any proposed model will predict the same failure rate at 150°C regardless of the activation energy because all nonhermetic data was for a 150°C test temperature. Therefore, assumption of a lower activation energy (i.e. the regression solution values for hermetic devices) resulted in a conservative failure rate estimate for all nonoperating temperatures less than 150°C.

The number of gates was determined to be a significant variable with 90% confidence. The preliminary model assumed that digital microcircuit nonoperating failure rate was proportional to the number of the gates raised to a constant value. The regression solution for the constant was 0.477. Upper and lower 90% confidence interval values were 0.624 and 0.330 respectively. The range of gate counts found in the available data was from 1 to 3100 gates. The observed relationship between nonoperating failure rate and the number of gates was an empirical relationship (as opposed to a theoretical relationship). Therefore, extrapolation of the observed relationship beyond 3100 gates could not be justified.

It was decided to include the gate count variable into an equation for base failure rate. The base failure rate for digital microcircuits was therefore given by the following equation:

$$\lambda_{nb} = A_b(\# \text{ gates})^{.477}$$

where

λ_{nb} = nonoperating base failure rate, (# gates \leq 3100)

A_b = constant

The constant term (A_b) was defined as a function of device technology and the assumed reference temperature of 298°K (or 25°C) due to normalization of the nonoperating temperature factor. The temperature factor was defined to be equal to a value of one for a temperature of 25°C. Therefore, the A_b constant must also correspond to 25°C. In addition, the technology dummy variable (TECH) coefficient was included in the equation for base failure rate. Determination of appropriate values for the A_b constant was computed by the following equation.

$$A_b = \exp(9.368 + 7.524(\text{TECH}) - A_n(1/298))$$

where all variables have been previously defined. The 9.368 and 7.524 values were the b_0 and TECH coefficients previously presented in Table

5.1.2-5. Only the observed A_n values of 4813 for TTL, DTL and ECL, and 7057 for CMOS and CMOS/SOS were used for the A_b determination process. The extrapolated A_n values for other logic types were to determine the relative (as opposed to absolute) effect of temperature. The respective base failure rate constants for bipolar and MOS were therefore determined to be,

bipolar: $A_b = \exp(9.368 - 4813(1/298)) = .001134 \text{ failures}/10^6 \text{ hrs.}$

MOS: $A_b = \exp(9.368 + 7.524 - 7057(1/298)) = .001126 \text{ failures}/10^6 \text{ hrs.}$

It was noted that the two base failure rate constant values were the same up to three significant digits. The fact that these two numbers are extremely close must in part be attributed to coincidence because failure rate estimation techniques are not accurate to three significant digits. However, it was concluded from this analysis that the nonoperating failure rates of bipolar and MOS devices were indistinguishable at 25°C, if all other parameters are equal.

The base failure rate expression was determined to be applicable from 1 to 3100 gates. This range of values includes all SSI/MSI devices and enters into the LSI range of devices. The gate count range for LSI devices begins at 100 gates. The cut-off between LSI and VLSI is less defined. Nonoperating failure rate estimation of digital devices with greater than 3100 gates was further investigated to determine whether extrapolated or assumed relationships beyond 3100 gates could be justified or were warranted.

It was considered essential to determine methods to predict the nonoperating failure rate for state-of-the-art devices. Continued advancements in integrated circuit fabrication and processing techniques have resulted in an electronics industry which is in a constant state of transition. Therefore, numerical analyses which require large quantities of observed field data are necessarily outdated by the time the data is collected. This problem was particularly acute for nonoperating failure rate prediction model development because of relatively long mean-time-to-

failures in the nonoperating state. As a result, prediction models for state-of-the-art devices could not be determined empirically. Nevertheless, one of the primary objectives of this study effort was to develop methods which can be applied to any conceivable equipment type and mission profile. Therefore, alternate methods to assess high gate count LSI and VLSI devices were considered.

One option which was considered to predict the nonoperating failure rate for high gate devices was to assume that the observed relationship for devices with less than 3100 gates (i.e. failure rate $\propto (\text{\#gates})^{.477}$) would continue to be accurate for higher gate counts. This option was rejected, however, based on the information provided in Reference 30. The results of this recent study (documented in Reference 30) concluded that no numerical correlation between operating failure rate and number of gates could be found for devices in the VLSI range with greater than 3000 gates. A possible reason for this lack of correlation was that the majority of VLSI failure mechanisms are directly related to particular fabrication process steps (such as mask registration). These failure mechanisms effect all similar components on a die uniformly, and not random individual die components as would be indicated by a complexity factor. Another factor confounding the results was the fact that as device complexity increases the associated fabrication processes are improving, thus masking any true effect complexity may have. It was assumed that this observed pattern would also be true for nonoperating failure rate.

It was determined that an approximate base failure rate value for random logic VLSI devices would be constant with respect to gate count within the VLSI range, and could be found by solving the previously determined expression for SSI/MSI/LSI devices for number of gates equal to 3100. Therefore, the approximate random logic VLSI nonoperating base failure rate was computed with the following expression.

$$\lambda_{nb,VLSI} = .00113(3100)^{.477} = .0523 \text{ failures}/10^6 \text{ hrs}$$

This value is different from the base failure rate presented in Section 5.1.1 because the model had not been normalized for environment at this stage of the model development process. It is emphasized that this average value is only approximate. However, the proposed value is intuitively appealing for two reasons. First, the nonoperating failure rate is independent of gate count for random logic VLSI devices. Second, the predicted nonoperating failure rates provide a smooth transition from SSI/MSI to the LSI and VLSI ranges of device complexities.

None of the three equipment power cycling variables were significant at the 60% confidence level. This observation was contrary to the assumption made in the theoretical model development process that equipment power cycling had an effect on observed nonoperating failure rate. Therefore, this observation was further studied. Given the size of the merged data set (i.e. 33 records), it was concluded that only the most significant variables could be identified through data analysis. In this case, temperature, technology, quality and complexity were identified as significant variables. Thus, results of the regression analysis were not necessarily that equipment power cycling had no effect on nonoperating failure rate, but that the effect was less evident than that of temperature, technology, quality and complexity over the range of values found in the data base.

The most obvious treatment of equipment power cycling was to exclude the variable from digital microcircuit nonoperating failure rate model development because of the apparent lack of correlation with failure rate. This probably would have been the proposed approach if not for the observation that equipment power cycling was determined to be a significant model parameter for linear/interface microcircuits (discussed in Section 5.1.3). The observed nonoperating failure rate difference resulting from power cycling was found to be 2.2 to 1 for linear devices. This difference was relatively small, and therefore it was not surprising that the effect could not be estimated for digital devices. A comparison was then made between the anticipated effects of power cycling for digital vs. linear devices.

One possible reason for the apparent difference between equipment power cycling effects of digital and linear devices was that a major failure mode resulting from power cycling is wire bond fatigue and failure. The rate at which wire bond fatigue occurs is related to the power dissipation and corresponding thermal/mechanical stresses which occur during the power on-off cycle. It was hypothesized that, on average, linear devices exhibit slightly higher levels of power dissipation than the primarily SSI/MSI digital devices included in the data base. This would possibly explain the apparently higher degree of dependence on equipment power cycling for linear devices. However, this can not be generalized for all linear and digital devices. Many linear devices have power dissipation equal to or lower than those typically encountered in digital devices.

It was determined from this comparison of power cycling effects for digital and linear devices that a proposed digital microcircuit model required an equipment power cycling factor. This determination was made because (1) the comparison did not reveal substantial reasons why power cycling would not effect digital nonoperating failure rate given that power cycling was observed to effect linear device failure rate, and (2) the series of microcircuit models should be consistent with regard to model parameters.

The assumed equipment power cycling factor was determined to be,

$$\pi_{\text{cyc}} = 1 + .02(\text{power cycles}/10^3 \text{ hours})$$

The (.02) constant term was based on two premises. First, the power cycling constant term would be less than or equal to the corresponding term developed for linear microcircuits. The second premise was that the power cycling factor would have less effect (over the range of values found in the available data) than the observed relationships for temperature, quality and complexity. The (.02) term represents the largest numerical value which satisfies the two constraints. It is noted

that this proposed power cycling factor will assume a value of one for essentially all missile storage test schedules.

The next phase of the model development process was to investigate the effects of the environment. The theoretical model developed for digital microcircuits included a nonoperating environmental factor. As previously stated, there were insufficient data to develop a complete series of nonoperating environmental factors empirically. Nevertheless, the objective of this study effort was to develop a methodology which can be employed for nonoperating reliability evaluation for any potential application. Therefore, it was imperative that appropriate nonoperating environmental factors were determined.

The methods presented in Section 4.5 were applied to develop appropriate nonoperating environmental factors. This method assumes that a series of nonoperating environmental factors can be generated from the MIL-HDBK-217D operating environmental factors based on a comparison of operating and nonoperating failure mechanism accelerating factors. Additionally, the differences between average temperature for operating and nonoperating states were investigated. Operating temperatures are higher because of the internal heat generation associated with applying power to the equipment. For microcircuits, the effect of this temperature difference was predicted by the respective operating and proposed nonoperating temperature factors. Thus, no temperature adjustment was required for environmental factor development purposes.

The proposed digital microcircuit nonoperating environmental factors were presented in Table 5.1.1-1 in the previous section. Separate nonoperating environmental factors were proposed for hermetic and nonhermetic devices because nonhermetic devices have been observed to be more sensitive to environmental stress, primarily humidity and contaminated environments. An environmental factor conversion was required because the operating environmental factor is part of a complex nonlinear model form as opposed to the proposed multiplicative model for nonoperating failure rate prediction. The conversion factor expression

for microcircuits was presented in Section 4.5. The conversion factor constants used to compensate for the difference in model forms were based on average MIL-HDBK-217D microcircuit values. For nonhermetic devices, the conversion factor constants were based on average factor values complemented by the results of the Panama nonhermetic microcircuit storage life testing (data entries 17 and 18 in Table 5.1.2-2). In addition, the nonoperating environmental factors were normalized to a ground benign value equal to one. This was done so that the proposed microcircuit nonoperating environmental factors would be consistent with the other proposed models, and to provide the proposed model with increased utility. Conversely, the MIL-HDBK-217D, Notice 1 operating microcircuit environmental factors are not normalized to any environment (i.e. no factor is equal to one), and therefore the numerical values for the base failure rate constants have no physical meaning by themselves.

Tables 5.1.2-8 through 5.1.2-10 present failure mechanism and failure acceleration factor distributions for MOS SSI/MSI, bipolar SSI/MSI and random logic LSI digital devices. References 31 through 40 included microcircuit failure mode or failure mechanism distribution information. Accurate quantitative failure mechanism information was difficult to obtain for nonoperating conditions and often conflicting for operating conditions. Therefore, the information presented in Tables 5.1.2-8 through 5.1.2-10 represent typical failure mechanism distributions which may not be similar for all specific device styles and applications.

The issue of device maturity was also addressed in this study effort. All digital microcircuits which were represented in the collected data were mature devices. Thus, the effect of device maturity could not be evaluated by data analysis. Additionally, it is strongly recommended that any equipment subjected to prolonged periods of storage be designed with only mature part types. Therefore, the proposed digital microcircuit nonoperating failure rate prediction model does not apply to any of the following conditions.

- 1) New device in initial production.

TABLE 5.1.2-8: MOS DIGITAL SSI/MSI FAILURE MECHANISM DISTRIBUTION

Failure Mode/Mechanism	Accelerating Factors	Operating Distribution (%)	Nonoperating Distribution (%)
Die			
Oxide Defects	voltage, temp.	20-50	0-20
Diffusion Defects	voltage, temp.	0-5	0-5
Surface Anomalies	moisture, temp., voltage	20-40	35-70
Metallization	current	1-15	0-5
Contamination	humidity, temp.	1-15	1-20
Package			
Die Bond	temp., shock, vibration	0-12	0-14
Lead	shock, vibration	1-14	1-18
Seal	shock, vibration	1-14	1-18
Interconnects			
Wire Bond	vibration, current	1-15	1-20
Wire	current	1-20	0-5

TABLE 5.1.2-9: BIPOLAR DIGITAL SSI/MSI FAILURE MECHANISM DISTRIBUTION

Failure Mode/Mechanism	Accelerating Factors	Operating Distribution (%)	Nonoperating Distribution (%)
Die			
Oxide Defects	voltage, temp.	0-10	0-10
Diffusion Defects	voltage, temp.	1-20	5-25
Surface Anomalies	moisture, temp., voltage	1-20	5-25
Metallization	current	5-25	0-10
Contamination	humidity, temp.	0-5	0-5
Package			
Die Bond	temp., shock, vibration	1-20	5-22
Lead	shock, vibration	1-20	5-23
Seal	shock, vibration	5-25	10-30
Interconnects			
Wire Bond	vibration, current	10-35	15-35
Wire	current	1-20	0-10

TABLE 5.1.2-10: RANDOM LOGIC LSI FAILURE MECHANISM DISTRIBUTION

Failure Mode/Mechanism	Accelerating Factors	Operating Distribution (%)	Nonoperating Distribution (%)
Die			
Oxide Defects	voltage, temp.	15-35	0-10
Diffusion Defects	voltage, temp.	0-5	0-5
Surface Anomalies	moisture, temp., voltage	0-5	0-5
Metallization	current	25-40	0-5
Contamination	humidity, temp.	5-25	20-40
Package			
Die Bond	temp., shock, vibration	1-15	5-25
Lead	shock, vibration	0-5	0-5
Seal	shock, vibration	0-5	0-5
Interconnects			
Wire Bond	vibration, current	5-30	30-65
Wire	current	1-15	0-5

- 2) Where major changes in design or process have occurred.
- 3) Where there has been an extended interruption in production or a change in line personnel (radical expansion).

The final phase of the model development process was to normalize the base failure rate constant to correspond to a ground benign environment. All observed field data were for a ground fixed environment. Therefore, the base failure rate constant of 0.00113 was divided by the ground fixed hermetic environmental factor of 2.4 to obtain a normalized base failure rate. Additionally, a relatively small numerical adjustment was required because of the assumed factor for equipment power on-off cycling. The base failure rate constant needed to correspond to a cycling rate of zero. Therefore, the base failure rate was multiplied by an adjustment factor of 0.80. This term was equal to the inverse of the average equipment power cycling factor for the cycling rate values found in the data base. The nonoperating base failure rate was therefore equal to .00038 after normalizing for environment and equipment power cycling. A corresponding change was also made for the approximate, constant base failure rate value for random logic microcircuits with greater than 3,100 gates.

A modification to the preliminary temperature factor was then required to prevent situations where the predicted nonoperating failure rate exceeds the MIL-HDBK-217D operating failure rate. The first phase of the model validation task (described in Section 5.1.5 for monolithic microcircuits) was to compare the proposed nonoperating models with MIL-HDBK-217D models. It was observed that in a very small percentage (<2%) of the failure rate comparisons, the preliminary nonoperating failure rate exceeded the corresponding operating failure rate prediction.

In each of the instances where the nonoperating failure rate was higher than the MIL-HDBK-217D failure rate, the part type in question had relatively low power dissipation and junction-to-case thermal resistance, and was exposed to a high ambient temperature. In other words, the difference between operating and nonoperating junction temperature was small, and temperature was the dominant failure causal stress. In these

cases, the "true" operating failure rate will be slightly higher than the "true" nonoperating failure rate, and given an infinite data supply, this would have been the result of the operating to nonoperating failure rate model comparisons. However, both the MIL-HDBK-217D models and the proposed nonoperating failure rate prediction models were based on data samples obtained from different data sources. The predicted failure rate is therefore a random variable distributed about an unknown "true" mean failure rate. As the difference between the "true" operating and nonoperating failure rates approach zero, the probability of the predicted nonoperating failure rate exceeding the predicted operating failure rate approaches 50%. Thus, the small percentage of instances where the preliminary nonoperating predicted failure rate exceeds the operating failure rate is a natural phenomenon, and is in no manner indicative of an incorrect analysis or invalid data. It must always be remembered that predicted failure rates are average failure rate values computed from a data sample of parts with similar characteristics. Predicted failure rates are not an inherent property of the part such as capacitance, device dimensions or number of gates.

Despite the conclusions of the previous paragraph, it is important that the proposed nonoperating failure rate prediction models are completely consistent with the operating failure rate prediction models. Therefore, a modified nonoperating temperature relationship was proposed and is given by the following equation.

$$\pi_{NT} = K_3 + K_4 \exp\left(-A_n\left(\frac{1}{T} - \frac{1}{298}\right)\right)$$

where

π_{NT} = nonoperating temperature factor

K_3, K_4 = constants (given in Table 5.1.2-11)

A_n = temperature coefficient (given in Table 5.1.2-7)

The K_3 and K_4 constants were determined by (1) assuming that the operating and nonoperating failure rates are asymptotic as temperature increases, and (2) defining the temperature factor to be equal to one at 25°C. The temperature factor modification process resulted in a factor of 1.29 difference between the regression solution failure rate and the modified temperature factor solution at 25°C. This difference was because the average temperature for the ground storage data was 20°C, and thus, both models predict an identical failure rate at 20°C. The difference between the two failure rate models increases with temperature and is equal to 1.29 at 25°C. The previously determined nonoperating base failure rates then had to be divided by 1.29 to be compatible with the modified temperature factor. The modified nonoperating base failure rate constant was equal to .00029 and the VLSI nonoperating base failure rate was equal to .014 failures/10⁶ hours.

TABLE 5.1.2-11: K_3 and K_4 TEMPERATURE FACTOR CONSTANTS FOR DIGITAL MICROCIRCUITS

Technology	K_3	K_4
TTL, HTTL, DTL, ECL	.91	.09
LTTL, STTL	.90	.10
LSTTL	.89	.11
IIL	.86	.14
MNOS	.61	.39
PMOS	.68	.32
NMOS, CCD	.65	.35
CMOS, CMOS/SOS	.58	.42

Normalization of the base failure rate and modification of the temperature factor concluded the model development process for digital microcircuits. The proposed nonoperating failure rate prediction model was found to be a function of gate count, technology, temperature, screening, hermeticity, equipment power on-off cycling and application environment. The model is presented in Section 5.1.1 and in Appendix A in a form compatible with MIL-HDBK-217D. Monolithic microcircuit model

validation was performed using data from AFCIQ and is described in Section 5.1.5.

5.1.3 Linear/Interface Microcircuits

A nonoperating failure rate modeling approach was also successfully applied for linear/interface microcircuits. The approach taken was similar to the digital microcircuit model development. A theoretical nonoperating failure rate prediction model was hypothesized, and then evaluated and quantified with the available data. The resultant nonoperating failure rate prediction model was found to be a function of complexity, quality, temperature, environment and equipment power on-off cycling frequency. The model is presented in Section 5.1.1 and in Appendix A in a format compatible with MIL-HDBK-217D.

The initial step in the model development process was to identify application and construction variables which characterize linear and interface microcircuits in a nonoperating environment. These variables represent possible failure rate model parameters and are presented in Table 5.1.3-1.

The theoretical model for linear/interface devices was essentially the same as the digital microcircuit theoretical model. It was assumed that the model would be multiplicative, but nonlinear due to the equipment power cycling factor. Additionally, the theoretical model included complexity, technology, hermeticity, screening, temperature, environment and equipment power cycling as model parameters.

The summarized linear/interface microcircuit nonoperating reliability data is presented in Table 5.1.3-2. The collected data consists of 76 observed failures, 3605.8×10^6 nonoperating part hours and 124 individual data records. Data was available for parts screened to S, B, B-1, B-2, D and D-1 quality levels.

TABLE 5.1.3-1: LINEAR/INTERFACE MICROCIRCUIT CHARACTERIZATION VARIABLES

- I. Style
 - A. Linear
 - B. Interface
- II. Technology

A. DTL	E. ECL	I. IIL	M. CCD
B. TTL	F. LTTL	J. MNOS	N. CMOS
C. HTTL	G. STTL	K. PMOS	O. CMOS/SOS
D. DTL	H. LSTTL	L. NMOS	P. HMOS
- III. Number of Transistors
- IV. Construction

A. Dip	E. Chip Carrier
B. Can	F. Quad In-Line (staggered leads)
C. Flatpack	G. In-Line
D. Square	
- V. Enclosure
 - A. Hermetic
 - B. Non-Hermetic
- VI. Package Material

A. Metal	E. Glass	I. Metal/Epoxy
B. Ceramic	F. Plastic/Ceramic	J. Silicon
C. Metal/Ceramic	G. Epoxy	K. Phenolic
D. Metal/Glass	H. Ceramic/Plastic/Window	
- VII. Number of Pins
- VIII. Number of Interconnects
- IX. Die Bond
 - A. Eutectic
 - B. Epoxy
 - C. Glass
- X. Quality Level

A. S	C. B-1	E. C	G. D
B. B	D. B-2	F. C-1	H. D-1
- XI. Application Environment
- XII. Temperature
 - A. Rated
 - B. Actual
- XIII. Number of Power On/Off Cycles per 10^3 Nonoperating Hours

TABLE 5.1.3-2: LINEAR/INTERFACE MICROCIRCUIT NONOPERATING
FAILURE RATE DATA

No.	Equipment/Source	Data Records	Complexity (# transistors)	Failures	Part Hours (x 10 ⁶)
1	Hawk/MICOM	3	1-30	3	1,123.0
2	Maverick/MICOM	4	1-30	6	885.4
3	F-16 HUD/RIW	8	1-30	5	285.5
4	F-16 HUD/RIW	11	31-100	15	519.0
5	F-16 HUD/RIW	1	>100	2	13.0
6	Martin Marietta	2	1-30	3	771.0
7	PRC	3	1-30	0	0.6
8	RAC (1)	66	1-30	6	4.7
9	RAC (1)	20	31-100	32	1.6
10	RAC (1)	2	>100	2	0.1
11	RAC (1)	4	(2)	2	1.9
Totals		124		76	3,605.8

Notes 1) High temperature storage life test data. Storage temperatures range from 150°C to 200°C

2) Unknown

The collected nonoperating failure rate data for linear and interface devices was initially subjected to a preliminary analysis. Weaknesses in the data base were identified, and correlation coefficients were computed for each pair of independent variables. Additionally, zero failure data were analyzed to determine which data entries had sufficient part hours to estimate an upper bound on nonoperating failure rate. Results from these initial analyses are the following:

- 1) All collected data were from a ground based environment or from storage life testing.
- 2) All data were for bipolar linear/interface devices.

- 3) 73% of the high temperature data records and 98% of the high temperature storage failures were for D or D-1 quality level parts.
- 4) 100% of the ground field data were for S or B quality level parts
- 5) The correlation coefficient for number of transistors vs. number of pins was equal to 0.70.

The distribution of quality levels presented a problem. The higher quality devices were concentrated in the lower temperature applications. Similarly, the lower quality devices were concentrated in the high temperature applications. Therefore, the effects of temperature and quality could not both be determined empirically. After consideration of several options, it was decided to assume that the nonoperating quality factors developed for digital microcircuits would also apply for linear/interface microcircuits. This assumption was based on the premise that screening impacts all monolithic microcircuits similarly. Thus, the nonoperating quality factors presented in Table 5.1.2-6 of the previous section were used for nonoperating failure rate prediction of linear/interface devices. To remove the effect of quality level from the data, the number of part hours were multiplied by the respective nonoperating quality factor to normalize the data. After normalizing the data for quality level, the effect of temperature could then be evaluated.

It had been desired to analyze the effect that both number of pins and number of transistors had on nonoperating failure rate. However, the apparent correlation between these two variables prevented evaluation of the effect of both variables by use of regression analysis. This observed correlation between number of transistors and number of pins was hardly unexpected. As a result of the high degree of correlation, it was concluded that only one measure of device complexity would be included in the model. The natural logarithm of number of transistors was chosen to be included in the regression and was designated C_1 .

It should also be noted that if two variables are correlated inherently (as opposed to coincidentally), then it would not be desirable

to determine separate factors. A model with separate factors for transistor count and pin count would be correct physically, but probably less accurate. At least one of the factors would have to be based on an assumption. Assumptions always introduce some degree of error. Determination of the other factor would be adversely effected by an inaccurate assumption, and thus, both factors would be incorrect. Conversely, an empirical relationship versus either one of the inherently correlated variables represents the actual failure experience of the device, and would be preferable.

The theoretical model for linear/interface devices included a factor for equipment power on-off cycling. The multiplicative factor was assumed to be of the following form.

$$\text{Cycling Factor} = 1 + K(\text{cycles}/10^3 \text{ hours})$$

where K is a constant. A model with a factor of this form is not linear and regression analysis could not be directly applied. This potential problem and a proposed solution is described in Section 4.3. The proposed solution involved performing iterative regression analyses. As recommended in Section 4.3, three qualitative "dummy" variables were defined (cyc1, cyc2 and cyc3) to represent four distinct equipment power cycling frequency categories, which are,

- o cycling rates less than one power cycle every two years (cyc1, cyc2, cyc3 = 0,0,0).
- o cycling rates between one cycle per year and one cycle every two years (cyc1, cyc2, cyc3 = 1,0,0).
- o cycling rates greater than one cycle per year (cyc1, cyc2, cyc3 = 0,1,0).
- o unknown cycling rates (cyc1, cyc2, cyc3 = 0,0,1).

The linear/interface nonoperating failure rate data were then merged according to equipment, temperature, quality level and transistor count. To maximize the number of failures and part hours per data record, data

within 10 transistor intervals were merged. For example, the observed failures and part hours were summed for all B quality linear devices in the Maverick missile with between 21 and 30 transistors. The average number of transistors for the category was used as the measure of complexity in the regression analysis. There were a total of 23 merged data records for linear/interface devices.

Regression analysis was then applied to the data. Results of the regression analysis are given in Table 5.1.3-3. The dependent variable was the natural logarithm of nonoperating failure rate. The number of transistors (C_1) and the inverse of temperature (designated $1/T$) were determined to significantly effect nonoperating failure rate with 90% confidence. The equipment power cycling variable for cycling rates greater than one cycle per year (cyc2) was significant with 70% confidence.

TABLE 5.1.3-3: LINEAR/INTERFACE INITIAL REGRESSION RESULTS

Variable	Coefficient	Standard Error	F-Ratio	Confidence Limit
$1/T$	-4027.505	555.208	52.62	0.90
C_1	0.841	0.340	6.11	0.90
cyc2	0.983	0.802	1.50	0.70
b_0	6.065	--	--	--

The coefficients given in Table 5.1.3-3 were the results of a regression analysis with the dependent variable equal to the natural logarithm of nonoperating failure rate normalized to remove the effects of quality level. Transforming the regression solution into an equation where nonoperating failure rate (as opposed to log of normalized nonoperating failure rate) is the dependent variable results in the following preliminary multiplicative model for linear/interface devices.

$$\lambda_{1/i} = 0.00058(\# \text{ transistors})^{.841} \exp(-4028(\frac{1}{T} - \frac{1}{298})) \pi_{NQ} \pi_{cyc} \epsilon$$

where

$\lambda_{1/i}$ = predicted linear/interface microcircuit nonoperating failure rate (failures/ 10^6 hours)

T = temperature ($^{\circ}$ K)

π_{NQ} = assumed nonoperating quality factors

π_{cyc} = equipment power cycling factor (preliminary)

= $\exp(0.983(\text{cyc}^2))$

= 1.0, cycling rate < .057 cycles/ 10^3 hour

= 1.0, $.057 \leq$ cycling rate < .114 cycles/ 10^3 hour

= 2.67, cycling rate \geq .114 cycles/ 10^3 hour

ϵ = residual

The reference temperature term of 298 $^{\circ}$ K was added to the previous equation for convenience. Therefore, the multiplicative constant of 0.000581 corresponds to a temperature equal to the reference temperature.

It was hypothesized that the reason that the cyc1 and cyc3 variables were not determined to be significant was that storage related failures (as opposed to failures induced by the power on-off cycle) dominate the total failure rate for cycling rates less than 0.114 cycles/ 10^3 hours. Therefore, the anticipated difference in failure rate would be less than the inherent variability in the data and could not be detected. It was considered encouraging that the unknown cycling frequency data entries were not significantly different than the data in the two lower cycling frequency categories. Although the cycling frequency was unknown for these data sources, it was known that the equipments were energized relatively infrequently.

The next step in the model development process was to perform iterative regression analyses to accommodate the assumed nonlinear model form. The process began by performing a two-dimensional regression with the cycling rate coefficients from the initial regression as the dependent variable, and the mean cycling rate for each category as the independent variable. The result was an expression for equipment power cycling factor

of the desired form (i.e. cycling factor = $mx + b$). As the iterative process continued, the equipment power cycling expression was assumed exact and the coefficients for all other variables were recalculated. Then, those coefficients were assumed exact and the equipment power cycling factor was recalculated. The iterative process continued until the observed changes in coefficient values were negligible. For linear/interface microcircuits, six iterations were required before the optimal nonlinear regression solution was found. On the final iteration, the temperature coefficient changed by 1/10th of 1% and the complexity coefficient changed by 4/10th of 1%. The coefficients for $1/T$, C_1 and b_0 after the sixth iteration are given in Table 5.1.3-4. The optimal form of the equipment power cycling factor expression was determined to be,

$$\pi_{cyc} = 1 + .0309(N_C)$$

where

N_C = number of equipment power on-off cycles per 10^3 nonoperating hours

TABLE 5.1.3-4: LINEAR/INTERFACE FINAL REGRESSION RESULTS

Variable	Coefficient	Standard Error	F-Ratio	Confidence Limit
$1/T$	-4748.303	448.970	111.85	0.90
C_1	0.887	0.297	9.24	0.90
b	6.065	--	--	--

As had been expected, temperature was determined to be the dominant variable effecting failure rate. The linear/interface temperature coefficient of -4748 is equivalent to an activation energy of 0.41eV. The standard error statistic allowed for computation of a 90% confidence interval around the point estimate temperature coefficient value. Upper and lower 90% confidence interval values for linear/interface devices were determined to be -3974 and -5523 respectively. These values are only

approximate because of the log transformation. It was decided to include the effect of temperature into a nonoperating temperature factor. For linear/interface devices, the temperature factor was determined to be the following equation. As previously stated, the 298 term is a reference temperature and was added for convenience.

$$\pi_{NT} = \exp(-4748(\frac{1}{T} - \frac{1}{298}))$$

where

π_{NT} = nonoperating temperature factor

A base failure rate for linear/interface devices was defined as a function of the number of transistors. Upper and lower 90% confidence interval values for the base failure rate complexity coefficient of 0.887 were computed and found to be 1.40 and 0.375 respectively. As this stage of the model development process, the base failure must be considered preliminary because the value has yet to be normalized for environment. A preliminary base failure rate expression was determined to be,

$$\lambda'_{nb} = 0.000576(\# \text{ transistors})^{.887}$$

where

λ'_{nb} = preliminary base failure rate

The next phase of the model development process for linear and interface microcircuits was to investigate the effects of the environment. Data were only available for ground based environments, and thus, a series of nonoperating environmental factors could not be determined empirically. However, it was essential that an appropriate series of factors were determined so the proposed model could be used for any potential application with linear/interface devices.

Several possibilities were evaluated to determine appropriate nonoperating environmental factors for linear and interface microcircuits. Consideration was given to development of a unique series of factors for linear/interface devices using the methods described in Section 4.5 of this report. However, it was eventually decided to apply the same factors developed for nonoperating failure rate prediction of digital microcircuits (presented in Table 5.1.1-3 in Section 5.1.1). This factor includes unique nonoperating environmental factor values for hermetic and nonhermetic microcircuits. This decision was made for two reasons. First, the use of one series of environmental factors for various microcircuit types has a precedent. The operating failure rate prediction procedure for microcircuits presented in MIL-HDBK-217D includes a single series of factors for all monolithic microcircuits. The second reason for using the digital nonoperating environmental factors was that the nonoperating environmental factor development process was only approximate. Therefore, the relatively smaller differences between specific microcircuit styles could not be justified.

The final step in the linear/interface model development process was to normalize the base failure rate equation to correspond to a ground benign environment. All observed field data were for a ground fixed environment. Therefore, the preliminary base failure rate constant of 0.000576 was divided by the ground fixed hermetic environmental factor of 2.4 to obtain a normalized base failure rate constant equal to 0.000240.

The first phase of the model validation task (described in Section 4.1.5) resulted in the observation that the preliminary nonoperating failure rate model exceeded the MIL-HDBK-217D failure rate prediction a small percentage of the time. To prevent these occurrences, a modification was made to the nonoperating temperature factor. The modified form of the temperature factor is given by the following equation.

$$\pi_{NT} = 0.50 + 0.50 \exp(-4748(\frac{1}{T} - \frac{1}{298}))$$

The 0.50 constants were based on a vigorous exercising of both operating and nonoperating failure rate models. A small adjustment was also required to the nonoperating base failure rate because the average temperature for the field data was 20°C compared to the reference temperature of 25°C (i.e. 298°K). The adjustment factor of 1.16 resulted in a nonoperating base failure rate constant equal to 0.000208 failures/10⁶ hours.

Definition and determination of a nonoperating temperature factor, base failure rate and nonoperating environmental factor, and normalization of the base failure rate constant concluded the model development process for linear/interface devices. The proposed model for linear/interface devices is thereby given by the following equation. The residual term was removed from the expression.

$$\lambda_{l/i} = \lambda_{nb} \pi_{NT} \pi_{NQ} \pi_{NE} \pi_{cyc}$$

where

$\lambda_{l/i}$ = predicted linear/interface microcircuit nonoperating failure rate

λ_{nb} = base failure rate (failure/10⁶ nonoperating hours)
 $= 0.00021(N_t)^{.887}$

where

N_t = number of transistors

π_{NT} = nonoperating temperature factor
 $= 0.50 + 0.50 \exp(-4748(\frac{1}{T_{avg}} - \frac{1}{298}))$

π_{NQ} = nonoperating quality factor (presented in Table 5.1.1-2 in Section 5.1.1)

π_{NE} = nonoperating environmental factor (presented in Table 5.1.1-3 in Section 5.1.1)

π_{cyc} = equipment power on-off cycling factor
 $= 1 + .031(N_c)$

determined microcircuit nonoperating failure rate factors for quality, environment, temperature and equipment power on-off cycling frequency. The results of the first regression indicated that these factors could also be applied for memory nonoperating failure rate prediction purposes. These factors were then assumed to be correct and the data were subjected to a second regression. Introduced into the second regression were variables for memory type, technology and the number of gates. Only the technology variable was significant with a 70% confidence. Interpretation of the regression results were that bipolar memory devices have a nonoperating failure rate which is 2.1 times higher than MOS memory devices at the reference temperature of 25°C.

TABLE 5.1.4-1: MEMORY DEVICE NONOPERATING FAILURE RATE DATA

No.	Equipment/Source	Data Records	Complexity (# bits)	Failures	Part Hours (x10 ⁶)
1	RAC (1)	7	< 256	1	0.4
2	RAC (1)	24	256	13	1.0
3	RAC (1)	4	320	3	1.1
4	RAC (1)	2	512	0	0.2
5	RAC (1)	1	567	0	0.1
6	RAC (1)	48	1024	23	4.0
7	RAC (1)	3	2048	2	0.2
8	RAC (1)	12	4096	8	1.5
9	RAC (1)	11	8192	67	0.9
10	RAC (1)	4	16384	1	0.6
11	F-16 HUD/RIW	1	64	0	77.9
12	F-16 HUD/RIW	2	1024	1	337.4
13	F-16 HUD/RIW	1	4096	3	181.7
14	F-16 HUD/RIW	1	16384	0	207.6
Totals		121		122	814.6

NOTES: (1) High temperature storage life test data.

Additional regression solutions were found to further investigate the effects of number of bits and memory type. The difference in nonoperating failure rate between RAM and ROM memory devices was not significant with 50% confidence. When forced into the regression solution, the ratio of RAM to ROM nonoperating failure rate was found to be 0.67. However,

where

N_C = number of equipment power on-off cycles per 10^3 nonoperating hours

The proposed linear/interface nonoperating failure rate prediction model is presented in Section 5.1.1 and in Appendix A in a form compatible with MIL-HDBK-217D. Monolithic microcircuit model validation including linear/interface devices is described in Section 5.1.4.

5.1.4 Memory Device Model Development

A nonoperating failure rate prediction model was also successfully developed for memory devices. The model development approach was similar to the digital and linear device model development processes. The proposed model was determined to be a function of device style, quality, temperature, environment, hermeticity and screening level. The model is presented in Section 5.1.1 and in Appendix A in a format compatible with MIL-HDBK-217D. This section describes the model development process for memory devices.

The theoretical model for memory devices was essentially the same as the models for other microcircuit types. The theoretical model was assumed to be a function of complexity, technology, hermeticity, screening, temperature, environment and equipment power on-off cycling.

The summarized memory device nonoperating failure rate data are presented in Table 5.1.4-1. The data collectively consists of 122 observed failures, 814.6×10^6 nonoperating part hours and 121 individual data records. All data were either from the F-16 HUD, or from high temperature storage life testing. The inherent data base weaknesses identified for other microcircuit types also applied for memory ICs.

Two regression analyses were applied to the data to quantify the theoretical model. A first regression was used to evaluate the previously

numerical values computed with low confidence are not necessarily meaningful. Similarly, the number of bits was not significant with 50% confidence. When forced into regression solution, the data indicated that nonoperating failure rate was negatively correlated with the number of bits. Intuitively incorrect solutions, such as this, are not unusual when variables are forced into a regression solution with very low confidence. Neither memory type or number of bits was included in the proposed model because of the low observed correlation with nonoperating failure rate.

It was considered unusual that complexity was not a significant variable for memory devices given that the number of gates and number of transistors were significant variables for random logic and linear microcircuits respectively. One possible explanation for this observation is that as complexity has historically increased, corresponding advances have been made to optimize manufacturing technology. Thus, the expected increase in failure rate may be negated by corresponding increases in production technology, quality control and screening. Another possible explanation for the observed lack of correlation was that the statistical noise in the data prevented all but the most significant variables from being identified. However, neither of these explanations indicate why complexity would be significant for random logic and linear devices, but not memories. It was decided not to assume a complexity relationship for several reasons. Including an assumed complexity factor would needlessly complicate the proposed model when no observed correlation can be detected, for whatever the reason.

The proposed model for memory devices is therefore given by the following equation. The nonoperating base failure rates are the numerical values determined from the data. The other factors were previously determined for random logic microcircuits.

$$\lambda_m = \lambda_{nb} \pi_{NT} \pi_{NQ} \pi_{NE} \pi_{cyc}$$

where

λ_m = memory device nonoperating failure rate

λ_{nb} = nonoperating base failure rate

= .0034, bipolar memory devices

= .0017, MOS memory devices

π_{NT} = nonoperating temperature factor

= $\exp(-A_n(\frac{1}{T} - \frac{1}{298}))$

where

T = nonoperating temperature ($^{\circ}\text{K}$)

A_n = temperature coefficient (given in Table 5.1.2-7 in Section 5.1.2)

π_{NQ} = nonoperating quality factor (given in Table 5.1.1-1 in Section 5.1.1)

π_{NE} = nonoperating environmental factor (given in Table 5.1.1-2 in Section 5.1.1)

π_{cyc} = equipment power on-off cycling frequency
= $1 + .02(N_c)$

where

N_c = number of equipment power on-off cycles per 10^3 nonoperating hours

Determination of the memory device nonoperating base failure rates was the final phase of the model development process. The proposed model is presented in Appendix A in a format compatible with MIL-HDBK-217D.

5.1.5 Monolithic Microcircuit Model Validation

The proposed microcircuit nonoperating failure rate prediction models were next subjected to a thorough model validation process. The first phase of the model validation process consisted of an in-depth comparison

of nonoperating failure rate prediction models to the MIL-HDBK-217D models. This phase served to identify cases where the predicted nonoperating failure rate exceeded the predicted operating failure rate. The second phase of the model validation task consisted of an extreme case analysis. Predictions were made using the proposed models for parameters beyond the ranges found in the data. The intent of the extreme case analysis was to identify any set of conditions which cause the predicted nonoperating failure rates to approach infinity or predict an intuitively incorrect failure rate. This exercise did not actually serve to validate the proposed model, but was an important step in the overall model development process and was useful to insure that the proposed models were physically correct. The third phase of the model validation task was to compare the predicted nonoperating failure rates with observed field data which had been withheld from the model development process. Nonoperating microcircuit data were collected from AFCIQ but not used because of part characterization problems.

The first phase of the model validation task consisted of a vigorous exercising of the models to identify cases where the predicted nonoperating failure rate exceeds the MIL-HDBK-217D operating failure rate. The probability of this seemingly unlikely event approaches 50% (if the failure rate estimates are distributed normally) as the inherent nonoperating failure rate becomes close to the inherent operating failure rate. This stems from the fact that failure rate is a random variable and the predicted failure rates represent averages computed from a limited data sample. The averages computed from different data samples would be distributed about some unknown inherent mean failure rate. Some of the average failure rates will be higher than the inherent failure rate and some will lower. Therefore, as the inherent operating and nonoperating failure rates become close, there will be close to a 50% probability that the average failure rate computed from a sample of nonoperating failure data will exceed the average failure rate computed from a sample of operating failure data. An example where the inherent nonoperating failure rate would be anticipated to be close to the inherent operating failure rate is for highly screened devices exposed to a high ambient

temperature and with a low power dissipation and IC junction-to-case thermal resistance. In other words, there would be little difference between operating and nonoperating junction temperature, and temperature would be the dominant failure causal stress.

Despite the conclusions of the previous paragraph, it was believed that nonoperating failure rate predictions which exceed the corresponding operating failure rate prediction (even if this occurs only a small percentage of the time) could seriously detract from the credibility of MIL-HDBK-217D. Many handbook users incorrectly treat MIL-HDBK-217D failure rate predictions as an inherent property of the device. It was determined that a modification to the model would have little effect on model accuracy yet would increase the credibility of the models.

To identify instances where the nonoperating failure rate prediction exceeded the MIL-HDBK-217D failure rate, a sample size of 40 microcircuits were selected. The selected microcircuits represented the full range of available quality levels, technologies, and complexities. These same 40 microcircuits are presented in Table 7.0-1 in Section 7.0, "Comparison of Operating and Nonoperating Failure Rates." Operating and nonoperating failure rate predictions were made using MIL-HDBK-217D and the preliminary nonoperating failure rate prediction model for three different ambient temperatures (20°C, 40°C, and 60°C) and two environments (ground, fixed and airborne, uninhabited fighter). Comparisons were then made for operating to nonoperating ground fixed environments (e.g., most ground based equipments), operating to nonoperating airborne uninhabited fighter environment (e.g., captive carry missiles), and operating airborne uninhabited fighter to nonoperating ground fixed environments (e.g., most avionic equipments). A total of 480 failure rate predictions and 360 failure rate comparisons were computed. The nonoperating failure rate prediction exceeded the MIL-HDBK-217D failure rate prediction in seven instances or in 1.9% of the comparisons. In each of these instances, the ambient temperature was 60°C.

After this phase of the model evaluation task, a modification was made to the nonoperating temperature factor as part of the model development task. The modified models have the same equivalent activation energy for high temperatures. The only difference is that the modified temperature factor model approaches a constant value as temperature becomes very low.

The second phase of the model validation task was an extreme case analysis. This analysis did not indicate any deficiencies with the proposed models. Quantitative factors for temperature, complexity and equipment power on-off cycling were tested by this method. At extremely high levels of equipment power cycling, the nonoperating failure rate for each microcircuit model becomes directly proportional to the equipment power cycling frequency. At low levels of equipment power cycling, the proposed microcircuit nonoperating failure rates approach a constant value. These extreme case results confirm intuitive reliability relationships. At extremely high equipment power cycling rates, the nonoperating failure rate would be expected to be dominated by failures induced by the power on-off cycle. Therefore, it would be anticipated that the relationship would be proportional. At extremely low equipment power cycling rates, the failure rate would be expected to be equal to the inherent storage/dormant failure rate, and independent of power cycling frequency.

The microcircuit nonoperating failure rate data collected from AFCIQ were not used in the model development process because device complexity, equipment power cycling frequency and screening level could not be determined. However, typical values for these parameters were assumed and the observed nonoperating failure rates were compared to the corresponding predicted values. Table 5.1.5-1 presents the model validation data. Additionally, the predicted nonoperating failure rate is included in Table 5.1.5-1. Equivalent quality levels were provided by AFCIQ. The complexity levels were known to be less than 100 gates for digital devices and 100 transistors for linear devices. Fifty gates and 50 transistors were assumed to compute the predicted failure rates. One equipment power cycle per 10^3 nonoperating periods was also assumed. Due to the number of

assumptions, the model validation with AFCIQ data could only serve to identify large errors.

TABLE 5.1.5-1: MONOLITHIC MICROCIRCUIT MODEL VALIDATION DATA

No.	Fail.	Part Hours (x10 ⁶)	Description	Temp. (°C)	Equiv. Quality	$\lambda_{.05}$	λ_0	$\lambda_{.95}$	λ_{pre}
1	0	22	digital, bipolar	(1)	D	--	--	.1361	.0115
2	0	240	digital, bipolar	25	D	--	.0042	.0125	.0115
3(2)	1	2	digital, bipolar	150	D	.0307	.5988	2.84	.0605
4	22	1330	digital, bipolar	5-30	D	.0111	.0165	.0235	.0115
5	2	59	digital, bipolar	5-30	B	.0060	.0339	.1067	.0046
6(3)	20	25	digital, bipolar	85-135	B	.5302	.8000	1.16	.0579
7	2	159	linear, bipolar	(1)	D	.0022	.0126	.0396	.0406
8	0	24	linear, bipolar	25	D	--	--	.1248	.0406
9(2)	0	<1	linear, bipolar	150	D	--	--	7.30	1.08
10	3	80	linear, bipolar	5-30	D	.0103	.0375	.0969	.0406
11	0	6	linear, bipolar	5-30	B	--	--	.4992	.0163

50 1947

NOTES: (1) Temperature was unknown for these data entries. 25°C was assumed.

(2) Data entry was from high temperature storage life testing.

(3) Data entry was from temperature cycling test (85°C to 135°C) Environment assumed to be airborne, uninhabited fighter.

The model evaluation process indicated that the proposed models were accurate. Although no substantial conclusion could be reached because of the assumptions. The geometric mean of the ratio of observed to predicted failure rate was equal to 2.1 for those data entries with observed failures or sufficient part hours to estimate a failure rate without observed failures (i.e. data entries 2, 3, 4, 5, 6, 7, 10). Strict interpretation would therefore indicate that the proposed model predicted a failure rate which is lower than actual. However, it should also be noted that the geometric mean of the ratio of observed to predicted failure rate is equal to 0.97 for only the field data entries. High temperature life test data is inherently more variable because it necessarily reflects only the beginning of the device lifetime.

Additionally, test data generally consists of many parts on test for a relatively short time each.

The proposed nonoperating failure rate prediction models for monolithic microcircuits are probably the most important models presented in this report. The proposed models provide proper discrimination against application variables which influence failure rate. Additionally, they are easy to apply and have been shown to be relatively accurate. The use of the proposed monolithic microcircuit nonoperating failure rate prediction models, as well as the other models presented in this report, will greatly enhance nonoperating failure rate assessment capabilities.

5.1.6 Hybrid Microcircuit Nonoperating Failure Rate Model

This section presents the proposed nonoperating failure rate prediction model for hybrid microcircuits. The proposed model is presented in Appendix A in a form compatible with MIL-HDBK-217D. The proposed model is given by the following relationship.

$$\lambda_p = \lambda_{nb} \pi_{NQ} \pi_{NE}$$

where

$$\begin{aligned} \lambda_p &= \text{predicted hybrid microcircuit nonoperating failure rate} \\ \lambda_{nb} &= \text{nonoperating base failure rate (includes an average failure} \\ &\quad \text{rate contribution for capacitors, packaged resistors, substrate} \\ &\quad \text{resistors and the substrate) (failures/10}^6 \text{ hours)} \\ &= A_1 \exp(.45(N_D) + .45(N_T) + .81(N_{IC})), N_D + N_T + 1.8N_{IC} \leq 12.2 \\ &= A_2 \exp(.033(N_D) + .033(N_T) + .059(N_{IC})), N_D + N_T + 1.8N_{IC} > 12.2 \end{aligned}$$

where

$$\begin{aligned} N_D &= \text{number of diodes} \\ N_T &= \text{number of transistors} \\ N_{IC} &= \text{number of integrated circuits} \end{aligned}$$

$A_1 = .0000817$

$A_2 = .013$

π_{NQ} = nonoperating quality factor

= 0.53, S

= 1.0, B

= 8.6, D

π_{NE} = nonoperating environmental factors (see Table 5.1.6-1)

The next section describes the nonoperating hybrid model development process.

5.1.7 Hybrid Model Development

The failure rate modeling approach described in Section 4.1 was implemented for hybrid devices. Two assumed theoretical models were investigated by analysis of the available hybrid nonoperating reliability data. Both resulting failure rate prediction models were thoroughly analyzed and an optimum model determined. The first theoretical model was a function of the number of diodes, transistors, integrated circuits (ICs), resistors and capacitors in the hybrid. The second theoretical model was similar to the operating hybrid failure rate model developed by IITRI (Reference 30) which was determined to be a function of the number of interconnects. In addition, the effects of device screening, seal perimeter, environment and equipment power on-off cycling frequency were investigated as part of each theoretical model.

The first step in the model development process was to identify application and construction variables which properly characterize hybrids in a nonoperating environment. Table 5.1.7-1 presents a list of the part characterization variables for hybrids. These variables are possible failure rate model input parameters which were analyzed using statistical methods when possible.

TABLE 5.1.6-1: HYBRID NONOPERATING ENVIRONMENT FACTORS (π_{NE})

Environment	π_{NE}
G _B	1
G _F	2.4
G _M	3.5
M _P	3.2
N _{SB}	3.4
N _S	3.4
N _U	4.5
N _H	4.6
N _{UU}	4.9
A _{RW}	6.3
A _{IC}	2.4
A _{IT}	2.7
A _{IB}	4.0
A _{IA}	3.4
A _{IF}	4.7
A _{UC}	2.7
A _{UT}	3.4
A _{UB}	5.7
A _{UA}	4.7
A _{UF}	6.7
S _F	1.3
M _{FF}	3.3
M _{FA}	4.3
U _{SL}	8.0
M _L	9.3
C _L	150

TABLE 5.1.7-1: HYBRID PART CHARACTERIZATION

- I. Functional Group
 - A. Digital
 - B. Linear
- II. Number of Components
 - A. Packaged Resistors
 - B. Capacitors (packaged/chip)
 - C. Diodes (packaged/die)
 - D. Transistors (packaged/die)
 - E. Microcircuits (packaged/die)
- III. Number of Chip and Substrate Resistors
- IV. Number of Active Interconnections
 - A. Bimetal Bonds
 - B. Single Metal Bonds
- V. Seal Perimeter (inches)
- VI. Substrate Area (Square Inches)
- VII. Quality Level
 - A. S
 - B. B
 - C. D
- VIII. Application Environment
- IX. Temperature
 - A. Rated
 - B. Actual
- X. Number of Equipment Power On/Off Cycles per 10^3 Nonoperating Hours

The first theoretical model for hybrids was determined to be the following equation (f denotes a function).

$$\lambda_{h1} = f(N_D, N_T, N_{IC}, N_{R1}, N_{R2}, N_C, S) \pi_{NQ} \pi_{NE} \pi_{cyc}$$

where

λ_{h1} = predicted hybrid nonoperating failure rate (failures/10⁶ hours)

N_D = number of diodes

N_T = number of transistors

N_{IC} = number of integrated circuits

N_{R1} = number of packaged resistors

N_{R2} = number of chip or substrate resistors

N_C = number of capacitors

S = seal perimeter (inches)

π_{NQ} = nonoperating quality factor, based on device screening

π_{NE} = nonoperating environmental factor

π_{cyc} = equipment power on-off cycling factor

$$= 1 + K(N_C)$$

where

K = constant

N_C = equipment power on-off cycling rate (cycles/10³ nonop. hours)

The second theoretical model was based on the premise that the total number of interconnections sufficiently characterizes hybrid device complexity. The number of interconnections is typically equal to one for each diode and external lead, equal to two for each transistor, capacitor and chip resistor and equal to the number of chip bonding pads for integrated circuits. The second theoretical model was the following equation.

$$\lambda_{h2} = f(N_I, S) \pi_{NQ} \pi_{NE} \pi_{cyc}$$

where

N_I = number of interconnects

S = seal perimeter (inches)

Presentation of these theoretical models does not imply that each of the variables is significant. Statistical methods were applied as a basis for establishing the significance of variables. The theoretical model was intended to define the relationship of the independent variables to each other.

The summarized hybrid nonoperating reliability data collected in support of this study is presented in Tables 5.1.7-2. The data consists of 27 individual data records, 2082 observed failures with $50,049.89 \times 10^6$ part hours.

TABLE 5.1.7-2: SUMMARIZED HYBRID NONOPERATING RELIABILITY DATA

Equipment/Source	# Data Records	# Failures	Part Hours ($\times 10^6$)
Maverick/MICOM	17	1,969	22,529.73
Hawk/MICOM	7	109	27,416.36
F-16 HUD/RIW	3	4	103.80
Totals	27	2,082	50,049.89

Point estimate failure rates were computed for data records with observed failures. The methods described in Section 3.3 were applied to determine which zero failure data records had sufficient part hours to be included in the analysis. All twenty seven data records had either observed failures or sufficient part hours to estimate a failure rate without observed failures.

The number of variables which could be analyzed empirically was limited by the nature of the available data. The following attributes of

the collected hybrid data were identified during a preliminary data analysis:

- 1) There was an insufficient range of environments represented in the data to develop a series of environmental factors based only on the data.
- 2) There was an insufficient range of quality levels to develop a quality factor series based upon the data.
- 3) There was an insufficient range of ambient temperature to study the effects of temperature analytically.
- 4) All data were for digital hybrids.
- 5) There was a high degree of correlation between many of the "independent" variables.

One major problem identified in the available data was a high level of correlation between a large number of the potential model variables. The following pairs of variables had a correlation coefficient greater than 0.40:

- o interconnects and number of resistors
- o interconnects and number of diodes
- o interconnects and number of ICs
- o interconnects and cycling rate
- o number of resistors and number of diodes
- o number of resistors and cycling rate
- o number of capacitors and number of transistors
- o number of diodes and seal perimeter
- o number of transistors number of ICs
- o number of transistors and seal perimeter
- o number of transistors and cycling rate
- o number of ICs and cycling rate

This many correlated variables made proper application of regression analysis impossible. A correlation coefficient matrix is presented in Table 5.1.7-3. A discussion of correlation coefficients is presented in Section 3.2.

TABLE 5.1.7-3: HYBRID VARIABLE CORRELATION COEFFICIENT MATRIX

	Variables							
	IN	R	C	D	T	IC	S	CYC
IN	1.0							
R	.67	1.0						
C	-.21	-.15	1.0					
D	.41	.75	-.25	1.0				
T	-.33	-.33	.45	.04	1.0			
IC	.69	.33	-.10	-.18	-.64	1.0		
S	.15	.21	.06	.42	.41	-.17	1.0	
CYC	.80	.57	-.26	.13	-.75	.78	-.25	1.0

NOTE (1): IN = # interconnects, R = # resistors, C = # capacitors, D = # diodes, T = # transistors, IC = # integrated circuits, S = seal perimeter (inches), CYC = equipment power cycling rate (cycles/10³ hrs.)

The correlation coefficients for hybrids were much larger than those for any other part type in this study. Probable reasons for the large coefficients were the small number of data sources available with hybrid nonoperating failure rate data, and the small number of hybrids typically used in an equipment. Also, many of the correlations were expected because as the hybrid becomes more complex, the size and the number of components must increase. As a result of the high correlation, multiple linear regression analysis could not be correctly applied to the data to simultaneously investigate the effects of all variables. This observation was one of the reasons to attempt two different modeling approaches. The high degree of correlation between interconnects and resistors, diodes, and ICs prevented a numerical analysis of both the number of interconnects and the number of components. However, if the number of interconnects sufficiently characterizes hybrid complexity by itself, then a two-dimensional regression (failure rate vs. number of interconnects) could be correctly applied to develop a hybrid nonoperating failure rate prediction model. This is not to say that only interconnects fail in a hybrid device. If the number of interconnects increase simultaneously

with the number of components, then a regression against either one of these parameters will include the effects of both.

It should be noted that the observed correlation between number of interconnects and number of active components was hardly unexpected. In fact, these two parameters must be correlated because of the nature of a hybrid design. Therefore, it would be undesirable to include both number of interconnects and number of components in a proposed prediction model, even though both factors intuitively have an effect on nonoperating failure rate. Quantifying two correlated variables separately must always rely on assumptions, thus introducing error.

The large correlation between equipment power on-off cycling frequency and interconnects, resistors, transistors, and ICs must be attributed to coincidence and the result of a relatively small data base. Therefore, the effects of equipment power on-off cycling could not be quantified with the available data. This was unfortunate because equipment power on-off cycling potentially has a significant effect on hybrid nonoperating failure rate. There was a wide range of power cycling values represented in the collected data. Equipment power cycling frequency values ranged from 0.038 cycles/ 10^3 nonoperating hours (i.e. approximately one power cycle every three years) for the Hawk missile to 40.12 cycles/ 10^3 nonoperating hours (i.e. approximately one power cycle every 25 hours) for the F-16 HUD. Therefore, the resultant hybrid microcircuit nonoperating failure rate prediction model corresponds to some unknown, average cycling rate.

Although no temperature relationship could be derived from the data, it was determined that temperature dependence hypothetically should be a factor in the failure rate prediction model. However, no temperature factor was proposed due to (1) the limited range of temperatures found in the data, (2) the fact that hybrids are made of a composite of devices each with different temperature characteristics, and (3) the large variety of hybrid designs precludes the assumption of a temperature factor.

Therefore, the proposed model is based on a constant average nonoperating temperature.

The preliminary model refinement process resulted in the conclusion that both theoretical models had merit. The variables analyzed for the first model were number of capacitors, number of resistors, number of diodes, number of transistors, number of ICs, seal perimeter, quality level, and environment. The variables evaluated versus nonoperating failure rate for the second model were number of interconnects, quality level, and environment. These variables, with the exception of quality and environment, were analyzed using statistical techniques. Both theoretical models were explored by application of regression analysis. The negative effect of correlated variables was minimized by carefully choosing independent variables.

For the first model, the dependent variables were number of resistors (N_R), number of capacitors (N_C), number of diodes (N_D), number of transistors (N_T), number of microcircuits (N_{IC}), and package seal perimeter (S). The results of this regression indicated that nonoperating failure rate was negatively correlated to N_C and S , as well as positively correlated with N_T , N_D and N_{IC} . These intuitively incorrect results were most likely the result of the scarcity of data, the intercorrelation between variables, and/or the large variability observed in the data. Next, the regression was run with these variables omitted. The results of this regression are presented in Table 5.1.7-4. N_T , N_D and N_{IC} were significant at a 70% confidence limit. A properly applied regression analysis requires that there is no correlation between independent variables. Therefore, the regression results must be considered approximate. The R-squared value for this regression was .44. This value was considered to be relatively low, but not unexpected due to the variability in the data.

In the second model, the dependent variable was the number of interconnects (I). The results of the second regression analysis are given in Table 5.1.7-5. Number of interconnects was significant at a 90%

confidence level. The R-squared value for this regression was .31. In other words, only 31% of the variability in the data could be explained by the regression solution. This relatively low value can be explained by the fact that there are many variables effecting hybrid nonoperating reliability, including design and processing variables which can not be quantified. An extremely accurate model was not considered feasible because of the problems associated with hybrid nonoperating failure modeling.

Interpretation of these two initial regression solutions are:

- 1) A nonoperating hybrid failure rate prediction model as a function of the number of interconnects can be supported with the data.
- 2) The number of transistors, diodes and microcircuits were significant at a 70% confidence limit for the first model.
- 3) The high level of intercorrelation between variables, the large variability in observed data, the scarcity of data, and the many variables involved make a highly accurate model unfeasible.
- 4) Although number of resistors, number of capacitors and seal perimeter were not significant factors in either analysis, this does not mean they do not have an effect on hybrid microcircuit nonoperating failure rates. Rather, the effect cannot be detected with the available data over the range of values found in the data base. In addition, since these devices have inherently lower failure rates than discrete semiconductors and microcircuits, the results of the regression were encouraging.

The first model does not include capacitors, packaged resistors, substrate resistors and the substrate implicitly in the proposed model. However, the model was based on observed data for hybrids designed with these components, and therefore, the base failure rate constant must include an average failure rate contribution for capacitors, packaged resistors, substrate resistors and the substrate itself. Thus, the effect of these factors was not ignored although they are not included specifically as part of the model.

The first model includes a count of integrated circuits without considering the complexity of individual IC chips. A model factor based on specific IC chip complexities would have been impossible to quantify from the available data.

TABLE 5.1.7-4: HYBRID REGRESSION RESULTS (I)

Variable	Coefficient	Standard Error	F-ratio	Confidence Limit
N_D	.6157	.1717	12.86	.70
N_T	.2843	.1724	2.73	.70
N_{IC}	.8115	.2696	9.06	.70
b_0	-8.5364	--	--	--

TABLE 5.1.7-5: HYBRID REGRESSION RESULTS (II)

Variable	Coefficient	Standard Error	F-ratio	Confidence Limit
N_I	2.1114	.6269	11.34	.90
b_0	-11.9330	--	--	--

The regression analyses were performed with the dependent variable equal to the natural logarithm of nonoperating failure rate. Transforming the regression solutions into equations where the dependent variable is simply the nonoperating failure rate results in the following preliminary models:

$$(I) \lambda_{h1} = A_1 \exp(\alpha_1(N_D) + \alpha_2(N_T) + \alpha_3(N_{IC}))$$

where

λ_{h1} = predicted hybrid nonoperating failure rate (failure/ 10^6 hours)

A_1 = constant (includes average failure rate contributions for capacitors, packaged resistors, substrate resistors and substrate)

= .000196

α_1 = constant

= .62

N_D = number of diodes

α_2 = constant

= .28

N_T = number of transistors

α_3 = constant

= .81

N_{IC} = number of integrated circuits

$$(II) \quad \lambda_{h2} = A_2(N_I)^{\alpha_4}$$

where

λ_{h2} = predicted hybrid nonoperating failure rate (failures/ 10^6 hours)

A_2 = constant

= .00000657

N_I = number of interconnections

α_4 = constant

= 2.11

These models are preliminary and only applicable to a ground fixed environment.

Both preliminary models had merit and were easy to apply. However, neither preliminary model was particularly accurate. This was not a result of an incorrect or oversimplified analysis, but was due to the

large variability associated with hybrid device failure behavior. Hybrid devices tend to be manufactured in lower quantities, and the design and processing controls are less uniform than with monolithic microcircuits. This observation and other factors result in the high variability. The decision was made to proceed with the first nonoperating failure rate prediction model, as a function of number of microcircuits, number of transistors and number of diodes. This decision was made because of the better fit to the data of the first regression solution.

The standard error statistic allows for computation of confidence intervals around regression solution coefficients. A brief discussion concerning confidence intervals is included in Section 3.2. Table 5.1.7-6 presents upper and lower 90% confidence interval values of the coefficients for N_D , N_T and N_{IC} . The coefficient for N_{IC} was considered to be intuitively correct. Interpretation of the coefficient was that the number of integrated circuits would have a greater influence on nonoperating failure rate than either the number of transistors or diodes. Conversely, the coefficients for diodes (N_D) and transistors (N_T) seemed conflicting. Intuitively, the number transistors should have a greater effect than the number of diodes. Initially, it was felt that the regression solution was erroneous. After further investigation of the respective coefficients and the confidence intervals (presented in Table 5.1.7-6), it was concluded that the results were not in error but that the relatively smaller difference between the coefficient values could not be detected with the available data. However, it was strongly believed that the proposed models should be physically correct. Therefore, an identical average value was included in the proposed model for both diodes and transistors.

TABLE 5.1.7-6: HYBRID COEFFICIENT CONFIDENCE INTERVALS

Variable	Lower 90% Limit	Coefficient	Upper 90% Limit
N _D	0.321	0.617	0.910
N _T	-0.011	0.284	0.580
N _{IC}	0.349	0.812	1.274

The next task in the model development was to determine a series of hybrid nonoperating quality factors for S, B and D quality levels. No quality factor was determined D-1 quality hybrids. This is consistent with MIL-HDBK-217D. The proposed series of nonoperating quality factors was developed based upon the operating hybrid quality factors and the relationship of the digital IC nonoperating quality factors (developed empirically in this study) to the monolithic microelectronic device operating values from MIL-HDBK-217D, Table 5.1.2.5-1. The derivation process was based on two assumptions. First, it was assumed that the ratio of S to B nonoperating quality factors was the same for hybrid microcircuits as monolithic microcircuits, or,

$$(\pi_{NQS}/\pi_{NQB})_{\text{monolithic ICs}} = (\pi_{NQS}/\pi_{NQB})_{\text{hybrids}} = .53$$

where

π_{NQS} is the nonoperating S level quality factor

π_{NQB} is the nonoperating B level quality factor

Thus making $\pi_{NQB} = 1.0$ and $\pi_{NQS} = 0.53$ for hybrids

The second assumption was that the relative difference between the proposed nonoperating quality factors and the operating quality factors were the same for hybrid microcircuits as monolithic ICs. In effect, the previously determined factors for monolithic ICs were used as a scaling

factor to determine the nonoperating quality factor for D level hybrids. This relationship is given by,

$$\left(\frac{\pi_{NQD}/\pi_{NQB}}{\pi_{QD}/\pi_{QB}} \right)_{\text{monolithic ICs}} = \left(\frac{\pi_{NQD}/\pi_{NQB}}{\pi_{QD}/\pi_{QB}} \right)_{\text{hybrids}}$$

where

π_{NQB} is the nonoperating B-level quality factor (= 1.0 for monolithic and hybrid)

π_{NQD} is the nonoperating D-level quality factor (= 2.5 for monolithic)

π_{QB} is the operating B-level quality factor (= 1.0 for monolithic and hybrid)

π_{QD} is the operating D-level quality factor (= 17.5 for monolithic and 60 for hybrid)

Solving for the hybrid π_{NQD} gives: $\pi_{NQD} = 8.57$

The resulting series of hybrid nonoperating quality factors are presented in Table 5.1.7-7. These numerical values are based on intuitive relationships, and should be evaluated when more hybrid nonoperating failure rate data becomes available. The proposed nonoperating quality factors are based on the screening of the hybrid and not on the screening of the components in the hybrid. It was assumed that a high level of hybrid screening was indicative of an overall quality part. Conversely, a low level of hybrid screening was believed to be indicative of an overall lower level of quality.

TABLE 5.1.7-7: HYBRID NONOPERATING QUALITY FACTORS

Quality Level	π_{NQ}
S	0.53
B	1.0
D	8.6

The next step in the model development process was to determine a series of nonoperating environmental factors for hybrid microcircuits. After consideration of several possibilities, it was assumed that the IC chip typically dominates the failure rate of the hybrid, and thus the nonoperating environmental factors for digital ICs could also be applied to hybrids. Table 5.1.6-1 in Section 5.1.6 presents a listing of the nonoperating environmental factors for devices with both hermetic and non-hermetic packaging.

Finally, the base failure rate constant for hybrids was normalized to correspond to a ground benign environment. The base failure rates determined from the data correspond to a ground fixed environment. The observed nonoperating base failure rate was divided by the ground fixed environment factor ($\pi_{NE,GF} = 2.4$ for hermetic devices). The normalized hybrid nonoperating base failure rate constant was therefore determined to be .0000817.

The proposed hybrid nonoperating failure rate prediction model was next subjected to an extreme case analysis. Predictions were made using the proposed model for parameter values beyond those found in the data base. It was found that the proposed model predicted extremely high nonoperating failure rates for quantities of active components beyond that found in the data base. This was not necessarily indicative of an incorrect analysis. Empirical relationships are only strictly applicable to the range of values found in the data. Nevertheless, it was essential that the proposed hybrid model be physically correct and not limited to lower complexity hybrids. Therefore a second base failure rate equation was hypothesized for complexities beyond that found in the data. Additionally a more definitive complexity numeric was defined to be equal to the number of diodes plus the number of transistors plus 1.8 times the

number of integrated circuits. The second base failure rate is given by the following equation.

$$\lambda_{nb} = .013\exp(.033(N_D) + .033(N_T) + .059(N_{IC}))$$

and is applicable when $N_D + N_T + 1.8N_{IC} > 12.2$

The 12.2 cut-off value was equal to the highest complexity found in the data. The second base failure rate is intuitively correct for several reasons. First, it provides continuity with the low complexity base failure rate. Additionally, it would be anticipated that an increase in hybrid components for very complex hybrids would have less overall effect on the hybrid nonoperating failure rate as a similar increase on a simple device. Additionally, the second base failure rate equation still increases with the number of diodes, number of transistors and number of integrated circuits.

Determination of the second base failure rate equation concluded the model development for hybrid microcircuits. Despite several difficulties, a viable approach was developed for hybrid model development and a proposed model was determined as a function of the number of integrated circuits, number of transistors, number of diodes, quality level and environment.

5.1.8 Proposed Magnetic Bubble Memory Nonoperating Failure Rate Prediction Model

The proposed model for magnetic bubble memory devices is represented by the following equation. The proposed model is presented in Appendix A in a form compatible with MIL-HDBK-217D.

$$\lambda_p = (\lambda_{nb1} \pi_{NT1} + \lambda_{nb2} \pi_{NT2}) \pi_{NE}$$

where

$$\begin{aligned}\lambda_p &= \text{magnetic bubble memory predicted nonoperating failure rate} \\ \lambda_{nb1} &= \text{control structure nonoperating base failure rate (failures/} \\ &\quad 10^6 \text{ nonoperating hours)} \\ &= .0015(N_g)^{.477}\end{aligned}$$

where

$$\begin{aligned}N_g &= \text{number of gates} \\ &= \text{number of transfer gates plus number of dissipative control} \\ &\quad \text{gates plus number of major loops} \\ \pi_{NT1} &= \text{control structure nonoperating temperature factor} \\ &= \exp\left(-6159\left(\frac{1}{T} - \frac{1}{298}\right)\right)\end{aligned}$$

where

$$\begin{aligned}T &= \text{temperature (}^\circ\text{K)} = 273 + T \text{ (}^\circ\text{C)} \\ \lambda_{nb2} &= \text{magnetic memory structure nonoperating base failure rate} \\ &\quad \text{(failures/} 10^6 \text{ nonoperating hours)} \\ &= .0089(N_L)\end{aligned}$$

where

$$\begin{aligned}N_L &= \text{number of loops} \\ &= \text{number of major loops plus number of functional minor loops} \\ \pi_{NT2} &= \text{magnetic memory structure nonoperating temperature factor} \\ &= \exp\left(-A_n\left(\frac{1}{T} - \frac{1}{298}\right)\right)\end{aligned}$$

where

$$\begin{aligned}A_n &= \text{temperature coefficient (see Table 5.1.2-7 in Section 5.1.2)} \\ T &= \text{temperature (}^\circ\text{K)} = 273 + T \text{ (}^\circ\text{C)} \\ \pi_{NE} &= \text{nonoperating environmental factors (see Table 5.1.1-2 in} \\ &\quad \text{Section 5.1.1)}\end{aligned}$$

5.1.9 Magnetic Bubble Memory Model Development

The magnetic bubble memory device is a hybrid assembly of two major structural elements. The first segment is a basic memory and control structure consisting of thin-film elements on a crystalline substrate. The second major structural segment is a magnetic structure to provide a controlled magnetic field consisting of a magnet, magnetic coils and a housing. These two major structural segments of the hybrid are interconnected by a mechanical substrate and lead frame. The interconnect substrate is normally a printed circuit board in present technology.

No quantitative nonoperating failure rate data were available for magnetic bubble memory devices. Therefore, a hypothetical model was developed based on the monolithic and hybrid microcircuit nonoperating failure rate prediction model development, and the MIL-HDBK-217D operating failure rate prediction model for magnetic bubble memories. The model was simplified because the anticipated precision of the proposed model did not warrant a very complex equation. The hypothetical model is represented by the following expression.

$$\lambda_{bm} = (A_{b1}(N_g)^{.477} \pi_{NT1} + A_{b2}(N_L) \pi_{NT2}) \pi_{NE}$$

where

λ_{bm} = magnetic bubble memory predicted nonoperating failure rate
(failures/ 10^6 nonoperating hours)

A_{b1} = control structure nonoperating base failure rate constant

N_g = number of gates

= number of transfer gates plus number of dissipative control
gates plus number of major loops

π_{NT1} = control structure nonoperating temperature factor

= $\exp(-6159(\frac{1}{T} - \frac{1}{298}))$

where

- T = ambient nonoperating temperature (°K)
- A_{b2} = magnetic memory structure nonoperating base failure rate constant
- N_L = number of loops
= number of major loops plus number of functional minor loops
- π_{NT2} = magnetic memory structure nonoperating temperature factor
= $\exp(-A_n(\frac{1}{T} - \frac{1}{298}))$

where

- A_n = temperature coefficient
- T = ambient nonoperating temperature (°K)
- π_{NE} = nonoperating environmental factor

The first term in the nonoperating failure rate equation represents the contribution of the control structure. The temperature coefficient was the previously determined value for NMOS technology. The complexity exponent was the previously determined value for random logic digital microcircuits. The second term in the equation represents the nonoperating failure rate contribution of the magnetic memory structure. It was assumed that the temperature coefficients and nonoperating environmental factors for monolithic microcircuits were applicable for magnetic bubble memory devices. This assumption was necessary because of the lack of nonoperating failure rate data.

The remaining factors to be quantified were the control structure nonoperating base failure rate constant and the magnetic memory structure nonoperating base failure rate. Estimates for these values were based on the ratio of operating to nonoperating failure rate for monolithic microcircuits, and the MIL-HDBK-217D magnetic bubble memory operating

failure rate prediction model. Estimates for A_{b1} and A_{b2} are the following.

A_{b1} = control structure nonoperating base failure rate constant
= 0.00153

A_{b2} = magnetic memory structure nonoperating base failure rate
constant
= 0.00885

Determination of the two nonoperating base failure rate constants concluded the model development process for magnetic bubble memories. The proposed model was based entirely on assumptions and must be considered approximate. It was essential that a nonoperating failure rate model for magnetic bubble memories devices was proposed because of the requirement for a comprehensive nonoperating failure rate prediction methodology.

5.2 Discrete Semiconductors

5.2.1 Discrete Semiconductor Nonoperating Failure Rate Prediction Models

This section presents the proposed nonoperating failure rate prediction models for discrete semiconductors. Separate models were developed for transistors, diodes, and opto-electronic semiconductor devices. These models are presented in Appendix A in a form compatible with MIL-HDBK-217D.

Transistors

The proposed model for transistors is:

$$\lambda_p = \lambda_{nb} \pi_{NT} \pi_{NQ} \pi_{NE} \pi_{cyc}$$

where

$$\begin{aligned} \lambda_p &= \text{predicted transistor nonoperating failure rate} \\ \lambda_{nb} &= \text{nonoperating base failure rate (failure/10}^6 \text{ hours)} \\ &= .00027, \text{ Si,NPN (Group I)} \\ &= .00027, \text{ Si,PNP (Group I)} \\ &= .00040, \text{ Ge,PNP (Group I)} \\ &= .00040, \text{ Ge,NPN (Group I)} \\ &= .00039, \text{ FET (Group II)} \\ &= .0013, \text{ Unijunction (Group III)} \\ &= .041, \text{ Microwave (Group IX)} \\ \pi_{NT} &= \text{nonoperating temperature factor} \\ &= \exp\left(-A_n\left(\frac{1}{T} - \frac{1}{298}\right) + \left(\frac{T}{T_m}\right)^P\right) \end{aligned}$$

where

$$\begin{aligned} T &= \text{temperature (}^{\circ}\text{K)} \\ A_n &= \text{temperature coefficient (see Table 5.2.1-1)} \end{aligned}$$

TABLE 5.2.1-1: DISCRETE SEMICONDUCTOR NONOPERATING TEMPERATURE FACTOR PARAMETERS

Part	Group	Style	A _n	T _m	P
Transistors	I	Si,NPN	3356	448	10.5
		Si,PNP	3541	448	14.2
		Ge,PNP	4403	373	20.8
		Ge,NPN	4482	373	19
	II	FET	3423	448	13.8
	III	Unijunction	4040	448	13.8
Diodes	IV	Si, Gen. Purpose	4399	448	17.7
		Ge, Gen. Purpose	5829	373	22.5
	V	Zener/Avalanche	3061	448	14
	VI	Thyristors	4311	448	9.6
	VII	Microwave	2738	423	16.6
	VIII	Impatt, Gunn, Varactor, Pin, Step Recovery & Tunnel	3423	448	13.8
Transistors	IX	Microwave	5700	623	20

$T_{m,P}$ = shaping parameters (see Table 5.2.1-1)

π_{NQ} = nonoperating quality factors

= 0.57, JANTXV

= 1.0, JANTX

= 3.6, JAN

= 13, lower, hermetic

= 23, plastic

π_{NE} = nonoperating environmental factor (see Table 5.2.1-2)

π_{cyc} = equipment power on-off cycling factor

= $1 + .050(N_C)$

where

N_C = number of equipment power on-off cycles per 10^3 nonoperating hours

Diodes

The proposed model for diodes is represented by the following equation.

$$\lambda_p = \lambda_{nb} \pi_{NT} \pi_{NQ} \pi_{NE} \pi_{cyc}$$

where

λ_p = predicted diode nonoperating failure rate

λ_{nb} = nonoperating base failure rate (failure/ 10^6 hours)

= .00017, Si, General Purpose (Group IV)

= .00042, Ge, General Purpose (Group IV)

= .00040, Zener/Avalanche (Group V)

= .0027, Microwave (Group VII)

= .00063, Thyristor (Group VI)

= .0027, Impatt, Gunn, Varactor, Pin, Step Recovery and Tunnel (Group VIII)

TABLE 5.2.1-2: TRANSISTOR NONOPERATING ENVIRONMENTAL FACTORS (π_{NE})

Env.	Group I	Group II	Group III	Group IX
GB	1	1	1	1
GF	5.8	4.0	4.0	2.0
GM	18	18	18	7.8
Mp	12	12	12	7.4
NSB	9.8	6.0	9.3	3.6
NS	9.8	8.6	9.3	4.7
NU	21	21	21	11
NH	19	19	19	11
NUU	20	20	20	12
ARW	27	27	27	16
AIC	9.5	7.5	9.5	2.5
AIT	15	9	15	3.5
AIB	35	35	35	6.0
AIA	20	30	20	3.5
AIF	40	40	40	6.0
AUC	15	10	15	5.0
AUT	25	15	25	7.0
AUB	60	55	60	10
AUA	35	50	35	7.0
AUF	65	65	65	10
SF	(1)	(1)	(1)	(1)
MFF	12	12	12	7.5
FFA	17	17	17	11
USL	36	36	36	22
ML	41	41	41	25
CL	690	690	690	250

NOTES: (1) This study did not address Space Flight environment

$$\begin{aligned}\pi_{NT} &= \text{nonoperating temperature factor} \\ &= \exp(-A_n(\frac{1}{T} - \frac{1}{298}) + (\frac{T}{T_m})^P)\end{aligned}$$

where

$$\begin{aligned}T &= \text{temperature (}^{\circ}\text{K)} \\ A_n &= \text{temperature coefficient (see Table 5.2.1-1)} \\ T_{m,P} &= \text{shaping parameters (see Table 5.2.1-1)} \\ \pi_{NQ} &= \text{nonoperating quality factors} \\ &= 0.57, \text{ JANTXV} \\ &= 1.0, \text{ JANTX} \\ &= 3.6, \text{ JAN} \\ &= 13, \text{ lower, hermetic} \\ &= 23, \text{ plastic} \\ \pi_{NE} &= \text{nonoperating environmental factor (see Table 5.2.1-3)} \\ \pi_{cyc} &= \text{equipment power on-off cycling factor} \\ &= 1 + .083(N_C)\end{aligned}$$

where

$$N_C = \text{number of equipment power on-off cycles per } 10^3 \text{ nonoperating hours}$$

Opto-electronic Devices

The proposed model for opto-electronic semiconductor devices is the following equation.

$$\lambda_p = \lambda_{nb} \pi_{NQ} \pi_{NE}$$

where

$$\lambda_p = \text{predicted opto-electronic semiconductor nonoperating failure rate}$$

TABLE 5.2.1-3: DIODE NONOPERATING ENVIRONMENTAL FACTORS (TME)

Env.	Group IV	Group V	Group VI	Group VII	Group VIII
G _B	1	1	1	1	1
G _F	3.9	3.9	3.9	6.4	3.9
G _M	18	18	18	31	18
M _P	12	12	12	35	12
NS _B	4.8	5.8	5.8	8.0	5.8
NS	4.8	8.7	8.7	11	8.7
NU	21	21	21	33	21
NH	19	19	19	54	19
NUU	20	20	20	58	20
ARW	27	27	27	78	27
A _{IC}	15	4.5	9.5	30	4.5
A _{IT}	20	6.5	15	40	6.5
A _{IB}	30	45	35	65	45
A _{IA}	25	25	20	50	25
A _{IF}	35	45	40	70	45
A _{UC}	25	7.5	15	50	7.5
A _{UT}	30	10	25	60	10
A _{UB}	50	70	60	105	70
A _{UA}	40	40	35	80	40
A _{UF}	50	70	65	110	70
S _F	(1)	(1)	(1)	(1)	(1)
M _{FF}	12	12	12	36	12
F _{FA}	17	17	17	50	17
U _{SL}	36	36	36	110	36
M _L	41	41	41	120	41
C _L	690	690	690	2000	690

NOTES: (1) This study did not address Space Flight environment

λ_{nb} = nonoperating base failure rate (failures/ 10^6 nonoperating hours)

= .00016, LED

= .00070, Single Isolator

= .00089, Dual Isolator

= .00038, Phototransistor

= .00028, Photodiode

= .00025, Alpha-Numeric Displays

π_{NQ} = nonoperating quality factors

= 0.57, JANTXV

= 1.0, JANTX

= 3.6, JAN

= 13, lower, hermetic

= 23, plastic

π_{NE} = nonoperating environmental factor (see Table 5.2.1-4)

TABLE 5.2.1-4: OPTO-ELECTRONIC SEMICONDUCTOR NONOPERATING ENVIRONMENTAL FACTORS (π_{NE})

Env.	π_{NE}	Env.	π_{NE}
GB	1	AIA	3.5
GF	2.4	AIIF	8.0
GM	7.8	AUC	3.0
Mp	7.7	AUT	5.5
NSB	3.7	AUB	8.0
NS	5.7	AUA	5.5
NU	11	AUF	10
NH	12	SF	(1)
NUU	13	MFF	7.8
ARW	17	MFA	11
AIC	2.5	USL	23
AIT	3.5	ML	26
AIB	5.5	CL	450

NOTES: (1) This study did not address Space Flight environment

5.2.2 Transistor Model Development

The general nonoperating failure rate model development approach described in Section 4.1 was successfully implemented for transistors. A theoretical model was hypothesized based on information located during the literature search. Selection and quantification of the independent variables was accomplished by analyzing the available data. The proposed nonoperating failure rate prediction model for transistors was found to be a function of device style, screening, temperature, application environment and equipment power on-off cycling frequency.

The application and construction variables which were identified for transistors are presented in Table 5.2.2-1. These variables represent possible nonoperating failure rate model parameters. Parameter values for these factors were identified whenever possible as part of the data collection effort. If sufficient detail could not be determined for a specific data entry, it was deleted from the analysis.

The general nonoperating reliability concepts presented in Section 4 for temperature, screening, environment and equipment power on-off cycling were studied for development of a transistor theoretical model. These concepts were complemented by an investigation of transistor nonoperating failure mechanisms to determine the theoretical model. For transistors, the theoretical model was multiplicative but nonlinear due to the assumed effects of equipment power on-off cycling and temperature. The theoretical transistor failure rate prediction model was initially determined to be a function of device style, application, complexity, rated power, quality, environment, temperature, and equipment power on-off cycling frequency. After further qualitative analyses, it was determined that application and rated power were important variables for operating failure rate prediction, but were not nearly as significant for nonoperating failure rate prediction. Therefore, these two variables were deleted from the theoretical model.

TABLE 5.2.2-1: TRANSISTOR PART CHARACTERIZATION

- I. Device Style
 - A. Group I
 - 1. Si,NPN
 - 2. Si,PNP
 - 3. Ge,NPN
 - 4. Ge,PNP
 - B. Group II
 - 1. Si,FET
 - 2. GaAs,FET
 - C. Group III (Unijunction)
 - D. Group IX (Microwave)
- II. Application

A. Linear	E. Driver
B. Switch	F. Pulse Amplifier
C. Low Noise	G. Continuous Wave
D. High Frequency	H. Oscillator
- III. Complexity

A. Single Device	E. Dual Emitter
B. Dual (matched)	F. Multiple Emitter
C. Dual (unmatched)	G. Complementary Pair
D. Darlington Pair	H. Tetrode
- IV. Rated Power (watts)
- V. Quality Level
 - A. JANTXV
 - B. JANTX
 - C. JAN
 - D. Lower, Hermetic
 - E. Plastic
- VI. Application Environment
- VII. Temperature
 - A. Rated
 - B. Actual
- VIII. Number of Power On/Off Cycles per 10^3 Nonoperating Hours

The collected transistor nonoperating reliability data is summarized in Table 5.2.2-2. The table presents the number of data records, observed failures and summed part hours for each transistor style and equipment represented in the collected data. The data were initially analyzed separately without merging data records. The data were subjected to a thorough preliminary analysis to determine weaknesses of the data set. The following attributes of the available data were identified.

- 1) All collected data were from a ground based environment. Therefore, appropriate nonoperating environmental factors could not be determined empirically.
- 2) Only one source had data for JAN level transistors.
- 3) All high temperature data were from AFCIQ, and were not screened to identical specifications.
- 4) High temperature storage data were only available for Si,PNP and Si,NPN device styles.

Application environment was hypothesized to be a significant variable in the theoretical model development. However, nonoperating environmental factors could not be determined empirically because all collected data was for ground based environments. The methods described in Section 4.5 were used to determine appropriate nonoperating environmental factors after statistically analyzing the other variables.

Matrices of "dummy variables" (0 or 1) were defined for device style and quality level to accommodate quantitative analyses. The matrix for transistor device style is presented in Table 5.2.2-3. The matrix was defined to represent (1) Si,NPN, (2) Si,PNP, (3) FET, and (4) microwave transistors. Data in sufficient quantity were not available for other transistor styles. The matrix for quality level was simply a "0" for JANTX parts and a "1" for JAN parts. This variable was designated as Q₁. Data were not available for quality levels other than JANTX and JAN, and therefore, the quality matrix was not defined to represent other quality levels.

TABLE 5.2.2-2: TRANSISTOR NONOPERATING FAILURE RATE DATA

Equipment/Source	Data Records	Quality	Style	Failures	Part Hours (X 10 ⁶)
Hawk/MICOM	9	JANTX	Si,NPN	6	5189.5
Hawk/MICOM	5	JANTX	Si,PNP	2	2484.1
Hawk/MICOM	5	JANTX	FET	3	2501.2
Hawk/MICOM	1	JANTX	Microwave	1	17.0
Maverick/MICOM	6	JANTX	Si,NPN	4	1400.1
Maverick/MICOM	3	JANTX	Si,PNP	4	1482.5
Maverick/MICOM	1	JANTX	FET	0	41.2
Sparrow/MICOM	1	JAN	Si,PNP	0	25.5
Sparrow/MICOM	9	JAN	Si,NPN	1	408.3
Sparrow/MICOM	3	JAN	FET	0	25.5
Sprint/MICOM	8	JANTX	Si,PNP	0	489.8
Sprint/MICOM	3	JANTX	Si,NPN	2	1446.2
TOW/MICOM	3	JANTX	Ge,PNP	0	13.1
TOW/MICOM	4	JANTX	Si,NPN	0	107.7
TOW/MICOM	3	JANTX	Si,PNP	0	39.4
Lance/MICOM	4	JANTX	Si,PNP	0	11.2
Lance/MICOM	4	JANTX	Si,NPN	0	15.7
Martin Marietta	3	JANTX	Si,PNP	1	1326.4
Martin Marietta	3	JANTX	Si,NPN	6	4076.1
Martin Marietta	1	JANTX	Ge,NPN	0	20.8
Martin Marietta	1	JANTX	Ge,PNP	0	44.8
Martin Marietta	1	JANTX	FET	0	71.7
Martin Marietta	1	JANTX	Unijunction	0	1.0
F-16 HUD/RIW	8	JANTX	Si,NPN	4	350.0
F-16 HUD/RIW	5	JANTX	Si,PNP	0	363.3
AFCIQ (1)	4	(2)	Si,PNP	3	8.7
AFCIQ (1)	4	(2)	Si,NPN	12	20.8
PRC	1	JANTX	FET	0	0.3
ERADCOM (3)	1	Plastic	Si,NPN	33	0.9
ERADCOM (3)	1	Plastic	Si,PNP	39	0.3
Totals	106			121	21983.1

- NOTES: 1) High temperature storage life test data. Storage temperatures range from 150°C to 200°C.
- 2) These devices not screened to identical specifications.
- 3) Panama life test data for nonhermetic devices. Ambient temperature = 30°C, relative humidity = 90%.

TABLE 5.2.2-3: TRANSISTOR STYLE VARIABLE MATRIX

Device Style	S ₁	S ₂	S ₃
Si,NPN	0	0	0
SI,PNP	1	0	0
FET	0	1	0

There were several problems associated with the determination of an appropriate nonoperating temperature factor for transistors. One problem with the high temperature storage life test data from AFCIQ was that the transistors were not screened to similar specifications as the other data. Another problem was that data were only available for Si,PNP and Si,NPN transistor styles. A third problem was that no empirical or theoretical relationship for nonoperating failure rate vs. temperature could be located in the literature. Additionally, the assumed transistor temperature relationship presented in Section 4.4 could not be transformed into a linear form. As a solution to this dilemma, approximate quality levels were determined and various nonlinear relationships were fit to the data after statistical analysis of the other variables and assumption of an applicable series of nonoperating environmental factors.

Three qualitative "dummy variables" were then defined to represent four distinct equipment power cycling rate categories. The three variables were designated cyc1, cyc2 and cyc3. The definitions of the three categories and the corresponding cyc1, cyc2 and cyc3 values are the following.

- o cycling rates less than one power cycle every two years (cyc1, cyc2, cyc3 = 0, 0, 0).
- o cycling rates between one cycle per year and one cycle every two years (cyc1, cyc2, cyc3 = 1, 0, 0).
- o cycling rates greater than one cycle per year (cyc1, cyc2, cyc3 = 0, 0, 1).
- o unknown cycling frequencies.

Definition of the cycling rate variables was necessary because of the nonlinear form of the proposed model. Equipment power on-off cycling was temporarily treated as a qualitative variable and an approximate cycling factor relationship was determined. Then, an iterative approach was taken for nonlinear regression. This procedure is described in Section 4.3. The assumed form of the equipment cycling factor is expressed by the following equation.

$$\text{Cycling Factor} = 1 + K_1(\text{cycles}/10^3 \text{ hours})$$

where

$$K_1 = \text{constant}$$

The data were then merged and regression analysis applied. The data were merged according to equipment, device style, complexity and quality level by summing the number of failures and part hours. For example, the number of failures and part hours were summed for all JANTX, FET devices in the Hawk missile. Initially, two regression analyses were performed. In each case the dependent variable was equal to the natural logarithm of nonoperating failure rate. One regression was performed to evaluate the validity of the diode nonoperating quality factor (described in Section 5.2.3) for transistor nonoperating failure rate prediction. This approach was taken because of the belief that screening effects transistors and diodes similarly, and because only one data source was available for JAN transistors.

The initial regression indicated that the ratio of JAN to JANTX device nonoperating failure rate was equal to 2.24. This was compared to the corresponding value of 3.63 for diodes. A 90% confidence interval around the point estimate ratio for transistors was computed to be 0.83 and 6.03. This relatively large interval was due in part to the limited amount of JAN device data. The data did not disprove that the observed ratio for diodes could also be applied for transistor nonoperating failure rate prediction. Therefore, the ratio of 3.63 determined for diodes was

applied to transistors. The complete series of nonoperating quality factors are presented in Table 5.2.3-6 in the following section. A second regression analysis was then performed assuming that the diode nonoperating quality factors were accurate. Results of the second regression analysis are presented in Table 5.2.2-4. The variable coefficient, the standard error and the F-ratio are presented for each significant variable.

TABLE 5.2.2-4: TRANSISTOR REGRESSION RESULTS II

Variable	Coefficient	Standard Error	F-Ratio	Confidence Limit
S ₃	4.054	0.501	65.43	0.90
cyc1	1.000	0.376	7.09	0.90
cyc2	1.651	0.376	19.29	0.90
b ₀	-6.887	--	--	--

Interpretation of the regression results are the following.

- 1) The nonoperating failure rate for microwave transistors was significantly different from the other transistor styles with 90% confidence.
- 2) The difference in failure rate between Si,NPN, Si,PNP, and FET devices was not significant at a 70% confidence limit.
- 3) There was no observed difference between single and dual complexity transistors.
- 4) The cyc1 and cyc2 equipment power cycling variables were significant at 90%. The resultant factors were in descending order from the highest to lowest cycling rates, as expected. There was no significant difference, with 70% confidence, between the lowest cycling rate category and the unknown cycling rate data entries.

The next step in the model development task for transistors was to perform iterative regression analyses to solve the nonlinear model form. The nonlinear form resulted from the assumed equipment power on-off cycling relationship. This process was described in Section 4.3. For

transistors, three iterations were required. The regression solution after the third iteration is given by the following equation. The dependent variable was transformed to nonoperating failure rate. Previously, the dependent variable was the natural logarithm of nonoperating failure rate adjusted to compensate for quality. The preliminary model at this stage of the model development process is:

$$\lambda_t = \lambda'_{nb} \pi_{NQ} \pi_{cyc}$$

where

- λ_t = predicted transistor nonoperating failure rate
- λ'_{nb} = preliminary nonoperating base failure rate (failure/ 10^6 nonoperating hours)
 - = .00130, Si,PNP
 - = .00130, Si,NPN
 - = .00130, FET
 - = .0588, Microwave
- π_{NQ} = assumed nonoperating quality factors
- π_{cyc} = equipment power on-off cycling factor
 - = $1 + .0689(N_C)$

where

- N_C = number of equipment power on-off cycles per 10^3 nonoperating hours

It must be emphasized that the above equation is preliminary, and only applies to a ground fixed environment with an average nonoperating ambient temperature of 20°C. The nonoperating base failure rate in the proposed model (Section 5.2.1) corresponds to a reference temperature of 25°C. Therefore, determination of the proposed nonoperating base failure rate was dependent on the determination of transistor nonoperating temperature factors.

The next phase of the nonoperating failure rate model development was to estimate appropriate nonoperating environmental factors. The methods presented in Section 4.5 were applied to determine applicable factors. This method assumes that a series of nonoperating environmental factors can be generated from the MIL-HDBK-217 operating environmental factors based on (1) a comparison of application temperature differences, and (2) a comparison of operating and nonoperating failure mechanism accelerating factors. Operating temperatures are typically higher because of the internal heat generation. However, the effects of this temperature difference are predicted by the respective operating and proposed nonoperating temperature factors. Therefore, no temperature adjustment was required for transistors. A comparison was made between operating and nonoperating failure mechanisms and failure accelerating factors. A summary of the failure mechanism comparisons are presented in Tables 5.2.2-5 and 5.2.2-6 for bipolar single and power transistors, and FETs respectively. References 42 and 43 included transistor failure mode/mechanism information. Quantitative failure mechanism distributions were essentially impossible to locate for nonoperating applications, and often conflicting for operating applications. Nevertheless, it was determined that the operating transistor environmental factors approximate the effect of environmental stress for nonoperating failure rate. These factors were presented in Table 5.2.1-2 in Section 5.2.1.

The next stage in the model development process was to determine nonoperating temperature factors. Data were available from AFCIQ with temperatures ranging from 150°C to 200°C for Si,PNP and Si,NPN transistors. However, this range of values was insufficient to determine whether the equivalent Arrhenius equation was applicable for transistor nonoperating failure rate. It was believed that the Arrhenius relationship was not applicable because of the relationship for transistor failure rate vs. temperature in MIL-HDBK-217D. Therefore, a modified Arrhenius equation was assumed. The modified temperature factor allowed for a nonlinear relationship between the natural logarithm of nonoperating failure rate and the inverse of temperature. Additionally, a reference temperature term of 298°K was added to increase the utility of the

TABLE 5.2.2-5: SIGNAL AND POWER TRANSISTOR FAILURE MECHANISM DISTRIBUTION

Failure Mode/Mechanism	Accelerating Factors	Operating Distribution (%)	Nonoperating Distribution (%)
open			
poor lead to die contact	vibration, shock	1-20	5-25
wire bond defects	vibration, shock	1-15	1-17
intermetallic formation	time, temperature	1-15	1-18
wire nicks	current	1-15	0-10
metallization melt	current, temperature	1-20	0-5
short			
bulk impurities	current	5-25	0-10
contamination	temp., moisture, vibration	1-20	5-25
drift, degraded			
corrosion	temp., humidity, vibration	1-20	5-25
die to header bond defects	shock, vibration	5-25	10-30
contamination	temp., moisture, shock, vibration	5-25	10-20

TABLE 5.2.2-6: FET FAILURE MECHANISM DISTRIBUTION

Failure Mode/Mechanism	Accelerating Factors	Operating Distribution (%)	Nonoperating Distribution (%)
open			
poor lead to die contact	vibration, shock	1-15	1-18
wire bond defects	vibration, shock	1-15	1-18
intermetallic formation	time, temperature	1-12	1-14
wire nicks	current	1-13	0-10
metallization melt	current, temperature	1-15	0-5
short			
dielectric breakdown	voltage, temperature	15-40	0-10
contamination	temp., moisture, vibration	1-20	5-25
drift, degraded			
corrosion	humidity, temp., vibration	1-20	5-25
die to header defects	shock, vibration	5-25	15-35
contamination	temp., moisture, shock, vibration	5-25	15-35

proposed model. The temperature factor for transistors was assumed to be the following equation.

$$\pi_{NT} = \exp(-A_n(\frac{1}{T} - \frac{1}{T_r}) + (\frac{T}{T_m})^P)$$

where

π_{NT} = nonoperating temperature factor

A_n = temperature coefficient

T = temperature (°K)

T_r = reference temperature = 298°K

T_m, P = shaping parameters

The form of the assumed nonoperating temperature factor was based on the relationship of operating failure rate versus temperature in MIL-HDBK-217D. In approximate terms, the T_m shaping parameter is the temperature (expressed in degrees Kelvin) where the equivalent Arrhenius relationship is no longer applicable, and the P shaping parameter provides an indication of how fast the assumed relationship deviates from the equivalent Arrhenius relationship.

Several decisions were required before the assumed temperature factor could be quantified. First, an equivalent quality level of lower, hermetic was determined for the high temperature storage data based on information provided by AFCIQ. Second, there were insufficient data to estimate all three unknowns (i.e., A_n , T_m , P) in the assumed temperature relationship. It was decided that the T_m and P parameters which are used for operating failure rate prediction would be applicable for nonoperating failure rate prediction purposes. Unique A_n values were then determined empirically. Ideally, it would have been preferable to solve for all three parameters. However, data limitations prevented this.

Five data entries were available for transistor high temperature storage life testing. To compute the A_n temperature coefficients, the regression solution was assumed to be exact for 20°C, and it was then

assumed that the relatively higher failure rates from the high temperature data were due only to the increased temperatures. The effects of the other variables were eliminated by using the previously determined factors for quality, equipment power cycling and environment. Specifically, two simultaneous equations were solved for each high temperature data entry. Unknown parameters were the nonoperating base failure rate and the A_n temperature coefficient. The nonoperating base failure rate was unknown because it was dependent on the reference temperature, and thus, also dependent on the temperature coefficient.

The two equations used for the temperature analysis, and solved simultaneously were the following. The first equation was the regression solution found earlier for an average field storage temperature of 200C (or 2930K). The second equation was the assumed model for the high temperature storage data. In the first equation, the preliminary base failure rate (.00130 f/10⁶ hours) corresponded to JANTX quality, a ground fixed environment, a temperature of 200C, and no equipment power on-off cycling. Therefore, the previously determined values for those parameters were inserted in the first equation given below. In the second equation, the observed high temperature storage life test failure rate corresponded to an equivalent quality of lower, hermetic, ground benign environment, temperatures ranging from 1500C to 2000C and approximately 3 power cycles per 10³ hours. The corresponding factors for these parameters were inserted in the second equation.

$$\begin{aligned}
 1) \quad \lambda_t &= \lambda_{nb} \pi_{NQ} \pi_{NE} \pi_{cyc} \left(\exp \left(-A_n \left(\frac{1}{293} - \frac{1}{298} \right) + \left(\frac{293}{T_m} \right)^P \right) \right) \\
 .00130 &= \lambda_{nb}(1)(5.8)(1 + .069(0)) \exp \left(-A_n \left(\frac{1}{293} - \frac{1}{298} \right) + \left(\frac{298}{T_m} \right)^P \right) \\
 2) \quad \lambda_t &= \lambda_{nb} \pi_{NQ} \pi_{NE} \pi_{cyc} \left(\exp \left(-A_n \left(\frac{1}{T_s} - \frac{1}{298} \right) + \left(\frac{T_s}{T_m} \right)^P \right) \right) \\
 \lambda_o &= \lambda_{nb}(3.63)(1)(1 + .069(3)) \exp \left(-A_n \left(\frac{1}{T_s} - \frac{1}{298} \right) + \left(\frac{T_s}{T_m} \right)^P \right)
 \end{aligned}$$

where

$T_m = 448$, Table 5.1.3-21, MIL-HDBK-217D

$P = 10.5$, Si,NPN, Table 5.1.3-2, MIL-HDBK-217D

$= 14.2$, Si,PNP, Table 5.1.3-2, MIL-HDBK-217D

T_s = storage temperature ($^{\circ}\text{K}$)

λ_0 = observed nonoperating failure rate (failures/ 10^6 hours)

Unique solutions for A_n were found for each of the five high temperature storage life test data entries. These data entries and the solutions for A_n are presented in Table 5.2.2-7. The proposed temperature coefficient of 3356 for Si,NPN transistors was the average A_n value for entries 1 and 2 in Table 5.2.2-7. Similarly, the proposed temperature coefficient of 3541 for Si,PNP transistors was the average A_n value for entries 3, 4 and 5. It was noted that the proposed values were higher than the corresponding operating temperature coefficients (N_T in Table 5.1.3-2, MIL-HDBK-217D). One possible explanation for this observation was that there are fewer stresses acting on a part during nonoperation, and therefore the failure rate is more sensitive to each individual stress. It was also noted that the absolute difference between the proposed A_n values for Si,PNP and Si,NPN was very similar to the corresponding difference between operating temperature coefficients.

TABLE 5.2.2-7: HIGH TEMPERATURE STORAGE LIFE TEST DATA

Entry No.	Failures	Part Hours ($\times 10^6$)	$\lambda_0(1)$	Style	Equivalent Quality	Temperature ($^{\circ}\text{C}$)	$A_n(2)$
1	3	7.35	0.41	Si,NPN	lower	150	4021
2	9	13.41	0.67	Si,NPN	lower	200	2690
3	3	0.88	3.41	Si,PNP	lower	175	4979
4	0	6.53	<0.15	Si,PNP	lower	150	<3159
5	0	1.30	<0.77	Si,PNP	lower	200	<2486

NOTES: (1) Observed failure rate. One failure was assumed for data entries without failures

(2) A_n = transistor temperature coefficient

Estimates of the temperature coefficients for Ge,PNP, Ge,NPN, FET, and Unijunction were calculated by (1) assuming that the nonoperating temperature coefficient rankings would be the same as the operating temperature coefficient rankings, and (2) the temperature coefficient difference between operating and nonoperating would be the same for the other device styles as the observed difference for Si,PNP and Si,NPN. The MIL-HDBK-217D failure rate prediction model for microwave transistors assumes the equivalent Arrhenius relationship applied for the entire temperature range found during normal usage. The complete set of temperature coefficients and shaping parameters is presented in Table 5.2.1-1 of Section 5.2.1.

A by-product of the temperature coefficient determination process was that the nonoperating base failure rate was also found for Si,NPN, and Si,PNP transistors. The value was computed to be 0.00027 failures/10⁶ nonoperating hours as part of the simultaneous equation solution. The same value could have been determined by dividing the preliminary base failure (0.00130 failures/10⁶ nonoperating hours) by both the ground fixed nonoperating environmental factor of 5.8 and the nonoperating temperature factor of 0.83 for 20°C. This would have been necessary to normalize the base failure rate to correspond to the desired parameters. A complete series of nonoperating base failure rates were then determined by normalizing the preliminary base failure rates to the desired parameters. Additionally, nonoperating base failure rates were determined by extrapolation for transistor types without data.

Determination of the nonoperating base failure rates concluded the model development process for transistors. The proposed model for transistor nonoperating failure rate is therefore given by,

$$\lambda_t = \lambda_{nb} \pi_{NT} \pi_{NQ} \pi_{NE} \pi_{cyc}$$

where

λ_t = transistor nonoperating failure rate

λ_{nb} = nonoperating base failure rate (failures/ 10^6 nonoperating hours)

= .00027, Si,NPN

= .00027, Si,PNP

= .00040, Ge,PNP

= .00040, Ge,NPN

= .00039, FET

= .0013, Unijunction

= .041,Microwave

π_{NT} = nonoperating temperature factor

π_{NQ} = assumed nonoperating quality factor

π_{NE} = nonoperating environmental factor

π_{cyc} = equipment power on-off cycling factor

= $1 + .069(N_C)$

where

N_C = number of equipment power on-off cycles per 10^3 nonoperating hours

The proposed transistor nonoperating failure rate prediction model is presented in Section 5.2.1 and in Appendix A in a form compatible with MIL-HDBK-217D. Transistor model validation is described in Section 5.2.5.

5.2.3 Diode Model Development

A nonoperating failure rate prediction model for diodes was developed by hypothesizing a theoretical model, and then by analyzing empirical data to quantify the model parameters. The proposed model was determined to be a function of device style, environment, temperature, quality level and equipment power on-off cycling. The model factors for device style, quality level and equipment power on-off cycling were determined

analytically. The factors for temperature and application environment were assumed. The proposed model is presented in Section 5.2.1 and in Appendix A in a form compatible with MIL-HDBK-217D.

The initial phase of the model development process was to identify application and construction variables which characterize diodes in a nonoperating environment. These variables, presented in Table 5.2.3-1, represent possible nonoperating failure rate model parameters. Additionally, identification of the application and construction variables was a prerequisite to both the theoretical model development and data collection tasks.

A theoretical model was developed for diode nonoperating failure rate by studying both documented and intuitive reliability relationships. The theoretical model was nonlinear due to the assumed effects of temperature and equipment power on-off cycling frequency. The theoretical model was also assumed to be a function of device style, application, rated power, quality level and application environment.

Further refinement of the theoretical model for diodes resulted in the deletion of part application and rated power from the model. It was believed that these parameters had negligible effect on diode nonoperating failure rate. The refined theoretical model formed the basis for model development and subsequent analyses.

An extensive data collection effort was performed in support of this study. The collected diode nonoperating failure rate data is presented in a summarized form in Table 5.2.3-2. Data were collected in sufficient quantity for general purpose, zener, microwave and thyristor diodes.

TABLE 5.2.3-1: DIODE CHARACTERIZATION VARIABLES

- I. Device Style
 - A. Group IV
 - 1. Si, General Purpose
 - 2. Ge, General Purpose
 - B. Group V (Zener & Avalanche)
 - C. Group VI (Thyristors)
 - D. Group VII (Microwave Diodes)
 - 1. Microwave Detector
 - 2. Microwave Mixer
 - 3. Schottky Detector
 - E. Group VIII
 - 1. Varactor
 - 2. PIN
 - 3. IMPATT
 - 4. Step recovery
 - 5. Tunnel
 - 6. Gunn
- II. Application
 - A. Analog Circuits
 - B. Switching
 - C. Power Rectifier
 - D. Voltage Regulator
 - E. Voltage Reference
- III. Rated Power (watts)
- IV. Quality Level
 - A. JANTXV
 - B. JANTX
 - C. JAN
 - D. Lower, Hermetic
 - E. Plastic
- V. Temperature
 - A. Rated
 - B. Actual
- VI. Application Environment
- VII. Number of Equipment Power On/Off Cycles per 10^3 Nonoperating Hours

TABLE 5.2.3-2: DIODE NONOPERATING FAILURE RATE DATA

Equipment/Source	Data Records	Quality	Style	Failures	Part Hours (X 10 ⁶)
Hawk/MICOM	6	JANTX	Si,Gen.Purpose	0	4355.8
Hawk/MICOM	13	JANTX	Zener	1	357.3
Hawk/MICOM	1	JANTX	Microwave	3	204.2
Maverick/MICOM	9	JANTX	Si,Gen.Purpose	2	4776.9
Maverick/MICOM	9	JANTX	Zener	1	411.8
Sparrow/MICOM	28	JAN	Si,Gen.Purpose	2	1084.6
Sparrow/MICOM	14	JAN	Zener	0	178.6
Sprint/MICOM	2	JANTX	Si,Gen.Purpose	0	11.6
Sprint/MICOM	7	JANTX	Zener	0	81.3
Sprint/MICOM	3	JANTX	SCR	1	509.2
TOW/MICOM	7	JANTX	Si,Gen.Purpose	0	162.9
TOW/MICOM	2	JANTX	Zener	0	5.3
Lance/MICOM	7	JANTX	Si,Gen.Purpose	0	67.1
Lance/MICOM	5	JANTX	Zener	0	10.1
Martin Marietta	2	JAN	Si,Gen.Purpose	41	6262.0
Martin Marietta	1	JAN	Zener	0	607.0
Martin Marietta	1	JANTX	Zener	1	898.0
Martin Marietta	1	JANTX	Tunnel	0	1.9
Martin Marietta	1	JANTX	Varactor	0	1.9
F-16 HUD/RIW	19	JANTX	Si,Gen.Purpose	5	2192.8
PRC	1	JANTX	Zener	0	0.3
Totals	139			57	22180.6

A preliminary analysis of the collected data was then performed to identify relative strengths and weaknesses. The primary weakness was that all data were from a ground based environment. Therefore, there were an insufficient range of environmental stresses represented in the data to develop a series of nonoperating environmental factors empirically. This deficiency was common to all generic part types considered in this study. An alternate nonoperating environmental factor development procedure was developed (described in Section 4.5) to compensate for this deficiency. This method was applied after application of regression analysis to evaluate the effects of device style and quality. Another major deficiency with the summarized data set was that there was an insufficient range of temperatures to study the effects of temperature analytically. It was considered to be essential that a proposed diode nonoperating failure rate prediction model include the effects of temperature. Therefore, an applicable nonoperating temperature factor was assumed based on the MIL-HDBK-217D diode failure rate prediction model, and the proposed temperature factor for transistors.

"Dummy variable" matrices were defined for device style and quality. Statistical techniques such as regression analysis and correlation coefficient analysis require that variables are quantitative. Conversely, device style and quality level are qualitative variables. Therefore, definition of the matrices was necessary to accommodate the techniques required for nonoperating failure rate model development. The matrix for device style is presented in Table 5.2.3-3. Three variables were required to represent four distinct diode styles. The three variables were designated S_1 , S_2 , and S_3 . The matrix for quality level was simply a "0" for JANTX diodes and a "1" for JAN diodes. This variable was designated Q_1 .

TABLE 5.2.3-3: DIODE STYLE VARIABLE MATRIX

Diode Style	S ₁	S ₂	S ₃
Si, General Purpose	0	0	0
Zener	1	0	0
Thyristor	0	1	0
Microwave	0	0	1

The correlation coefficient analysis indicated no large correlation between independent variables. The data were then merged according to equipment, device style and quality level by summing the observed failures and the part hours. For example, all JANTX zener diode data were merged for the Maverick missile by summing the observed failures and part hours.

Similar to the discussion for transistor model development, three equipment power on-off cycling variables (cyc1, cyc2 and cyc3) were defined to represent four distinct equipment cycling rate categories. An approach of this type was necessary because the assumed relationship between nonoperating failure rate and equipment power on-off cycling resulted in a nonlinear model form. An iterative approach was taken to solve the nonlinear model. The four cycling rate categories were designated as (1) low, (2) intermediate, (3) high, and (4) unknown cycling rates, and were defined as,

- o cycling rates less than one power cycle every two years (cyc1, cyc2, cyc3 = 0,0,0).
- o cycling rates between one cycle per year and one cycle every two years (cyc1, cyc2, cyc3 = 1,0,0).
- o cycling rates greater than one cycle per year (cyc1, cyc2, cyc3 = 1,0,0).
- o unknown cycling rates (cyc1, cyc2, cyc3 = 0,0,1).

At this stage of the model development process, regression analysis was applied to the data. Results of the initial regression analysis are presented in Table 5.2.3-4. The dependent variable was the natural logarithm of nonoperating failure rate and the independent variables

introduced into the analysis were S_1 , S_2 , S_3 , Q_1 , cyc1, cyc2 and cyc3. The S_3 variable was significant with 90% confidence, the Q_1 variable was significant with 70% and S_1 , S_2 and cyc2 were significant with 60% confidence.

TABLE 5.2.3-4: DIODE INITIAL REGRESSION RESULTS

Variable	Coefficient	Standard Error	F-ratio	Confidence Limit
S_1	0.916	0.716	1.64	0.60
S_2	1.309	1.155	1.29	0.60
S_3	3.322	1.155	8.28	0.90
Q_1	1.291	0.740	3.05	0.70
cyc2	1.459	1.155	1.60	0.60
b_0	-7.542	--	--	--

The regression results were next evaluated. Interpretation of the regression solution was:

- 1) Microwave diode nonoperating failure rate was significantly different from S_i , general purpose diode failure rate with 90% confidence.
- 2) Zener diode and thyristor nonoperating failure rates were significantly different from S_i , general purpose diode failure rate with 60% confidence.
- 3) It was determined with 70% confidence that quality significantly affects diode nonoperating failure rate.
- 4) The nonoperating failure rate for high equipment power cycling rates was significantly larger, with 60% confidence, from devices with low, intermediate or unknown cycling rates. There was no significant difference, at the 60% confidence limit, between low, intermediate and unknown cycling rates.

The coefficients given in Table 5.2.3-4 were the results of a regression with the dependent variable equal to the natural logarithm of nonoperating failure rate. Transforming the regression solution into an

equation where failure rate (as opposed to log of failure rate) is the dependent variable results in the following multiplicative model.

$$\lambda_d = \lambda_{nb} \pi_{NQ} \pi_{cyc} \epsilon$$

where

- λ_d = predicted diode nonoperating failure rate
- λ_{nb} = preliminary nonoperating base failure rate (failures/ 10^6 nonoperating hours)
 - = $\exp(-7.542 + 0.916(S_1) + 1.309(S_2) + 3.322(S_3))$
 - = 0.000530, Si, General Purpose
 - = 0.00133, Zener
 - = 0.00196, Thyristor
 - = 0.0147, Microwave
- π_{NQ} = nonoperating quality factor
 - = $\exp(1.291(Q_1))$
 - = 1.0, JANTX
 - = 3.63, JAN
- π_{cyc} = equipment power on-off cycling factor
 - = $\exp(1.459(cyc2))$
 - = 1.0, cycling rate < .057 cycles/ 10^3 hr.
 - = 1.0, .057 \leq cycling rate < .114 cycles/ 10^3 hr.
 - = 4.30, cycling rate \geq .114 cycles/ 10^3 hr.
- ϵ = residual

The variables S_1 , S_2 , S_3 , Q_1 and $cyc2$ have been previously defined. It must be emphasized that this equation represents a preliminary model, which is only applicable to a ground based environment with an average nonoperating temperature of 20°C.

The next step in the model development process was to perform iterative regression analyses to accommodate the assumed nonlinear model form. For diodes, only one iteration was required. The regression after the first iteration is presented in Table 5.2.3-5. It was noted that the

respective confidence limits for S_1 , S_2 and Q_1 increased after one iteration. It was believed that this was evidence that the nonlinear model form was indeed the optimal form for predicting diode nonoperating failure rate. The preliminary model at this stage of the model development process is given by the following equation. The residual term was dropped from the equation at this point. However, the fact that a residual term should be included as part of a predictive model is implied.

$$\lambda_d = \lambda'_{nb} \pi_{NQ} \pi_{cyc}$$

where

λ'_{nb} = preliminary nonoperating base failure rate (failures/ 10^6 nonoperating hours)

= 0.000528, Si, general purpose

= 0.00132, Zener

= 0.00196, Thyristor

= 0.0146, Microwave

π_{NQ} = nonoperating quality factor

= 1.0, JANTX

= 3.64, JAN

π_{cyc} = equipment power on-off cycling factor

= $1 + .083(N_C)$

where

N_C = number of equipment power on-off cycles per 10^3 nonoperating hours

TABLE 5.2.3-5: DIODE FINAL REGRESSION RESULTS

Variable	Coefficient	Standard Error	F-ratio	Confidence Limit
S ₁	0.917	0.607	2.28	0.70
S ₂	1.310	1.011	1.68	0.70
S ₃	3.323	1.011	10.80	0.90
Q ₁	1.291	0.640	4.08	0.80
b ₀	-7.547	--	--	--

The magnitude of the ratio of the JAN to JANTX nonoperating quality factors was small in comparison to the corresponding ratio from MIL-HDBK-217D. It was hypothesized that observation was due to a significantly slower rate of failure for inherently weak devices in the nonoperating state. This trend is described in Section 4.6 of this report.

Data were only available for JANTX and JAN diode quality levels. However, it was essential that a proposed diode nonoperating failure rate prediction model include applicable nonoperating quality factors for each quality level presented previously in Table 5.2.3-1. Therefore, appropriate nonoperating quality factor values were extrapolated by assuming (1) that the nonoperating values would have a similar numerical ranking as the corresponding operating values, and (2) that the nonoperating values follow an increasing geometric progression. Table 5.2.3-6 presents the regression solution quality factor values, the extrapolated values for JANTXV, lower and plastic, and a 90% confidence interval computed around the point estimate value for JAN quality. The proposed values are normalized to a JANTX factor equal to one by definition. Conversely, the MIL-HDBK-217D diode quality factors do not appear to be normalized to any quality level.

TABLE 5.2.3-6: DIODE NONOPERATING QUALITY FACTORS

Quality Level	$\pi_{NQ,.05}$	$\pi_{NQ1}(1)$	$\pi_{NQ,.95}$	$\pi_{NQ2}(2)$
JANTXV	--	--	--	0.57
JANTX	--	1.0	--	1.0
JAN	1.00	3.64	13.2	3.6
Lower, Hermetic	--	--	--	13
Plastic	--	--	--	23

NOTES: (1) π_{NQ1} are the observed point estimate nonoperating quality factors.

(2) π_{NQ2} are the point estimate values complemented by extrapolated values for JANTXV, lower and plastic.

The next phase of the model development process was to apply the methods described in Section 4.5 to determine nonoperating environmental factors. This method assumed that appropriate nonoperating environmental factors could be generated from the corresponding MIL-HDBK-217D operating environmental factors by (1) comparing the difference in temperature, and (2) comparing the operating and nonoperating failure mechanism accelerating factors. No temperature adjustment was required for diode nonoperating environmental factors because the operating base failure rate (which is a function of temperature) and the proposed nonoperating temperature factor account for relative failure rate differences caused by internally generated heat. The comparison of failure mechanisms and failure mechanism accelerating factors indicated that the effects of environmental stress on nonoperating failure rate could be predicted by use of the MIL-HDBK-217D environmental factors. The complete series of diode nonoperating environmental factors is presented in Table 5.2.1-3 in Section 5.2.1. Tables 5.2.3-7 and 5.2.3-8 on the following pages present failure mode/mechanism and failure acceleration factor distributions for diodes in both the operating and nonoperating state. Accurate quantitative nonoperating failure mechanism information was extremely difficult to locate. Therefore, much of the information provided in Tables 5.2.3-7 and 5.2.3-8 was hypothesized. References 41, 42 and 43 proved to be useful for developing these distributions.

TABLE 5.2.3-7: ZENER DIODE FAILURE MODE/MECHANISM DISTRIBUTIONS

Failure Mode/Mechanism	Accelerating Factors	Operating Distribution (%)	Nonoperating Distribution (%)
open			
poor lead to die contact	shock, vibration, temp.	10-30	10-30
wire bond defects	shock, vibration	1-12	1-13
intermetallic formation	time, temp.	1-12	1-12
wire nicks	current	1-11	0-5
short			
bulk impurities	current	1-20	0-5
contamination	shock, vibration	1-20	1-20
relief loops touching	shock, vibration	1-15	1-15
degraded, intermittent, drift			
poor bonding of die to header	shock, vibration	15-30	20-40
moisture intrusion	humidity, temp., vibration	15-35	20-40

TABLE 5.2.3-8: SMALL SIGNAL DIODE FAILURE MODE/MECHANISM DISTRIBUTIONS

Failure Mode/Mechanism	Accelerating Factors	Operating Distribution (%)	Nonoperating Distribution (%)
open			
poor lead to die contact	shock, vibration, temp.	10-30	5-35
wire bond defects	shock, vibration	1-15	1-15
intermetallic formation	time, temp.	1-15	1-15
wire nicks	current	1-15	0-5
short			
bulk impurities	current	5-25	0-5
contamination, particles	shock, vibration	5-25	5-25
relief loops touching	shock, vibration	1-20	1-20
degraded, intermittent, drift			
poor bonding of die to header	shock, vibration	5-25	15-35
moisture intrusion	humidity, temp., vibration	1-20	5-25

The effect of nonoperating temperature was the next parameter evaluated. There was an insufficient range of temperature values represented in the data to determine a nonoperating temperature factor by the desired analytical techniques. However, the objective of this study was to develop nonoperating failure rate prediction methodologies which could be used for any conceivable mission profile (with the exception of satellites). Therefore, alternate methods were explored to determine an appropriate temperature factor. In the general discussion of temperature effects described in Section 4.4, a nonoperating temperature factor was presented for transistors and diodes. The factor was represented by the following equation.

$$\pi_{NT} = \exp(-A_n(\frac{1}{T} - \frac{1}{298}) + (\frac{T}{T_m})^P)$$

where

π_{NT} = nonoperating temperature factor

T = temperature (°K)

A_n = temperature coefficient

T_m, P = shaping parameters

High temperature storage life test data for transistors were used to estimate A_n terms during the transistor nonoperating failure rate model development. The T_m and P shaping parameter terms were assumed because of data limitations. Nevertheless, the transistor temperature factor was based on empirical data, and, therefore, is accurate in the range of 150°C to 200°C. For other temperatures, accuracy of the proposed transistor temperature factor is dependent on the accuracy of the assumptions. A_n values for transistor styles without data were extrapolated using the MIL-HDBK-217D relationship for failure rate vs. temperature. It was decided to extend the extrapolation process to also include diodes as a method to determine appropriate diode nonoperating temperature factors. This assumption was justified because of documented similarities (i.e. MIL-HDBK-217D) between the temperature relationships of transistors and

diodes. The extrapolated series of A_n values and the assumed values for T_m and P are presented in Table 5.2.1-1 of Section 5.2.1.

The final phase of the diode nonoperating failure rate model development process was to normalize the preliminary base failure rates to correspond to a ground benign environment and a nonoperating temperature of 25°C (i.e. the reference temperature). Additionally, base failure rate values were extrapolated for diode types without data. Table 5.2.3-9 presents the normalized nonoperating base failure rates, the extrapolated base failure rate values and 90% confidence limits for zener, thyristor and microwave diodes. Use of the standard error statistic and the t -statistic allows for computation of the 90% confidence interval values. Because of log transformation, the values are only approximate.

TABLE 5.2.3-9: DIODE NONOPERATING BASE FAILURE RATES

Device Style	$\lambda_{b,.05}$	$\lambda_{b1}(1)$	$\lambda_{b,.95}$	$\lambda_{b2}(2)$
S_i , General Purpose	--	.000174	--	.000174
Ge, General Purpose	--	--	--	.000420
Zener/Avalanche	.000118	.000402	.00136	.000402
Microwave	.000349	.00266	.0205	.00266
Thyristor	.000083	.000632	.00485	.000632
Group VIII (3)	--	--	--	.00266

- NOTES:
- (1) λ_{b1} is the observed point estimate base failure rates
 - (2) λ_{b2} is the observed values complemented with extrapolated values.
 - (3) Group VIII diodes include varactor, PIN, IMPATT, step recovery, tunnel and gunn devices

Normalization of the nonoperating base failure rates was the final phase of the diode model development process. The proposed model is,

$$\lambda_p = \lambda_{nb} \pi_{NT} \pi_{NQ} \pi_{NE} \pi_{cyc}$$

where all factors have been previously defined.

The proposed model is presented in Section 5.2.1 and in Appendix A in a form compatible with MIL-HDBK-217D. Model validation for discrete semiconductors is presented in Section 5.2.5.

5.2.4 Opto-electronic Semiconductor Model Development

The desired modeling approach utilizing analysis of a large data base was not feasible for opto-electronic semiconductor devices. No nonoperating failure rate data were collected for light emitting diodes (LEDs), isolators, phototransistors, photodiodes or alpha-numeric displays. Nevertheless, the objective of this study was to develop nonoperating failure rate prediction models which could be used for any proposed electronic equipment in any conceivable mission profile. Therefore, an alternate modeling approach was taken based on the ratio of operating to nonoperating failure rate for other semiconductor devices.

Initially, it was believed that sufficient nonoperating reliability data would be collected for opto-electronic semiconductors, and the general failure rate modeling approach (described in Section 4.1) would also be implemented for these devices. As a prerequisite for the planned data collection and theoretical model development, a list of application and construction variables were determined for opto-electronic devices. These variables are presented in Table 5.2.4-1, and represent possible nonoperating failure rate model parameters.

TABLE 5.2.4-1: OPTO-ELECTRONIC DEVICE CHARACTERIZATION VARIABLES

- I. Device Style
 - A. Light Emitting Diode (LED)
 - B. Isolator
 - 1. Photodiode Detector
 - 2. Phototransistor Detector
 - 3. Light Sensitive Resistor
 - C. Phototransistor
 - D. Photodiode
 - E. Alpha-numeric Display
- II. Complexity
 - A. Single Isolator
 - B. Dual Isolator
- III. Quality Level
 - A. JANTXV
 - B. JANTX
 - C. JAN
 - D. Lower, Hermetic
 - E. Plastic
- IV. Number of Pins
- V. Temperature
- VI. Application Environment
- VII. Number of Equipment Power On/Off Cycles per 10^3 Nonoperating Hours

A theoretical model was developed for opto-electronic devices based primarily on intuitive reliability relationships. Very little documented information concerning the storage/dormant reliability of these devices was available. The theoretical model was determined to be a function of device style, complexity, quality level, number of pins and equipment power on-off cycling frequency. In the absence of data, the theoretical model development process was the basis of the proposed nonoperating failure rate prediction model.

Despite extensive data collection efforts, no data were collected for opto-electronic semiconductors. Therefore, the anticipated failure behavior of opto-electronic devices was compared with other semiconductor devices. Two conclusions were made based on this comparison. First, the relative effect of device screening was anticipated to be similar for opto-electronic devices as the effect on transistors and diodes. As a result of this conclusion, the proposed nonoperating quality factors for diodes (also applied for transistors) were used to assess the effect of quality on opto-electronic semiconductors. These proposed nonoperating quality factors were presented in Table 5.2.3-6 in the previous section. The second conclusion was based on the observation that the MIL-HDBK-217D operating environmental factors were also assumed to accurately predict the effects of environmental stress during nonoperating periods. A similar assumption was made for opto-electronic devices. The MIL-HDBK-217D opto-electronic environmental factors were also applied for nonoperating failure rate prediction purposes, and were presented in Table 5.2.1-4 in Section 5.2.1.

The theoretical model for opto-electronic semiconductor devices was also assumed to be a function of device style, complexity, temperature and equipment power on-off cycling. It would have been extremely presumptuous to assume relationships for each of these variables without additional justification (i.e. observed data). A proposed nonoperating failure rate prediction model based entirely on assumptions must be considered approximate at best. Therefore, the only additional factor included in the proposed model was a nonoperating base failure rate as a function of

device style. Additional factors would only serve to complicate the proposed model without resulting in any significant improvement in model accuracy. The proposed model is therefore represented by the following equation.

$$\lambda_{oe} = \lambda_{nb} \pi_{NQ} \pi_{NE}$$

where

λ_{oe} = opto-electronic semiconductor predicted nonoperating failure rate

λ_{nb} = nonoperating base failure rate (failures/ 10^6 nonoperating hours)
= f(device style)

π_{NQ} = assumed nonoperating quality factor

π_{NE} = nonoperating environmental factor

Determination of numerical quantities for the opto-electronic base failure rate was conducted in two phases. The first phase was the selection of device style categories. It was decided to estimate separate base failure rate values for (1) LEDs, (2) single isolators, (3) dual isolators, (4) phototransistors, (5) photodiodes, and (6) alpha-numeric displays. There are obviously other variables within each of these categories which effect nonoperating failure rate. However, no finer division was justified because of the lack of quantitative information. The second phase of the nonoperating base failure rate determination process was to calculate an average nonoperating to operating failure rate ratio based on the proposed nonoperating failure rate prediction models for transistors and diodes, and the corresponding sections of MIL-HDBK-217D. It was found the average ratio for other semiconductor types was equal to 1:8. Thus, this adjustment factor was applied to the operating failure rate prediction model values. The resultant nonoperating base failure rates are presented in Table 5.2.4-2.

TABLE 5.2.4-2: OPTO-ELECTRONIC NONOPERATING BASE FAILURE RATES

Device Style	λ_{nb} (Failures/ 10^6 nonoperating hours)
Single LED	.000163
Single Isolator	.000699
Dual Isolator	.000885
Phototransistor	.000375
Photodiode	.000275
Alpha-numeric Display	.000254

It is emphasized that the proposed nonoperating failure rate prediction model for opto-electronic semiconductors is based solely on assumptions, and therefore must be considered approximate. However, a viable approach was taken to determine numerical values for the proposed model. It is strongly recommended that the accuracy of the proposed model is evaluated when nonoperating failure rate data becomes available for opto-electronic semiconductors.

5.2.5 Model Validation

The proposed discrete semiconductor nonoperating failure rate prediction models were next subjected to an extreme case analysis and a model evaluation process with observed data. The extreme case analysis consisted of computing nonoperating failure rate predictions with the proposed models for parameters beyond the ranges found in the data. The intent of the extreme case analysis was to identify any set of conditions which cause the proposed models to approach infinity, or predict intuitively inconsistent results. The proposed models were then tested with observed data which had been withheld from the model development process. Nonoperating failure rate data for discrete semiconductors had been collected from AFCIQ. However, only the high temperature storage life test data from AFCIQ were used for model development purposes.

The extreme case analyses did not indicate any deficiencies with the proposed models. At extremely high levels of equipment power cycling, the

nonoperating failure rate become proportional to the equipment power cycling frequency. This was considered to be an intuitively satisfactory result because, at high cycling frequencies, true storage related failures would be negligible in comparison to the number of failures induced by power on-off cycling. At extremely low cycling frequencies, the proposed models would predict nonoperating failure rates independent of equipment power cycling frequency. This was also considered to be an intuitively appealing result.

The field experience nonoperating failure rate data from AFCIQ were not used in the model development process because vital information such as equipment power cycling frequency and part screen class could not be precisely determined. However, these parameters were estimated and the data were used for model validation purposes. Tables 5.2.5-1 and 5.2.5-2 presents the model validation data for transistors and diodes respectively.

On average, the model validation process indicated that the proposed models were extremely accurate. However, individual data entries varied substantially from the predicted values. The geometric mean of the ratio of observed to predicted nonoperating failure rate was equal to 1.03 for those data entries with either observed failures or sufficient part hours to estimate a failure rate without failures. When the two most divergent data entries (numbers 4 and 13 in Table 5.2.5-2) were deleted, the geometric mean of the ratio became equal to 1.16. For transistors alone, the ratio of observed to predicted nonoperating failure rate was equal to 0.81. The geometric mean of the diode data, except entries 4 and 13, was equal to 1.35. These ratios were very close to unity, and this observation was considered to be indicative of accurate nonoperating failure rate prediction models.

TABLE 5.2.5-1: TRANSISTOR MODEL VALIDATION DATA

No.	Failures	Part Hours (x10 ⁶)	Style	Temp. (°C)	Equiv. Quality	$\lambda_{.05}$	λ_0	$\lambda_{.95}$	$\lambda_{pre(1)}$
1	6	1900	Si,PNP	20-30	JAN	.00138	.00316	.0062	.00567
2	0	18	Si,PNP	25	JAN	--	(3)	.166	.00567
3	0	38	Si,PNP	25	JAN	--	(3)	.0788	.00567
4	0	5	Si,PNP	25	JAN	--	(3)	.599	.00567
5	3	1100	Si,PNP	20-30	JAN	.00075	.00273	.0071	.00567
6	0	72	Si,NPN	25-30	JAN	--	(3)	.0416	.00567
7	0	42	Si,NPN	25-30	JAN	--	(3)	.0713	.00567
8	1	30	Si,NPN	25	JAN	.00171	.03333	.158	.00567
9	4	2800	Si,NPN	20-30	JAN	.00049	.00143	.0033	.00567
10	1	1253	Si,NPN	(2)	JANTX	.00004	.00080	.0038	.00157
11	8	1000	FET	20-30	JAN	.00398	.00800	.0144	.00565
12	0	28	FET	25	JAN	--	(3)	.107	.00565
13	0	6	FET	25	JAN	--	(3)	.499	.00565
14	0	6	FET	25	JAN	--	(3)	.499	.00565
15	0	96	FET	5-30	JAN	--	(3)	.0312	.00565
16	0	5	Unijun.	25	JAN	--	(3)	.599	.00565
Totals		23	8422						

- Notes:
- 1) λ_{pre} = predicted nonoperating failure rate. A cycling rate of 0.114 cycles/10³ nonoperating hours was assumed.
 - 2) Temperature was unknown for this data entry. Temperature assumed to be 25°C.
 - 3) There were insufficient part hours for these data entries to estimate a failure rate without observed failures.

TABLE 5.2.5-2: DIODE MODEL VALIDATION DATA

No.	Failures	Part Hours (x10 ⁶)	Style	Temp. (°C)	Equiv. Quality	$\lambda_{.05}$	λ_0	$\lambda_{.95}$	$\lambda_{pre}(1)$
1	20	779	Si,GP	(2)	Plastic	.01702	.02567	.0371	.01539
2	5	675	Si,GP	(2)	Plastic	.00292	.00741	.0156	.01539
3	2	136	Si,GP	20-30	JAN	.00261	.01471	.0463	.00241
4	2	16000	Si,GP	20-30	JAN	<.00001	.00001	.0004	.00241
5	4	906	Si,GP	(2)	JAN	.00151	.00442	.0101	.00241
6	0	41	Si,GP	25	JAN	--	(5)	.0730	.00241
7	1	247	Si,GP	25	JAN	.00021	.00405	.0192	.00241
8	0	36	Si,GP	25	JAN	--	(5)	.0832	.00241
9	1	400	Si,GP	5-30	JAN	.00013	.00250	.0119	.00241
10	1	1200	Si,GP	0-30	JAN	.00004	.00083	.0040	.00241
11(3)	0	3422	Si,GP	(2)	JANTX	--	.00029	.0009	.00067
12	5	47	Zener	(2)	Plastic	.04191	.1064	.2237	.03622
13	2	14	Zener	20-30	JAN	.02539	.1429	.4496	.00567
14	1	130	Zener	(2)	JAN	.00039	.00769	.0365	.00567
15	0	12	Zener	25	JAN	--	(5)	.2496	.00567
16	0	24	Zener	25	JAN	--	(5)	.1249	.00567
17	0	150	Zener	5-30	JAN	--	(5)	.0200	.00567
18	0	624	Zener	0-30	JAN	--	.00160	.0048	.00567
19(3)	1	175	Zener	(2)	JANTX	.00029	.00571	.0271	.00157
20	15	104	Si,GP	(2)	Plastic	.0889	.1442	.2205	.01539
21	0	30	Si,GP	25	JAN	--	(5)	.0998	.00241
22	0	67	Si,GP	5-30	JAN	--	(5)	.0447	.00241
23	0	72	Si,GP	(2)	JANTX	--	(5)	.0416	.00067
24(4)	16	10	Thyr.	(2)	Plastic	(4)	(4)	(4)	.0570
25	0	2	Thyr.	(2)	Plastic	--	(5)	1.498	.0570
26	0	19	Thyr.	20-30	JAN	--	(5)	.0365	.00893
27	1	130	Thyr.	20-30	JAN	.00039	.00769	.0365	.00893
28	0	16	Thyr.	0-30	JAN	--	(5)	.1872	.00893
Totals	77	25468							

- NOTES:
- 1) λ_{pre} = predicted nonoperating failure rate. A cycling rate of 0.114 cycles/10³ hours was assumed.
 - 2) Temperature was unknown for these data entries. Temperature assumed to be 25°C.
 - 3) The application environment was unknown for these data entries. An environment of ground fixed was assumed.
 - 4) This part was over-stressed.
 - 5) There were insufficient part hours for these data entries to estimate a failure rate without observed failures.

Inspection of the diode model validation data (Table 5.2.5-2) gives a good indication of the inherent variability which exists for nonoperating failure rates. It is not unusual for there to be order of magnitude differences for similar devices in similar applications. For this reason, incorrect conclusions can be made if insufficient data resources were available for analysis. This was one reason such a large emphasis was placed on the data collection effort in this study, and why model validation was an integral part of the overall model development process.

5.3 Resistors

5.3.1 Proposed Resistor Nonoperating Failure Rate Prediction Model

This section presents the proposed nonoperating failure rate prediction model for resistors. The proposed model is presented in Appendix A in a form compatible with MIL-HDBK-217D. The proposed model is:

$$\lambda_p = \lambda_{nb} \pi_{NQ} \pi_{NE} \pi_{cyc}$$

where

- λ_p = predicted resistor nonoperating failure rate
- λ_{nb} = nonoperating base failure rate (failures/ 10^6 hours)
 - = .000063, fixed composition (RC, RCR)
 - = .00010, fixed film (RN, RD, RL, RLR, RNR)
 - = .00043, film network (RZ)
 - = .00057, fixed wire wound (RW, RB, RE, RBR, RWR, RER)
 - = .00099, variable wirewound trimmer (RT, RTR)
 - = .0052, precision, semiprecision or power variable wirewound (RR, RA, RK, RP)
 - = .0052, variable non-wirewound (RV, RJ, RVC, RQ, RJR)
 - = .0027, thermistor (RTH)
- π_{NQ} = nonoperating quality factor
 - = 0.15, S
 - = 0.28, R
 - = 0.52, P
 - = 1.0, M
 - = 2.4, MIL-SPEC
 - = 4.4, lower
- π_{NE} = nonoperating environmental factor (see Table 5.3.1-1)

TABLE 5.3.1-1: RESISTOR NONOPERATING ENVIRONMENTAL FACTORS (π_{NE})

Env.	Comp.	Film	Network	WW	Therm.	Var. WW	Var. non-WW
GB	1	1	1	1	1	1	1
GF	2.9	2.4	2.4	2.1	4.8	2.5	2.5
GM	8.3	8.3	7.8	8.8	23	13	13
MP	8.5	9.9	8.8	11	17	18	19
NSB	4	4.7	4.2	5	7.9	7	7
NS	5.2	4.9	4.7	5	14	7	7
NU	12	15	14	15	17	14(3)	17
NH	13	16	14	17	25	29	29
NUU	14	17	15	18	27	31	31
ARW	19	22	19	24	33	41	41
AIC	3	3	2.5	4.3	4.3	5.5	12
AIT	3.5	4.5	3	7.3	7.7	6.6	16
AIB	5	6.8	6.5	12	19	9.5	24
AIA	3.5	5.8	6	9.7	15	8.6	22
AIIF	6.5	9.5	9	13	38	14	33
AUC	5	7.5	6	10	4.6	6.5(3)	19
AUT	7	11	6.5	13	8.6	9 (3)	25
AUB	10	18	15	23	21	18 (3)	37
AUA	7	13	15	18	17	13 (3)	32
AUF	15	23	20	28	42	20 (3)	52
SF	(2)	(2)	(2)	(2)	(2)	(2)	(2)
MFF	8.6	10	8.9	11	15	20 (3)	19
MFA	13	14	12	16	21	28 (3)	26
USL	25	30	26	33	49	58 (3)	56
ML	29	35	30	38	51	66 (3)	64
CL	490	590	510	610	950	1100 (3)	1100

- NOTES:
- 1) WW = Wirewound
 - 2) Space flight environment was not considered in this study
 - 3) These factors are not applicable for semiprecision wirewound or high power wirewound variable resistors.

$$\begin{aligned}\pi_{\text{cyc}} &= \text{equipment power on-off cycling factor} \\ &= 1 + .063(N_C)\end{aligned}$$

where

N_C = number of equipment power on-off cycles per 10^3 nonoperating hours

5.3.2 Model Development

The failure rate modeling approach described in Section 4.1 was successfully implemented for resistors. An assumed theoretical model was supplemented by analysis of the available resistor nonoperating reliability data to derive the failure rate prediction model. The model was determined to be a function of device style, quality level, environment and equipment power on-off cycling frequency. The proposed nonoperating failure rate prediction model for resistors is presented in Appendix A in a form compatible with MIL-HDBK-217D. This section describes the model development process.

The first step in the model development process was to identify application and construction variables which properly characterize resistors in a nonoperating environment. Table 5.3.2-1 presents a list of the part characterization variables for resistors. These variables represent possible failure rate model input parameters which were analyzed in greater depth using statistical methods. The part characterization variables were determined whenever possible for all collected data. If sufficient detail could not be determined for an individual data entry, then it was removed from the model development process.

The general nonoperating reliability concepts presented in Section 4.0 were complemented by a study of resistor nonoperating failure mechanisms and physics of failure information to determine a theoretical model for resistors. The theoretical model assumes a nonlinear failure rate equation which is constant with respect to time. The theoretical model

TABLE 5.3.2-1: RESISTOR PART CHARACTERIZATION

- I. Device Style
 - A. Fixed
 - 1. Composition (RC, RCR)
 - 2. Film (RN, RD, RL, RLR, RNR)
 - 3. Network, Film (RZ)
 - 4. Wirewound (RW, RB, RE, RBR, RWR, RER)
 - B. Variable
 - 1. Non-wirewound (RV, RJ, RVC, RQ, RJR)
 - 2. Wirewound (RA, RP, RR, RT, RK, RTR)
 - C. Thermistor (RTH)
 - 1. Bead
 - 2. Disk
 - 3. Rod
- II. Resistance (ohms)
- III. Rated Power (watts)
- IV. Quality Level

A. S	D. M
B. P	E. Mil-Spec
C. R	F. lower
- V. Number of Potentiometer Taps
- VI. Construction Class
 - A. Enclosed
 - B. Unenclosed
- VII. Number of Pins (style RZ only)
- VIII. Number of Resistors (style RZ only)
- IX. Temperature
 - A. Rated
 - B. Actual
- X. Application Environment
- XI. Number of Power On/Off Cycles per 10^3 Nonoperating Hours

developed for resistors is described by the following equation (f denotes a function).

$$\lambda_r = f(\text{device style, temp., } R, P,)\pi_{NQ}\pi_{NE}\pi_{cyc}$$

where

λ_r = predicted resistor nonoperating failure rate (failures/ 10^6 hrs)

R = resistance (ohms)

P = rated power (watts)

π_{NQ} = nonoperating quality factor, based on device screening

π_{NE} = nonoperating environmental factor

π_{cyc} = equipment power on-off cycling factor = $1 + K_1(N_c)$

K_1 = constant

N_c = equipment power on-off cycling rate (cycles/ 10^3 nonop. hrs.)

Presentation of the theoretical model does not imply that each of these variables was significant by anything other than theoretical grounds. Statistical methods, where appropriate, were used as a basis for decisions regarding significance of variables. The theoretical model was intended to define the relationship of the independent variables to each other.

The summarized resistor nonoperating reliability data collected in support of this study is presented in Table 5.3.2-2. The data collectively consists of 413 individual data records, 34 observed failures and $113,119 \times 10^6$ part hours.

Initially the data was evaluated with each data record separate (i.e. no data records were merged). Point estimate failure rates were computed for data records with observed failures. The methods described in Section 3.3 were applied to determine which zero failure data records had sufficient part hours to be included in the analysis, and to estimate failure rate for those records. It was found that 43 data records either

TABLE 5.3.2-2: RESISTOR NONOPERATING FAILURE RATE DATA

Equipment/Source	Data Records	Style	Failures	Parts Hours (x10 ⁶)
Sprint/MICOM	3	Wirewound	0	31.0
Sprint/MICOM	4	Composition	0	4300.0
Sprint/MICOM	1	Film	0	147.1
Sparrow/MICOM	116	Composition	2	4478.9
Sparrow/MICOM	173	Film	0	5346.6
Sparrow/MICOM	13	Wirewound	1	268.0
Sparrow/MICOM	6	Var., Non-WW	1	102.1
Sparrow/MICOM	1	Thermistor	0	13.0
TOW/MICOM	6	Film	0	609.7
TOW/MICOM	7	Composition	0	141.9
TOW/MICOM	1	Wirewound	0	42.1
Lance/MICOM	4	Film	0	122.0
Lance/MICOM	4	Composition	0	239.3
Lance/MICOM	2	Wirewound	0	23.4
Lance/MICOM	1	Var., WW	0	2.2
Lance/MICOM	1	Thermistor	0	1.1
Lance/MICOM	1	Film Ntwk.	0	1.1
Hawk/MICOM	8	Film	0	38576.5
Hawk/MICOM	4	Wirewound	1	1225.1
Hawk/MICOM	1	Thermistor	0	51.0
Hawk/MICOM	3	Var., Non-WW	0	102.1
Hawk/MICOM	1	Var., WW	0	17.0
Maverick/MICOM	8	Film	0	5806.4
Maverick/MICOM	4	Wirewound	0	782.4
Maverick/MICOM	7	Composition	0	3486.5
Maverick/MICOM	3	Var., Non-WW	0	370.6
Maverick/MICOM	2	Var., WW	1	514.8
Martin Marietta	2	Composition	0	11548.7
Martin Marietta	4	Film	1	15937.5
Martin Marietta	3	Thermistor	3	102.0
Martin Marietta	6	Wirewound	2	4339.0
Martin Marietta	2	Var., Non-WW	1	24.1
Martin Marietta	1	Var., WW	0	1.5
PRC	1	Composition	0	159.0
PRC	1	Film	0	192.0
F-16 HUD/RIW	3	Film	18	10328.2
F-16 HUD/RIW	2	Wirewound	2	570.9
F-16 HUD/RIW	2	Composition	0	2893.5
F-16 HUD/RIW	1	Var., WW	1	220.6
Totals	413		34	113,118.9

had observed failures or had sufficient part hours to estimate a failure rate without observed failures.

The number of variables which could be analyzed empirically was restricted because of the nature of the available data. The following attributes of the collected nonoperating resistor data were identified from the preliminary data analysis.

- 1) All collected data were from a ground based environment. Therefore, there was not a sufficient range of environments to develop a series of environmental factors based solely on the data.
- 2) There was an insufficient range of ambient temperatures to study the effects of temperature analytically.
- 3) The inherent failure rate of resistors in storage/dormant applications is very low. Therefore, the number of data records with observed failures and the number of failures per data record were naturally limited. Precise estimates of field failure rates and quantification of failure rate model parameters can not be made without observed failures. Thus, the number of variables which could be analyzed empirically was also limited.

The theoretical model was further scrutinized to determine the relative effect of the independent variables so that decisions could be made regarding the selection of variables. Failure mechanism acceleration factors were studied to aid in the variable evaluation process.

The preliminary model refinement process resulted in the conclusion that resistor device style, quality level, application environment and equipment power on-off cycling frequency are the dominant variables effecting nonoperating failure rate. These variables, with the exception of application environment, were further analyzed using statistical techniques. It was also determined that resistance level, and rated power were significant variables for assessing operating resistor failure rate, but theoretically had little effect on nonoperating failure rate. These two variables were not included in subsequent analyses.

It was assumed that application environment was a very important parameter effecting resistor nonoperating failure rate. Therefore it was essential that a proposed resistor nonoperating failure rate prediction model include an appropriate environmental factor to properly discriminate against known failure accelerating factors. All data collected in support of this study was for ground based environments, and therefore environmental factors could not be developed empirically. This was a major obstacle to the successful completion of this study and is discussed in Section 4.5 of this report. Section 4.5 also proposes a method to develop appropriate environmental factors based on a comparison of operating and nonoperating failure mechanisms, and a study of the documented MIL-HDBK-217D operating environmental factors. This method was applied to resistor nonoperating failure rate modeling after statistically analyzing the other variables.

The fact that temperature could not be empirically analyzed was also a problem. However, after careful consideration of many factors, it was decided not to include temperature in the failure rate prediction model. This decision was based on three reasons or observations. First, a temperature relationship could not be determined from the data. Therefore, any proposed temperature factor would be based on assumptions, which introduce inaccuracies. The second reason was that no theoretical relationship for resistor nonoperating failure rate vs. temperature could be located in the literature. In addition, there was no basis for assumptions that the nonoperating failure rate behaves similarly to the operating rate with respect to temperature. The stresses on the part are necessarily different due to the absence of an applied current. Therefore an approach of that nature was determined to be invalid. The third reason was that the temperature dependence of resistor nonoperating failure rate was believed to be significantly less than the temperature dependence for microcircuits and discrete semiconductors. The proposed nonoperating failure rate for these devices (described in Sections 5.1 and 5.2 of this report) does include a temperature factor. Therefore, the absence of a temperature factor for low failure rate devices, such as resistors, would not significantly effect equipment-level failure rate predictions. It also

should be noted that the very high temperatures during operation are not observed during nonoperating periods because of the absence of internal heat generation and the associated cooling problems. In conclusion, it is emphasized that direct numerical analysis of the relationship of resistor nonoperating failure rate and temperature would have been desirable. However, it is also emphasized that deletion of ambient temperature from the model development process was believed to have little effect on the accuracy of the proposed resistor nonoperating failure rate prediction model.

Matrices of "dummy variables" (0 or 1) were defined for device style and quality level so that correlation coefficient analysis and regression analysis could be applied to the data. These analyses require quantitative variables, whereas device style and quality level are qualitative variables. The matrix for device style is given in Table 5.3.2-3. No distinction was made between the different styles of variable resistors. The specific styles of variable resistors with data were wirewound precision, non-wirewound trimmer, wirewound trimmer, and non-wirewound film. This was done because of the limited amount of data (i.e. only 4 variable resistor observed failures) and because the failure rate difference between specific variable resistor types was assumed to be much less than the difference between variable and fixed resistors. The difference in failure rate between the specific styles of variable resistors were analyzed at a later stage of the model development process. The matrix for quality level was simply a "0" for high-reliability parts and a "1" for mil-spec quality parts. This variable was designated as Q_1 . The quality matrix was not defined to accommodate lower quality resistors because no data was available for lower quality resistors.

The data were then merged according to equipment, device style, and quality level. The data were merged by summing observed failures and summing part hours. For example, all data for B screen class, fixed composition resistors in the Hawk missile were merged. The correlation coefficient analysis indicated no large correlation between independent variables for the merged data set.

TABLE 5.3.2-3: RESISTOR STYLE VARIABLE MATRIX

Device Style	S ₁	S ₂	S ₃	S ₄
Variable	0	0	0	0
Fixed, Wirewound	1	0	0	0
Fixed, Film	0	1	0	0
Fixed, Composition	0	0	1	0
Thermistor	0	0	0	1

The theoretical resistor model was nonlinear due to the assumed relationship for equipment power cycling frequency. Thus, linear regression analysis could not be directly applied. An iterative approach to nonlinear regression was described in Section 4.3. As suggested in Section 4.3, equipment power cycling frequency was temporarily treated as a qualitative variable. Constant multiplicative values were computed by regression for three distinct cycling rate categories. Then a two-dimensional regression was performed with the cycling rate coefficients from the initial regression as the dependent variable, and the mean cycling rate value for each category as the independent variable. The result would be an expression for equipment cycling factor of the desired form (i.e. cycling factor = $mx + b$). As the iterative process continued, the equipment power cycling factor expression would be assumed exact, and the coefficients for all other variables recalculated. Then, those coefficients would be assumed to be exact and the equipment cycling factor recalculated. The iterative process would continued until observed changes were negligible.

Three qualitative "dummy" variables were defined (cyc1, cyc2, and cyc3) to represent four distinct equipment power cycling rate categories, which are,

- o cycling rates less than one power cycle every two years (cyc1, cyc2, cyc3 = 0,0,0),
- o cycling rates between one cycle per year and one cycle every two years (cyc1, cyc2, cyc3 = 1,0,0),
- o cycling rates greater than one cycle per year (cyc1, cyc2, cyc3 = 0,1,0), and

- o unknown cycling rates (cyc1, cyc2, cyc3 = 0,0,1).

The first three categories were designated as (1) low, (2) intermediate, and (3) high cycling frequencies, respectively.

Results of the initial regression analysis are given in Table 5.3.2-4. The dependent variable was $\ln(\text{failure rate})$. The independent variables were S_1 , S_2 , S_3 , S_4 , Q_1 , cyc1, cyc2, and cyc3, which were previously defined. Device style variables S_1 , S_2 , S_3 , quality variable Q_1 and equipment power cycling variable cyc2 were significant at a 90% confidence limit. No other variables were significant at a 70% confidence limit. The R-squared value for the regression was 0.85. That is, 85% of the variability in the observed data can be explained by the regression solution. Interpretation of the regression results are:

- 1) The nonoperating failure rates for fixed composition, fixed film, and fixed wirewound resistors were significantly different, with a 90% confidence, from the variable resistor and thermistor failure rate, as would be expected.
- 2) The difference in failure rate between variable resistors and thermistors was not significant at a 70% confidence limit.
- 3) As expected, it was determined with 90% confidence that resistor screening impacts the field nonoperating failure rate. Interpretation of the regression results was that the failure rate of Mil-spec quality resistors is 4.8 times higher than resistors screened to the established reliability specification.
- 4) The cyc2 equipment power cycling variable was significant with 90% confidence. This substantiated the assumption that equipment power cycling is an important variable for predicting nonoperating failure rate. The significance of cyc2 also served as a rationale to proceed with the cycling factor analysis. The failure rate difference between low, intermediate and unknown cycling frequencies was not significant even at a 70% confidence.

Regression solutions for confidence limits lower than 70% were computed to further investigate the difference between thermistor and variable resistor failure rate. At 50% confidence, the difference became significant (i.e. the f-ratio for the S_4 variable exceeded the critical-f

value). Interpretation of the results were that the ratio of thermistor to variable resistor failure rate was equal to 2.0. However, after careful consideration, it was decided that there was insufficient confidence to propose unique values for variable resistors and thermistors.

TABLE 5.3.2-4: RESISTOR INITIAL REGRESSION RESULTS

variable	coefficient	standard error	f-ratio	confidence limit
S ₁	-2.386	0.637	14.04	.90
S ₂	-3.957	0.584	45.91	.90
S ₃	-4.257	0.622	46.80	.90
Q ₁	1.560	0.512	9.28	.90
cyc2	1.294	0.622	4.33	.90
b ₀	-5.014	--	--	--

The coefficients given in Table 5.3.2-4 were the results of a regression with the dependent variable equal to the natural logarithm of failure rate. Transforming the regression results into an equation where failure rate (as opposed to log of failure rate) is the dependent variable results in the following preliminary multiplicative model:

$$\lambda_r = \lambda_{nb} \pi_{NQ} \pi_{cyc} \epsilon$$

where

λ_r = predicted resistor nonoperating failure rate (failures/10⁶ hours)

λ_{nb} = base failure rate, preliminary

= $\exp(-5.014 - 2.386(S_1) - 3.957(S_2) - 4.257(S_3))$

= .00611, fixed wirewound resistors

= .000127, fixed film resistors

= .0000941, fixed composition resistors

= .00664, variable resistors

= .00664, thermistors
 π_{NQ} = quality factor
 = $\exp(1.560(Q_1))$
 = 1.0, Hi-rel
 = 4.76, Mil-spec
 π_{cyc} = equipment power cycling factor (preliminary)
 = $\exp(1.294(cyc2))$
 = 1.0, cycling rate < .057 cycles/10³ hr.
 = 1.0, .057 ≤ cycling rate < .114 cycles/10³ hr.
 = 3.65, cycling rate ≥ .114 cycles/10³ hr.
 ϵ = residual

The variables S_1 , S_2 , S_3 , Q_1 and $cyc2$ have been previously defined. It is emphasized that the above equation represents a preliminary model, which is only applicable to ground based environments.

Two hypothetical reasons were determined as to why the intermediate and low equipment power cycling frequency data were statistically indistinguishable. The first reason was that "true" storage related failures (as opposed to failures induced by the power-on cycle) dominate the total failure rate for cycling rates less than .114 cycles/10³ hr (i.e. powered-up less than once a year). Therefore, the anticipated difference in failure rate would potentially be less than the inherent variability in the data, and therefore would not be detected. The second hypothetical reason was that the merged data set included only one data entry in the intermediate range of cycling frequencies. Therefore, if the data from that one source was biased, then the results would be effected. It is also noted that the unknown cycling frequency data entries were statistically indistinguishable from the data entries with low and intermediate power cycling frequencies. This was considered to be an encouraging sign. Although the cycling frequency was unknown for these data entries, the data was from missile storage applications where it was known that the cycling was relatively infrequent.

The next step in the model development process was to perform the iterative regression analyses to accommodate the assumed non-linear model form. It has been documented (Reference 42) that the effect of equipment power on-off cycling is best represented by an equation of the following form:

$$\pi_{\text{cyc}} = 1 + K_1(\text{cycles}/10^3 \text{ hr.})$$

As previously described, the iterative process began by performing a two-dimensional regression analysis for "equipment power cycling factor" versus average cycling rate for the three previously defined cycling rate categories. The average cycling rate for resistors exposed to low equipment cycling rates was .042 cycles/ 10^3 hrs. The data in this category was primarily from the Sparrow and Hawk missile program. A regression coefficient was also computed for the intermediate cycling rate category, so that the method could be properly applied. The average cycling rate for the intermediate category was .079 cycles/ 10^3 hr. This data was primarily from the TOW missile program. The average cycling rate for resistors exposed to high equipment cycling frequencies was 40.12 cycles/ 10^3 hr. This data was from the F-16 HUD RIW data. The data from sources with unknown cycling frequencies were not included in this regression. The data entries were weighted by the number of observations per category. An explanation of weighted regression is included in Section 3.2. The first iteration for equipment power cycling factor resulted in the following equation.

$$\begin{aligned} K_2 \pi_{\text{cyc}} &= 0.977 + .0614(\text{cycles}/10^3 \text{ hr.}) \\ \pi_{\text{cyc}} &= 1 + .0628(\text{cycles}/10^3 \text{ hr.}) \end{aligned}$$

where

$$\begin{aligned} K_2 &= \text{normalization constant} \\ &= 1/0.977 = 1.023 \end{aligned}$$

For resistors, only one iteration was required. The preliminary model at this stage of the model development process is given by the following equation:

$$\lambda_r = \lambda_{nb} \pi_{NQ} \pi_{cyc}$$

where

λ_r = predicted resistor nonoperating failure rate (failures/10⁶ hr.)

λ_{nb} = base failure rate, preliminary

= .000617, fixed wirewound resistors

= .000128, fixed film resistors

= .0000953, fixed composition resistors

= .00671, variable resistors

= .00671, thermistors

π_{NQ} = quality factor

= 1.0, Hi-rel

= 4.69, Mil-spec

π_{cyc} = equipment power cycling factor

= 1 + .0628(cycles/10³ hr.)

The magnitude of the nonoperating quality factor for Mil-spec resistors was small in comparison to the ratio of Mil-spec to established reliability (i.e. S, R, P and M) operating quality factors from MIL-HDBK-217D. In other words, screening apparently has less effect on nonoperating failure rate than operating failure rate. It was hypothesized that this trend was due to a significantly slower rate of failure for "infant mortality" failures (i.e. weak devices remaining and subsequently failing after the screen) during nonoperating periods. This trend was noted for every electronic component generic family, and is discussed in Section 4.6 of this report.

It was decided to derive unique nonoperating quality factor values for the established reliability (ER) quality levels defined in the ER specifications. A complete series of quality factors were required to

provide the models with maximum utility and to properly discriminate against known quality related factors. The available nonoperating failure rate for ER (or Hi-rel) resistors did not specify the particular established reliability level. In general, the average quality level was R or P. It was assumed that the average ER level for the collected data was P to determine a complete series of nonoperating quality factors. The assumption was made that nonoperating quality factors would follow a geometric progression. This was based on the observation that the MIL-HDBK-217D operating quality factors follow a similar progression. Table 5.3.2-5 presents point estimate nonoperating quality factors, upper and lower 90% confidence interval values, extrapolated nonoperating quality factors for S, R, M and lower qualities, and a series of quality factors normalized to an M factor equal to one.

TABLE 5.3.2-5: RESISTOR NONOPERATING QUALITY FACTORS

Quality Level	$\pi_{NQ,.05}$	$\pi_{NQ1(1)}$	$\pi_{NQ,.95}$	$\pi_{NQ2(2)}$	$\pi_{NQ3(3)}$
S	--	--	--	.28	0.15
R	--	--	--	.55	0.28
P	--	1.0	--	1.0	0.52
M	--	--	--	1.9	1.0
Mil-spec	2.2	4.7	10.1	4.7	2.4
lower	--	--	--	8.6	4.4

- NOTES: (1) π_{NQ1} is the observed point estimate quality factor.
- (2) π_{NQ2} is the point estimate quality factors supplemented by extrapolated values for S, R, M and lower quality levels.
- (3) π_{NQ3} is the quality factor normalized to M quality factor equal to one.

The next task in the model development process was to apply the methods presented in Section 4.5 to determine nonoperating environmental factors. This method assumes that a series of nonoperating environmental factors can be derived from the MIL-HDBK-217D operating environmental factors. A conversion algorithm was determined based on a comparison of

failure mechanism accelerating factors, and differences in average temperature. In general, if the distribution of failure mechanism accelerating factors were equivalent for operating and nonoperating conditions, then the one series of environmental factors would apply. Conversely, if the failure mechanism distributions were significantly different, then methods were determined to estimate the magnitude of the difference, if any. Since every MIL-HDBK-217D resistor model has a unique temperature factor, no numerical adjustment was required to account for the difference in average temperature between operating and nonoperating applications. An adjustment was required, however, for the thermistor nonoperating environmental factor.

The proposed resistor nonoperating environmental factors were presented in Table 5.3.1-1 in the previous section. It was determined that a minimum of seven different series of environmental factors were required to properly assess the effects of environmental stress on nonoperating failure rate. The results of the nonoperating environmental factor development were that the thermistor environmental factors required an adjustment to account for temperature differences. The appropriate temperature adjustment factor was based on anticipated differences between operating and nonoperating applications of up to 24°C for airborne uninhabited environments. The other MIL-HDBK-217D resistor environmental factors approximate the effects of environmental stress on resistor nonoperating failure rate. MIL-HDBK-217D includes 15 separate series of environmental factors for resistors. The decision was made to group and average the environmental factors for similar resistor styles. This was done for several reasons. The primary reason was that the nonoperating environmental factor development process was inexact. Therefore, the relatively small differences in environmental factors between similar styles were not justified for nonoperating failure rate prediction purposes.

Tables 5.3.2-6 through 5.3.2-11 show failure mode/mechanism and failure acceleration factor distributions for resistors. Accurate failure mode/mechanism information was difficult to obtain for operating

TABLE 5.3.2-6: COMPOSITION RESISTOR FAILURE MECHANISM DISTRIBUTION

Failure Mode	Failure Mechanism	Accelerating Factors	Operating Distribution (%)	Nonoperating Distribution (%)
resistance drift	moisture intrusion	moisture, temp.	35-55	45-65
	non-uniform comp. material	voltage/current, temp.	5-25	5-20
	contaminants	voltage/current, temp.	5-25	5-20
open	lead defects	moisture, temp., voltage/current	15-35	15-30

TABLE 5.3.2-7: FILM RESISTOR FAILURE MECHANISM DISTRIBUTION

Failure Mode	Failure Mechanism	Accelerating Factors	Operating Distribution (%)	Nonoperating Distribution (%)
resistance drift	moisture ingress	moisture, temp., contamination	20-40	30-50
	substrate defects	moisture, temp., voltage/current	15-35	5-25
	film imperfections	moisture, temp., voltage/current	15-35	5-25
open	lead termination	shock, vibration, temp., voltage/current	1-20	1-20
	film material damage	moisture, temp., voltage/current	1-20	1-20

TABLE 5.3.2-8: WIREWOUND RESISTOR FAILURE MECHANISM DISTRIBUTION

Failure Mode	Failure Mechanism	Accelerating Factors	Operating Distribution (%)	Nonoperating Distribution (%)
resistance drift	wire im-perfection	voltage/current, temp.	10-35	1-10
	wire insulation flow	voltage/current, temp.	15-40	1-15
	corrosion	temp., humidity	10-35	35-55
open	lead defect	shock, vibration, voltage/current	1-20	1-20
	wire im-perfection	voltage/current	1-20	1-10
	corrosion	temp., humidity	1-20	15-40
short	intrawinding insulation breakdown	temp., voltage/current	1-10	1-10

TABLE 5.3.2-9: VARIABLE WIREWOUND RESISTOR FAILURE MECHANISM DISTRIBUTION

Failure Mode	Failure Mechanism	Accelerating Factor	Operating Distribution (%)	Nonoperating Distribution (%)
resistance drift	contamination	temp., contamination	15-35	20-45
	noise	moisture, temp.	1-18	5-40
short	insulation breakdown	moisture, temp., voltage/current	5-25	5-15
	contamination bridging	contamination, moisture, temp.	1-12	5-20
open	wiper arm wear	mechanical actuations	1-20	0-5
	seal defects	contamination, moisture, temp.	1-20	5-30
mechanical	jamming, stripping	mechanical actuations	7-27	0-5

TABLE 5.3.2-10: VARIABLE COMPOSITION RESISTOR FAILURE MECHANISM DISTRIBUTION

Failure Mode	Failure Mechanism	Accelerating Factors	Operating Distribution (%)	Nonoperating Distribution (%)
resistance drift	corrosion	temp., humidity	40-60	45-65
	moisture intrusion	moisture, temp.	20-40	25-45
	wiper movement	shock, vibration	1-20	5-25
mechanical failure	binding, jamming	mechanical actuation, corrosion	1-15	1-5
open	terminal defect	voltage/current, temp.	1-13	1-5
	burnout of resistive element	voltage/current	1-12	0

TABLE 5.3.2-11: THERMISTOR FAILURE MECHANISM DISTRIBUTION

Failure Mode	Failure Mechanism	Accelerating Factors	Operating Distribution (%)	Nonoperating Distribution (%)
resistance drift	moisture intrusion	moisture, temp.	25-45	35-55
	body anomalies	temp., voltage/current	20-40	14-35
open	lead termination defect	vibration, temp., voltage/current	10-30	5-25
	non-uniform resistance material	temp., voltage	1-20	1-20
short	various	temp., contamination, voltage/current	0-15	0-15

applications and essentially impossible to locate for nonoperating applications. Therefore, much of information presented in Tables 5.3.2-6 through 5.3.2-11 was theorized. References 41, 42, and 43 provided important resistor failure mode information. Relationships identified during the failure mechanism analysis and the failure mechanism comparisons are,

- o Operating and nonoperating failure mechanisms for composition resistors, thermistors and all types of variable resistors are primarily accelerated by environmental stresses.
- o Operating failure mechanisms for fixed film and wirewound resistors are accelerated by a combination of environmental and operational stresses.
- o Carbon composition resistors are affected by moisture but usually keep themselves dry during operation because of self-generated heat. However, if the equipment must stand for long periods under humid conditions without power applied, then the resistance value will change.
- o Contaminants, especially when combined with moisture, can result in resistance shifts for composition resistors. The probability of experiencing contamination-related resistance drifts increases with storage time.

The next step in the model development process was to extrapolate base failure rate values for resistor styles which had no data. In addition, the base failure rate values were normalized to correspond to a ground benign environment and a M quality level. It was considered desirable to normalize the base failure rate values to be consistent with MIL-HDBK-217D. The base failure rates determined from the data correspond to a ground fixed environment and a P screen class. The observed base failure rates were divided by the ground fixed environmental factor and the P quality factor ($\pi_{NQ3} = 0.52$ in Table 5.3.2-5) to obtain the normalized base failure rates. The nonoperating environmental factor and nonoperating quality factor had previously been normalized to the desired levels. The normalization process had no effect whatsoever on the resultant resistor nonoperating failure rate prediction. In fact, the base failure rate, nonoperating environmental factor, and nonoperating

quality factor could have been normalized to any combination of environment and quality without effecting the resultant prediction. The increase in one factor would be compensated by a decrease in another.

Table 5.3.2-12 presents the normalized base failure rates, the extrapolated base failure rate values, and upper and lower confidence interval values for resistor styles with data. The upper and lower 90% confidence interval values were also normalized to correspond to a ground benign environment and M quality level.

TABLE 5.3.2-12: RESISTOR NONOPERATING BASE FAILURE RATES

Type	Style	$\lambda_{nb,.05}$	λ_{nb}	$\lambda_{nb,.095}$
Fixed	Composition	.000022	.000063	.00018
Fixed	Film	.000039	.000103	.00027
Fixed	Film Network	--	.000433	--
Fixed	Wirewound	.000195	.000565	.00164
Variable	Wirewound	--	.00516	--
Variable	Non-wirewound	--	.00516	--
Thermistor	Any	--	.00267	--

The final phase of the resistor model development process was to investigate the failure rate differences between the specific styles of variable resistors. The regression analysis indicated that there was no significant difference between thermistors and variable resistor failure rate in the ground fixed environment. However, the specific styles of variable resistors were grouped because of data limitations and failure rate differences could not be detected. Point estimate failure rates, predicted failure rates and 90% chi-squared confidence interval values were computed for each variable resistor data record. No data record had greater than one failure and thus the observed failure rate estimates were imprecise. A description of chi-squared confidence intervals is included in Section 3.2 of this report. If the regression solution (or predicted) failure rate was contained in the 90% chi-squared confidence interval,

then the variable resistor point estimate base failure rate previously presented in Table 5.3.2-12, was applied to the respective variable resistor style. This was the case for non-wirewound trimmer, wirewound precision, and non-wirewound film variable resistors. For wirewound trimmer variable resistors, the upper 90% confidence interval value was less than the predicted failure rate. Therefore, it was concluded that the nonoperating failure rate of wirewound trimmer variable resistors was divergent from the remaining variable resistor styles and required a unique base failure rate value. A multiplicative base failure rate adjustment factor for wirewound trimmer variable resistors was derived by computing the ratio of the observed point estimate failure rate to the predicted failure rate (Adjustment Factor = .00453/.0237 = .191). The variable resistor base failure rate was then adjusted accordingly. For variable resistor styles where no data were available, the operating failure rate rankings found from MIL-HDBK-217 were inspected to aid in the analysis. It was found that the operating failure rates for the variable resistor styles without data (i.e. wirewound semiprecision, wirewound power, non-wirewound composition, and non-wirewound precision) were ranked between non-wirewound trimmer and wirewound precision. It was assumed that the nonoperating failure rates would have a similar ranking and therefore the regression solution base failure rate would also be applicable to these resistor styles. It should also be noted that the operating MIL-HDBK-217D failure rate prediction for wirewound trimmer variable resistors was also substantially lower than other variable resistor styles.

Adjustment of the base failure rate value for wirewound trimmer variable resistors concluded the resistor model development process. The proposed nonoperating failure rate prediction model for resistors is given by the following equation. Two significant digits were used for all factors.

$$\lambda_r = \lambda_{nb} \pi_{NQ} \pi_{NE} \pi_{cyc}$$

where

- λ_r = predicted resistor nonoperating failure rate
- λ_{nb} = base failure rate (failures/ 10^6 hours)
 - = .000063, fixed composition
 - = .00010, fixed film
 - = .00043, film network
 - = .00057, fixed wirewound
 - = .00099, variable wirewound, trimmer
 - = .0052, precision, semiprecision or power variable wirewound
 - = .0052, variable non-wirewound
 - = .0027, thermistor
- π_{NQ} = nonoperating quality factor (π_{NQ3} in Table 5.3.2-5)
- π_{NE} = nonoperating quality factor (given in Table 5.3.1-1)
- π_{cyc} = equipment power on-off cycling factor
 - = $1 + .063(N_C)$

where

- N_C = number of equipment power on-off cycles per 10^3 nonoperating hours

The proposed resistor nonoperating failure rate prediction model is presented in a format similar to MIL-HDBK-217D in Appendix A.

5.3.3 Model Validation

The proposed resistor nonoperating failure rate prediction model was next subjected to a thorough model validation process. The model validation process took place in two phases. The first phase consisted of an extreme case analysis. Predictions were made using the proposed model for parameters beyond the ranges found in the data. The intent of the extreme case analysis was to identify any set of conditions which cause the proposed model to numerically "blow up", and also to identify any set of conditions which predict a failure rate which is theoretically

inconsistent (e.g. a negative failure rate) or intuitively wrong. The second phase of the model validation process was to compare the proposed model with observed field data which had been withheld from the model development process. Nonoperating resistor failure rate data had been collected from the French Organization AFCIQ (Reference 8) but not used because of part characterization problems.

The extreme case analysis did not indicate any deficiencies with the proposed model. At extremely high levels of equipment power cycling, the nonoperating failure rate becomes directly proportional to the equipment power cycling frequency. At low levels of equipment power cycling, the proposed resistor nonoperating failure rate approaches a constant value. These extreme case results confirm initiative reliability relationships. At extremely high equipment power cycling rates, the nonoperating failure rate would be expected to be dominated by failures induced by the power on-off cycle. Thus, the proportional relationship between the two variables was anticipated. At extremely low equipment power cycling rates, the failure rate would be expected to be equal to the inherent storage/dormant failure rate, and independent of power cycling frequency.

The resistor nonoperating failure rate data collected from AFCIQ were not used in the model development process because vital information such as equipment power cycling frequency and part screen class could not be precisely determined. However, the AFCIQ data was extremely useful for model evaluation purposes. Table 5.3.3-1 presents the AFCIQ resistor nonoperating failure rate data and the corresponding failure rate prediction from the proposed model. The part types were not screened according to identical specifications. However, equivalent quality levels were determined. Additionally, one equipment power cycle per year was assumed to compute the failure rate prediction. All AFCIQ data records were for a ground fixed environment except record number 13, which corresponds to a laboratory environment.

The model evaluation process substantiated the accuracy of the proposed resistor model. The geometric mean of the ratio of observed to

predicted failure rate was equal to 1.23 for those data entries with observed failures or sufficient part hours to estimate a failure rate without observed failures (i.e. record numbers 5, 9, 10, 14, 15, 16, 17 in Table 5.3.3-1). It is also noted that data records 5, 9 and 17 were for commercial grade resistors. The proposed nonoperating quality factor for commercial quality resistors was an extrapolated value. Therefore, it was considered very encouraging that the geometric mean of the ratio of observed to predicted failure rate for these three data entries was equal to 0.91. It should also be noted that the predicted failure rate was not within the 90% chi-squared confidence interval for two of these three commercial quality data records. Field failure rates for lower quality parts always exhibit a higher degree of variability, and therefore this observation was not surprising.

The proposed resistor nonoperating failure rate prediction model is an integral part of the methodology, presented in this report, which provides capabilities to assess the effects of nonoperating periods on equipment reliability. The proposed resistor nonoperating failure rate prediction model provides proper discrimination against application variables which influence failure rate. Additionally, the proposed model is relatively easy to use, and has been shown to be accurate. The application of the nonoperating failure rate prediction methods developed in this study will greatly enhance nonoperating failure rate assessment capabilities.

TABLE 5.3.3-1: RESISTOR MODEL VALIDATION DATA

No.	Failures	Part Hours (x10 ⁶)	Style	Equiv. Quality	$\lambda_{.05}$	$\lambda_0(1)$	$\lambda_{.95}$	$\lambda_{pre}(2)$
1	0	20	Comp.	MIL-SPEC	--	(3)	.150	.00044
2	0	40	Comp.	MIL-SPEC	--	(3)	.0749	.00044
3	0	147	Comp.	MIL-SPEC	--	(3)	.0204	.00044
4	0	420	Comp.	MIL-SPEC	--	(3)	.0071	.00044
5	1	143	WW	lower	.00036	.00699	.0332	.00530
6	0	13	WW	MIL-SPEC	--	(3)	.230	.00289
7	0	36	WW	MIL-SPEC	--	(3)	.0832	.00289
8	0	10	WW	MIL-SPEC	--	(3)	.300	.00289
9	9	3,422	film	lower	.00137	.00263	.0046	.00106
10	0	2,383	film	MIL-SPEC	--	.00042	.0013	.00058
11	0	155	film	MIL-SPEC	--	(3)	.0193	.00058
12	0	84	film	MIL-SPEC	--	(3)	.0357	.00058
13(4)	0	55	film	MIL-SPEC	--	(3)	.0546	(4)
14	1	299	film	MIL-SPEC	.00017	.00334	.0159	.00058
15	2	4,448	film	MIL-SPEC	.00008	.00045	.00142	.00058
16	0	4,273	film	HI-REL	--	.00023	.00070	.00013
17	4	300	var. (5)	lower	.00455	.01333	.0305	.0576
18	0	78	var. (5)	MIL-SPEC	--	(3)	.0384	.0314
19	0	11	var. (5)	HI-REL	--	(3)	.272	.00681
20	0	28	var., ww	MIL-SPEC	--	(3)	.107	.0314
21	0	25	v., trimm.	MIL-SPEC	--	(3)	.120	.00598
Totals	17	16,390						

- NOTES:
- 1) λ_0 is the point estimate failure rate
 - 2) λ_{pre} is the predicted failure rate. A cycling rate of 0.114 cycles/10³ nonoperating hours was assumed.
 - 3) There were insufficient part hours to estimate a failure rate without observed failures.
 - 4) This data record was from life testing performed at 155°C.
 - 5) Specific variable resistor style unknown.

5.4 Capacitors

5.4.1 Proposed Capacitor Nonoperating Failure Rate Prediction Model

This section presents the proposed nonoperating failure rate prediction model for capacitors. The proposed model is presented in Appendix A in a form compatible with MIL-HDBK-217D. The proposed model is:

$$\lambda_p = \lambda_{nb} \pi_{NQ} \pi_{NE} \pi_{cyc}$$

where

- λ_p = predicted capacitor nonoperating failure rate
- λ_{nb} = nonoperating base failure rate (failure/10⁶ hours)
 - = .0011, fixed paper/plastic film (CP, CZ, CA, CPV, CH, CHR, CQ, CQR, CFR, CRH)
 - = .00039, fixed ceramic (CC, CCR, CK, CKR)
 - = .00075, fixed mica (CB, CM, CMR)
 - = .00045, fixed glass (CY, CYR)
 - = .00018, fixed tantalum, solid (CSR)
 - = .0064, fixed tantalum, non-solid (CL, CLR)
 - = .0064, fixed electrolytic, aluminum (CE, CU)
 - = .015, variable air trimmer (CT)
 - = .012, variable ceramic (CV)
 - = .0038, variable piston (PC)
 - = .046, variable vacuum (CG)
- π_{NQ} = nonoperating quality factor
 - = .05, T (mica capacitors only)
 - = .10, S
 - = .23, R
 - = .46, P
 - = 1.0, M
 - = 1.7, L
 - = 2.5, MIL-SPEC

= 5.3, lower

π_{NE} = nonoperating environmental factor (See Table 5.4.1-1)

π_{cyc} = equipment power on-off cycling factor

= $1 + .16(N_C)$

where

N_C = number of equipment power on-off cycles per 10^3 nonoperating hours

5.4.2 Model Development

An accurate and useful nonoperating failure rate prediction model for capacitors was developed by applying the modeling approach described in Section 4.1. Analysis of the available capacitor nonoperating reliability data and development of an assumed theoretical model were used to derive the failure rate prediction model. The model was determined to be a function of device style, quality level, environment and equipment power on-off cycling frequency.

Initially, application and construction variables were identified which characterize capacitors in a nonoperating environment. Table 5.4.2-1 presents a list of the part characterization variables for capacitors. These variables were analyzed in greater depth to determine their effect on capacitor nonoperating reliability. Statistical methods were used when appropriate. The part characterization variables were determined whenever possible as an integral part of the data collection task. If sufficient detail could not be determined for an individual data entry, then it was removed from the model development process.

A theoretical nonoperating failure rate prediction model for capacitors was developed by studying documented and intuitive nonoperating reliability relationships. The theoretical model assumes a nonlinear failure rate equation because of the assumed effect of equipment power on-off cycling. In addition, the theoretical model is constant with respect

TABLE 5.4.1-1: CAPACITOR NONOPERATING ENVIRONMENTAL FACTORS (π_{NE})

Env.	Film	Mica/Glass	Cer.	Tant. Solid	Tant. Nonsolid	Elec. Al.	Variable
GB	1	1	1	1	1	1	1
GF	2.2	2.1	2.0	2.4	1.4	2	3.3
GM	8.3	8.8	8.3	7.8	10	12	9.6
Mp	9.9	11	11	9.2	11	12	17
NSB	4.7	5.0	5.0	4.4	5.0	5.8	7.7
NS	6.3	5.9	5.2	4.9	6.7	6.7	8.2
NU	14	15	15	13	15	13	18
NH	15	16	16	14	16	19	25
NUU	16	17	18	15	17	20	27
ARW	21	23	24	20	23	27	36
AIC	3.2	3.5	2.7	2.5	2.5	9.5	5
AIT	4.3	4.0	3.3	2.5	4.0	10	5.3
AIB	7.0	8.0	6.2	7	6.5	10	7.7
AIA	4.9	4.0	5.0	3	6	15	13
AIIF	9.2	10	8.0	7.5	10	15	13
AUC	7.6	15	6.0	4.5	8.5	28	20
AUT	13	15	12	6.0	15	30	38
AUB	23	35	15	25	20	30	57
AUA	17	15	17	10	20	30	50
AUF	33	40	30	30	40	40	85
MFF	9.9	11	11	9.3	11	12	16(1)
MFA	13	15	15	13	15	17	22
USL	23	31	32	27	31	36	47(1)
ML	33	36	36	31	36	41	54(1)
CL	560	610	610	510	610	690	930

Notes: (1) This environment not applicable for vacuum or gas, fixed and variable (CG) type capacitors.

(2) Cer. = Ceramic, Tant. = Tantalum, Elec. Al. = Aluminum Electrolytic

TABLE 5.4.2-1: CAPACITOR PART CHARACTERIZATION

- I. Device Style
 - A. Fixed
 - 1. Paper/Plastic Film (CP,CZ,CA,CPV,CH,CHR,CQ,CQR,CFR,CRH)
 - 2. Mica (CR,CM,CMR)
 - 3. Glass (CY,CYR)
 - 4. Ceramic (CC,CCR,CR,CRR)
 - 5. Electrolytic (CE,CL,CLR,CSR,CU)
 - 6. Fixed Vacuum or Gas (CG)
 - B. Variable (CV,CT,PC,CG)
- II. Capacitance (microfarads)
- III. Quality level
 - A. T
 - B. S
 - C. R
 - D. P
 - E. M
 - F. L
 - G. Mil-Spec
 - H. Lower
- IV. Construction (CLR type only)
 - A. Slug
 - B. Foil
- V. Seal
 - A. Hermetic
 - B. Nonhermetic
- VI. Body Dimensions
- VII. Temperature
 - A. Rated
 - B. Actual
- VIII. Application Environment
- IX. Number of Power On/Off Cycles per 10^3 Nonoperating Hours.

to time. The theoretical model for capacitors is given by the following equation (f denotes a function).

$$\lambda_c = f(\text{device style, temperature, } C) \pi_{NQ} \pi_{NE} \pi_{cyc}$$

where

λ_c = predicted capacitor nonoperating failure rate (failures/ 10^6 hours)

C = capacitance (microfarads)

π_{NQ} = nonoperating quality factor, based on device screening

π_{NE} = nonoperating environmental factor

π_{cyc} = equipment power on-off cycling factor = $1 + K_1(N_c)$

K_1 = constant

N_c = equipment power on-off cycling rate (cycles/ 10^3 nonop. hrs.)

The summarized capacitor nonoperating reliability data collected in support of this study is presented in Table 5.4.2-2. The data collectively consists of 324 individual data records, 48 observed failures and $41,840.6 \times 10^6$ part hours.

A preliminary analysis was then performed to identify strengths and weaknesses of the collected data set. Initially the data was evaluated without merging data records. The methods described in Section 3.3 were applied to determine which zero failure data records had sufficient part hours to estimate a failure rate without observed failures. Ninety eight data records either had observed failures or had sufficient part hours to estimate a failure rate without observed failures. Limitations imposed by the nature of the available data restricted the number of variables which could be statistically evaluated. Four deficiencies of the collected nonoperating capacitor data base were identified from the preliminary data analysis. These deficiencies are,

- 1) All collected data was from a ground based environment. Therefore, there was not a sufficient range of environments to

TABLE 5.4.2-2: CAPACITOR NONOPERATING FAILURE RATE DATA TABLE

Equipment/Source	Data Records	Style	Failures	Part Hours (x10 ⁶)
Hawk/MICOM	2	Film	0	1271.9
Hawk/MICOM	10	Ceramic	2	7299.3
Hawk/MICOM	3	Mica	0	1071.9
Hawk/MICOM	3	Electrolytic	0	3896.4
Hawk/MICOM	2	Variable	0	85.1
Maverick/MICOM	4	Film	1	453.0
Maverick/MICOM	1	Ceramic	0	1997.2
Maverick/MICOM	2	Mica	0	1235.4
Maverick/MICOM	2	Electrolytic	0	4838.7
Sparrow/MICOM	50	Film	6	1620.6
Sparrow/MICOM	77	Ceramic	0	650.8
Sparrow/MICOM	14	Mica	0	51.0
Sparrow/MICOM	42	Electrolytic	0	663.6
Sparrow/MICOM	34	Glass	0	1225.0
Sprint/MICOM	6	Mica	1	230.4
Sprint/MICOM	1	Glass	0	71.6
Sprint/MICOM	5	Ceramic	0	909.9
Sprint/MICOM	4	Electrolytic	0	104.6
Sprint/MICOM	1	Variable	1	9.7
TOW/MICOM	3	Film	1	63.1
TOW/MICOM	1	Mica	0	65.7
TOW/MICOM	1	Ceramic	0	131.4
TOW/MICOM	2	Electrolytic	0	63.1
Lance/MICOM	6	Film	0	32.4
Lance/MICOM	3	Mica	0	4.4
Lance/MICOM	6	Ceramic	0	11.2
Lance/MICOM	4	Electrolytic	2	17.9
Lance/MICOM	7	Film	4	413.3
Martin Marietta	4	Mica	1	660.0
Martin Marietta	2	Glass	0	299.4
Martin Marietta	2	Ceramic	5	3832.4
Martin Marietta	5	Electrolytic	7	2613.2
Martin Marietta	4	Variable	1	133.4
F-16 HUD/RIW	7	Ceramic	14	4748.9
F-16 HUD/RIW	2	Electrolytic	2	1012.1
F-16 HUD/RIW	1	Glass	0	25.6
PRC	1	Electrolytic	0	27.0
Totals	324		48	41,840.6

develop a series of environmental factors based solely on the data.

- 2) There was an insufficient range of ambient temperatures to study the effects of temperature analytically.
- 3) The inherent failure rate of capacitors in storage/dormant applications is very low. Therefore, the number of data records with observed failures and the number of failures per data record were naturally limited. Precise estimates of field failure rates and quantification of failure rate model parameters can not be made without observed failures. Thus, the number of variables which could be analyzed empirically was limited.
- 4) No data was available for Aluminum Oxide electrolytic capacitors or for any variable capacitor style except variable, air trimmer.

The theoretical capacitor nonoperating failure rate prediction model was further studied to determine the relative effect of the independent variables. It was concluded that capacitor device style, quality level, application environment and equipment power on-off cycling frequency were the dominant variables effecting nonoperating failure rate. Capacitance level was not anticipated to have a significant effect on nonoperating failure rate. This variable was therefore not included in subsequent analyses due to data limitations.

A matrix of "dummy variables" (0 or 1) was defined for capacitor device style so that correlation coefficient analysis and regression analysis could be applied to the data. Device style is a qualitative variable, whereas regression and correlation analyses require quantitative variables. The "dummy variable" matrix allows for application of these numerical methods. The matrix for device style is given in Table 5.4.2-3. Of particular interest was the specific device styles within the electrolytic capacitors category. Aluminum electrolytic capacitors are a "shelf life" item which is known to significantly degrade during storage. Non-solid tantalum capacitors are also believed to be sensitive to prolonged storage. The non-solid dielectric is particularly sensitive to a loss of seal. Unfortunately no data were available for aluminum electrolytic capacitors. However, data were available for both solid tantalum and non-solid tantalum electrolytic capacitors, and the device

style matrix was defined to allow for a comparison of observed nonoperating failure rate.

A qualitative matrix was also defined for quality level. The matrix was simply a "0" for high-reliability parts and a "1" for mil-spec quality parts. This variable was designated as Q₁. The quality matrix was not defined to accommodate lower quality capacitors because no data of this type was available.

TABLE 5.4.2-3: CAPACITOR DEVICE STYLE VARIABLE MATRIX

Device Style	S ₁	S ₂	S ₃	S ₄	S ₅
Paper/plastic film	0	0	0	0	0
Ceramic	1	0	0	0	0
Mica	0	1	0	0	0
Solid tantalum	0	0	1	0	0
Non-solid tantalum	0	0	0	1	0
Variable, air trimmer	0	0	0	0	1

The correlation coefficient analysis indicated no large correlation between independent variables for the merged data set. The data were merged according to equipment, device style, and quality level. For example, all data for B screen class, fixed mica capacitors in the Hawk missile were merged.

Since the theoretical capacitor model was nonlinear due to the assumed relationship for equipment power cycling frequency, the approach to nonlinear regression described in Section 4.3 was implemented to quantify the nonlinear model. Equipment power cycling frequency was temporarily treated as a qualitative variable. Constant multiplicative values were computed by regression for three distinct cycling rate categories. Then a two-dimensional regression was performed with the cycling rate coefficients from the initial regression as the dependent variable, and the mean cycling rate value for each category as the independent variable. The result would be an expression for equipment cycling factor of the desired form (i.e. cycling factor = $mx + b$). An iterative process was

then required. First, the equipment power cycling factor expression was assumed exact, and the coefficients for all other variables recalculated. Then, those coefficients were assumed to be exact and the equipment cycling factor recalculated. The iterative process would continue until observed changes were negligible. For capacitors, this process required three iterations.

Three qualitative "dummy" variables were defined to represent four distinct equipment power cycling rate categories. The three variables were designated as cyc1, cyc2 and cyc3. The categories were defined as,

- o cycling rates less than one power cycle every two years (cyc1, cyc2, cyc3 = 0,0,0).
- o cycling rates between one cycle per year and one cycle every two years (cyc1, cyc2, cyc3 = 1,0,0), (3) cycling rates greater than one cycle per year (cyc1, cyc2, cyc3 = 0,1,0).
- o cycling rates greater than one cycle per year (cyc1, cyc2, cyc3 = 1,0,0).
- o unknown cycling rates (cyc1, cyc2, cyc3 = 0,0,1).

The first three categories were designated as (1) low, (2) intermediate, and (3) high cycling frequencies, respectively.

Application environment was assumed to be a significant variable effecting capacitor nonoperating failure rate. It was essential that a proposed capacitor nonoperating failure rate prediction model include an appropriate environmental factor to properly discriminate against known failure accelerating environmental stresses. Unfortunately, all collected data was for ground based environments. Therefore, environmental factors could not be developed empirically. This data deficiency existed for the model development of each part type, and is discussed in-depth in Section 4.5 of this report. Section 4.5 also proposes a method to develop appropriate environmental factors based on a comparison of operating and nonoperating failure mechanisms. This method was used to determine

capacitor nonoperating environmental factors after application of regression analysis.

The fact that temperature could not be empirically analyzed was also a problem. However, after careful consideration of many factors, it was decided not to include temperature in the nonoperating failure rate prediction model. Similar to the discussion for resistor nonoperating failure rate model development, there were three reasons determined to support this decision. The first was that no temperature relationship could be derived from the data due to the limited range of temperatures available. The second reason was that no theoretical relationship was identified in the literature which corresponded to nonoperating conditions. The third reason was that the effect of temperature on nonoperating failure was believed to be relatively low in comparison to microcircuits and discrete semiconductors. Therefore, an approximate assumed temperature relation for capacitors was not warranted.

At this stage of the model development process, the data were in the format required for application of regression analysis. Results of the initial regression analysis are presented in Table 5.4.2-4. The dependent variable was $\ln(\text{failure rate})$. The independent variables were S_1 , S_2 , S_3 , S_4 , S_5 , Q_1 , cyc1 , cyc2 and cyc3 .

Device style variables S_3 , S_4 , and S_5 were significant at a 90% confidence limit. Device style variable S_1 , device quality variable Q_1 and equipment cycling frequency variables cyc1 , cyc2 , and cyc3 were significant at a 80% confidence limit. Device style variable S_2 was significant at a 65% confidence limit. The R-squared value for the regression was .85. That is 85% of the variability in the observed data can be explained by the regression solution. Interpretation of the regression results are:

- 1) The variable, non-solid and solid tantalum capacitor styles were significantly different, with a 90% confidence limit from the other device styles.

- 2) All other styles were significantly different from paper/plastic film at a 60% confidence limit.
- 3) The difference in predicted failure rate between mica and paper plastic film capacitors was not significant at a 80% confidence limit.
- 4) As expected, it was determined with 80% confidence that capacitor screening effects the field nonoperating failure rate. Interpretation of the initial regression solution was that the failure rate of mil-spec quality resistors is 3.9 times higher than capacitors screened to the established reliability specification.
- 5) The cyc1, cyc2 and cyc3 equipment power cycling variables were significant with 80% confidence. This substantiated the assumption that equipment power cycling is an important variable for predicting nonoperating failure rate.

TABLE 5.4.2-4: CAPACITOR INITIAL REGRESSION RESULTS

Variable	Coefficient	Standard Error	f-ratio	Confidence Limit
S1	-1.578	.528	8.94	.80
S2	-0.601	.622	0.93	.65
S3	-2.180	.627	12.08	.90
S4	0.875	.662	1.75	.90
S5	2.283	.817	7.80	.90
Q1	1.189	.505	5.55	.80
cyc1	0.891	.541	2.71	.80
cyc2	2.624	.736	12.70	.80
cyc3	1.500	.440	11.63	.80
b ₀	-6.775	--	--	--

The coefficients given in Table 5.4.2-4 were the results of a regression with the dependent variable equal to the natural logarithm of failure rate. Transforming the regression results into an equation where failure rate (as opposed to log of failure rate) is the dependent variable results in the following multiplicative model:

$$\lambda_c = \lambda_{nb} \pi_{NQ} \pi_{cyc} \epsilon$$

where

λ_c = predicted capacitor nonoperating failure rate (failures/ 10^6 hours)

λ_{nb} = base failure rate
 $= \exp(-7.089 - 1.306(S_1) - 1.879(S_3) + 1.120(S_4) + 2.650(S_5))$
 $= .000834$, paper/plastic film
 $= .000834$, mica
 $= .000226$, ceramic
 $= .000127$, solid tantalum
 $= .00256$, nonsolid tantalum
 $= .0118$, variable

π_{NQ} = quality factor
 $= \exp(1.361(Q_1))$
 $= 1.0$, hi-rel
 $= 3.9$, mil-spec

π_{cyc} = equipment power cycling factor
 $= \exp(.970(cyc1) + 2.651(cyc2) + 1.446(cyc3))$
 $= 1.0$, cycling rate $< .057$ cycles/ 10^3 hr.
 $= 2.64$, $.057 \leq$ cycling rate $< .114$ cycles/ 10^3 hr.
 $= 14.17$, cycling rate $\geq .114$ cycles/ 10^3 hr.
 $= 4.25$, unknown cycling rate

ϵ = residual

The variables S_1 , S_2 , S_3 , S_4 , S_5 , Q_1 , $cyc1$, $cyc2$ and $cyc3$ have been previously defined. It is emphasized that the above equation represents a preliminary model, which is only applicable to ground based environments.

The observation that equipment power cycling variables $cyc1$ and $cyc2$ were identified as significant variables supports the assumption that equipment power on-off cycling effects nonoperating failure rate. The $cyc3$ variable for unknown power cycling was also observed to be significantly different, with 80% confidence, from the low cycling frequency values. This was attributed to several possible reasons. This observation may be because the average cycling frequency for the unknown

data entries was greater than 0.114 cycles/10³ nonoperating hours. Another possible reason was that the data in the unknown category may have been biased and that the observed failure rates are not representative of capacitors in a nonoperating environment. Neither contention can be proved. However, the magnitude of the ratio of unknown to low equipment cycling was not large enough to cause any concern.

The next step in the model development process was to perform the iterative regression analyses to accommodate the assumed non-linear model form. It has been documented (Reference 5) that the effect of equipment power on-off cycling is best represented by an equation of the following form:

$$\pi_{\text{cyc}} = 1 + K_1(\text{cycles}/10^3 \text{ hr.})$$

As previously described, the iterative process began by performing a two-dimensional regression analysis for "equipment power cycling factor" versus average cycling rate for the three previously defined cycling rate categories. The average cycling rate for capacitors exposed to low equipment cycling rates was .042 cycles/10³ hrs. The data in this category was primarily from the Sparrow and Hawk missile programs. The average cycling rate for the intermediate category was .079 cycles/10³ hr. This data was primarily from the Maverick and TOW missile programs. The average cycling rate for capacitors exposed to high equipment cycling frequencies was 40.12 cycles/10³ hr. This data was from the F-16 HUD RIW data. The data from sources with unknown cycling frequencies were not included in this regression. The data entries were weighted by the number of observations per category. An explanation of weighted regression is included in Section 3.2. The third iteration for equipment power cycling factor resulted in the following equation.

$$K_2 \pi_{\text{cyc}} = .60 + .0962(\text{cycles}/10^3 \text{ hr.})$$

$$\pi_{\text{cyc}} = 1 + .16(\text{cycles}/10^3 \text{ hr.})$$

where

$$\begin{aligned} K_2 &= \text{normalization constant} \\ &= 1/.60 = 1.66 \end{aligned}$$

The preliminary model at this stage of the model development process is given by the following equation. The residual was dropped from the equation at this stage of model development.

$$\lambda_c = \lambda_{nb} \pi_{NQ} \pi_{cyc}$$

where

$$\begin{aligned} \lambda_{nb} &= \text{preliminary base failure rate} \\ &= .00231 \text{ paper plastic/film} \\ &= .000782 \text{ ceramic} \\ &= .00158 \text{ mica} \\ &= .000434 \text{ solid tantalum} \\ &= .00896 \text{ non-solid tantalum} \\ &= .05001 \text{ variable} \\ \pi_{NQ} &= \text{quality factor} \\ &= 1.0, \text{ Hi-rel} \\ &= 2.47, \text{ mil-spec} \\ \pi_{cyc} &= \text{equipment power cycling factor} \\ &= 1 + .16(\text{cycles}/10^3 \text{ hr.}) \end{aligned}$$

It was noticed that the ratio of non-solid tantalum to solid tantalum preliminary base failure rates was greater than twenty to one. It had been anticipated that the non-solid tantalum nonoperating failure rate would be relatively higher because of the sensitivity of the non-solid dielectric to even minimal loss of seal properties. The observation that the observed nonoperating failure rate was twenty times as high was considered to be additional evidence that non-solid tantalum capacitors are relatively more sensitive to nonoperating periods. The corresponding operating failure rate ratio (from MIL-HDBK-217D) is approximately 1.2 to

1. This difference between operating and nonoperating ratios was another reason why operating and nonoperating failure rate prediction must be treated separately.

The magnitude of the nonoperating quality factor for mil-spec capacitors was small in comparison to the ratio of mil-spec to established reliability (i.e. T, S, R, P, M and L) operating quality factors from MIL-HDBK-217D. It was hypothesized that this trend was due to a significantly slower rate of failure for "infant mortality" failures (i.e. weak devices remaining after the screen and subsequently failing) during nonoperating periods. This trend is discussed in Section 4.6 of this report.

It was decided to derive unique nonoperating quality factor values for the established reliability (ER) quality levels defined in the ER specifications. The available nonoperating failure rate for ER (or Hi-rel) capacitors did not specify the particular established reliability level. In general, the average capacitor quality level was R, P, or M. It was assumed that the average ER level for the collected data was M. A P quality level had been assumed for resistors. However the observed effect of quality was less for capacitors and it was decided to make a "worst case" assumption. Inspection of the MIL-HDBK-217D capacitor quality factors revealed that the numerical values increase geometrically. The assumption was made that nonoperating quality factors would also follow a geometric progression. Ideally, a unique nonoperating quality factor series may have been required for each capacitor style. However, due to the amount of available data, a single series of nonoperating quality factors was proposed for all capacitor styles. Numerical values for quality levels without data were extrapolated by assuming a similar ranking as the MIL-HDBK-217D operating quality factors. Table 5.4.2-5 presents point estimate nonoperating quality factors, upper and lower 90% confidence interval values, and extrapolated nonoperating quality factors for T, S, R, P, L and lower qualities.

TABLE 5.4.2-5: CAPACITOR NONOPERATING QUALITY FACTORS

Quality Level	$\pi_{NQ,.05}$	$\pi_{NQ1(1)}$	$\pi_{NQ,.95}$	$\pi_{NQ2(2)}$
T	--	--	--	.05
S	--	--	--	.10
R	--	--	--	.23
P	--	--	--	.46
M	--	1.0	--	1.00
L	--	--	--	1.70
MIL-SPEC	.810	2.47	7.46	2.47
Lower	--	--	--	5.25

- NOTES: (1) π_{NQ1} is the observed point estimate nonoperating quality factor.
- (2) π_{NQ2} is the point estimate quality factors supplemented by extrapolated values for T, S, R, P, L and Lower quality levels.

The next task in the capacitor model development process was to apply the methods presented in Section 4.5 to determine nonoperating environmental factors. The proposed capacitor nonoperating environmental factors are presented in Table 5.4.1-1 in Section 5.4.1. Eight series of environmental factors were required to properly assess the effect of environmental stress on capacitor nonoperating failure rate. The 19 different environmental factor series in MIL-HDBK-217D were grouped and averaged for similar capacitor styles. Since the nonoperating environmental factor development process was inexact, the small environmental factor differences between similar styles for the operating condition were not justified for nonoperating failure rate prediction purposes.

Table 5.4.2-6 through 5.4.2-13 present failure mode/mechanism and failure acceleration factor distributions for capacitors in both the operating and nonoperating conditions. Accurate distribution information for operating applications was difficult to find and essentially impossible to find for nonoperating applications. Therefore, much of the

TABLE 5.4.2-6: PAPER AND PLASTIC CAPACITOR FAILURE MECHANISM DISTRIBUTION

<u>Failure Mode</u>	<u>Failure Mechanism</u>	<u>Accelerating Factors</u>	<u>Operating Distribution (%)</u>	<u>Nonoperating Distribution (%)</u>
short	dielectric breakdown	temp, volt, pwr. cycles	15 - 35	1 - 15
	dielectric decomposition	temp	1 - 20	1 - 20
	dielectric contamination	time, temp	1 - 15	1 - 20
open	weld joint failure	temp, current, vibration	15 - 35	1 - 20
drift	corrosion	temp, humidity	1 - 20	25 - 45
	moisture intrusion	temp, humidity	20 - 40	35 - 60

TABLE 5.4.2-7: CERAMIC CAPACITOR FAILURE MECHANISM DISTRIBUTION

<u>Failure Mode</u>	<u>Failure Mechanism</u>	<u>Accelerating Factors</u>	<u>Operating Distribution (%)</u>	<u>Nonoperating Distribution (%)</u>
short	contamination	temp	5 - 25	5 - 25
	ceramic cracks	temp, vibration	5 - 25	5 - 25
	dielectric anomalies	temp, voltage	5 - 25	0 - 15
	silver migration	temp, voltage	1 - 15	0 - 15
open	faulty internal connection	temp, vibration	10 - 30	10 - 30
low insulation resistance	surface contamination	humidity	1 - 5	0 - 5
	defective encapsulation	humidity, temp	1 - 5	0 - 5
drift	moisture intrusion	temp, humidity, time	20 - 40	25 - 45

TABLE 5.4.2-8: MICA CAPACITOR FAILURE MECHANISM DISTRIBUTION

<u>Failure Mode</u>	<u>Failure Mechanism</u>	<u>Accelerating Factors</u>	<u>Operating Distribution (%)</u>	<u>Nonoperating Distribution (%)</u>
short	dielectric breakdown	voltage, temp	30 - 50	0 - 15
	moisture absorption	humidity, temp	10 - 30	30 - 55
	silver migration	humidity, volt, temp	1 - 20	0 - 15
open	weak internal connections	shock, vibration	5 - 25	20 - 45
drift	fatigued mica film		1 - 15	1 - 20
	moisture absorption		1 - 15	1 - 20

TABLE 5.4.2-9: GLASS CAPACITOR FAILURE MECHANISM DISTRIBUTION

<u>Failure Mode</u>	<u>Failure Mechanism</u>	<u>Accelerating Factors</u>	<u>Operating Distribution (%)</u>	<u>Nonoperating Distribution (%)</u>
short	dielectric breakdown	volt, temp	45 - 70	0 - 15
open	weak internal connection	shock, vibration	20 - 45	70 - 95
drift	degradation of crystalline structure	storage below 45°C (temp)	1 - 15	5 - 25

TABLE 5.4.2-10: WET FOIL CAPACITOR FAILURE MECHANISM DISTRIBUTION

<u>Failure Mode</u>	<u>Failure Mechanism</u>	<u>Accelerating Factors</u>	<u>Operating Distribution (%)</u>	<u>Nonoperating Distribution (%)</u>
short	electrolytic leakage	temp, cycling, vibration	1 - 20	1 - 21
	breakdown	voltage, temp	1 - 20	0 - 15
	insulation defect	temp, cycling, volt	1 - 20	0 - 15
open	faulty external lead welds	shock, vibration, temp, cycling	10 - 30	15 - 35
drift	foil separation	temp cycling, temp	10 - 30	15 - 35
	electrolyte vaporization	temp, voltage	10 - 30	15 - 35
excessive leakage	electrolyte leakage	temp cycling	1 - 15	1 - 17
	insulation defects	temp cycling	1 - 15	1 - 17

TABLE 5.4.2-11: SOLID TANTULUM CAPACITOR FAILURE MECHANISM DISTRIBUTION

<u>Failure Mode</u>	<u>Failure Mechanism</u>	<u>Accelerating Factors</u>	<u>Operating Distribution (%)</u>	<u>Nonoperating Distribution (%)</u>
short	oxide defect	voltage, temp	25 - 50	0 - 15
	solder reflow	vibration	1 - 15	1 - 20
	mechanical defects	shock, vibration	5 - 25	20 - 40
	dielectric breakdown	voltage	1 - 15	0 - 5
open	mechanical defect	shock, vibration	1 - 20	1 - 20
drift	poor slug adhesion	temp cycling	5 - 25	15 - 35
	oxide defects	temp cycling	1 - 20	15 - 35

TABLE 5.4.2-12: ALUMINUM ELECTROLYTIC CAPACITOR FAILURE MECHANISM DISTRIBUTION

<u>Failure Mode</u>	<u>Failure Mechanism</u>	<u>Accelerating Factors</u>	<u>Operating Distribution (%)</u>	<u>Nonoperating Distribution (%)</u>
short	oxide breakdown	voltage	1 - 20	0 - 5
	mechanical defect	temp, voltage, vibration	20 - 40	5 - 25
open	defective connections	shock, vibration	20 - 45	15 - 35
capacitance degradation	oxide film deterioration	temp, lack of voltage	1 - 20	20 - 40
excessive leakage	oxide film deterioration	temp, lack of voltage	5 - 25	20 - 40

TABLE 5.4.2-13: VARIABLE CAPACITOR FAILURE MECHANISM DISTRIBUTION

<u>Failure Mode</u>	<u>Failure Mechanism</u>	<u>Accelerating Factors</u>	<u>Operating Distribution (%)</u>	<u>Nonoperating Distribution (%)</u>
short	mechanical defects	temp cycling, vibration	20 - 40	10 - 30
open	mechanical defects	temp cycling, vibration	1 - 20	1 - 20
drift	moisture intrusion	humidity	15 - 35	20 - 40
	contamination	humidity	15 - 35	20 - 40
	mechanical deformation	vibration, temp cycling	1 - 20	1 - 20

information in these tables was theorized. References 33 and 41 provided capacitor failure mode information. The following relationships were identified during the failure mechanism analysis:

- o For aluminum electrolytic capacitors, the aluminum cases corrode in salt air environment.
- o Both glass and mica capacitors are adequate for most military environments which include exposure to humidity and high levels of shock and vibration.
- o In the nonoperating mode, shorts and opens in ceramic capacitors can be accelerated by temperature cycling and to a lesser extent, mechanical stress. Low insulation resistance may occur as a result of surface conditioning during manufacture or because of moisture penetration through a defective epoxy encapsulation. Monolithic ceramics when properly cured and fixed are impervious to moisture as the chip itself is concerned, but the shunt path formed by contaminants surface moisture may result in circuit failure.

The next step in the model development process was to extrapolate base failure rate values for capacitor styles for which there was no data. In addition, the base failure rate values were normalized to a ground benign environment. The observed data corresponded to a ground fixed environment. Table 5.4.2-14 presents the normalized base failure rates, the extrapolated base failure rates, and upper and lower confidence interval values for capacitor styles for which there were observed data.

TABLE 5.4-14: CAPACITOR NONOPERATING BASE FAILURE RATES

Type	Style	$\lambda_{nb}, .05$	λ_{nb}	$\lambda_{nb}, .95$
Fixed	Paper/plas. film	--	.00105	--
Fixed	Ceramic	.000119	.000391	.00128
Fixed	Mica	.000182	.000752	.00314
Fixed	Glass	--	.000450	--
Fixed	Ta, Solid	.0000436	.000181	.000750
Fixed	Ta, Nonsolid	.00143	.00640	.0287
Fixed	Al Oxide	--	.00640	--
Variable	Air, Trimmer	.00265	.0152	.0867
Variable	Ceramic	--	.0122	--
Variable	Piston	--	.00376	--
Variable	Vacuum	--	.0456	--

Normalization of the base failure rates concluded the model development process. The capacitor nonoperating failure rate prediction model was found to be a function of device style, quality, environment power on-off cycling frequency. The proposed model is presented in Section 5.4.1 and in Appendix A in a format compatible with MIL-HDBK-217D.

5.4.3 Model Validation

The proposed capacitor nonoperating failure rate prediction model was subjected to a thorough model validation process. First, the model was subjected to an extreme case analyses. That is, predictions were made using the proposed model for parameters beyond the ranges in the data. The purpose of this analysis was to test the model for any set of conditions for which this model would "blow up," or predict a failure rate which is theoretically inconsistent. No deficiencies with the proposed model were found. Secondly, the prediction model was compared with field data (AFCIQ) which was purposely withheld from the model development process. Table 5.4.3-1 presents this nonoperating field data and the corresponding failure rate prediction from the proposed model. Although these parts were not screened according to the identical specifications used for the model development data, equivalent quality levels were able to be determined.

Except where otherwise indicated, all data was from a ground, fixed environment. Generally, the Hi-rel quality level was equivalent to a level of M.

TABLE 5.4.3-1: CAPACITOR MODEL VALIDATION DATA

No.	Failures	Part Hours (x10 ⁶)	Style	Equiv. Quality	$\lambda_{.05}$	$\lambda_0(1)$	$\lambda_{.95}$	$\lambda_{pre}(2)$
1	1	25	Ceramic	MIL-SPEC	.00205	.0400	.190	.00197
2	5	1637	Ceramic	MIL-SPEC	.00120	.00305	.0064	.00197
3	0	84	Ceramic	MIL-SPEC	--	(4)	.036	.00197
4	0	835	Ceramic	MIL-SPEC	--	.00120	.0036	.00197
5(3)	0	82	Ceramic	HI-REL	--	(4)	.037	(3)
6(3)	0	518	Ceramic	HI-REL	--	(4)	.0058	(3)
7	1	42	Film	MIL-SPEC	.00122	.0238	.113	.00581
8	0	37	Film	MIL-SPEC	--	(4)	.081	.00581
9	0	18	Film	MIL-SPEC	--	(4)	.170	.00581
10(3)	0	31	Film	HI-REL	--	(4)	.097	(3)
11	0	30	Mica	MIL-SPEC	--	(4)	.100	.00397
12	0	87	Mica	MIL-SPEC	--	(4)	.034	.00397
13	0	2	Paper	MIL-SPEC	--	(4)	1.497	.00581
14	0	36	Paper	MIL-SPEC	--	(4)	.083	.00581
15	0	4	ta, solid	Lower	--	(4)	.749	.00231
16	1	42	ta, solid	MIL-SPEC	.00122	.0238	.113	.00109
17	2	855	ta, solid	MIL-SPEC	.00042	.00234	.0074	.00109
18	0	46	ta, solid	MIL-SPEC	--	(4)	.065	.00109
19	1	27	ta, solid	MIL-SPEC	.00190	.0370	.176	.00109
20(3)	0	5	ta, solid	HI-REL	--	(4)	.599	(3)
21	3	560	ta, non-s	MIL-SPEC	.00146	.00536	.0138	.0225
22	0	1	Glass	MIL-SPEC	--	(4)	2.995	.00238
Totals	14	5004						

(1) λ_0 is the point estimate failure rate.

(2) λ_{pre} is the predicted failure rate. A cycling rate of .114 cycles/10³ nonoperating hours was assumed.

(3) Environment was unknown, so prediction with this data entry was not possible.

(4) Insufficient part hours to estimate a failure rate without observed failures.

The model validation process indicated that the proposed nonoperating failure rate prediction model for capacitors was relatively accurate. Three data entries (i.e. 1, 16 and 19) indicated that the proposed model was optimistic, and one data entry (i.e. 21) indicated that the proposed model was pessimistic. The predicted failure rate for four data entries (i.e. 2, 4, 7 and 17) was contained within the 90% chi-squared confidence interval and were considered to be representative of an accurate model. Further investigation of the model validation data proved to be enlightening. Data entry number one was for ceramic capacitors and suggested that the proposed model was optimistic. However, data entry number 2 was also for ceramic capacitors and had a greater number of failures and part hours. The predicted and observed failure rates were close for this data entry. Similarly, data entries 16 and 19 were for solid tantalum capacitors and indicated that the proposed model was optimistic. However, data entry number 17 was also for solid tantalum capacitors and had more observed failures and part hours than either of the other two data entries. As before, this data entry indicated that the proposed model was accurate. The apparent variability of some of the observed failure rates with a small number of failures and part hours was not unusual. It was concluded that observed nonoperating failure behavior requires some minimum time interval to stabilize. It was considered very encouraging that the three model validation data entries with the largest number of part hours (e.g. 2, 4 and 17) each indicated that the proposed model was accurate.

The proposed capacitor nonoperating failure rate prediction model provides proper discrimination against application variables which influence nonoperating failure rate, and is an integral part of the methodology presented in this report. It was designed to be easy to use, and has been proven to be relatively accurate.

5.5 Inductive Devices

5.5.1 Proposed Inductor Nonoperating Failure Rate Prediction Model

This section presents the proposed nonoperating failure rate prediction model for inductive devices. The proposed model is presented in Appendix A in a format compatible with MIL-HDBK-217D. The proposed model is:

$$\lambda_p = \lambda_{nb} \pi_{NQ} \pi_{NE} \pi_{cyc}$$

where

λ_p = predicted inductor nonoperating failure rate

λ_{nb} = nonoperating base failure rate

= .000055, low power pulse and audio transformers

= .00028, high power pulse, power and RF transformers

= .00015, RF coils

π_{NQ} = nonoperating quality factor

= .06, S

= .15, R

= .38, P

= 1.0, M

= 3.1, Mil-spec

= 11, lower

π_{NE} = nonoperating environmental factor (see Table 5.5.1-1)

π_{cyc} = equipment power on-off cycling factor

= $1 + .75(N_C)$, transformers

= $1 + .38(N_C)$, coils

where

N_C = number of equipment power on-off cycles per 10^3 nonoperating hours

TABLE 5.5.1-1: INDUCTOR NONOPERATING ENVIRONMENTAL FACTORS

Environment	Transformers	Coils
GB	1	1
GF	5.7	3.6
GM	12	12
MP	11	11
NSB	5.1	5.1
NS	5.7	5.7
NU	14	14
NH	16	16
NUU	18	18
ARW	24	24
AIC	4.5	4
AIT	6	4.5
AIB	6	5.5
AIA	6	4.5
AIF	9	9
AUC	6.5	5
AUT	6.5	6.5
AUB	7.5	7.5
AUA	7.5	6.5
AUF	10	10
SF	(1)	(1)
MFF	11	11
MFA	15	15
USL	32	32
ML	36	36
CL	310	610

NOTES: (1) Space flight environment was not considered in this study.

5.5.2 Inductor Model Development

The failure rate modeling approach described in section 4.1 was implemented for inductors. Analysis of the available nonoperating inductor failure rate data was complemented by an assumed theoretical model to derive the failure rate prediction model. The model was determined to be a function of inductor style, quality level, environment, and power on-off cycling frequency. For the purposes of this study, inductive devices were considered to be pulse, audio, power and RF transformers and RF coils. The proposed nonoperating failure rate prediction model for inductors is included in Appendix A in a format similar to MIL-HDBK-217D models.

Identification of application and construction variables which properly characterize inductors in a nonoperating environment was the first step of the preliminary model development. Table 5.5.2-1 presents a list of these variables for inductors. The part characterization variables represent possible failure rate model input parameters, analyzed in greater depth using statistical methods. As with all other models, the part characterization variables were determined whenever possible for all inductor data. If sufficient detail could not be achieved for an individual data entry, it was then removed from the model development process.

A theoretical model for inductors was determined based upon the general nonoperating reliability concepts presented in section 4.0 and a study of inductor nonoperating failure mechanisms and physics of failure information. The theoretical model was assumed to be a nonlinear failure rate equation because of the contribution of equipment power on-off cycling.

TABLE 5.5.2-1: INDUCTOR PART CHARACTERIZATION

- I. Device Style
 - A. Coils
 - 1. Construction
 - a. Fixed, RF
 - b. Variable, RF
 - c. IF
 - 2. Insulation Class
 - a. A
 - b. B
 - c. C
 - d. F
 - B. Transformers
 - 1. Type
 - a. Audio (MIL-T-27)
 - b. Power (MIL-T-27)
 - c. High Power Pulse (MIL-T-27)
 - d. Low Power Pulse (MIL-T-21038)
 - e. IF (MIL-T-55631)
 - f. RF (MIL-T-55631)
 - g. Discriminator (MIL-T-55631)
- II. Device Construction
 - A. Coils
 - 1. Numbers of Coils per Device
 - 2. Core Material
 - 3. Potting Material
 - B. Transformers
 - 1. Number of Primary Windings
 - 2. Number of Secondary Windings
 - 3. Core Material
 - 4. Potting Material
- III. Inductance (coils only)
- IV. Quality Level

A. S	D. M
B. R	E. MIL-SPEC
C. P	F. Lower
- V. Temperature
 - A. Rated
 - B. Actual
- VI. Application Environment
- VII. Number of Power On/Off Cycles per 10^3 Nonoperating Hours

The summarized inductor nonoperating reliability data collected in support of this study is presented in Table 5.5.2-2. The data consists of 73 individual data records, with 87 failures and $49,833 \times 10^6$ part hours.

TABLE 5.5.2-2: INDUCTOR NONOPERATING FAILURE RATE DATA

Equipment/Source	Data Records	Style	Failures	Part Hours ($\times 10^6$)
Hawk/MICOM	3	RF Coil	2	935.8
Hawk/MICOM	1	Discriminator	0	17.0
Hawk/MICOM	3	RF Transformer	0	204.2
Hawk/MICOM	1	Power Transformer	0	17.0
Maverick/MICOM	1	RF Coil	0	329.4
Maverick/MICOM	1	Transformer	0	41.2
Sparrow/MICOM	3	RF Coil	0	599.7
Sparrow/MICOM	4	Transformer	0	140.4
Sprint/MICOM	6	RF Coil	0	118.1
Sprint/MICOM	5	Power Transformer	0	17.4
Sprint/MICOM	5	RF Transformer	0	65.8
Sprint/MICOM	2	AF Transformer	0	9.7
Sprint/MICOM	3	Pulse Transformer	0	21.3
TOW/MICOM	2	Transformer	0	3.7
Martin Marietta	2	RF Coil	0	291.2
Martin Marietta	2	Transformer	12	3437.3
F-16 HUD/RIW	5	RF Coil	5	1831.8
AFCIQ	4	RF Coil	1	243.4
AFCIQ	9	Transformer	18	429.0
Southern Tech.	3	RF Coil	16	32235.9
Southern Tech.	8	Transformer	33	8843.7
Totals	73		87	49,833.0

The data was evaluated initially with each data record separate (no data records merged). Point estimate failure rates were computed for data records with observed failures. The methods described in Section 3.3 were applied to determine which zero failure data records had sufficient part hours to be included in the analysis, and to estimate failure rates for those records. Twenty data records in total were found to have either observed failures or sufficient part hours to estimate a failure rate without observed failures.

The number of variables which could be analyzed empirically was restricted because of the nature of the available data. The following attributes of the nonoperating inductor data were observed from the preliminary data analysis:

- 1) There was not a sufficient range of environments in the data to develop a series of environmental factors based solely on the data.
- 2) There was an insufficient range of ambient temperature to study the effects of temperature analytically.
- 3) Data were not available in sufficient quantity to evaluate specific device styles within the generic categories of coils and transformers.

The previously derived theoretical model was further examined to determine the relative effect of the independent variables, leading to the selection of variables. Failure mechanism acceleration factors were studied to aid in the variable evaluation process.

The preliminary model refinement process resulted in the conclusion that inductor device style, quality level, application environment and equipment power on-off cycling frequency were the dominant variables effecting inductor nonoperating failure rate. These variables, with the exception of application environment, were further analyzed using statistical methods. Other application and construction variables were considered to have minimal effect on inductor nonoperating failure rate.

It was assumed that application environment was an important factor effecting inductor nonoperating failure rate. Therefore, it was essential that a proposed inductor nonoperating failure rate prediction model included an appropriate environment factor to properly discriminate against known failure accelerating factors. Section 4.5 proposes a method to develop appropriate environmental factors based on a comparison of operating and nonoperating failure mechanisms, and a study of the documented MIL-HDBK-217D operating environmental factors. This method was

applied to the inductor nonoperating failure rate model after statistically analyzing the other variables.

The fact that the effect of temperature could not be empirically analyzed was also a problem. However, after careful consideration, it was decided not to include temperature in the inductor failure rate prediction model. This decision was based on the following observations:

- o A temperature relationship could not be determined from the data. Therefore, any proposed temperature factor would be based on assumptions, which introduce inaccuracies.
- o No theoretical relationship for inductor nonoperating failure rate vs. temperature could be located in the literature.
- o There is no basis for the assumption that the nonoperating failure rate behaves similarly to the operating rate with respect to temperature. The stresses on the part are necessarily different due to the absence of an applied current.
- o The average effect of ambient temperature will be included in the environmental factor since average ambient temperature changes with application environment.
- o The temperature dependence of inductor nonoperating failure rate was believed to be much less than the temperature dependence of microcircuits and discrete semiconductors, which do have a temperature factor in their proposed model.

The absence of a temperature factor for inductors was therefore not expected to have a significant effect on equipment level failure rate predictions.

To allow correlation coefficient analysis and regression analysis to be applied to the data, matrices of "dummy variables" (0 or 1) were defined for device style and quality level. These analyses require quantitative variables and device style and quality are qualitative variables. Table 5.5.2-3 illustrates the matrix for device quality level. The matrix for device style was simply a "0" for coils and a "1" for transformers. This variable was designated as S_1 . The device style

matrix was not defined to accommodate a further breakdown of the styles since sufficient detail in the data were not available.

TABLE 5.5.2-3: DEVICE QUALITY VARIABLE MATRIX

Device Quality	Q ₁	Q ₂
Hi-Rel	0	0
MIL-SPEC	1	0
Lower	0	1

Data were then merged according to equipment, device style and quality level by summing failures and part hours. For example, all data for Hi-Rel coils from the Hawk missile were merged. The correlation coefficient analysis indicated no large correlation between independent variables for the merged data set. Quality levels for inductors in the F-16 data were not available. It was therefore assumed that these parts were Hi-rel because of the requirements of the military application (Air Inhabited). Regression results later indicated that this assumption was reasonable.

The theoretical inductor model was nonlinear due to the assumed relationship for equipment power cycling frequency. An iterative approach was used to determine the nonlinear regression solution. Initially, two qualitative "dummy" variables were defined (cyc1 and cyc2) to represent three distinct equipment power cycling rate categories within the inductor data. For other part types, four categories were used. However there was an insufficient spread of equipment cycling frequency values to propose four categories for inductors. The three categories are:

- o Cycling rate less than one power cycle every two years (cyc1, cyc2 = 0, 0)
- o Cycling rate greater than one cycle per year (cyc1, cyc2 = 1, 0)
- o Unknown cycling rates (cyc1, cyc2 = 0, 1)

These categories were designated as low, high, and unknown cycling frequencies.

The data were then in a form suitable for regression analysis. Results of the initial regression analysis are given in Table 5.5.2-4. The dependent variable was $\ln(\text{failure rate})$. The independent variables introduced into the analysis were S_1 , Q_1 , Q_2 , cyc1 , cyc2 , which were previously defined.

TABLE 5.5.2-4: INDUCTOR INITIAL REGRESSION RESULTS

Variable	Coefficient	Standard Error	F-Ratio	Confidence Limit
S_1	1.689	1.103	2.34	.80
Q_2	2.477	1.208	4.20	.80
cyc1	3.414	1.636	4.36	.75
b_0	-7.504	--	--	

Device style (S_1) and the lower device quality variable (Q_2) were significant at a 80% confidence limit. The cycling rate variable (cyc1) was significant at a 75% confidence limit. No other variables were significant with 70% confidence. The available data did not indicate a significant difference between nonoperating failure rate for Hi-Rel and MIL-SPEC coils. This was unusual because screening was expected to have a significant effect. The R-squared value for the regression was .69. That is, 69% of the variability in the observed data can be explained by the regression solution. Interpretation of the regression results are:

1. The nonoperating failure rates for coils and transformers are significantly different from each other with a 80% confidence limit.
2. There were insufficient data to determine the difference between Hi-Rel and MIL-SPEC coils.
3. The lower device quality level was significantly different from Hi-Rel and MIL-SPEC at 80% confidence limit.

4. The cycl equipment power cycling variable was significant at a 75% confidence limit.
5. The low cycling rate variable and the unknown cycling rate variable were statistically indistinguishable.

Although cycling frequency was unknown for several data entries, it was not surprising that the unknown cycling data entries would be statistically indistinguishable from the low cycling frequency data entries. It was known that this data were from missile storage applications where cycling were relatively infrequent.

The coefficients in Table 5.5.2-4 were the result of a regression with the dependent variable equal to the natural logarithm of failure rate. Transforming the regression solution into an equation where failure rate is the dependent variable results in the following multiplicative model

$$\lambda_i = \lambda_{nb} \pi_{NQ} \pi_{cyc} \epsilon$$

where

λ_i = predicted inductor nonoperating failure rate (failure/ 10^6 nonoperating hours)

λ_{nb} = base failure rate, preliminary
 $= \exp(-7.509 + 1.689(S_1))$
 $= .000551$, Coils
 $= .002982$ Transformers

π_{NQ} = quality factor
 $= \exp(2.477(Q_1))$
 $= 1.0$, Hi-Rel and MIL-SPEC
 $= 11.91$, Lower

π_{cyc} = equipment power cycling factor (preliminary)
 $= \exp(3.414(cyc_1))$
 $= 1$, low cycling rate ($\approx .039$ cycles/ 10^3 hours)
 $= 30.386$, high cycling rate (≈ 40.12 cycles/ 10^3 hours)

ϵ = residual

The variables S_1 , Q_1 , and $cycl$ have been previously defined. The above equation represents a preliminary model, applicable only to ground based environments.

The next step in the model development was to apply iterative regression analyses to quantify the assumed nonlinear model form. As previously discussed, the effect of equipment power on-off cycling was represented by an equation of the following form:

$$\pi_{cyc} = 1 + K_1(\text{cycles}/10^3 \text{ hours})$$

The data in the first category, low cycling rate, was primarily from the Hawk missile program, with an average cycling rate of .038 cycles/ 10^3 hour. The data in the second category, high equipment cycling, was from the F-16 HUD RIW data with a cycling rate of 40.12 cycles/ 10^3 hour. The following equation for a power cycling factor resulted:

$$\begin{aligned} K_2 \pi_{cyc} &= .972 + .730(\text{cycles}/10^3 \text{ hour}) \\ \pi_{cyc} &= 1 + .751(\text{cycles}/10^3 \text{ hour}) \end{aligned}$$

where

$$\begin{aligned} K_2 &= \text{normalization constant} \\ &= 1/.972 = 1.029 \end{aligned}$$

Only one iteration was required for changes in the regression solution to be negligible. The preliminary model at this stage of the development process is given by:

$$\lambda_i = \lambda_{nb} \pi_{NQ} \pi_{cyc}$$

where

$$\begin{aligned} \lambda_{nb} &= \text{base failure rate} \\ &= .000555, \text{ coils} \end{aligned}$$

= .00328, transformers
 π_{NQ} = nonoperating quality factor
 = 1.0, Hi-Rel and Mil-spec
 = 11.36, lower
 π_{cyc} = inductor equipment power cycling factor
 = $1 + .751(\text{cycles}/10^3 \text{ hour})$

Transformers were anticipated to be one of the more sensitive part types to equipment power on-off cycling. The nonoperating failure rate of coils was also anticipated to be sensitive to equipment power on-off cycling. However, the relative effect was thought to be less for coils. Unfortunately, there were insufficient data to determine unique factors for both part classes. It was strongly believed that the proposed models should be physically correct. Therefore a separate, hypothesized power cycling constant was proposed for coils. The hypothesized value was one half of the observed constant for the inductor family.

The observation that coil nonoperating failure rate was statistically indistinguishable for Hi-Rel and Mil-Spec devices was further studied. The fact that the lower quality variable (Q_2) was significant at a 75% confidence limit was considered to be sufficient rationale to assume that quality provisions result in a lower observed nonoperating failure rate. Theoretically, screening effectiveness properties supported the premise that screening improves failure rate. Also, a complete series of nonoperating quality factors were required to provide the models with maximum utility and to properly discriminate against known quality related factors.

To determine a complete series of coil nonoperating quality factor values, the point estimate quality factors for Hi-Rel and Mil-Spec quality levels were assumed to correspond to an average quality level of M (according to applicable ER specifications). Only Mil-spec and lower quality levels are applicable for transformers. Coil nonoperating quality factors for S, R, P and Mil-spec were determined by extrapolation by

assuming (1) the observed nonoperating quality factors are accurate for M and lower quality levels, (2) nonoperating quality factors would follow a similar ranking to the MIL-HDBK-217D coil operating quality factors, and (3) the nonoperating quality factors are distributed geometrically. Table 5.5.2-5 presents point estimate nonoperating quality factors, upper and lower 90% confidence interval values, and extrapolated nonoperating quality factors for S, R, P, and Mil-spec. Transformer data were only for Mil-spec and lower categories. Therefore, the preliminary transformer base failure rate was divided by the Mil-spec nonoperating quality factor of 3.08. In this manner, one nonoperating quality factor can be used for all inductive devices.

TABLE 5.5.2-5: INDUCTOR NONOPERATING QUALITY FACTORS

Quality Level	$\pi_{NQ}, .05$	$\pi_{NQ1}(1)$	$\pi_{NQ}, .95$	$\pi_{NQ2}(1)$
S	--	--	--	.06
R	--	--	--	.15
P	--	--	--	.38
M	--	1.0	--	1.00
MIL-SPEC	--	--	--	3.08
Lower	1.37	11.36	94.51	11.36

NOTES: (1) π_{NQ1} are the observed nonoperating quality factors. π_{NQ2} are the observed factors supplemented by extrapolated values for S, R, P and MIL-SPEC qualities.

The next task in the inductor model development process was to determine nonoperating environmental factors by the methods described in Section 4.5. This method assumes that a series of nonoperating environmental factors can be generated from the MIL-HDBK-217D operating environmental factors. The proposed indicator nonoperating factors were presented in Table 5.5.1-1 in the previous section. It was determined that separate environmental factors would be applied for coils and transformers.

Tables 5.5.2-6 and 5.5.2-7 show failure mode/mechanism and failure acceleration factor distributions for inductors. Accurate failure mode/mechanism information was difficult to obtain for operating applications and essentially impossible for nonoperating applications. Much of the information in these tables was therefore theorized, although References 33, 41 and 42 provided important failure mode information.

The final phase of the inductive device model development process was to normalize the preliminary base failure rates to correspond to a ground benign environment. The preliminary base failure rates were normalized by dividing with the respective ground fixed environmental factors. Additionally a unique base failure rate value for RF transformers, power transformers and high power pulse transformers was extrapolated by assuming the base failure rate was the average value for all transformer styles and using the operating failure rate relationships from MIL-HDBK-217D. The nonoperating base failure rates were therefore determined to be:

λ_{nb} = nonoperating base failure rate
= .000055, lower power pulse and audio transformers
= .00028, high power pulse, power and RF transformers
= .00015, RF coils

Normalization of the nonoperating base failure rates concluded the model development for inductive devices. The proposed model is presented in its entirety in Section 5.5.1.

TABLE 5.5.2-6: RF COIL FAILURE MECHANISM DISTRIBUTION

Failure Mode	Failure Mechanism	Accelerating Factors	Operating Distribution (%)	Nonoperating Distribution (%)
open	wire over-stress	voltage, current	25 - 45	0 - 5
	faulty lead	vibration, shock	5 - 25	20 - 40
short	insulation breakdown	voltage, humidity, temperature	5 - 20	5 - 20
unstable, drift	insulation deterioration	temp., humidity	20 - 40	40 - 65

TABLE 5.5.2-7: TRANSFORMER FAILURE MECHANISM DISTRIBUTION

Failure Mode	Failure Mechanism	Accelerating Factors	Operating Distribution (%)	Nonoperating Distribution (%)
open	wire over-stress	voltage, current	15 - 35	0 - 5
	faulty leads	vibration, shock	0 - 15	0 - 15
short	corroded windings	humidity, temp.	15 - 35	20 - 45
	insulation breakdown	voltage, humidity, temp.	15 - 35	20 - 40
	insulation deterioration	humidity, temp.	10 - 30	20 - 40

5.6 Lasers

5.6.1 Proposed Laser Nonoperating Failure Rate Prediction Models

This section presents the proposed nonoperating failure rate prediction models for lasers. The proposed models are presented in Appendix A in a format compatible with MIL-HDBK-217D. The proposed nonoperating failure rate prediction models are approximate, and based on the observed operating to nonoperating ratios for vacuum tubes.

Helium Neon Lasers

The proposed model for helium/neon lasers is:

$$\lambda_p = .11 \pi_{NE}$$

where

λ_p = helium/neon laser nonoperating failure rate (failures/ 10^6 nonoperating hours)

π_{NE} = nonoperating environmental factor (see Table 5.6.1-1)

Argon Ion Lasers

The proposed model for argon ion lasers is:

$$\lambda_p = .61 \pi_{NE}$$

where

λ_p = argon ion laser nonoperating failure rate (failure/ 10^6 nonoperating hours)

π_{NE} = nonoperating environmental factor (see Table 5.6.1-1)

Carbon Dioxide, Sealed Lasers

The proposed model for CO₂ sealed lasers is:

$$\lambda_p = (.65 + .013(N_{op})) \pi_{NE}$$

where

λ_p = CO₂ sealed laser nonoperating failure rate (failures/10⁶ nonoperating hours)

N_{op} = number of active optical surfaces

π_{NE} = nonoperating environmental factor (see Table 5.6.1-1)

Carbon Dioxide, Flowing Lasers

The proposed model for CO₂ flowing lasers is:

$$\lambda_p = .039(N_{op}) \pi_{NE}$$

where

λ_p = CO₂ flowing laser nonoperating failure rate (failures/10⁶ nonoperating hours)

N_{op} = number of active optical surfaces

π_{NE} = nonoperating environmental factor (see Table 5.6.1-1)

Solid State Lasers (Nd:YAG or Ruby Rod)

The proposed model for solid state lasers is:

$$\lambda_p = (0.062 + .021(N_{op})) \pi_{NE}$$

where

λ_p = solid state laser nonoperating failure rate (failures/10⁶
nonoperating hours)

N_{op} = number of active optical surfaces

π_{NE} = nonoperating environmental factor (see Table 5.6.1-1)

The proposed model for solid state lasers is for either Nd:YAG or ruby rod lasers, and for either xenon or krypton flashlamps.

TABLE 5.6.1-1: LASER NONOPERATING ENVIRONMENTAL FACTORS

Environment	π_{NE}	Environment	π_{NE}
G_B	1	A_{IA}	44
G_F	9.0	A_{IF}	62
G_M	44	A_{UC}	35
M_p	22	A_{UT}	42
N_{SB}	10	A_{UB}	71
N_S	49	A_{UA}	57
N_U	49	A_{UF}	71
N_H	35	S_F	(1)
N_{UU}	38	M_{FF}	21
A_{RW}	46	M_{FA}	29
A_{IC}	26	U_{SL}	69
A_{IT}	35	M_L	71
A_{IB}	58	C_L	-

NOTES: (1) Space Flight environment was not addressed in this study.

5.6.2 Laser Model Development

A series of simple laser nonoperating failure rate prediction models were determined based on assumptions. The nonoperating failure rate model development process consisted of five separate steps, which are:

1. Compute average MIL-HDBK-217D operating failure rates.
2. Determine an appropriate operating to nonoperating failure rate ratio.
3. Compute approximate nonoperating failure rates.
4. Assume a nonoperating environmental factor.
5. Normalize the failure rates.

The first step in the process was simple enough. Average operating failure rates were computed for helium/neon, argon ion, CO₂, and solid state lasers by using the methods in MIL-HDBK-217D. It was preferable to proceed with the average failure rate values rather than assuming the operating factors would also apply during nonoperating periods. Many of laser operating factors would clearly not apply during nonoperating periods. For example, factors for pulse repetition, cooling, tube current and pulse energy would intuitively not apply to nonoperating periods.

In general, the dominant nonoperating failure mechanisms for the generic laser family are either related to the tube (i.e. laser tube for a He/Ne laser, flashlamp for a Nd:YAG laser) or degraded optical surfaces. The operating to nonoperating failure rate ratio for vacuum tubes was selected because of similar tube failure mechanisms. For the electronic vacuum tubes with data, the average ratio was 84.8 to 1. This ratio was then applied to the average operating failure rates to determine approximate nonoperating failure rates.

The next phase of the model development process was to assume a series of nonoperating environmental factors. It was determined that the operating environmental factor could not accurately be applied for

nonoperating failure rate prediction purposes. Therefore, a series of nonoperating environmental factors were generated using the methods presented in Section 4.5. The proposed laser nonoperating environmental factors were presented in Table 5.6.1-1 of the previous section.

The final step for laser model development was to normalize the approximate nonoperating failure rates to correspond to a ground benign environment. This was done to provide consistency with the other proposed models. The normalization process consisted of dividing the failure rates by the ground fixed environmental factor of nine.

The proposed laser nonoperating failure rate prediction models must be considered approximate because they were based exclusively on assumptions. However, the objective of this study was not to analyze data but to develop models which can be used to predict the nonoperating failure rate of any equipment type. Additionally, laser target designators and range finders with Nd:YAG solid state lasers generally are exposed to significant periods of nonoperation. Therefore, a laser nonoperating failure rate prediction methodology is essential.

5.7 Tubes

5.7.1 Proposed Tube Nonoperating Failure Rate Prediction Model

This section presents the proposed tube nonoperating failure rate model. The model is also presented in Appendix A in a form compatible with MIL-HDBK-217D. The proposed model for electronic vacuum, microwave and other tube types is given by the following equation.

$$\lambda_p = \lambda_{nb} \pi_{NE}$$

where

- λ_p = predicted tube nonoperating failure rate
- λ_{nb} = nonoperating base failure rate (failure/10⁶ hrs.)
 - = .0040, receiver; triode, tetrode or pentode
 - = .0090, receiver; power rectifier
 - = .049, vidicon
 - = .013, CRT
 - = .32, thyatron
 - = 1.29, crossed field amplifier
 - = 1.03, pulsed gridded
 - = .56, transmitting; triode, tetrode or pentode
 - = 1.61, transmitting, any style with peak power \leq 200 kW, frequency \leq 200 MHz, or average power \leq 2 kW
 - = 2.60, twystron
 - = 1.02, magnetron
 - = 1.20, CW klystron
 - = 1.15, pulsed klystron
 - = .69, TWT
- π_{NE} = nonoperating environmental factor (see Table 5.7.1-1)

TABLE 5.7.1-1: TUBE NONOPERATING ENVIRONMENTAL FACTORS

Environment	π_{NE}	Environment	π_{NE}
G _B	1	A _{IA}	23
G _F	3.0	A _{IF}	35
G _M	31	A _{UC}	8.2
M _p	31	A _{UT}	23
N _{SB}	15	A _{UB}	33
N _S	29	A _{UA}	27
N _U	47	A _{UF}	43
N _H	110	S _F	(1)
N _{UU}	120	M _{FF}	63
A _{RW}	140	M _{FA}	91
A _{IC}	6.2	U _{SL}	210
A _{IT}	19	M _L	220
A _{IB}	25	C _L	3600

NOTES: (1) Space Flight environment was not addressed in this study.

5.7.2 Tube Model Development

The modeling approach discussed in Section 4.1 was implemented for tubes. Analysis of the available tube nonoperating reliability data and development of a theoretical model were used to determine the nonoperating failure rate prediction model. The proposed model was determined to be a function of tube style and environment.

Application and construction variables were identified which characterize tubes in a nonoperating environment. Table 5.7.2-1 presents a list of the device classification variables. These variables were possible nonoperating failure rate model input parameters which were analyzed using statistical methods where appropriate. These variables were determined whenever possible for all collected data. If sufficient information could not be determined for any specific data entry, then it was removed from the model development process.

TABLE 5.7.2-1: TUBE PART CLASSIFICATION

- I. Type
 - A. Receiver
 - 1. Triode
 - 2. Tetrode
 - 3. Pentode
 - 4. Power Rectifier
 - B. CRT
 - C. Vidicon
 - D. Thyatron
 - E. Crossed Field Amplifier
 - F. Pulsed Gridded
 - G. Transmitting
 - 1. Triode
 - 2. Tetrode
 - 3. Pentode
 - H. TWT
 - I. Twystron
 - J. Magnetron
 - 1. Conventional
 - 2. Coaxial
 - K. Klystron
- II. Pulsed vs. CW
- III. Temperature
 - A. Rated
 - B. Actual
- IV. Rated Power
- V. Frequency
- VI. Application Environment
- VII. Number of Power On/Off Cycles per 10^3 Nonoperating Hours

The nonoperating reliability concepts presented in Section 4.0 and a study of tube nonoperating failure mechanisms were combined to determine a theoretical model for tubes. The theoretical model assumes a nonlinear failure rate equation which is time dependent. The theoretical nonoperating failure rate model for tubes is represented by the following equation (f denotes a function).

$$\lambda_t = f(\text{device style, } P, F, \text{time, temp.}) \pi_{NE} \pi_{cyc}$$

where

λ_t = predicted tube nonoperating failure rate (failures/10⁶ hrs.)

P = rated power

F = operating frequency

π_{NE} = nonoperating environmental factor

π_{cyc} = equipment power on-off cycling factor = $1 + K_1(N_C)$

where

K_1 = constant

N_C = equipment power on-off cycling rate (cycles/10³ nonop. hrs.)

It was hypothesized that the theoretical tube model would be time dependent. This assumption was based on two observations. First, many of the anticipated storage failure mechanisms are degradation mechanisms. For example, the dominate electronic vacuum tube failure mechanism according to Reference 1 is a loss of vacuum during prolonged storage. A loss of vacuum integrity would tend to cause failures later in a tube nonoperating life (as opposed to early in the tube life). Even though a microscopic leak in the tube envelope may be present early, the tube would not actually fail as a result of the leak until a later point in time. This mechanism would be indicative of a time increasing nonoperating failure rate. Another tube storage failure mechanism is corrosion and embrittlement of the filament structure. Again, the frequency of occurrence for these failures would not be anticipated to be random with

time, but would increase with time. The second observation which led to the time dependent tube nonoperating failure rate conclusion was the "shelf life" phenomenon. Even if nothing were known about tube storage failure mechanisms, the fact that some tube types are believed to have some inherent "shelf life" was considered as evidence of a time dependent failure rate. In general terms, it can be assumed that the nonoperating failure rate is relatively low until the specified "shelf life" and then the instantaneous failure rate would be expected to increase dramatically. It should also be noted that many high quality military tube types including TWTs and magnetrons are no longer believed to have a "shelf life" and thus, the nonoperating failure rate could be accurately assumed to be constant with time. However, this is certainly not true for all tube styles considered in this study.

Unfortunately, there was little which could have done to quantify a time dependent nonoperating failure rate model. All available data were in the form: X observed failures in Y nonoperating part hours. Individual nonoperating times-to-failure would have been required to quantify a time dependent model. It is doubtful that accurate times-to-failure can ever be detected during nonoperating applications because a failure generally can not be detected until power is applied to the tube. If power were applied to the tube frequently enough to determine times-to-failures, then the majority of failures would probably have been induced by the frequent power on-off cycling. As a result of this lack of time to failure information, the model development process continued by computing average nonoperating failures. It should be cautioned that instantaneous failure rates can differ significantly from the average for short time intervals.

The summarized tube nonoperating reliability data collected in support of this study is presented in Table 5.7.2-2. The data consists of 47 individual data records, 364 observed failures, and 794.8×10^6 part hours. The source for each data record was the MICOM storage data base. Forty-seven data records were found to either have observed failures or

had sufficient part hours to estimate a failure rate without observed failures.

TABLE 5.7.2-2: TUBE NONOPERATING FAILURE RATE DATA

Data Records	Style	Failures	Part Hours (X10 ⁶)
11	Magnetron	163	156.5
2	TWT	11	3.6
2	Twystron	8	1.6
11	Klystron, pulsed	98	31.3
14	Klystron, CW	32	11.0
4	Pulsed Gridded	38	8.7
1	Vidicon	3	20.6
1	Receiver, Triode	1	191.4
1	Receiver, Pentode	10	370.1
<hr/>			
47		364	794.8

The number of variables which could be analyzed empirically was limited by the nature of the available data. The following attributes of the collected nonoperating tube data were identified from the preliminary data analysis.

- 1) There was not a sufficient range of environments to develop a series of environmental factors based solely on the data.
- 2) There was an insufficient range of ambient temperatures to study the effects of temperature analytically.
- 3) There was insufficient cycling rate information to analyze the effects of power on-off cycling on the nonoperating failure rate of tubes.

It was unfortunate that equipment power on-off cycling could not be analyzed empirically. The change in temperature resulting from turning the equipment power on and off would hypothetically have an adverse effect on nonoperating failure rate. However, no relationship could be determined empirically and no theoretical relationship could be located in the literature. Thus, the proposed model corresponds to some average, unknown equipment power on-off cycling frequency.

The preliminary model refinement process resulted in the conclusion that tube style and application environment were the dominant variables effecting nonoperating failure rate. Variables such as rated power and frequency were believed to have little effect on nonoperating failure rate. The effect of style was further analyzed using statistical techniques. It was assumed that application environment was an important parameter effecting nonoperating failure rate. Although a series of environmental factors could not be derived from the data, it was essential to include applicable factors in the proposed tube nonoperating failure rate prediction model. This was essential to properly discriminate against known failure accelerating environmental factors. Section 4.5 proposes a method to develop appropriate nonoperating environmental factors. This method was applied to tube nonoperating failure rate model after evaluating the effect of tube style.

A matrix of "dummy variables" (0 or 1) was defined for tube style so that correlation coefficient analysis and regression analysis could be applied to the data. These analyses require quantitative variables and device style is a qualitative variable. The matrix for tube style is illustrated in Table 5.7.2-3.

TABLE 5.7.2-3: DEVICE STYLE VARIABLE MATRIX

Device Style	S ₁	S ₂	S ₃	S ₄	S ₅	S ₆	S ₇	S ₈
Klystron, Pulsed	0	0	0	0	0	0	0	0
Twystron	1	0	0	0	0	0	0	0
Klystron, CW	0	1	0	0	0	0	0	0
Magnetron	0	0	1	0	0	0	0	0
TWT	0	0	0	1	0	0	0	0
Receiver, Triode	0	0	0	0	1	0	0	0
Vidicon	0	0	0	0	0	1	0	0
Receiver, Pentode	0	0	0	0	0	0	1	0
Pulsed Gridded	0	0	0	0	0	0	0	1

As the model development process continued, regression analysis was then applied to the data. Results of the regression analysis are given in Table 5.7.2-4. The dependent variable was the natural logarithm of nonoperating failure rate. The independent variables were S_1 through S_8 . Device style variables S_5 , S_6 , and S_7 were significant at a 90% confidence limit. S_1 was significant with 70% confidence, and S_4 with 50% confidence. The R-squared value for the regression was .65, so 65% of the variability in the observed data can be explained by the regression solution. There was no significant difference, with 50% confidence, between the nonoperating failure rate for pulsed klystrons, CW klystrons, magnetrons and pulsed gridded tubes.

TABLE 5.7.2-4: TUBE REGRESSION RESULTS

Variable	Coefficient	Standard Error	f-ratio	Confidence Limit
S_1	.819	.770	1.13	0.70
S_2	.147	.404	.01	<0.50
S_3	-.115	.427	.07	<0.50
S_4	-.512	.770	.44	0.50
S_5	-6.491	1.047	38.46	0.90
S_6	-3.163	1.047	9.13	0.90
S_7	-4.848	1.047	21.45	0.90
S_8	-.106	.585	.03	<0.50
b_0	1.237	--	--	--

Regression solutions below 50% were then computed to further evaluate the nonoperating failure rate of CW klystrons, magnetrons, and pulsed gridded tubes. As a general practice in this study, unique failure rate modifying factors were not proposed for variables which did not significantly effect nonoperating failure rate with greater than 70% confidence. However, an exception was made to this general rule for tubes. These various tube styles belong to the same generic part family, but are physically very different. Therefore it was decided to propose the best estimates available for nonoperating failure rate regardless of the significance level.

The coefficients given in Table 5.7.2-4 were the results of a regression with the dependent variable equal to the natural logarithm of the nonoperating failure rate. Transforming the regression results into an equation where nonoperating failure rate (as opposed to log of nonoperating failure rate) was the dependent variable resulted in the following preliminary multiplicative model.

$$\lambda_t = \exp(1.237 + .819(S_1) + .147(S_2) - .115(S_3) - .512(S_4) - 6.491(S_5) - 3.163(S_6) - 4.848(S_7) - .106(S_8))$$

- = 3.44, klystron, pulsed
- = 7.81, twystron
- = 3.61, klystron, CW
- = 3.07, magnetron
- = 2.06, TWT
- = .00523, Receiver, triode
- = .146, Vidicon
- = .0271, Receiver, pentode
- = 3.10, Pulsed gridded

The next phase of the model development process for tubes was to develop appropriate nonoperating environmental factors using the methods presented in Section 4.5. Tubes presented a unique situation for determination of nonoperating environmental factors. The anticipated failure mechanisms in the operating state are dominated by failures which are accelerated by the internal heat rise due to either the current flow from one element of the tube to another element, the power used to raise an electron-emitting cathode to operating temperature, or another source of internal heat rise. Excessive heat can result in several general failure mechanisms including deterioration of the seal, wearout of electron emission surfaces, evolution of gas, and contaminated or damaged emission surfaces resulting in increased electronic emission. It was concluded from the failure mechanism comparisons that the MIL-HDBK-217D operating environmental factors clearly do not represent the effects of environmental stress in a nonoperating application.

Part types which have operating failure rates which are dominated by factors unique to the operating state were categorized in Section 4.5. Tubes, as well as incandescent lamps and laser tubes, fit into this category. For these part types, the difference between operating and nonoperating failure rate was believed to be relatively large. However, the rate of increase for failure rate versus environmental stress would be greater in the nonoperating state. Failures due to purely environmental stresses, such as vibration and mechanical shock, would not occur in greater numbers in the nonoperating state, but these failures would be a much larger percentage of the total failures. Thus, a similar increase in the number of failures due to a more stressful environment would have a much more apparent effect for nonoperating applications. Proper determination of applicable nonoperating environmental factors was not possible with the available information. However, an approximate formula was developed (and described in Section 4.5) to estimate nonoperating environmental factors for these part types.

The nonoperating environmental factor conversion was based on the MIL-HDBK-217D operating environmental factors, the fraction of failures due to purely operational stress, the fraction of failures due to purely environmental stress, and the fraction of total failures due to simultaneous exposure to operational/environmental stresses. To compute the environmental factors, it was estimated that 50% of operating tube failures could be attributed to entirely operational stress. The remaining percentage was attributed to combined operational/environmental stress or other factors such as environment related temperature rises. The resultant factors were presented in Table 5.7.1-1 of the previous section. It is emphasized that these values are approximate. However, the described approach did not ignore the observation that the operating and nonoperating environmental factors would not be expected to be the same for tubes. Therefore, this approach was preferable to the erroneous assumption that the environmental factors would be the same. Additionally, the tube nonoperating environmental factors were normalized to a ground benign value equal to one to be consistent with the other models presented in this report.

The next phase of the tube model development process was to extrapolate nonoperating failure rates for those tube styles without data. Table 5.7.2-5 presents the observed nonoperating failure rate, the corresponding MIL-HDBK-217D operating failure rate for a ground fixed environment, and the ratio between the two. The results of this exercise were very interesting. First, the correlation coefficient for operating and nonoperating failure rate was found to be 0.73. This was considered to be extremely high in consideration of the inherent failure rate variability. The high correlation coefficient provides justification for using the operating failure rates to extrapolate nonoperating failure rates for tube types without data. Another important observation was the ratios fell into two categories. There was a high ratio (geometric mean = 374) for receiving tubes and vidicons, and a somewhat lower ratio (geometric mean = 51.7) for the remaining tube styles. No explanation for this apparent difference was determined. However, it was decided to group the tube styles without data into one of the two groups based on device construction. CRTs was grouped with vidicons and receiving tubes. Thyratrons, crossed field amplifiers, and transmitting tubes were grouped with the remaining tube types. The appropriate ratios were then used to determine ground fixed nonoperating failure rates.

The final phase of nonoperating failure rate model development was to normalize the ground fixed failure rates to correspond to a ground, benign environment. It was desired that all models presented in this report be normalized to a ground benign environment to provide consistency. The normalization was done by dividing the previously presented failure rates by the ground fixed nonoperating environmental factor of three.

Normalizing the tube nonoperating failure rate concluded the model development process. The proposed models were based on data in ground based environments and accurately predicts the nonoperating failure rate in those environments. A series of nonoperating environmental factors were assumed based largely on intuitive reliability relationships. These factors should be evaluated when additional tube nonoperating failure rate data becomes available for airborne and other stressful environments.

TABLE 5.7.2-5: TUBE OPERATING AND NONOPERATING FAILURE RATE COMPARISON

Tube Type	Operating Failure Rate (f/10 ⁶ hrs.)	Nonoperating Failure Rate (f/10 ⁶ hrs.)	Ratio ($\lambda_{op}/\lambda_{nonop}$)
Receiver			
Triode, Tetrode, Pentode	5	.012(2)	417
Power Rectifier	10	--	--
Vidicon	49(1)	.146	336
CRT	15	--	--
Thyratron	50(2)	--	--
Crossed Field Amplifier	200(2)	--	--
Pulsed Gridded	200(2)	3.10	64.5
Transmitting			
Triode, Tetrode, Pentode	87(2)	--	--
Other (3)	250	--	--
Twystron	460(2)	7.81	58.9
Magnetron	435(2)	3.07	141
CW Klystron	68(2)	3.61	18.8
Pulsed Klystron	84(2)	3.44	24.4
TWTs	160(2)	2.06	77.7

NOTES: (1) Vidicon failure rates from Reference 45.

(2) Geometric mean is given.

(3) Any transmitting tube with peak power \leq kW, frequency \leq 200 MHz, or average power \leq 2 kW.

5.8 Mechanical/Electromechanical Devices

There are a number of families of electromechanical devices that are susceptible to degradation damage when exposed to many of the military environments for long periods of time in a nonoperating state. In some cases this degradation may be more severe than the operating effects in the same environment. The device families in question include switches, relays, electric motors, servomechanisms, and connectors.

The following sections present the proposed nonoperating failure rate prediction models for mechanical and electromechanical devices. Additionally, discussions are presented which address the nature of the degradation effects and actions which may ameliorate the impact of long term exposure in a nonoperating state. The elements of the environment which cause degradation include vibration, shock, ambient temperature, humidity, and airborne contamination such as salt, sulfur and products of petroleum combustion.

Very little nonoperating failure rate data were collected for mechanical/electromechanical devices. Therefore, model development for these devices was based on intuitive nonoperating reliability relationships supplemented by whatever data were available. It was decided to propose simple models for these part types because of the general lack of quantitative information. More complex assumed models would not necessarily be more accurate but would delude the model users into thinking that they were.

5.8.1 Proposed Mechanical/Electromechanical Device Nonoperating Failure Rate Prediction Models

This section presents the proposed nonoperating failure rate prediction models for mechanical and electromechanical devices. The devices studied are those mechanical and electromechanical devices included in MIL-HDBK-217D. Separate models were developed for relays, switches and connectors. A table of average nonoperating failure rates

was determined for rotating mechanisms. The proposed models are presented in Appendix A in a format compatible with MIL-HDBK-217D.

Rotating Mechanisms

Table 5.8.1-1 presents average nonoperating failure rates for motors, synchros, resolvers, and elapsed time meters. The average nonoperating failure rate for motors pertains to motors with power ratings below one horsepower.

TABLE 5.8.1-1: ROTATING DEVICE AVERAGE NONOPERATING FAILURE RATES

Device	Nonoperating Failure Rate (failures/10 ⁶ nonoperating hours)
Motors (ac or dc)	.045
Synchros	.14
Resolvers	.14
Elapsed Time Meters	1.2

Relays

The proposed nonoperating failure rate prediction model for relays is:

$$\lambda_p = \lambda_{nb} \pi_{NQ} \pi_{NE}$$

where

λ_p = relay nonoperating failure rate

λ_{nb} = nonoperating base failure rate (failures/10⁶ hours)

= .010, nonhermetic, contact voltage \leq 50 millivolts when operated

= .002, nonhermetic, contact voltage $>$ 50 millivolts when operated

= .0004, hermetic packaged relays

π_{NQ} = nonoperating quality factor

= 0.46, established reliability

= 1.0, Mil-spec

= 4.2, lower

π_{NE} = nonoperating environmental factor (see Table 5.8.1-2)

TABLE 5.8.1-2: RELAY NONOPERATING ENVIRONMENTAL FACTORS

Environment	π_{NE}	Environment	π_{NE}
GB	1	AIA	7.5
GF	2.3	AIF	10
GM	8.2	AUC	8.0
Mp	21	AUT	9.0
NSB	8.0	AUB	15
NS	8.0	AUA	10
NU	14	AUF	15
NH	32	SF	(1)
NUU	34	MFF	21
ARW	46	MFA	29
AIC	5.5	USL	62
AIT	6	ML	71
AIB	10	CL	N/A

NOTES: (1) Space Flight environment was not addressed in this study.

Switches

The proposed nonoperating failure rate prediction model for switches is:

$$\lambda_p = \lambda_{nb} \pi_{NQ} \pi_{NE}$$

where

λ_p = switch nonoperating failure rate

λ_{nb} = nonoperating base failure rate (failures/ 10^6 hours)

= .030, contact voltage \leq 50 milliamps when operated

= .006, contact voltage > 50 milliamps when operated

π_{NQ} = nonoperating quality factor

= 0.46, established reliability

= 1.0, Mil-spec

= 4.2, lower

π_{NE} = nonoperating environmental factor (see Table 5.8.1-3)

TABLE 5.8.1-3: SWITCH NONOPERATING ENVIRONMENTAL FACTORS

Environment	π_{NE}	Environment	π_{NE}
GB	1	AIA	14
GF	2.9	AIF	18
GM	13	AUC	9
MP	21	AUT	9
NSB	7.9	AUB	18
NS	7.9	AUA	18
NU	18	AUF	23
NH	32	SF	(1)
NUU	34	MFF	19
ARW	41	MFA	26
AIC	7.2	USL	63
AIT	7.2	ML	64
AIB	14	CL	1200

NOTES: (1) Space Flight environment was not addressed in this study.

Connectors

The proposed nonoperating failure rate prediction model for connectors is:

$$\lambda_p = \lambda_{nb} \pi_{NE}$$

where

λ_p = connector nonoperating failure rate

λ_{nb} = connector nonoperating base failure rate (failures/ 10^6 hours)

= .00044, circular, coaxial and power connectors

= .0029, rack and panel, and printed wiring board connectors

π_{NE} = nonoperating environmental factor (see Table 5.8.1-4)

TABLE 5.8.1-4: CONNECTOR NONOPERATING ENVIRONMENTAL FACTORS

Environment	π_{NE}	Environment	π_{NE}
GB	1	AIA	5.3
GF	2.3	AIF	11
GM	8.3	AUC	4.3
Mp	8.5	AUT	15
NSB	4.1	AUB	9.8
NS	5.5	AUA	8.0
NU	13	AUF	15
NH	13	SF	(1)
NUU	14	MFF	8.5
ARW	19	MFA	12
AIC	2.8	USL	25
AIT	4.8	ML	29
AIB	7.0	CL	490

NOTES: (1) Space Flight environment was not addressed in this study.

5.8.2 Rotating Mechanisms

The rotating mechanisms included in MIL-HDBK-217D are motors, synchros, resolvers and elapsed time meters. Average nonoperating failure rates were determined for each of these device types. Additionally, a qualitative assessment of rotating mechanisms was performed, and is described in this section.

The following discussion is limited to low torque electric motors and servomechanisms, their nonoperating degradation mechanisms, and the associated environmental causal stresses.

Ball bearings are normally used to support the rotating member in those devices using grease as a lubricant. Prior to assembly of the bearings into the device, they are uniformly packed with grease. In the first few rotations of the device, the balls form a channel in the grease. This channel, if uniform without voids or discontinuities, serves to concentrate the oils released from the grease on the wear path insuring good lubrication and long bearing life. The grease must be uniformly packed initially or a continuous channel will not be formed and short life will result. Prolonged nonoperating periods can effect the uniformity of the packed grease. In the nonoperating state, temperatures above 70^o, vibration, or both will cause the grease to sag resulting in a nonuniform channel when the device is again operated.

It is recommended that these devices be run up to speed every six months when exposed to 70^oF or higher temperatures. Where these rotating mechanisms are simultaneously exposed to temperatures in excess of 70^oF and vibration, the time between run ups should not exceed three months. If the time between run ups is longer than these recommended intervals, it would be anticipated that the nonoperating failure rate would be higher.

Commutator devices such as DC motors and certain servomechanisms may develop resistive coatings on the commutator much as contact devices (discussed in Section 5.8.3). Prolonged storage results in the formation of resistive surface films. When less than six volts potential exist, running these devices up to speed every three months will also preclude erratic operations.

It was hypothesized that device style would be the most significant variable effecting the nonoperating failure rate of motors. Commutator motors have two major nonoperating failure mechanisms; contamination of

commutative surfaces and loss of a uniform lubricant. Conversely, the loss of lubricant is the dominant mechanism acting on non-commutator motors. In general, AC motors are non-commutator devices. DC motors may be either commutator or non-commutator.

Nonoperating failure rate data for rotating mechanisms were available from MICOM. This data are presented in Table 5.8.2-1. The data collectively consists of 20 observed failures in 149.0×10^6 nonoperating part hours. There were insufficient data to statistically analyze the effects of independent variables with regression analysis.

TABLE 5.8.2-1: ROTATING MECHANISM NONOPERATING FAILURE RATE DATA

Equipment/Source	Device Style	Failures	Part Hours ($\times 10^6$)
Martin Marietta	AC motor	1	2.16
Martin Marietta	torque motor	0	4.16
Martin Marietta	resolver	2	14.20
MICOM	DC motor	3	6.34
MICOM	AC motor	0	0.15
MICOM	DC motor	0	55.25
Maverick/MICOM	torque motor	14	41.18
Sparrow/MICOM	DC motor	0	25.52
Totals		20	148.96

The nonoperating failure rate for the merged AC motor data was over 12 times as high as the nonoperating failure rate for the merged DC motor data. This observation was contrary to the earlier hypothesis that commutator motors (if some of the DC motors were commutators) should have a higher nonoperating failure rate. It was assumed that there were insufficient data to accurately distinguish the difference between commutator and non-commutator motor types. Therefore, an average nonoperating failure rate was computed by dividing the sum of the failures by the sum of the part hours for both AC and DC motor styles. The average nonoperating failure rate was therefore found to be 0.0447 failures per 10^6 nonoperating hours.

Similar to the discussion for motors, there were insufficient data for synchros and resolvers to develop nonoperating failure rate prediction models analytically. Therefore, an average nonoperating failure rate of 0.14 was determined from the data. It was then assumed that this value was applicable for all styles of synchros and resolvers.

No nonoperating failure rate data were available for elapsed time meters. Therefore, an average nonoperating failure rate was determined by (1) calculating an average operating failure rate using MIL-HDBK-217D, (2) determine an operating to nonoperating ratio for rotating devices using the data for other devices, and (3) computing an average, approximate failure rate. The applicable ratio was determined to be 54:1 and the average nonoperating failure rate for elapsed time meters was computed to be 1.2 failures/10⁶ nonoperating hours.

Failure rates based on small sample sizes are potentially biased. However, the average nonoperating failure rates presented in this section for motors, synchros, resolvers and elapsed time meters represent the best possible values given the data constraints. It is recommended that these average failure rates be evaluated when additional data resources become available.

5.8.3 Contact Device Model Development

For the purpose of this study, contact devices were considered to be switches and relays. The desired analytical model development approach could not be applied for contact devices because of a general lack of quantitative nonoperating failure rate data. Therefore, intuitive nonoperating reliability relationships formed the basis of the model development process. The limited data supply was used to complement the intuitive relationships. The proposed nonoperating failure rate prediction model for relays was determined to be a function of package type, contact voltage, quality level and application environment. The switch nonoperating failure rate prediction model was found to be a function of contact voltage, quality level and application environment.

A list of construction and application variables were determined for both relays and switches. These variables are presented in Table 5.8.3-1 and 5.8.3-2 respectively. In each case, these variables represent possible nonoperating failure rate prediction model parameters.

Switches and nonhermetic relays utilized to control low voltage and current (typical of digital circuits) are of concern regarding nonoperating reliability. This type of operation is called low level circuit operation where the voltage and current are less than 50 millivolts and 50 microamps respectively. The contacts are particularly a reliability concern when contacts are normally open. The voltage in digital circuits is too low to produce an arc on contact closure which would break thru resistive surface films which form during nonoperating periods. The transfer is by a tunneling mechanism which can not take place thru a resistive surface film. Therefore, the contact voltage/current and the number of normally open contacts are important variables for predicting the nonoperating failure rate for nonhermetic contact devices. Conversely, contact voltage/current would not be anticipated to be a significant variable for hermetic relays because the hermetic seal would preclude the formation of substantial resistive surface films.

The rate of build up and nature of the surface resistive film is a function of the environment to which the contacts are exposed, as well as the contact material. The ability of the contact to remove a surface film depends on the design, contact material, surface roughness, and contact pressure.

From the previous paragraph, it can be said that reliable operation depends on maintaining clean contact surfaces and that long term nonoperating conditions may defeat this objective. The alternative approach to prevent nonoperating contact failures is periodic actuation when long periods of nonoperation are the rule. The literature contains no quantitative information in this regard. A survey of leading manufacturers was more helpful in a qualitative sense, but not

TABLE 5.8.3-1: RELAY PART CHARACTERIZATION

- I. Application Type
 - A. Low Level Circuit
 - B. General Purpose
 - C. Sensitive (0-100 mw)
 - D. Polarized
 - E. Vibrating Reed
 - F. High Speed
 - G. Time Delay
 - H. Latching
 - I. High Power
 - J. Medium Power
 - K. Contactors
- II. Construction
 - A. Armature
 - B. Dry Reed
 - C. Mercury Wetted
 - D. Solenoid
 - E. Magnetic Latching
 - F. Vacuum
 - G. Mechanical Latching
- III. Configuration
 - A. SPST
 - B. DPST
 - C. SPDT
 - D. 3PST
 - E. 4PST
 - F. DPDT
 - G. 4PDT
 - H. 6PDT
- IV. Contact Rating (Amps)
- V. Operating Load Type
 - A. Resistive
 - B. Inductive
 - C. Lamp
- VI. Quality Level
 - A. R
 - B. P
 - C. M
 - D. L
 - E. Mil-Spec
 - F. Lower
- VII. Temperature
 - A. Rated
 - B. Actual
- VIII. Application Environment
- IX. Number of Power On/Off Cycles per 10^3 Nonoperating Hours

TABLE 5.8.3-2: SWITCH PART CHARACTERIZATION

- I. Device Style
 - A. Toggle
 - B. Push Bottom
 - C. Rotary
 - D. Basic Sensitive
 - E. Heavy Duty Contactor
 - F. Inertial
- II. Actuation Style
 - A. Snap Action
 - B. Non-Snap Action
- III. Configuration

A. SPST	E. 4PST
B. DPST	F. DPDT
C. SPDT	G. 4PDT
D. 3PST	H. 6PDT
- IV. Operating Load Type
 - A. Resistive
 - B. Inductive
 - C. Lamp
- V. Contact Rating (Amps)
- VI. Number of Switch Positions
- VII. Actuation Differential
- VIII. Temperature
 - A. Rated
 - B. Actual
- IX. Application Environment
- X. Number of Power On/Off Cycles Per Unit Time
- XI. Quality
 - A. Mil-Spec
 - B. Lower
- XII. Wafer Material
 - A. Ceramic
 - B. Glass

quantitatively. The manufacturers all agreed to the wisdom of periodic actuation. However, due to varying experience, the manufacturers contacted had different views on the optimal frequency of actuation. Frequencies were expressed ranging from daily for a dirty industrial environment to every six months in a computer room like environment. None of the manufacturers contacted took exception to monthly actuation as being adequate for all but worst case environments.

The philosophy of periodic actuations for contact devices is the reverse of the observation that equipment power on-off cycling degrades electronic component device reliability. For contact devices, it would be anticipated that as equipment power on-off cycling increases, the observed nonoperating failure rate due to the formation of resistive films would decrease. This trend would be expected for all equipment power on-off cycling frequencies encountered during equipment storage. For equipments which are power cycled frequently (e.g. every day), the observed failure rate would be anticipated to begin to increase due to contact wear. However, it was hypothesized that the effect of equipment power on-off cycling was not a significant variable over the range of equipment power cycling frequencies typically found during normal usage. The beneficial effects of periodic actuation would be approximately canceled by the effects of contact wear. Therefore, the proposed models for contact devices did not include an equipment power on-off cycling factor.

As a result of the qualitative assessment of contact devices, it was determined that the dominant variables effecting relay nonoperating failure rate were package type (i.e. hermetic vs. nonhermetic), contact voltage/current, quality level, environment and the number of normally open contacts. It was believed that these variables were more significant than the respective differences between specific relay styles. It was anticipated that there would not be a large nonoperating failure rate difference between specific relay styles because the dominant nonoperating failure mechanisms act on the contacts (which are relatively similar), and do not act on the actuation mechanisms (which vary considerably).

The nonoperating failure rate data collected for relays is presented in Table 5.8.3-3. The data were merged according to data source, construction and quality level. Merged data records with zero failures were evaluated by the methods presented in Section 3.3 to determine whether there were sufficient part hours to estimate a nonoperating failure rate. There were a total of seven merged data entries available for analysis. This was considered to be insufficient data to quantify the effects of the independent variables by use of regression analysis.

TABLE 5.8.3-3: RELAY NONOPERATING FAILURE RATE DATA

Equipment/Source	Construction	Quality	Failures	Part Hours (X10 ⁶)
Maverick/MICOM	Armature	Mil-spec	2	61.7
Maverick/MICOM	Other	Mil-spec	0	20.6
Sparrow/MICOM	Other	Mil-spec	2	382.8
Lance/MICOM	Armature	Mil-spec	0	4.5
MICOM	Other	Lower	1	3.6
Hughes	Armature	Mil-spec	0	22.1
Hughes	Other	Mil-spec	20	620.0
Martin Marietta	Other	Mil-spec	0	153.5
Martin Marietta	Other	Mil-spec	0	12.3
AFCIQ	Armature	Lower	11	57.0
AFCIQ	Other	Lower	0	1.5
AFCIQ	Other	Lower	0	1.8
AFCIQ	Other	Lower	0	19.0
Totals			36	1360.4

The proposed model form for relays was then hypothesized to be the following equation.

$$\lambda_r = \lambda_{nb} \pi_{NQ} \pi_{NE}$$

where

λ_r = relay nonoperating failure rate

λ_{nb} = nonoperating base failure rate (failures/10⁶ nonoperating hrs.)

= f(package type, contact voltage/current)

π_{NQ} = nonoperating quality factor

π_{NE} = nonoperating environmental factor

The number of normally open contacts was not included in the model because it could not be determined for the collected data. Therefore the proposed model corresponds to an average, unknown quantity of normally open contacts.

A nonoperating base failure rate for nonhermetic relays was determined from the available data for armature relays. It was assumed that the data typically were for low level circuit applications. Nonoperating base failure rates for hermetic relays and nonhermetic relays with greater than 50 millivolts across the contacts were hypothesized. The data where the construction and application were unknown provided a lower limit on hypothesized nonoperating failure rate. The preliminary base failure rates were determined to be:

$\lambda_{nb,pre}$ = preliminary nonoperating base failure rate
 = .023 nonhermetic, contact voltage \leq 50 millivolts when
 operated
 = .005 nonhermetic, contact voltage $>$ 50 millivolts when
 operated
 = .001 hermetic relays

The base failure rates are preliminary because they correspond to a ground fixed environment. Conversely, the proposed model corresponds to a ground benign environment. Only one base failure rate was required for hermetic relays because the effect of contact voltage is negligible without the build-up of surface films.

A ratio between lower quality relays and mil-spec relays was computed from the available data to determine a nonoperating quality factor for commercial grade relays. Both the armature and unknown relay style data were utilized to calculate a commercial grade nonoperating quality factor equal to 4.2. An average established reliability (ER) quality factor was

obtained from RADC-73-248 (Reference 5). This document presented generic relay nonoperating data for established reliability and Mil-spec devices. The ratio of the observed failure rates was equal to 0.46. It was assumed that this ratio was applicable for all relay types. The relay nonoperating quality factors are presented in Table 5.8.3-4. The table presents the proposed factors for established reliability, Mil-spec and commercial grade relays.

TABLE 5.8.3-4: RELAY NONOPERATING QUALITY FACTORS

Quality Level	π_{NQ}
Established Reliability	0.46
Mil-spec	1.0
Lower	4.2

The next phase of the model development process was to assume appropriate nonoperating environmental factors. Based on a comparison of failure mechanism accelerating factors, it was assumed that the operating relay environmental factors would be applicable for nonoperating failure rate prediction purposes. These factors were given in Table 5.8.1-2 in Section 5.8.1. Table 5.8.3-5, on the following page, presents the summarized results of the failure mechanism comparison for relays. References 41, 42 and 46 provided failure mode or mechanism information for relays.

The final phase of the nonoperating failure rate model development for relays was to normalize the base failure rates by dividing by the ground fixed environmental factor of 2.3. The proposed model is presented in Section 5.8.1 and in Appendix A in a format compatible with MIL-HDBK-217D.

A similar intuitive approach to model development was taken for switches. Similar to the discussion for relays, it was hypothesized that the nonoperating failure rate of the switch actuation mechanism is small in comparison to the nonoperating failure rate of the contacts.

TABLE 5.8.3-5: ARMATURE RELAY FAILURE MECHANISM COMPARISON

<u>Failure Mode/Mechanism</u>	<u>Accelerating Factors</u>	<u>Operating Distribution (%)</u>	<u>Nonoperating Distribution (%)</u>
open			
contact contamination	moisture, temp.	10 - 30	30 - 40
poor contact alignment	actuators, vibration	1 - 15	1 - 14
contact corrosion	actuators, voltage, humidity	1 - 12	1 - 13
opened coil	current, vibration	1 - 16	1 - 6
unstable coil	humidity, voltage, temp.	5 - 25	5 - 25
short			
contact welding	current	1 - 13	1 - 13
spring fatigue	actuators	1 - 17	0 - 5
drift, intermittent			
contact corrosion	humidity, temp.	10 - 30	10 - 30
mechanical			
binding, jamming	actuators, contaminants	1 - 20	1 - 10

Therefore, the dominant variables were believed to be contact voltage/current and the number of normally open contacts. Additionally, it was assumed that application environment and quality were significant variables.

All collected nonoperating switch data were for Mil-spec quality devices. Therefore, the nonoperating quality factors developed for relays were also applied for switches. This assumption was justified because the contacts are physically similar for both generic part families.

A series of nonoperating environmental factors for switches was then determined by applying the methods presented in Section 4.5. This method assumed that nonoperating environmental factors could be generated from the corresponding operating factors. The conversion process was conducted in two phases. First, typical temperature differences between operating and nonoperating applications were compared. A temperature adjustment was required for switches because the MIL-HDBK-217D switch models do not have a unique temperature factor to account for the temperature difference. Temperature adjustment factors were multiplied with the operating environmental factors. The temperature adjustment factors were based on documented relationships (i.e. MIL-HDBK-217D) of failure rate vs. temperature for other component types. The second phase of the nonoperating environmental factor determination process was to compare typical operating and nonoperating failure mechanism accelerating factors. Table 5.8.3-6 presents the results of the failure mechanism comparison for toggle switches. References 41, 42 and 46 contained valuable switch failure mode and mechanism information. It was concluded, based on the comparison, that the temperature adjusted switch environmental factors also represented the effect of environmental stress on nonoperating failure rate. The proposed switch nonoperating environmental factors were presented in Table 5.8.1-3 in Section 5.8.1.

The next phase of the switch model development process was to determine an average base failure rate from the available switch nonoperating failure rate data. Table 5.8.3-7 presents the summarized

TABLE 5.8.3-6: TOGGLE SWITCH MECHANISM COMPARISONS

<u>Failure Mode/Mechanism</u>	<u>Accelerating Factors</u>	<u>Operating Distribution (%)</u>	<u>Nonoperating Distribution (%)</u>
open			
misaligned contacts	vibration, actuations	1 - 13	1 - 15
contaminated contacts	temp., humidity	1 - 20	5 - 35
contact wear	actuations	1 - 12	0 - 5
short			
contact welding	current	1 - 15	1 - 10
spring fatigue	actuations	1 - 15	0 - 5
mechanical			
binding, jamming, wear	actuations, humidity, temp.	25 - 45	5 - 30
intermittent, drift			
corrosion, contaminated contacts	humidity, temp., contaminants	20 - 50	40 - 65

switch data. The average nonoperating base failure rate was determined by dividing the sum of the failures by the sum of the part hours, and then dividing by the ground fixed environmental factor. The average nonoperating base failure rate was determined to be 0.030 failures per 10^6 nonoperating hours.

TABLE 5.8.3-7: SWITCH NONOPERATING FAILURE RATE DATA

Equipment/Source	Device Style	Failures	Part Hours ($\times 10^6$)
Martin Marietta	Toggle/Pushbutton	0	1.61
Martin Marietta	Pressure	4	48.30
Martin Marietta	Sensitive	0	1.64
Martin Marietta	Stepping	2	5.00
Martin Marietta	Inertial	9	137.10
Hawk/MICOM	Toggle/Pushbutton	1	17.00
Maverick/MICOM	Thermostatic	0	20.59
Maverick/MICOM	Solenoid	9	82.36
Sparrow/MICOM	Toggle/Pushbutton	0	12.76
Sparrow/MICOM	Pressure	0	25.52
Sparrow/MICOM	Inertial	0	12.76
TOW/MICOM	Toggle/Pushbutton	0	5.26
MICOM	Toggle/Pushbutton	0	1.88
MICOM	Pressure	10	31.00
MICOM	Thermostatic	0	3.88
MICOM	Sensitive	0	1.64
Totals		35	408.30

The contact voltage/current was unknown for the available data. However, this was considered to be the most important variable for assessing switch nonoperating failure rate. Resistive films on the contact surfaces are much more harmful for low voltage, low current switching applications. Higher voltage applications produce an arc on contact closure which would break thru resistive surface films which form during storage. It was assumed that the available data corresponded to low level circuit applications to compute separate base failure rates. Additionally, it was assumed that the relative difference between low level circuit and other applications was the same as for relays. Two

unique nonoperating base failure rates were determined by applying these assumptions and are given by,

$$\begin{aligned}\lambda_{nb} &= \text{nonoperating base failure rate (failures/10}^6 \text{ hours)} \\ &= 0.006, \text{ contact voltage} > 50 \text{ millivolts when operated} \\ &= .030, \text{ contact voltage} \leq 50 \text{ millivolts when operated}\end{aligned}$$

Determination of the nonoperating base failure rates concluded the model development for contact devices. Both the proposed model for switches and relays are presented in Section 5.8.1 and in Appendix A. Both models are based primarily on intuitive rather than empirical relationships. The dominant model parameters were determined by carefully evaluating device construction and the anticipated failure mechanisms. When more data becomes available, the proposed models can be evaluated. It is hypothesized that the number of normally open contacts is the most significant variable not included in the proposed model.

5.8.4 Connectors

The model development for connectors is described in this section. Additionally, a qualitative assessment of connector nonoperating failure rate is provided. The proposed model is presented in Section 5.8.1 and in Appendix A in a format compatible with MIL-HDBK-217D.

Printed wiring board, and rack and panel connectors are the most simply constructed of all connector types. This does not mean they are the most reliable since they are not designed to seal against moisture assimilation or protect the contacts from harmful agents in the atmosphere. How this effects performance in a nonoperating state requires an understanding of the nature of the contact and certain chemical effects on the contact.

Achieving good electrical contact in a connector is a function of surface films (oxides and sulphides), surface roughness, contact area, plastic deformation of the contacting materials and load applied.

Since even the best machined, polished and coated surfaces look rough and uneven when viewed microscopically, the common concept of a flat, smooth contact is grossly oversimplified. In reality, the connector interface is basically an insulating barrier with a few widely scattered points of microscopic contact. The performance of the connector is dependent upon the chemical, thermal and mechanical behavior at these contact points.

Current flow between mating metals is constricted at the interface to the small points on the surfaces which are in electrical contact. This flow pattern causes differences of potential to exist along the contact interface, and causes current bunching at points of lower resistance. As a result, contact resistance and capacitance are introduced into the circuit, and certain chemical effects evolve.

Most nonoperating failures of connectors are induced by the growth of films at points of contact. These films can cause increased contact resistance or an open circuit when power is applied. Contact resistance causes higher temperatures during equipment turn on at the point of contact and thus, increasing chemical activity.

Normally, the purity of metals in contact is not considered a reliability problem. However, ions in impurities or contamination in the surface pores will migrate to the points of highest potential, which are frequently the localized hotspots. Ions interfacing with electrons and other constituents at the points of high chemical activity generate films, usually non-conducting. There is also a continuous supply of material for the growth of insulating films from environments where there are corrosive elements such as hydrogen sulfide, water vapor, oxygen, ozone, hydrocarbons and various dusts.

The connector plugged to its mate during much of its life is characterized by a typical catastrophic nonoperating failure rate based on the factors described. It would appear that periodic demating and mating whether operational or nonoperational would be beneficial. However, such

action exposes, by repeated opening of the mating pin surfaces, the contacts to a fresh supply of local corrosive contaminants. There is also the problem of physical wear on the connecting interfaces. Surface contact points become worn which cause unsymmetrical contacts. The result is increased interface resistance and degradation of the connection.

It was hypothesized that the dominant variables influencing connector nonoperating failure rate were the connector style, the number of pins and the application environment. The device style was considered to be an extremely important variable for connectors because the amount of protection to the environment can vary considerable depending on the specific connector style. In general, all connector styles can be grouped into one of two categories. Circular, coaxial, and power connectors are characterized by good protection from the environment which minimizes the build-up of resistive surface films during storage. Conversely, rack and panel, and printed wiring board (both one-piece and two-piece) connectors offer less protection from the environment and would be anticipated to have a higher nonoperating failure rate.

The collected nonoperating reliability data for connectors is presented in Table 5.8.4-1. All available connector data were from MICOM. Unfortunately, no part characterization information was available.

TABLE 5.8.4-1: CONNECTOR NONOPERATING FAILURE RATE DATA

No.	Equipment/Source	Failures	Part Hours (X10 ⁶)
1	Martin Marietta	0	163.0
2	Hawk/MICOM	0	2024.7
3	Sparrow/MICOM	1	344.5
4	Lance/MICOM	0	3.4
5	MICOM	0	47.4
6	MICOM	0	79861.0
Totals		1	82444.0

Analysis of the data revealed large variability. Data entry number six in Table 5.8.4-1 indicated such a low nonoperating failure rate that it was considered suspect. There were insufficient data to statistically

test for outliers. However, data entry number six was not further considered in the analysis because of the belief that the extremely low failure rate was not indicative of connectors in nonoperating applications. Of the remaining data, only data entries 2 and 3 had failures or sufficient part hours to estimate nonoperating failure rate. As stated before, no part characterization information was available. However, it was assumed that the two calculated nonoperating failure rates provided a typical lower and upper bound on connector nonoperating failure rate, and were set equal to preliminary base failure rates for (1) circular, coaxial and power connectors and (2) rack and panel, and printed wiring board connectors, respectively. These values were preliminary because a series of nonoperating environmental factors were later determined and the base failure rates were normalized to a ground benign value equal to one. The preliminary base failure rates are,

$\lambda_{nb,pre}$ = preliminary nonoperating base failure rate
 = .00044, circular, coaxial, and power connectors
 = .0029, rack and panel, and printed wiring board connectors

The methods presented in Section 4.5 were then applied to determine approximate nonoperating environmental factors. A comparison of failure mechanism accelerating factors was used as a rationale to assume that the operating environmental factors would also predict the effect of environmental stress on nonoperating failure rate. The proposed nonoperating environmental factors were presented in Table 5.8.1-4 in Section 5.8.1. These numerical values are average values of printed wiring board (Table 5.1.12.2-4, MIL-HDBK-217D) and other connector styles (Table 5.1.12.1-6, MIL-HDBK-217D).

The final stage of the model development process was to normalize the nonoperating base failure rates by dividing by the ground fixed nonoperating environmental factor of 2.3. The proposed nonoperating base failure rates were presented in Section 5.8.1.

It must be emphasized that the objective of this proposed study was to develop nonoperating failure rate prediction models which can be applied for any equipment type. Therefore, it was absolutely essential that the proposed methodology include a nonoperating failure rate prediction model for connectors. The proposed connector model was based on practically no quantitative information and must be considered approximate. However, the proposed model is physically correct with proposed factors for device style and environment.

5.9 Interconnection Assemblies

5.9.1 Proposed Interconnection Assembly Nonoperating Failure Rate Prediction Model

This section presents the proposed interconnection assembly nonoperating failure rate prediction model. The interconnection assembly model predicts the nonoperating failure rate of the printed wiring board and the solder connections. The model is also presented in Appendix A in a format compatible with MIL-HDBK-217D. The proposed model is:

$$\lambda_p = \lambda_{nb} \times N_{pth} \times \pi_{NE}$$

where

λ_p = interconnection assembly nonoperating failure rate (includes both the interconnection board and the solder connections)

λ_{nb} = nonoperating base failure rate (failures/ 10^6 nonoperating hours)

= .0000014, double-sided soldered printed wiring boards

= .0000028, multilayer soldered printed wiring boards

= .0000089, discrete wiring w/electroless deposited PTH

N_{pth} = number of functional plated-through holes (includes nonsoldered functional via holes)

π_{NE} = nonoperating environmental factor (see Table 5.9.1-1)

This model pertains to all interconnection assemblies using plated through holes.

TABLE 5.9.1-1: INTERCONNECTION ASSEMBLY NONOPERATING ENVIRONMENTAL FACTORS

Environment	π_{NE}	Environment	π_{NE}
G _B	1	A _{IA}	5.0
G _F	2.3	A _{IF}	9.0
G _M	6.9	A _{UC}	5.4
M _p	6.9	A _{UT}	11
N _{SB}	4.1	A _{UB}	18
N _S	5.3	A _{UA}	14
N _U	11	A _{UF}	25
N _H	13	S _F	(1)
N _{UU}	14	M _{FF}	7.8
A _{RW}	17	M _{FA}	11
A _{IC}	2.3	U _{SL}	25
A _{IT}	4.1	M _L	26
A _{IB}	7.2	C _L	500

NOTES: (1) Space Flight environment was not addressed in this study.

5.9.2 Interconnection Assembly Model Development

An interconnection assembly failure rate prediction model simultaneously predicts the failure rate of the printed wiring board (or discrete wiring board) and the solder connections. The failure rate modeling approach described in Section 4.1 was implemented for interconnection assemblies. A theoretical model was developed and then quantified with the available data. Selection of significant variables was accomplished as part of the theoretical model development because a relatively small nonoperating failure rate data base prevented the selection of variables empirically. The proposed model was determined to be a function of interconnection technology, the number of circuit planes, the number of functional plated through holes, and the application environment. The proposed model is presented in Appendix A in a format compatible with MIL-HDBK-217D.

Identification of application and construction variables which properly characterize interconnection assemblies was the first step of the model development process. Table 5.9.2-1 presents a list of the variables identified for interconnection assemblies. These variables represent possible nonoperating failure rate prediction model parameters which were further studied by both qualitative and quantitative techniques.

A theoretical model for interconnection assemblies was developed based on information located during the literature search. The theoretical model assumed a multiplicative model as a function of the number of circuit planes, the number of plated through holes, solder application technique, application environment and equipment power on-off cycling frequency. Additionally, the theoretical nonoperating failure rate prediction model was hypothesized to be directly proportional to the number of plated through holes. This hypothesis was based on two observations. First, the dominate areas of failure for interconnection assemblies are (1) the plated through hole and substrate interface, (2) the plated through hole barrel, (3) the plated through hole and solder connection interface, (4) the solder connection, and (5) the solder connection and component lead interface. In each instance, the number of potential failure areas is approximately equal to the number of plated through holes. Specific examples may exist where the number of plated through holes and the number of solder connection are not correlated. However, on the average, the number of solder connections can be accurately approximated by the number of plated through holes. The second observation was that each potential failure area is physically isolated from each other. Therefore, it follows that the assembly failure rate would be equal to the sum of the individual plated through hole, solder connection and interface failure rates. Thus, the assembly nonoperating failure rate would be proportional to the number of plated through holes.

The summarized printed wiring board and solder connection nonoperating failure rate data is presented in Table 5.9.2-2. The data collectively consists of 11 data records, 3 observed failures, 2976.6×10^6 assembly hours and $2,065,262.2 \times 10^6$ connection hours. Two data entries were

TABLE 5.9.2-1: INTERCONNECTION ASSEMBLY CHARACTERIZATION

- I. Interconnection Technology
 - A. Printed Wiring
 - B. Discrete Wiring
- II. Number of Circuit Planes
- III. Number of Functional Plated Through Holes
- IV. Board Dimensions
- V. Solder Application Technique
 - A. Wave Solder
 - B. Hand Solder
 - C. Reflow Solder
- VI. Percentage of Solder Connections Requiring Rework
- VII. Conformal Coating
- VIII. Quality Level
 - A. MIL-SPEC
 - B. Lower
- IX. Temperature
 - A. Rated
 - B. Actual
- X. Application Environment
- XI. Number of Equipment Power On/off Cycles per 10^3 Nonoperating Hours

available for double sided printed wiring boards and six data entries were available for multilayer printed wiring boards. Efforts to determine specific circuit plane quantities for multilayer boards proved to be futile. Additionally, it was assumed that the average number of plated through holes per board was equal to 600 to determine the number of connection hours. The 600 value was based on a sample from the Maverick missile.

TABLE 5.9.2-2: INTERCONNECTION ASSEMBLY NONOPERATING FAILURE RATE DATA

Equipment/Source	Data Records	Description(1)	Failures	Assembly Hours (X10 ⁶)	Connection Hours (X10 ⁶)
Hawk/MICOM(2)	1	Multilayer PWB	0	2,569.2	1541520.0
Maverick/MICOM(2)	1	Multilayer PWB	0	308.9	185310.0
Sprint/MICOM(2)	1	Multilayer PWB	1	67.8	40655.4
TOW/MICOM(2)	1	Multilayer PWB	1	26.3	15768.0
Lance/MICOM(2)	1	Multilayer PWB	0	4.5	2683.8
AFCIQ	1	Multilayer PWB	1	(3)	405000.0
AFCIQ	2	Double Sided PWB	0	(3)	5940.0
Totals	8		3	>2,976.7	2196877.2

NOTES: (1) PWB = printed wiring board

(2) 600 plated through holes per PWB assumed for these data records.

(3) Unknown.

The number of observed variables which could be evaluated empirically was limited because of the nature of the available data. Environment, temperature and equipment power on-off cycling could not be properly evaluated because there were an insufficient range of these parameters represented in the data. The number of circuit planes, solder application technique and solder rework percentage could not be determined for the majority of data sources, and therefore these variables also could not be evaluated. As a result of the data restrictions, it was decided that a

relatively simple model was warranted for interconnection assembly nonoperating failure rate.

Selection of significant variables was then done based primarily on intuitive nonoperating reliability relationships. The assumed form of the interconnection nonoperating failure rate prediction model was determined to be the following equation.

$$\lambda_{ia} = \lambda_{nb} \times N_{pth} \times \pi_{NE}$$

where

- λ_{ia} = interconnection assembly nonoperating failure rate
- λ_{nb} = nonoperating base failure rate (failures/ 10^6 nonoperating hrs.)
= f(interconnection technology)
- N_{pth} = number of plated through holes
- π_{NE} = nonoperating environmental factor

The next phase of the model development process was to determine appropriate nonoperating environmental factors by applying the methods described in Section 4.5. This method assumes that a series of nonoperating environmental factors can be generated from the MIL-HDBK-217D environmental factors by (1) comparing anticipated differences in application temperature, and (2) comparing operating and nonoperating failure mechanism accelerating factors. Operating temperatures are necessarily higher because of the heat generation associated with power being applied. It was required that the interconnection assembly MIL-HDBK-217D environmental factors be adjusted to compensate for the higher temperature differences in the more stressful environments. The environmental factor temperature conversion was computed by the following equation.

$$\pi_{NE} = A_T \pi_{OE}$$

where

π_{NE} = nonoperating environmental factor

A_T = temperature adjustment factor

π_{OE} = operating environmental factor

The A_T factor values ranged from a value of 1.0 for all ground based environments to a value of 0.72 for all airborne, uninhabited environments. The temperature adjustment factors were determined based on the average, documented temperature dependence for other part types. It was determined that the resultant π_{NE} factors sufficiently characterized the effects of nonoperating environmental stress on interconnection assembly nonoperating failure rate. These factors were presented in Table 5.9.1-1 in the previous section.

Determination of a nonoperating base failure rate for multilayer printed wiring assemblies was the next step in the model development process. A preliminary base failure rate was computed by taking the geometric average of the connection nonoperating failure rate (i.e. failures divided by connection hours) for those data entries with observed failures or sufficient connection hours to estimate failure rate without observed failures. The preliminary base failure for multilayer printed wiring assemblies was determined to be 0.00000642 failures per 10^6 hours. This numerical value is equivalent to the failure rate of one plated through hole/solder joint connection in a ground fixed environment. The final base failure rate was computed by dividing the preliminary base failure rate by the ground fixed nonoperating environmental factor of 2.3. This was required because the nonoperating environmental factors were normalized to a ground benign value equal to one. Thus, the multilayer printed wiring assembly base failure rate was equal to 0.00000279.

There were insufficient connection hours to estimate a base failure rate constant for doubled sided printed wiring assemblies. Therefore, an extrapolated value was determined from the corresponding MIL-HDBK-217D, Notice 1 operating interconnection assembly model (Reference 47).

Additionally, a base failure rate value was extrapolated for discrete wiring with electroless deposited plated through holes. The final nonoperating base failure rates were therefore given by,

λ_{nb} = nonoperating base failure rate
= .00000140, double sided printed wiring assemblies
= .00000279, multilayer printed wiring assemblies
= .00000885, discrete wiring w/electroless deposited PTH

Extrapolation of the base failure rates concluded the model development process. The proposed model is largely intuitive due to deficiencies with the collected data. It is recommended that the proposed model be evaluated when additional interconnection assembly nonoperating failure rate data becomes available.

5.10 Connections

5.10.1 Proposed Connections Nonoperating Failure Rate Prediction Model

The proposed model for connections is given by the following equation.

$$\lambda_p = \pi_{NE} \sum_{i=1}^n (N_i \lambda_{nbi})$$

where

- λ_p = connections nonoperating failure rate
- π_{NE} = nonoperating environmental factor (see Table 5.10.1-1)
- N_i = number of connections of the i^{th} type
- λ_{nbi} = nonoperating base failure rate of the i^{th} type connection
(failures/ 10^6 nonoperating hours)
 - = .000089, hand solder
 - = .000013, crimp
 - = .0000017, weld
 - = .00000012, solderless wrap
 - = .0000048, wrapped and soldered
 - = .0000041, clip termination
 - = .0000024, reflow solder

This nonoperating failure rate prediction model applies to connections used on all interconnection assemblies except those with plated through holes. The nonoperating failure rate of the structure which supports the connections and components should be considered to have a negligible nonoperating failure rate.

TABLE 5.10.1-1: CONNECTIONS NONOPERATING ENVIRONMENTAL FACTORS

Environment	π_{NE}	Environment	π_{NE}
GB	1	AIA	4.5
GF	2.1	AIF	6.8
GM	6.6	AUC	2.7
MP	7.3	AUT	5.4
NSB	3.5	AUB	6.8
NS	4.4	AUA	6.3
NU	8.9	AUF	8.6
NH	11	SF	(1)
NUU	12	MFF	6.6
ARW	14	MFA	9.0
AIC	2.3	USL	22
AIT	4.1	ML	23
AIB	5.0	CL	420

5.10.2 Model Development

The nonoperating failure rate model development for connections could not be performed by the desired analytical approach because of a complete lack of quantitative information. However, the objective of this study effort was to determine a nonoperating failure rate prediction methodology which could be applied for any equipment in any conceivable mission profile (with the exception of satellite applications). Therefore, an alternative nonoperating failure rate model development approach was determined. The alternate approach was based solely on assumptions and therefore must be considered approximate.

The alternate nonoperating failure rate development approach for connections was conducted in three phases. The first phase was to determine appropriate nonoperating environmental factors using the methods described in Section 4.5. The second phase of the alternate model development approach was to determine an applicable operating to

nonoperating failure rate ratio. Computation of approximate connection nonoperating base failure rates using this ratio was the final phase of the alternate model development process. It would have been preferable to analyze observed nonoperating failure rate data. However, the alternate approach represents the best possible method to determine connections nonoperating failure rate prediction models given the data constraints.

Connections nonoperating environmental factors were determined using the methods presented in Section 4.5. This method assumes that appropriate nonoperating environmental factors can be generated from the corresponding MIL-HDBK-217D environmental factors. Specifically, the environmental factor conversion process required two quantitative comparisons. First, the difference between typical operating and nonoperating temperatures were investigated. The operating temperature is generally higher because of the internal heat generation. For connections, a temperature adjustment was required because there was no separate temperature dependent factor to account for the temperature difference. The second part of the nonoperating environmental factor determination process was to compare operating and nonoperating failure mechanism accelerating factors. The MIL-HDBK-217D factors were not applicable for part types with operating failure mechanisms which are primarily accelerated by "operational stress" (e.g. current, voltage, actuations). However, this was not the case for connections. Most connection failure mechanisms are accelerated by environmental stress in both operating and nonoperating states. Therefore, the temperature adjusted environmental factors approximate the effect of environmental stress on connections nonoperating failure rate. The connections nonoperating environmental factors were presented in Table 5.10.1-1 in the previous section.

The second phase of the alternate model development approach was to assume an appropriate operating to nonoperating failure rate ratio. It was determined that the most comparable part category was interconnection assemblies. The interconnection assembly failure rate predicts the failure rate of both the printed wiring board and the solder connections.

The average operating to nonoperating ratio for interconnection assemblies was equal to 29:1.

The final phase of the connections model development approach was to compute approximate base failure rate values. The proposed values were computed by dividing the operating base failure rates (Table 5.1.14-1, MIL-HDBK-217D, Notice 1) by the assumed ratio. In this manner, nonoperating base failure rates were determined for hand solder, crimp, weld, solderless wrap, wrapped and soldered, clip termination and reflow solder. One average base failure rate value was proposed for crimp connections. Without additional justification, the crimp connection factors for tool type and quality could not be assumed to apply for nonoperating failure rate prediction purposes.

The proposed model for connections was based entirely on assumptions. In a project the magnitude of this study, it was inevitable that sufficient data would not be collected for all parts. However, the proposed model represents the best possible nonoperating failure rate values and are based on sound assumptions. When additional information becomes available, the proposed model should be evaluated, and updated if required.

5.11 Miscellaneous Parts

5.11.1 Proposed Miscellaneous Parts Nonoperating Failure Rates

Table 5.11.1-1 presents average nonoperating failure rates for miscellaneous parts. the part types considered in this section include all parts in Table 5.1.15-1, MIL-HDBK-217D.

TABLE 5.11.1-1: NONOPERATING FAILURE RATES FOR MISCELLANEOUS PARTS

Part Type	Nonoperating Failure Rate (failures/10 ⁶ hours)
Vibrators	3.3
Quartz Crystals	.039
Fuses	.0014
Lamps	
Neon	.029
Incandescent	.11
Fiber Optic Cables (single fiber types only)	.014 (per fiber km)
Single Fiber Optic Connectors	.014
Meters	1.4
Circuit Breakers	.29
Microwave Elements (coaxial and waveguide)	
Attenuators	(1)
Fixed Elements (directional couplers, fixed stubs and cavities)	Negligible
Variable Elements (tuned stubs and tuned cavities)	.014
Microwave Ferrite Devices	.043
Dummy Loads	.011
Terminations (thin or thick film loads used in stripline and thin film circuits)	.010

NOTES: (1) The nonoperating failure rate of attenuators should be calculated the same as for Style RD resistors.

5.11.2 Model Development

The miscellaneous part types considered in this study are the same miscellaneous parts which are included in MIL-HDBK-217D. Nonoperating failure rate data were available for quartz crystals, fuses, neon lamps and incandescent lamps. The operating to nonoperating failure rate ratio for crystals and incandescent lamps were then applied for the other miscellaneous parts. There were insufficient data to estimate nonoperating failure rate for fuses and neon lamps.

There was no physical reason for proportional failure rate assumption to be true. However, both incandescent lamps and crystals are part styles which degrade in storage. Therefore, the assumption represents a worst case scenario. Additionally, the geometric mean of the numerical values for vibrators, microwave ferrite devices and dummy loads was used. The average ratio for operating to nonoperating failure rate was determined to be 7:1. The average fuse nonoperating failure rate was divided by an additional factor of ten because of the nature of fuse operating and nonoperating failure mechanisms.

The available nonoperating failure rate data for miscellaneous parts is presented in Table 5.11.2-1. All available data were from MICOM or Martin Marietta. The merged nonoperating failure rate for crystals was computed to be .039 failures per 10^6 nonoperating hours, and the merged nonoperating failure rate was equal to 0.11 for incandescent lamps.

TABLE 5.11.2-1: MISCELLANEOUS PART NONOPERATING FAILURE RATE DATA

Equipment/Source	Part Type	Failures	Part Hours (X 10^6)
Hawk/MICOM	Crystals	4	51.0
Maverick/MICOM	Crystals	0	21.0
Sprint/MICOM	Crystals	0	9.7
Martin Marietta	Crystals	0	20.1
Martin Marietta	Fuses	0	2.1
Martin Marietta	Inc. Lamps	1	9.5
Sparrow/MICOM	Neon Lamps	0	12.8
TOW/MICOM	Fuses	0	2.6
Totals		5	128.8

The miscellaneous part nonoperating failure rates are approximate for all devices except crystals or incandescent lamps. However, the part types are all low population parts and therefore inaccurate nonoperating failure rates would have little effect on the equipment level nonoperating failure rate prediction.

6.0 APPLICATION OF NONOPERATING RELIABILITY MODELS

6.1 Comprehensive Reliability Models

With the inclusion of nonoperating failure rate models as a part of this document, comprehensive reliability models are made feasible. A comprehensive reliability model is one which considers all possible states and the time in each state which an equipment must survive. While it is true that most contractual reliability requirements are given in operational equipment terms (i.e. MTBF or probability of survival for a given mission time), the performance of an electronic equipment depends on the effects of other events such as transportation, testing, equipment power on-off cycling and nonoperation.

A simple comprehensive model which considers only one operational and one nonoperational state takes the following form.

$$R = \exp\left(-\left(\lambda_o\left(\frac{t_o}{t_o + t_N}\right) + \lambda_N\left(\frac{t_N}{t_o + t_N}\right)\right) T\right)$$

where

R = reliability for a service life time of T

λ_o = equipment operating failure rate

λ_N = equipment nonoperating failure rate

t_o = one mission operating time

t_N = nonoperating time between missions

T = $t_o + t_N$

The $(t_o/(t_o + t_N))$ term is simply the operating duty cycle, and the $(t_N/(t_o + t_N))$ term is the nonoperating duty cycle. In cases where there is no definitive service life time interval (T), estimates can often be made of the respective duty cycles. Reliability would then be a function of one unknown instead of two.

This form also reduces to the following simpler equation.

$$R = \exp(-(\lambda_0 t_0 + \lambda_N t_N))$$

However, the fractional time terms represent duty cycle, and is best viewed as initially presented in many instances.

This is a simple model which could be applied to a ground fixed electronic system since the two equipment states are exposed to the same environment.

The model for an avionics system becomes more complex. A possible scenario of events would consist of preflight power up testing, the airborne mission comprised of operating and nonoperating periods, postflight power up testing, and a nonoperating period. The model for this scenario takes the following form.

$$R = \exp(-(\lambda_{OG} (\frac{t_{OG}}{T}) + \lambda_{OA} (\frac{t_{OA}}{T}) + \lambda_{NA} (\frac{t_{NA}}{T}) + \lambda_{NG} (\frac{t_{NG}}{T})) T)$$

where

- λ_{OG} = ground operating equipment failure rate
- λ_{OA} = airborne operating equipment failure rate
- λ_{NA} = airborne nonoperating equipment failure rate
- λ_{NG} = ground nonoperating equipment failure rate
- t_{OG} = ground power on test time
- t_{OA} = airborne power on time
- t_{NA} = airborne nonoperating time
- t_{NG} = ground nonoperating time
- T = total time covered by the scenario

This model quantifies reliability in terms of the major events that effect, in varying degree, the reliability of a system. It can be seen that such a model can be developed for virtually any system exposed to a

single or combination of environments. The model has the virtue of focusing attention on the impact on reliability of both the operating and nonoperating states, as well as the environments in which these states occur.

6.2 Proposed Comprehensive Reliability Prediction Method

An eight part procedure was defined to use the proposed nonoperating failure rate prediction models together with existing MIL-HDBK-217D operating reliability assessment techniques. Table 6.2-1 presents the eight specific tasks.

TABLE 6.2-1: COMPREHENSIVE RELIABILITY PREDICTION TASKS

Task No.	Description
1	Define Mission Profile
2	Define Use Scenario
3	Determine Component Operating Failure Rates
4	Determine Equipment Operating Failure Rate
5	Determine Component Nonoperating Failure Rates
6	Determine Equipment Nonoperating Failure Rate
7	Compute Average Service Life Failure Rate
8	Compute Reliability

Definition of a mission profile (task 1) must be the initial phase of any reliability assessment process. Specific time intervals and stresses in every applicable operating environment must be defined as part of the mission profile definition. For this study, a use scenario was considered to be equal to the mission profile plus the nonoperating time between missions. In addition to the information provided from the mission profile, specific time intervals and stresses encountered during the nonoperating phase of the use scenario must be defined as part of task 2.

Tasks 3 and 4 are well established and will not be further discussed. Tasks 5 and 6 represent the corresponding reliability assessment tasks for nonoperating periods. An equipment nonoperating failure rate is determined based on the use scenario. The product of Tasks 3 through 6 is

the determination of two unique parameters characterizing equipment reliability; the inherent equipment operating failure rate and the inherent nonoperating failure rate. At this point in the comprehensive reliability prediction process, the two parameters are seemingly independent and do not complement one another.

The next task is to compute an average service life failure rate. A service life failure rate was defined as the number of failures per unit time regardless of operational mode. The service life failure rate is therefore dependent on operating failure rate, nonoperating failure rate, operating duty cycle and nonoperating duty cycle, and is given by the following equation for one operational state and one nonoperational state.

$$\lambda_{SL} = \lambda_o \left(\frac{t_o}{t_o + t_N} \right) + \lambda_N \left(\frac{t_N}{t_o + t_N} \right)$$

where

λ_{SL} = service life failure rate

$\frac{t_o}{t_o + t_N}$ = operating duty cycle

$\frac{t_N}{t_o + t_N}$ = nonoperating duty cycle

The equation becomes more complex when there are more than two states. However, the equation would take the same general form with more operational or nonoperational states. The service life failure rate can be the most informative comprehensive reliability parameter for some equipment types. The service life failure rate is constant with time, and is therefore useful for comparing or evaluating the total reliability for equipments with an indeterminate mission duration. The service life parameter is generally a good indication of the reliability for equipments which are exposed to intermediate amounts of both operating and nonoperating periods. For equipments with a use scenario dominated by

dormancy, the service life failure rate approximates the dormant equipment failure rate. Note in the equation that as t_0 approaches zero, λ_{SL} approaches λ_N . Regardless of the relative merit of this parameter, the service life failure rate should be computed for every electronic equipment exposed to nonoperating periods. The service life failure rate can be computed with specific values for t_0 and t_N , or with appropriate duty cycle values.

Computation of the equipment reliability is the final phase of the comprehensive reliability prediction method. Given the specific time intervals defined as part of the use scenario, the equipment reliability is given as

$$R = \exp(-(\sum \lambda_{oi} t_{oi} + \sum \lambda_{Ni} t_{Ni}))$$

where

R = reliability

λ_{oi} = operating failure rate in the i^{th} operating state

t_{oi} = time in the i^{th} operating state

λ_{Ni} = nonoperating failure rate in the i^{th} nonoperating state

t_{Ni} = time in the i^{th} nonoperating state

Reliability is the more important parameter for equipments exposed to prolonged periods of nonoperation. Failures can not be detected when the equipment is not operating, and therefore the probability of surviving a specified nonoperating time interval without failure is essential information. However, regardless of the relative merit of this reliability parameter, the reliability should be computed for every electronic equipment for the time interval equal to the mission duration plus the time between missions.

These sections described two key comprehensive reliability parameters which should be evaluated as part every reliability program for equipments exposed to nonoperating periods. The equations to compute service life failure rate and comprehensive reliability were also described.

7.0 COMPARISON OF OPERATING AND NONOPERATING FAILURE RATES

Operating and nonoperating failure rates were compared using MIL-HDBK-217D and the proposed nonoperating failure rate prediction models. Table 7.0-1 presents the calculated failure rates for a wide range of microcircuits. Table 7.0-2 presents the ratio of operating to nonoperating failure rate for three possible mission profiles; (1) ground fixed operating to nonoperating, (2) airborne uninhabited fighter operating to nonoperating, and (3) airborne uninhabited fighter operating to ground fixed nonoperating, and three different ambient temperatures. Table 7.0-3 presents operating to nonoperating failure rate ratios for discrete semiconductors.

It was noted that in Table 7.0-2 the ratio for microcircuits was greater for lower quality parts. This was the anticipated result. As the device screening increases, the operating and nonoperating failure rate difference decreases. This trend is because inherently weak devices fail more quickly in the operating state, and was discussed in Section 4.6. Additionally, it was noted that the ratios for nonhermetic unscreened microcircuits was lower than the ratios for hermetic unscreened microcircuits. This would mean that package type is a relatively more significant variable in the nonoperating state than in the operating state.

Ratios for airborne avionic equipments are necessarily different from ground based equipments. Airborne equipments typically operate in ground fixed, ground mobile and airborne environments. In the nonoperating state, the same equipment is primarily exposed to a ground fixed environment. The predicted operating failure rate is higher (than the ground fixed case) because of the numerically higher environmental factors and increased temperatures. The predicted nonoperating failure rate would also increase due to a higher level of equipment power on-off cycling. The operating to nonoperating ratio is approximately 2-5 times higher for airborne equipments.

TABLE 7.0-1: SAMPLE CALCULATIONS COMPARING NONOPERATING
AND MIL-HDBK-217D MODELS

PART #	VENDOR	DESCRIPTION	COMPLEXITY	TECHNOLOGY	QUALITY	TYPE	6F-20C	6F-40C	6F-60C	AUF-20C	AUF-40C	AUF-60C
100102DC	FSC	GATE	6G	ECL	D	O	.5007	.5079	.5237	1.791	1.798	1.814
100102DC	FSC	GATE	6G	ECL	D	N	.0040	.0045	.0057	.0112	.0126	.0160
10470	FSC	4K RAM	4096B	ECL	D	O	1.618	3.230	6.460	2.796	4.409	7.638
10470	FSC	4K RAM	4096B	ECL	D	N	.0200	.0227	.0287	.0559	.0633	.0803
1103	SIGNETICS	1K RAM	1024B	PMOS	C	O	.4364	.8582	1.790	.8943	1.316	2.247
1103	SIGNETICS	1K RAM	1024B	PMOS	C	N	.0087	.0120	.0182	.0243	.0337	.0507
14015B	MOT	SHIFT REGISTER	666	CMOS	D-1	O	.6085	.7910	2.075	2.135	2.318	3.602
14015B	MOT	SHIFT REGISTER	666	CMOS	D-1	N	.0638	.1399	.5442	.2072	.4546	1.360
1821	RCA	1K RAM	1024B	CMOS	S	O	.0132	.0271	.0760	.0370	.0509	.0998
1821	RCA	1K RAM	1024B	CMOS	S	N	.0019	.0041	.0122	.0052	.0114	.0340
2114A	INTEL	4K RAM	4096B	NMOS	B-1	O	.1638	.3530	.8675	.3777	.5668	1.081
2114A	INTEL	4K RAM	4096B	NMOS	B-1	N	.0051	.0091	.0213	.0142	.0254	.0595
2513	SIGNETICS	ROM	2560B	PMOS	D	O	.5369	.8172	1.526	1.582	1.862	2.571
2513	SIGNETICS	ROM	2560B	PMOS	D	N	.0093	.0152	.0315	.0258	.0425	.0880
2580	SIGNETICS	8K ROM	8192B	PMOS	D-1	O	2.576	7.588	25.16	5.392	10.40	27.98
2580	SIGNETICS	8K ROM	8192B	PMOS	D-1	N	.0537	.0883	.1829	.1745	.2868	.5943
25L04	AMD	SHIFT REGISTER	2636	LTTL	D	O	.6052	.8426	1.359	1.793	2.031	2.547
25L04	AMD	SHIFT REGISTER	2636	LTTL	D	N	.0245	.0283	.0384	.0671	.0789	.1073
25LS299	AMD	SHIFT REGISTER	1046	LSTTL	S	O	.0131	.0160	.0235	.0439	.0468	.0542
25LS299	AMD	SHIFT REGISTER	1046	LSTTL	S	N	.0033	.0039	.0059	.0092	.0111	.0164
2901A	AMD	MICROPROCESSOR	5426	LSTTL	B-1	O	.1515	.2029	.3328	.4810	.5324	.6623
2901A	AMD	MICROPROCESSOR	5426	LSTTL	B-1	N	.0191	.0230	.0341	.0532	.0641	.0953
3601	INTEL	1K PROM	1024B	LTTL	D-1	O	.6812	.8884	1.420	2.199	2.406	2.938
3601	INTEL	1K PROM	1024B	LTTL	D-1	N	.1147	.1077	.2148	.3729	.3499	.6982

TABLE 7.0-1: SAMPLE CALCULATIONS COMPARING NONOPERATING
AND MIL-HDBK-217D MODELS (CONT'D)

PART #	VENDOR	DESCRIPTION	COMPLEXITY	TECHNOLOGY	QUALITY	TYPE	GF-20C	GF-40C	GF-60C	AUF-20C	AUF-40C	AUF-60C
4004	INTEL	4 BIT MICROPROCESSOR	7596	PMOS	D-1	O	.8208	1.597	4.674	2.455	3.231	6.308
4004	INTEL	4 BIT MICROPROCESSOR	7596	PMOS	D-1	N	.2163	.3555	.7368	.7030	1.155	2.395
4009N	NSC	BUFFER	66	CMOS	D-1	O	.5311	.5741	.8784	1.899	1.942	2.246
4009N	NSC	BUFFER	66	CMOS	D-1	N	.0203	.0557	.1135	.0659	.1810	.3687
4020A	RCA	BINARY COUNTER	1326	CMOS	D	O	.2556	.3290	.6162	.8723	.9458	1.233
4020A	RCA	BINARY COUNTER	1326	CMOS	D	N	.0153	.0336	.1005	.0427	.0938	.2804
4515B	RCA	LATCH DECODER	1026	CMOS	C	O	.2183	.2530	.3866	.7627	.7974	.9310
4515B	RCA	LATCH DECODER	1026	CMOS	C	N	.0125	.0273	.0818	.0348	.0763	.2282
54C221	NSC	FLIP-FLOP	206	CMOS	B-1	O	.0497	.0551	.0766	.1755	.1809	.2025
54C221	NSC	FLIP-FLOP	206	CMOS	B-1	N	.0035	.0077	.0229	.0098	.0214	.0640
54LS197	TI	BINARY COUNTER	346	LSTTL	D	O	.2576	.2853	.3626	.8981	.9258	1.003
54LS197	TI	BINARY COUNTER	346	LSTTL	D	N	.0084	.0109	.0163	.0253	.0305	.0454
6116	ZILOG	16K RAM	16384B	CMOS	D	O	1.398	3.337	10.42	3.637	5.576	12.66
6116	ZILOG	16K RAM	16384B	CMOS	D	N	.0088	.0192	.0574	.0244	.0536	.1603
732	FSC	DEMULATOR	39T	BIPOLAR	D-1	O	7.238	17.14	65.88	21.36	31.26	80.01
732	FSC	DEMULATOR	39T	BIPOLAR	D-1	N	.1664	.2987	.5993	.5407	.9708	1.948
74H72	TI	JK FLIP-FLOP	86	HTTL	D-1	O	.4608	.4801	.5279	1.634	1.653	1.701
74H72	TI	JK FLIP-FLOP	86	HTTL	D-1	N	.0265	.0301	.0382	.0863	.0978	.1240
74S206	NSC	256 BIT RAM	256B	STTL	C-1	O	.3922	.6840	1.339	.9656	1.257	1.913
74S206	NSC	256 BIT RAM	256B	STTL	C-1	N	.0190	.0223	.0303	.0530	.0623	.0847
9080A	AMD	MICROPROCESSOR	1100G	NMOS	B-2	O	.5324	.7978	1.473	1.582	1.848	2.523
9080A	AMD	MICROPROCESSOR	1100G	NMOS	B-2	N	.0349	.0625	.1466	.0975	.1744	.4094
921B	AMD	16K ROM	16384B	NMOS	B-1	O	.1911	.3853	.9075	.4660	.6602	1.182
921B	AMD	16K ROM	16384B	NMOS	B-1	N	.0051	.0091	.0021	.0142	.0254	.0595

TABLE 7.0-1: SAMPLE CALCULATIONS COMPARING NONOPERATING
AND MIL-HDBK-217D MODELS (CONT'D)

PART #	VENDOR	DESCRIPTION	COMPLEXITY	TECHNOLOGY	QUALITY	TYPE	GF-20C	GF-40C	GF-60C	AUF-20C	AUF-40C	AUF-60C
93425	FSC	1K RAM	1024B	TTL	C-1	O	.5063	.8882	1.686	1.164	1.546	2.344
93425	FSC	1K RAM	1024B	TTL	C-1	N	.0192	.0218	.0276	.0536	.0608	.0770
93481	FSC	MEMORY	4096B	IIL	D-1	O	3.715	18.42	88.93	6.005	20.71	91.22
93481	FSC	MEMORY	4096B	IIL	D-1	N	.1127	.1502	.2733	.3662	.4880	.8915
93L415	FSC	1K RAM	1024B	LTTL	B	O	.0602	.1295	.2790	.1026	.1719	.3214
93L415	FSC	1K RAM	1024B	LTTL	B	N	.0079	.0093	.0126	.0221	.0260	.0353
9401	FSC	GENERATOR	114G	IIL	D-1	O	.6630	1.619	6.175	1.903	2.859	7.415
9401	FSC	GENERATOR	114G	IIL	D-1	N	.0920	.1226	.2240	.2990	.3985	.7280
9900A	TI	MICROPROCESSOR	3100G	IIL	D-1	O	2290	6300	15871	2297	6307	15878
9900A	TI	MICROPROCESSOR	3100G	IIL	D-1	N	.4449	.5929	1.083	1.446	1.927	3.520
C2416	INTEL	16K CCD SERIAL MEM.	16384B	CCD	D	O	2.296	5.795	14.98	4.098	7.596	16.78
C2416	INTEL	16K CCD SERIAL MEM.	16384B	CCD	D	N	.0091	.0162	.0381	.0253	.0453	.1063
CD4025AK	RCA	GATE	3G	CMOS	B-1	O	.0309	.0336	.0443	.1096	.1122	.1229
CD4025AK	RCA	GATE	3G	CMOS	B-1	N	.0014	.0031	.0092	.0039	.0086	.0258
DM74L85N	NSC	COMPARATOR	33G	LTTL	D-1	O	.6179	.6673	.8069	2.174	2.223	2.362
DM74L85N	NSC	COMPARATOR	33G	LTTL	D-1	N	.0517	.0608	.0827	.1681	.1976	.2685
LM111	NSC	VOLTAGE COMPARATOR	23T	BIPOLAR	S	O	.0100	.0170	.0426	.0304	.0375	.0630
LM111	NSC	VOLTAGE COMPARATOR	23T	BIPOLAR	S	N	.0038	.0068	.0137	.0106	.0191	.0383
LM741	NSC	DUAL OP AMP	23T	BIPOLAR	D	O	.2815	.3869	.7845	.9469	1.052	1.450
LM741	NSC	DUAL OP AMP	23T	BIPOLAR	D	N	.0180	.0322	.0647	.0501	.0900	.1806
MC1355P-2	MOT	FREQUENCY AMP	22T	BIPOLAR	D-1	O	1.763	6.939	33.28	3.879	9.055	35.39
MC1355P-2	MOT	FREQUENCY AMP	22T	BIPOLAR	D-1	N	.1001	.1798	.3607	.3254	.5842	1.172
MC1408L-8	MOT	D/A CONVERTER	60T	BIPOLAR	D	O	.6463	.9056	1.963	2.136	2.396	3.453
MC1408L-8	MOT	D/A CONVERTER	60T	BIPOLAR	D	N	.0420	.0755	.1514	.1173	.2107	.4227

TABLE 7.0-1: SAMPLE CALCULATIONS COMPARING NONOPERATING
AND MIL-HDBK-217D MODELS (CONT'D)

PART #	VENDOR	DESCRIPTION	COMPLEXITY	TECHNOLOGY	QUALITY	TYPE	GF-20C	GF-40C	GF-60C	AUF-20C	AUF-40C	AUF-60C
MD3636	INTEL	16K PROM	16384B	TTL	D	0	1.014	1.639	2.983	2.457	3.082	4.326
MD3636	INTEL	16K PROM	16384B	TTL	D	N	.0200	.0227	.0287	.0559	.0633	.0803
MM5205D	MMI	2K ROM	2048B	LTTL	D	0	.3318	.4260	.6444	1.059	1.153	1.372
MM5205D	MMI	2K ROM	2048B	LTTL	D	N	.0198	.0233	.0464	.0552	.0649	.0882
MM6276N	MMI	16K ROM	16384B	LTTL	D-1	0	1.568	2.586	5.019	4.237	5.255	7.688
MM6276N	MMI	16K ROM	16384B	LTTL	D-1	N	.1147	.1349	.1833	.3729	.4383	.5958
TLC271CP	TI	OP AMP	4T	LIN CMOS	D-1	0	1.162	7.209	31.79	2.594	9.187	32.77
TLC271CP	TI	OP AMP	4T	LIN CMOS	D-1	N	.0221	.0396	.0795	.0717	.1288	.2584

TABLE 7.0-2: RATIOS OF MIL-HDBK-217D
TO NONOPERATING FAILURE RATES

PART #	VENDOR	DESCRIPTION	COMPLEXITY	TECHNOLOGY	QUALITY	PKG	PIN	GFO/GFN	AUFO/AUFN	AUFO/GFN
100102DC	FSC	GATE	66	ECL	D	HDIP	24	125.17	142.73	449.58
10470	FSC	4K RAM	4096B	ECL	D	HDIP	18	80.88	69.64	220.43
1103	SIGNETICS	1K RAM	1024B	PMOS	C	HDIP	18	50.16	39.05	151.27
14015B	MOT	SHIFT REGISTER	66G	CMOS	D-1	NDIP	16	9.53	5.09	36.32
1821	RCA	1K RAM	1024B	CMOS	S	HDIP	16	6.95	4.46	26.77
2114A	INTEL	4K RAM	4096B	NMOS	B-1	HDIP	18	32.12	13.33	111.15
2513	SIGNETICS	ROM	2560B	PMOS	D	HDIP	19	57.73	43.82	200.25
2580	SIGNETICS	8K ROM	8192B	PMOS	D-1	NDIP	24	47.97	36.27	193.72
25L04	AMD	SHIFT REGISTER	263G	LTTTL	D	HDIP	21	24.70	25.73	82.87
25LS299	AMD	SHIFT REGISTER	104G	LSTTL	S	HDIP	20	3.98	4.21	14.17
2901A	AMD	MICROPROCESSOR	542G	LSTTL	B-1	HDIP	40	7.94	8.30	27.93
3601	INTEL	1K PROM	1024B	LTTTL	D-1	NDIP	16	5.93	6.87	20.98
4004	INTEL	4 BIT MICROPROCESSOR	759G	PMOS	D-1	NDIP	16	3.79	2.79	14.93
4009N	NSC	BUFFER	66	CMOS	D-1	NDIP	15	2.61	10.72	95.66
4020A	RCA	BINARY COUNTER	132G	CMOS	D	HFPK	16	16.70	10.08	61.81
4515B	RCA	LATCH DECODER	102G	CMOS	C	HFPK	24	17.46	10.45	63.79
54C221	NSC	FLIP-FLOP	20G	CMOS	B-1	HDIP	16	14.19	8.45	5.16
54LS197	TI	BINARY COUNTER	34G	LSTTL	D	HDIP	14	30.66	30.34	110.22
6116	ZILOG	16K RAM	16384B	CMOS	D	HDIP	24	158.81	104.02	633.61
732	FSC	DEMODULATOR	39T	BIPOLAR	D-1	NDIP	14	43.49	32.20	187.9
74H72	TI	JK FLIP-FLOP	86	HTTL	D-1	NDIP	13	17.38	16.90	62.38
74S206	NSC	25P BIT RAM	256B	STTL	C-1	HDIP	16	20.64	20.18	66.17
9080A	AMD	MICROPROCESSOR	1100G	NMOS	B-2	HDIP	40	15.25	10.59	52.94
9218	AMD	16K ROM	16384B	NMOS	B-1	HDIP	24	37.47	25.99	129.44

TABLE 7.0-2: RATIOS OF MIL-HDBK-217D
TO NONOPERATING FAILURE RATES (CONT'D)

PART #	VENDOR	DESCRIPTION	COMPLEXITY	TECHNOLOGY	QUALITY	PKG	PIN	GFO/GFN	AUFO/AUFN	AUFO/GFN
93425	FSC	1K RAM	1024B	TTL	C-1	HDIP	16	26.37	25.42	80.51
93481	FSC	MEMORY	4096B	IIL	D-1	NDIP	16	32.95	42.42	183.71
93L415	FSC	1K RAM	1024B	LTTL	B	HFPK	16	7.62	6.61	21.75
9401	FSC	GENERATOR	114G	IIL	D-1	NDIP	12	7.20	7.22	31.07
9900A	TI	MICROPROCESSOR	3100G	IIL	D-1	NDIP	59	5148.1	3273.5	14178.0
C2416	INTEL	16K CCD SERIAL MEM.	16384B	CCD	D	HDIP	18	252.34	167.68	834.72
C04025AK	RCA	GATE	3G	CMOS	B-1	HFPK	14	22.07	13.07	80.17
DM74L85N	NSC	COMPARATOR	33G	LTTL	D-1	NDIP	16	11.95	11.24	42.99
LM111	NSC	VOLTAGE COMPARATOR	23T	BIPOLAR	S	HCAN	8	2.63	1.96	9.86
LM741	NSC	DUAL OP AMP	23T	BIPOLAR	D	HCAN	7	15.69	11.69	58.44
MC1355P-2	MOT	FREQUENCY AMP	22T	BIPOLAR	D-1	NDIP	14	17.61	15.50	90.46
MC1408L-8	MOT	D/A CONVERTER	60T	BIPOLAR	D	HDIP	16	15.39	11.37	57.05
MD3636	INTEL	16K PROM	16384B	TTL	D	HDIP	24	50.70	48.69	154.12
MM5205D	MMI	2K ROM	2048B	LTTL	D	HDIP	16	16.07	17.77	58.02
MM6276N	MMI	16K ROM	16384B	LTTL	D-1	NDIP	24	13.67	11.98	45.81
TLC271CP	TI	OP AMP	4T	LIN CMOS	D-1	NDIP	8	73.12	63.56	370.5

NOTE: The given data values are based on the information provided in the MIL-HDBK-217D document. The values are not intended to be used for design purposes. The values are provided for informational purposes only.

TABLE 7.0-3: DISCRETE SEMICONDUCTOR OPERATING TO NONOPERATING
FAILURE RATE RATIOS

Part Description	JANTX	Commercial
Transistor, Si, NPN, hermetic	7.5	15
Transistor, Si, NPN, nonhermetic	--	16
Transistor, Si, PNP, hermetic	11	22
Transistor, Si, PNP, nonhermetic	--	24
Transistor, Ge, PNP, hermetic	47	98
Transistor, Ge, PNP, nonhermetic	--	110
Transistor, FET, hermetic	21	39
Transistor, FET, nonhermetic	--	45
Transistor, Unijunction, hermetic	7.0	7.0
Transistor, Unijunction, nonhermetic	--	1.5
Transistor, Microwave, hermetic	1.1	0.4
Diodes, Si, GP, hermetic	1.5	2.0
Diodes, Si, GP, nonhermetic	--	3.1
Diodes, Ge, GP, hermetic	3.6	6.9
Diodes, Ge, GP, nonhermetic	--	7.7
Diodes, Zener, hermetic	1.3	2.6
Diodes, Zener, nonhermetic	--	29
Diodes, Thyristor, hermetic	4.0	7.8
Diodes, Thyristor, nonhermetic	--	8.8
Diodes, Si, mixer, hermetic	37	7.0
Opto-electronic LED	3.5	7.6
Opto-electronic, display	1.8	4.0
Geometric mean for all discrete semiconductors	5.5	9.7

8.0 CONCLUSIONS

Nonoperating failure rate prediction models were developed at the component level for the entire range of device types included in MIL-HDBK-217D. The models were primarily based on empirical data analysis and represent accurate, easy to use and essential nonoperating reliability assessment tools. Additionally, a comprehensive reliability prediction method was presented to allow for use of the proposed nonoperating failure rate prediction models together with the documented MIL-HDBK-217D methods. The proposed methods will greatly improve upon current failure rate prediction capabilities.

Previously, no single source of nonoperating failure rates were available. A large number of intuitive and, for the most part, invalid methods were generally used to estimate nonoperating reliability. The inclusion of the proposed methods as part of a reliability program fills a large void and will allow for more consistent evaluations of nonoperating reliability predictions, reliability trade-offs and life cycle cost analyses.

Sufficient nonoperating failure rate data were available for most major part classes. However, for the following part classes, the proposed models were largely intuitive and complemented with whatever data were available.

- o Magnetic Bubble Memories
- o Opto-electronic Semiconductors
- o Relays
- o Switches
- o Connectors
- o Motors

None of the nonoperating failure rate prediction models developed during this study are as sophisticated as was originally intended. This

was entirely due to a lack of sufficient data, or a lack of detail in the data. Several of the reasons for these data deficiencies are:

- o The inherent nonoperating failure rate for some parts is extremely low. Thus, observed failure data is very limited.
- o Many part types in MIL-HDBK-217 are low population part types.
- o Data contributors are generally reluctant to incur any expenditure to further refine data and information they provide without charge.
- o It is often difficult to segregate nonoperating failures from operating failures or total maintenance actions.
- o The wide scope of the study (i.e. all MIL-HDBK-217 parts) made it impossible to concentrate efforts on one part type.
- o Potential data contributors are hesitant to allow visitors access to their proprietary data bases.

Consequently, many of the factors initially considered could not be properly evaluated as part of the data analysis phase. Nevertheless, sufficient data were collected and models developed for all major part classes.

Additionally, it was concluded that the present MIL-HDBK-217D failure rate prediction models may be influenced by nonoperating failures. The extent to which the MIL-HDBK-217D models are affected by nonoperating failures is dependent on,

- o whether nonoperating failures were segregated from the total number of failures during model development
- o the ratio of operating to nonoperating failure rate
- o the ratio of operating to nonoperating time

It was impossible to accurately estimate the difference between the MIL-HDBK-217D models and the inherent mean operating failure rate. However, it was concluded that the difference was small based on the model development information which was studied.

9.0 RECOMMENDATIONS

It is recommended that the proposed nonoperating failure rate prediction models developed during this study be incorporated into MIL-HDBK-217. Additionally, it is recommended that nonoperating failure rate prediction models be updated periodically to reflect changes in technology or other factors which temporarily result in an inaccurate or missing model.

Although the proposed nonoperating failure rate prediction procedures greatly improve prediction capabilities, several recommendations are necessary in light of all available information. Due to the nature of nonoperating failure rates, plentiful amounts of data were not always available for analysis and consequently, many of the proposed models were based on limited data resources. The nonoperating failure rate of many of these devices can constitute a large percentage of the total nonoperating equipment reliability. Therefore, the respective nonoperating failure rate prediction models should be further investigated to enhance their accuracy and sensitivity. Included among these part types are:

- o Hybrid Microcircuits
- o Bubble Memories
- o Relays
- o Switches
- o Rotating Mechanisms
- o Connectors
- o Opto-electronic Devices
- o Lasers
- o Tubes

It is also recommended that a study be initiated to investigate the feasibility of predicting nonoperating failure rate based on accelerated life testing to simulate more stressful environments. This would allow for expeditious analyses of emerging technologies and would possibly allow for the development of unique nonoperating environmental factors.

Additionally, it is recommended that future studies be initiated to address the issue of equipment power cycling effects for mechanical and electromechanical part types. For this family of parts, periodic equipment power cycling can be a useful tool to decrease the probability of failure during extended nonoperating periods. Unfortunately, there were insufficient data for this class of part types to properly investigate this effect. A study should therefore be established which specifically analyzes both qualitatively and quantitatively the effects of equipment power on-off cycling on mechanical and electromechanical part types, and to determine optimal testing/operational schedules.

The availability of empirical data is essential for any valid reliability assessment. When inherent difficulties prevent the availability of data, an exhaustive data collection effort must be undertaken, thereby, consuming valuable funds and manpower. Therefore, it is recommended that the government should investigate methods of identifying when reliability data are generated, of analyzing the merits of available data, of providing a method of purchasing the data (if required) and of storing the data in a central repository which is available to all government contractors.

REFERENCES

1. Kern, G. A. and T. M. Drnas, Operational Influences on Reliability, RADC-TR-76-366, Hughes Aircraft Co., December 1976.
2. Kern, G. A., I. Quart, S. Tung and K. Wong, Nonoperating Failure Rates for Avionics Study, Hughes Aircraft Co., RADC-TR-80-136, April 1980.
3. Malik, D., Storage Reliability Analysis Summary Report, LC-78-2, Raytheon, January 1978.
4. Kremp, B. F. and E. W. Kimball, Revision of Environmental Factors for MIL-HDBK-217B, RADC-TR-80-299, Martin Marietta, September 1980.
5. Bauer, J. A., D. F. Cottrell, T. R. Gagnier and E. W. Kimball, et. al., Dormancy and Power On-Off Cycling Effects on Electronic Equipment and Part Reliability, RADC-TR-73-248, Martin Marietta, August 1973.
6. Neuner, G. E. and E. H. Barnett, An Investigation of the Ratio Between Stand-by and Operating Part Failure Rates, GIDEP Report E151-1405, TRW Systems Group, November 1971.
7. Graber, R., et. al., An Approach In Assessing Missile System Dormant Reliability, BDM/A-81-016-TR, January 1981.
8. Association Francais Pour le Control Industrial et la Qualite, Donnes de Faibilite en Stockage des Composants Electroniques, Second Edition, July 1983.
9. Coit, D. W., K. A. Dey, and W. E. Turkowski, "Operation & Analysis of A Reliability Database," Proceedings of the 8th Advances in Reliability Technology, University of Bradford, April 1984.
10. Draper, N. R. and H. Smith, Applied Regression Analysis, Wiley, 1966.

REFERENCES (CONT'D)

11. Bean, E. E. and C. E. Bloomquist, An Investigation of On/Off Effects on Equipment Operating in Space, PRC-R-1293, Planning Research Corporation, October 1969.
12. Bean, E. E. and C. E. Bloomquist, The Effects of Ground Storage, Space Dormancy, Standby Operation, and On/Off Cycling on Satellite Electronics, PRC-R-1435, Planning Research Corp., May 1970.
13. Bean, E. E. and C. E. Bloomquist, Reliability Data from In-flight Spacecraft, 1958-1970, PRC-R-1453, Planning Research Corporation, November 1971.
14. Bloomquist, C., and W. Grahm, Analysis of Spacecraft On-Orbit Anomalies and Lifetimes, PRC-R-3579, Planning Research Corporation, February 1983.
15. Boteilko, R. J., "Effects of On/Off Cycling on Equipment Reliability", Proceedings of the Seventh National Symposium on Reliability and Quality Control in Electronics, January 1961.
16. Stanbery, R. L., "Military Electronics Field Effectiveness," Washington, D.C. Presentations, March 1983.
17. Stanbery, R. L., "TOW Failure Rates in Test and Flight," Washington, D.C. Presentations, March 1983.
18. MIL-HDBK-217D, Military Handbook, Reliability Prediction of Electronic Equipment, January 1982.
19. Rickers, H. C., LSI/Microprocessor Reliability Prediction Model Development, RADC-TR-79-97.

REFERENCES (CONT'D)

20. Hommey, G. A., and T. E. Paquette, Linear/Interface Data, RAC Publication MDR-6, Autumn 1977.
21. Flint, S., J. Steinkirchner and E. Edwards, Avionic Environmental Factors for MIL-HDBK-217, RADC-TR-81-374, IIT Research Institute, January 1982.
22. Fiorentino, Eugene, The Use of Air Force Field Maintenance Data for R&M Assessments of Ground Electronic Systems, RADC-TR-79-103, April 1979.
23. Reed, A. C., Failure Rates of Non-Homogeneous Parts Populations, Report No. TOR-0172 (2133)-1, September 1971.
24. Livesay, B. R. and E. J. Scheibner, Reliability Factors for Electronic Components in a Storage Environment, DD-14-23 Georgia Institute of Technology, September 1977.
25. Frank, R., L. McTigue and R. Provence, "Storage Reliability of Chip and Bond Wire Electronic Devices", Proceedings 1976 Reliability and Maintainability Symposium, January 1976.
26. Hakim, E. and H. Shaver, "Panama Field Test Results of Plastic Encapsulated Devices," Proceedings of the Symposium on Plastic Encapsulated/Polymer Sealed Semiconductor Devices for Army Equipment, U.S. Army ERADCOM, May 1978.
27. Merren, G. T., "Dormant Storage Reliability Assessments - Data Based," IEEE Transactions on Components, Hybrids, and Manufacturing Technology, Vol. CHMT-4, No. 4, Sandia National Laboratories, December 1981.

REFERENCES (CONT'D)

28. Coit, D., et. al., VLSI Device Reliability Models, RADC-TR-84-182, IIT Research Institute, 1984.
29. Manno, P., Failure Rate Prediction Methodology (Today and Tomorrow), Rome Air Development Center.
30. Peck, D. S., "New Concerns About Integrated Circuit Reliability," International Reliability Physics Symposium, 1978.
31. Electronic Reliability Design Handbook, IIT Research Institute, MIL-HDBK-338 (Proposed).
32. Cook, D., S. Rosenburg, and B. Euzert, "HMOS Reliability," International Reliability Physics Symposium, 1978.
33. Edwards, J. R., et. al., "VMOS Reliability," International Reliability Physics Symposium Proceedings, 1978.
34. Branner, J. B., et. al., IEEE Transactions on Reliability, R-24, 1975 p. 238.
35. Reynolds, F. H., and J. W. Stevens, "Semiconductor Components Reliability in an Equipment Operating in Electromechanical Telephone Exchanges," International Reliability Physics Symposium Proceedings, 1978.
36. Bramhilla, D. F., F. Funtini and A. Mattona, "Reliability Problems with VLSI," Microelectronics Reliability, Vol. 24, No. 2, 1984.
37. Dey, K. A., and W. E. Turkowski, Memory/Digital LSI Data, RAC Publication MDR-18, Winter 81/82.

REFERENCES (CONT'D)

38. Ballou, T. A., Digital SSI/MSI Data, RAC Publication MDR-19, Spring 1984.
39. European Space Research and Technology Center, Specification QRA-4, Issue 3, February 1976.
40. Information for Reliability Prediction, G.E. Technical Memorandum, Report No. ASD-R-05-64-1, General Electric Co., May 1964.
41. Transistor/Diode Data, RAC Publication DRS-3, Winter 1979/80.
42. Tyler, D. and J. Wilbur, FMECA R&M Standard, Naval Avionics Center Standard No. NAC-83-RM-914-00C-1, May 1984.
43. Coit, D., and J. Steinkirchner, Reliability Modeling of Critical Electronic Devices, RADC-TR-83-108, IIT Research Institute, May 1983.
44. Arno, R., Nonelectronic Parts Reliability Data, RAC Publication NPRD-2, Summer 1981.
45. Coit, D. W., Printed Wiring Assembly and Interconnection Reliability, RADC-TR-81-318, IIT Research Institute, November 1981.

APPENDIX A
Proposed Revision Pages
For
MIL-HDBK-217

MIL-HDBK-217

5.2 Nonoperating Reliability Prediction

5.2.1 Discussion of Nonoperating Failure Rate Prediction

5.2.1.1 Applicability

The nonoperating failure rate prediction models are applicable when most of the design is completed and a detailed parts list is available. This section contains nonoperating failure rate models for a wide variety of parts used in electronic equipment. The models are to be used when a subsystem, or assembly is experiencing none of the electrical or mechanical stresses inherent in the designed activation of that subsystem or system. It may, however, be experiencing stress caused by the environment, transportation and handling, captive carry G-forces, etc.

5.2.1.2 General Model Factors

The following factors are common for the majority of the nonoperating failure rate prediction models.

- o π_{NQ} - Nonoperating Quality Factor, accounts for effects of different quality levels.
- o π_{NE} - Nonoperating Environmental Factor, accounts for the influence of all environmental stresses. For microelectronic devices and discrete semiconductors, the factor accounts for all environmental stress except temperature.
- o π_{NT} - Nonoperating Temperature Factor, accounts for the effects of nonoperating ambient temperature.
- o π_{CYC} - Equipment Power On-Off Cycling Factor, accounts for the effects of transients due to equipment power cycling.

MIL-HDBK-217

5.2.1.3 Model Application

The nonoperating failure rate prediction models can be used separately to predict nonoperating failure rate and reliability, or can be used to complement the operating failure rate prediction models in Section 5.1. The following three equations illustrate the methods for predicting nonoperating reliability, service life failure rate and combined operating/nonoperating reliability.

$$(1) R_n = \exp(-\sum \lambda_{ni} t_{ni})$$

$$(2) \lambda_{SL} = \sum D_{oi} \lambda_{oi} + \sum D_{ni} \lambda_{ni}$$

$$(3) R_{o/n} = \exp(-(\sum \lambda_{ni} t_{ni} + \sum \lambda_{oi} t_{oi}))$$

where

R_n = nonoperating reliability

λ_{ni} = nonoperating failure rate in the i^{th} nonoperating environment

t_{ni} = nonoperating time in the i^{th} nonoperating environment

λ_{SL} = service life failure rate, equal to the number of failures per unit time regardless of operational mode

D_{oi} = duty cycle in the i^{th} operating environment, equal to the time in the i^{th} operating environment divided by total operating time plus total nonoperating time

λ_{oi} = operating failure rate in the i^{th} operating environment

MIL-HDBK-217

D_{ni} = duty cycle in the i^{th} nonoperating environment, equal to the time in the i^{th} nonoperating environment divided by total operating time plus total nonoperating time

$R_{o/n}$ = Reliability for the mission duration plus nonoperating time between missions

5.2.1.4 Cautions

The following cautions are offered to prevent the misuse of the nonoperating failure rate models.

- o Temperature in the models for discrete semiconductors and microelectronic devices is the ambient nonoperating temperature, not operating case or junction temperatures.
- o Nonoperating environment is the actual environment to which the component is exposed. For example, an airborne radar between missions is most likely exposed to a ground fixed environment.
- o Equipment power on-off cycling is determined at the equipment level. The parameter does not refer to actuations of switches or relays, nor specific circuit applications within the operating state.

MIL-HDBK-217
 MICROELECTRONIC DEVICES
 MONOLITHIC

5.2.2 Microelectronic Devices

5.2.2.1 Monolithic (Bipolar and MOS) Digital SSI/MSI, Random Logic LSI, and Microprocessor Devices

This section represents the nonoperating failure rate prediction model for monolithic (bipolar and MOS) digital SSI/MSI, random logic LSI and microprocessor devices. The prediction model is as follows:

$$\lambda_p = \lambda_{nb} \pi_{NT} \pi_{NQ} \pi_{NE} \pi_{cyc} \quad \text{failures}/10^6 \text{ nonoperating hours}$$

where

λ_p = predicted monolithic microelectronic device nonoperating failure rate

λ_{nb} = nonoperating base failure rate, based on gate count (N_g)

= $.00029(N_g)^{.477}$ for $N_g \leq 3100$ gates (See Table 5.2.2.4-1)

= $.014$ for $N_g > 3100$ gates (See Table 5.2.2.4-1)

π_{NT} = nonoperating temperature factor, based on technology (See Table 5.2.2.4-3)

π_{NQ} = nonoperating quality factor (See Table 5.2.2.4-5)

π_{NE} = nonoperating environmental factor (See Table 5.2.2.4-8)

π_{cyc} = equipment power on-off cycling factor (See Table 5.2.2.4-6)

MIL-HDBK-217
 MICROELECTRONIC DEVICES
 MONOLITHIC

5.2.2.2 Monolithic (Bipolar and MOS) Linear/Interface Devices

This section represents the nonoperating failure rate prediction model for monolithic (bipolar and MOS) linear/interface devices. The prediction model is as follows:

$$\lambda_p = \lambda_{nb} \pi_{NT} \pi_{NQ} \pi_{NE} \pi_{cyc} \quad \text{failures}/10^6 \text{ nonoperating hours}$$

where

λ_p = linear/interface device predicted nonoperating failure rate

λ_{nb} = nonoperating base failure rate, based on transistor count (N_t)

$\lambda_{nb} = 0.00021(N_t)^{.887}$ where N_t = number of transistors (See Table 5.2.2.4-2)

π_{NT} = nonoperating temperature factor, based on technology (See Table 5.2.2.4-3)

π_{NQ} = nonoperating quality factor (See Table 5.2.2.4-5)

π_{NE} = nonoperating environmental factor (See Table 5.2.2.4-8)

π_{cyc} = equipment power on-off cycling factor (See Table 5.2.2.4-7)

MIL-HDBK-217
 MICROELECTRONIC DEVICES
 MONOLITHIC

5.2.2.3 Monolithic RAM, CCD, ROM, and PROM Memory Devices

This section represents the nonoperating failure rate prediction model for monolithic (bipolar and MOS) memory devices (RAMs, CCDs, ROMs and PROMs). The prediction model is as follows:

$$\lambda_p = \lambda_{nb} \pi_{NT} \pi_{NQ} \pi_{NE} \pi_{cyc} \quad \text{failures}/10^6 \text{ nonoperating hours}$$

where

λ_p = memory device predicted nonoperating failure rate

λ_{nb} = nonoperating base failure rate, based on technology

= 0.0034 for Bipolar Memory Devices

= 0.0017 for MOS Memory Devices

π_{NT} = nonoperating temperature factor, based on technology (See Table 5.2.2.4-3)

π_{NQ} = nonoperating quality factor (See Table 5.2.2.4-5)

π_{NE} = nonoperating environmental factor (See Table 5.2.2.4-8)

π_{cyc} = equipment power on-off cycling factor (See Table 5.2.2.4-6)

MIL-HDBK-217
MICROELECTRONIC DEVICES
MONOLITHIC

5.2.2.4 Monolithic Microcircuit Nonoperating Failure Rate Tables

TABLE 5.2.2.4-1: DIGITAL SSI/MSI, RANDOM LOGIC LSI AND MICROPROCESSOR
NONOPERATING BASE FAILURE RATE (λ_{nb})

No. Gates	λ_{nb} ($f/10^6$ hrs)	No. Gates	λ_{nb} ($f/10^6$ hrs)
1	.00029	80	.00234
2	.00040	90	.00248
4	.00056	100	.00261
6	.00068	150	.00317
8	.00078	200	.00363
10	.00087	250	.00404
12	.00095	300	.00440
14	.00102	350	.00474
16	.00109	400	.00505
18	.00115	450	.00534
20	.00121	500	.00562
22	.00127	550	.00588
24	.00132	600	.00613
26	.00137	650	.00637
28	.00142	700	.00660
30	.00147	750	.00682
32	.00151	800	.00704
34	.00157	850	.00724
36	.00160	900	.00744
38	.00164	950	.00763
40	.00169	1000	.00786
42	.00172	1200	.00855
44	.00176	1400	.00916
46	.00180	1600	.00977
48	.00184	1800	.0104
50	.00188	2000	.0109
55	.00196	2400	.0119
60	.00205	2800	.0128
65	.00212	3100	.0134
70	.00220	>3100	.014

$\lambda_{nb} = .00029(N_g)^{.477}$

where

N_g = number of gates

MIL-HDBK-217
MICROELECTRONIC DEVICES
MONOLITHIC

TABLE 5.2.2.4-2: LINEAR/INTERFACE MICROCIRCUIT NONOPERATING
BASE FAILURE RATE (λ_{nb})

No. Transistors	λ_{nb} (f/10 ⁶ hrs.)	No. Transistors	λ_{nb} (f/10 ⁶ hrs.)
4	.00072	148	.0177
8	.00133	156	.0186
12	.00190	164	.0193
16	.00246	172	.0202
20	.00299	180	.0210
24	.00352	188	.0219
28	.00403	196	.0227
32	.00454	204	.0235
36	.00504	220	.0251
40	.00746	236	.0268
44	.00603	252	.0284
48	.00651	268	.0299
52	.00699	284	.0315
56	.00746	300	.0331
60	.00794	350	.0379
64	.00840	400	.0427
68	.00884	450	.0474
72	.0936	500	.0521
76	.0098	550	.0566
80	.0102	600	.0612
84	.0107	650	.0656
88	.0111	700	.0701
92	.0116	750	.0746
96	.0121	800	.0789
100	.0125	850	.0833
108	.0134	900	.0875
116	.0143	950	.0919
124	.0151	1000	.0963
132	.0160		
140	.0168		

$$\lambda_{nb} = .00021(N_t)^{.887}$$

where

N_t = number of transistors

MIL-HDBK-217
MICROELECTRONIC DEVICES
MONOLITHIC

TABLE 5.2.2.4-3: MONOLITHIC DEVICE NONOPERATING TEMPERATURE FACTOR
(π_{NT})

T (°C)	TTL, HTTL, DTL, ECL	L TTL, STTL	LSTTL	IIL	MNOS	PMOS	NMOS, CCD	CMOS, CMOS/SOS	Linear Devices
0	0.93	0.92	0.91	0.88	0.66	0.73	0.70	0.63	0.62
5	0.94	0.93	0.91	0.89	0.69	0.76	0.73	0.66	0.66
10	0.95	0.94	0.93	0.90	0.73	0.79	0.76	0.70	0.72
20	0.98	0.97	0.97	0.95	0.88	0.91	0.89	0.86	0.88
25	1.00	1.00	1.00	1.00	1.00	1.00	1.00	1.00	1.00
30	1.03	1.03	1.04	1.06	1.17	1.12	1.14	1.20	1.15
35	1.06	1.08	1.10	1.15	1.41	1.28	1.34	1.49	1.34
40	1.11	1.14	1.17	1.27	1.74	1.49	1.59	1.88	1.58
45	1.16	1.21	1.27	1.43	2.18	1.75	1.94	2.44	1.86
50	1.23	1.30	1.39	1.65	2.77	2.10	2.39	3.20	2.22
55	1.31	1.41	1.54	1.94	3.57	2.54	2.97	4.23	2.65
60	1.41	1.55	1.74	2.32	4.62	3.09	3.73	5.63	4.62
65	1.54	1.72	1.99	2.82	5.98	3.79	4.69	7.49	3.80
70	1.68	1.93	2.30	3.46	7.73	4.67	5.95	9.97	4.55
75	1.86	2.18	2.68	4.29	10.0	5.73	7.49	13.2	5.44
80	2.06	2.50	3.14	5.34	12.9	7.05	9.42	17.3	6.50
85	2.30	2.87	3.71	6.69	16.6	8.66	11.8	22.7	7.70
90	2.58	3.31	4.41	8.38	21.2	10.6	14.9	29.7	9.15
95	2.92	3.83	5.25	10.5	27.0	13.0	18.6	38.5	10.9
100	3.30	4.45	6.27	13.1	34.2	15.9	23.0	49.6	12.8
105	3.74	5.18	7.46	16.3	43.0	19.3	28.5	63.4	15.1
110	4.28	6.03	8.90	20.3	53.9	23.3	35.1	81.0	17.7
115	4.85	7.02	10.6	25.1	67.1	28.1	43.1	102	20.7
120	5.52	8.18	12.6	31.1	83.5	33.8	52.6	129	24.1
125	6.29	9.51	14.9	38.2	103	40.3	63.8	161	27.9
130	7.16	11.0	17.6	46.7	126	48.0	77.2	201	32.3
135	8.14	12.8	20.8	56.8	154	57.0	93.0	249	37.2
140	9.26	14.8	24.6	69.0	187	67.7	112	307	42.8
145	10.5	17.1	28.8	83.4	227	79.6	133	376	49.0
150	11.9	19.7	33.7	100	273	93.4	158	457	56.0
155	13.5	22.6	39.4	120	328	109	188	558	63.5
160	15.2	26.0	45.7	143	390	127	221	667	72.5

$$\pi_{NT} = K_1 + K_2 \exp\left(-A_n\left(\frac{1}{T + 273} - \frac{1}{298}\right)\right)$$

T = ambient nonoperating temperature (°C)

K₁, K₂, A_n = temperature coefficients, based on technology (See Table 5.2.2.4-4)

MIL-HDBK-217
MICROELECTRONIC DEVICES
MONOLITHIC

TABLE 5.2.2.4-4: NONOPERATING TEMPERATURE COEFFICIENT (A_n)

Technology	A_n	K_1	K_2
TTL, HTTL, DTL, ECL	4813	0.91	0.09
LTTL, STTL	5261	0.90	0.10
LSTTL	5711	0.89	0.11
IIL	6607	0.86	0.14
MNOS	6607	0.61	0.39
PMOS	5711	0.68	0.32
NMOS, CCD	6159	0.65	0.35
CMOS, CMOS/SOS	7057	0.58	0.42
Linear	4748	0.50	0.50

$$\pi T = K_1 + K_2 \exp\left(-A_n\left(\frac{1}{T + 273} - \frac{1}{298}\right)\right)$$

TABLE 5.2.2.4-5: MONOLITHIC DEVICE NONOPERATING QUALITY FACTOR (πNQ)

Quality Level*	πNQ
S	0.53
B	1.0
B-1	1.4
B-2	2.0
C	2.3
C-1	2.4
D	2.5
D-1	8.7

*Quality level definitions are provided in Table 5.1.2.5-1 in Section 5.1.2.5-1

MIL-HDBK-217
 MICROELECTRONIC DEVICES
 MONOLITHIC

TABLE 5.2.2.4-6: DIGITAL/MEMORY EQUIPMENT POWER ON-OFF
 CYCLING FACTOR (π_{cyc})

Cycling Rate* (N_C) (Power Cycles/ 10^3 hrs.)	Mean-Time-Between Power Cycles (Hours)	π_{cyc}
<1	>1000	1
1	1000	1.02
2	500	1.04
3	333	1.06
4	250	1.08
5	200	1.10
10	100	1.20
20	50	1.40
50	20	2.00

$$\pi_{cyc} = 1 + .02(N_C)$$

N_C = Number of equipment power on-off cycles per 1000 nonoperating hours

* An equipment power on-off cycle is defined as the state during which an electronic equipment goes from zero electrical activation level to the normal design activation level plus the state during which it returns to zero.

MIL-HDBK-217
 MICROELECTRONIC DEVICES
 MONOLITHIC

TABLE 5.2.2.4-7: LINEAR/INTERFACE EQUIPMENT POWER ON-OFF
 CYCLING FACTOR (π_{cyc})

Cycling Rate* (N_C) (Power Cycles/ 10^3 hrs.)	Mean-Time-Between Power Cycles (Hours)	π_{cyc}
<1	>1000	1
1	1000	1.03
2	500	1.06
3	333	1.09
4	250	1.12
5	200	1.16
10	100	1.31
20	50	1.62
50	20	2.55

$$\pi_{cyc} = 1 + .031(N_C)$$

N_C = Number of equipment power on-off cycles per 1000 nonoperating hours

- * An equipment power on-off cycle is defined as the state during which an electronic equipment goes from zero electrical activation level to the normal design activation level plus the state during which it returns to zero.

MIL-HDBK-217
 MICROELECTRONIC DEVICES
 MONOLITHIC

TABLE 5.2.2.4-8: MONOLITHIC DEVICE NONOPERATING
 ENVIRONMENTAL FACTORS (MNE)

Environment	Hermetic Devices	Nonhermetic Devices
GB	1	1
GF	2.4	4.0
GM	3.5	6.5
Mp	3.2	5.9
NSB	3.4	6.2
NS	3.4	6.2
NU	4.5	8.6
NH	4.6	8.9
NUU	4.9	9.5
ARW	6.3	13
AIC	2.4	4.0
AIT	2.7	4.7
AIB	4.0	7.6
AIA	3.4	6.2
AIF	4.7	9.0
AUC	2.7	2.7
AUT	3.4	3.4
AUB	5.7	11
AUA	4.7	9.0
AUF	6.7	13
SF	1.0	1.0
MFF	3.3	6.0
MFA	4.3	8.2
USL	8.0	16
ML	9.3	19
CL	150	310

MIL-HDBK-217
MICROELECTRONIC DEVICES
MONOLITHIC

5.2.2.5 Example Nonoperating Failure Rate Calculations

Example One

Given: A hermetically sealed monolithic linear device, M38510/11402P is being used in a ground fixed environment at an ambient nonoperating temperature of 20°C. The quality level is class S and the equipment on-off cycling rate is 1 per 1,000 hours.

Step 1: The nonoperating failure rate model is shown in Section 5.2.2.2 to be $\lambda_p = \lambda_{nb} \pi_{NT} \pi_{NQ} \pi_{NE} \pi_{cyc}$

Step 2: Examine Table 5.1.2.5-28 "Microelectronic Parameters" in Section 5.1.2.5 and determine the number of transistors for an M385010/11402P. Thirty-two transistors is the correct number.

Step 3: Refer to Table 5.2.2.4-2 and find the correct nonoperating base failure rate (λ_{nb}) of 0.00454 failures per million hours for the 32 transistor device.

Step 4: Refer to Table 5.2.2.4-3 and find the nonoperating temperature factor π_{NT} of 0.88 for a linear device at 20°C ambient nonoperating temperature.

Step 5: Next refer to Table 5.2.2.4-5 and find correct nonoperating quality factor (π_{NQ}) of 0.53 for a quality level S device.

Step 6: Refer to Table 5.2.2.4-7 and find correct π_{cyc} factor of 1.03 for a cycling rate of 1 per 1000 hours.

Step 7: Refer to Table 5.2.2.4-8 and find correct nonoperating environmental factor (π_{NE}) of 2.4 for a hermetically sealed linear device.

Step 8: Determine the predicted linear monolithic device failure rate as follows:

$$\lambda_p = \lambda_{nb} \pi_{NT} \pi_{NQ} \pi_{NE} \pi_{cyc}$$

$$\lambda_p = .00454 \times 0.88 \times 0.53 \times 2.4 \times 1.03$$

$$\lambda_p = .00523 \text{ failures for million hours}$$

MIL-HDBK-217
MICROELECTRONIC DEVICES
MONOLITHIC

Example Two

Given: A hermetically sealed monolithic bipolar memory device TTL, M38510/20202-F is being used in a ground mobile environment at an ambient nonoperating temperature of 40°C. The quality level is class B and the equipment on-off cycling rate is 3 every 1000 hours.

Step 1: The nonoperating failure rate model is shown in section 5.2.2.3 to be $\lambda_p = \lambda_{nb} \pi_{NT} \pi_{NQ} \pi_{NE} \pi_{cyc}$

Step 2: Refer to nonoperating base failure rate constant λ_{nb} of 0.0034 for a bipolar memory device from Section 5.2.2.3.

Step 3: Refer to Table 5.2.2.4-3 and find the nonoperating temperature factor (π_{NT}) of 1.11 for a TTL memory device at 40°C ambient nonoperating temperature.

Step 4: Next refer to Table 5.2.2.4-5 and find correct nonoperating quality factor (π_{NQ}) of 1.0 for a quality level-B device.

Step 5: Refer to Table 5.2.2.4-6 and find correct π_{cyc} factor of 1.06 for a cycling rate of 3 per 1000 hours (refer to digital/memory device listing).

Step 6: Refer to Table 5.2.2.4-8 and find correct nonoperating environmental factor π_{NE} of 3.5 for ground mobile (G_M), hermetically sealed TTL memory device.

Step 7: Determine the predicted TTL monolithic memory device failure rate as follows:

$$\lambda_p = \lambda_{nb} \pi_{NT} \pi_{NQ} \pi_{NE} \pi_{cyc}$$

$$\lambda_p = 0.0034 \times 1.11 \times 1.0 \times 3.5 \times 1.06$$

$$\lambda_p = .0140 \text{ failures per million hours}$$

MIL-HDBK-217
MICROELECTRONIC DEVICES
MONOLITHIC

Example Three

Given: A hermetically sealed monolithic TTL, M38510/00903-A, device is being used in the ground mobile environment at an ambient nonoperating temperature of 60°C. The quality level is Class B and the equipment on-off cycling rate is 1 per 500 hours.

Step 1: The nonoperating failure rate model is shown in Section 5.2.2.1 to be $\lambda_p = \lambda_{nb} \pi_{NT} \pi_{NQ} \pi_{cyc} \pi_{NE}$

Step 2: Examine Table 5.1.2.5-28, "Microelectronic Parameters" in Section 5.1.2.5 and determine the number of gates for a TTL type, M38510/00903-A device. Thirty-six gates is the correct number.

Step 3: Refer to Table 5.2.2.4-1 and find the correct nonoperating base failure rate (λ_{nb}) of 0.00160 failures per million hours for the 36 gate device.

Step 4: Refer to Table 5.2.2.4-3 and find the nonoperating temperature factor (π_{NT}) of 1.41 for a TTL device at 60°C ambient nonoperating temperature.

Step 5: Next refer to Table 5.2.2.4-5 and find correct nonoperating quality factor (π_{NQ}) of 1.0 for a quality level B device.

Step 6: Refer to Table 5.2.2.4-6 and find correct π_{cyc} factor of 1.04 for a mean-time-between power cycles of 500 hours.

Step 7: Refer to Table 5.2.2.4-8 and find correct nonoperating environmental factor (π_{NE}) of 3.5 for a ground mobile (G_M), hermetically sealed TTL device.

Step 8: Determine the predicted TTL monolithic device nonoperating failure rate as follows:

$$\lambda_p = \lambda_{nb} \pi_{NT} \pi_{NQ} \pi_{NE} \pi_{cyc}$$

$$\lambda_p = .00160 \times 1.41 \times 1.0 \times 3.5 \times 1.04$$

$$\lambda_p = 0.00821 \text{ failures per million hours}$$

MIL-HDBK-217
MICROELECTRONIC DEVICES
HYBRID

5.2.2.6 Hybrid Microcircuits

This section includes the nonoperating failure rate prediction model for hybrids.

The general model for hybrid devices is as follows:

$$\lambda_p = \lambda_{nb} \pi_{NQ} \pi_{NE} \quad \text{failures}/10^6 \text{ nonoperating hours}$$

where

λ_p = predicted hybrid microelectronic device nonoperating failure rate

λ_{nb} = nonoperating base failure rate, based on component count (See Table 5.2.2.6-1)

π_{NQ} = nonoperating quality factor (see Table 5.2.2.6-2)

π_{NE} = nonoperating environmental factor (see Table 5.2.2.6-3)

5.2.2.6.1 Example Failure Rate Calculation

Given: A hermetically sealed hybrid procured to MIL-STD-883, Method 5004, 5005 and MIL-M-38510 contains 18 diodes, 15 transistors, and 3 integrated circuits, and is installed in a ground fixed environment.

Step 1: The nonoperating failure rate model is shown in Section 5.2.2.6 to be $\lambda_p = \lambda_{nb} \pi_{NQ} \pi_{NE}$

Step 2: The next step is to determine which hybrid nonoperating base failure rate equation to use. Refer to Table 5.2.2.6-1. Adding the number of diodes (18) plus the number of transistors (15) plus 1.8 times the number of integrated circuits (3) yields 38.4. Therefore, since 38.4 is greater than 12.2, the second base failure rate equation is selected to determine the hybrid nonoperating base failure rate. Do not count capacitors, packaged resistors, substrate resistors, substrate and interconnections as these parameters are all included in the base failure rate constant.

MIL-HDBK-217
 MICROELECTRONIC DEVICES
 HYBRID

Step 3: The correct nonoperating base failure rate model (Equation 2) is shown in Section 5.2.2.6 to be

$$\lambda_{nb} = 0.013 (e^{.033(N_D + N_T)} + .059N_{IC})$$

$$= 0.046$$

Step 4: Refer to Table 5.2.2.6-2 and select the nonoperating quality factor of 1.0 for a quality level B hybrids.

Step 5: Refer to Table 5.2.2.6-3 and select the ground fixed (G_F) nonoperating environmental factor of 2.4 for the hermetically sealed hybrid.

Step 6: Determined the predicted hybrid nonoperating failure rate as follows:

$$\lambda_p = \lambda_{nb} \pi_{NQ} \pi_{NE}$$

$$= .046 \times 1.0 \times 2.4$$

$$= .110 \text{ failures}/10^6 \text{ nonoperating hours}$$

MIL-HDBK-217
 MICROELECTRONIC DEVICES
 HYBRID

TABLE 5.2.2.6-1: HYBRID NONOPERATING BASE FAILURE RATE (λ_{nb})

Nonoperating Base Failure Rate Model*					
$\lambda_{nb} = A \exp(b_1 N_D + b_2 N_T + b_3 N_{IC})$ <p>where</p> <p>N_D = number of diodes N_T = number of transistors N_{IC} = number of integrated circuits</p>					
Case	Complexity	A	b ₁	b ₂	b ₃
I	$N_D + N_T + 1.8 N_{IC} \leq 12.2$.000817	.45	.45	.81
II	$N_D + N_T + 1.8 N_{IC} > 12.2$.013	.033	.033	.059

- * Hybrid base failure rate includes the contribution of an average number of capacitors, packaged resistors, and substrate resistors.

MIL-HDBK-217
 MICROELECTRONIC DEVICES
 HYBRID

TABLE 5.2.2.6-2: HYBRID NONOPERATING QUALITY FACTORS (π_{NQ})

QUALITY LEVEL	DESCRIPTION	π_Q
S	The test procedures for this quality level are currently being developed. Until such time that they are included in MIL-STD-883 and MIL-M-38510, the procuring activity will provide the necessary testing requirements.	0.53
B	Procured to the Class B requirements of: MIL-STD-883, Method 5008 and Appendix G of MIL-M-38510	1.0
	or MIL-STD-883, Methods 5004 and 5005 and MIL-M-38510	
D	Commercial Part, hermetically sealed, with no screening beyond manufacturer's normal quality assurance practices.	8.6

MIL-HDBK-217
 MICROELECTRONIC DEVICES
 HYBRID

TABLE 5.2.2.6-3: HYBRID NONOPERATING ENVIRONMENT FACTORS (π_{NE})

Environment	π_{NE}
GB	1
GF	2.4
GM	3.5
Mp	3.2
NSB	3.4
NS	3.4
NU	4.5
NH	4.6
NUU	4.9
ARW	6.3
AIC	2.4
AIT	2.7
AIB	4.0
AIA	3.4
AIF	4.7
AUC	2.7
AUT	3.4
AUB	5.7
AUA	4.7
AUF	6.7
SF	1.3
MFF	3.3
MFA	4.3
USL	8.0
M _L	9.3
C _L	150

MIL-HDBK-217
MICROELECTRONIC DEVICES
BUBBLE MEMORIES

5.2.2.7 Magnetic Bubble Memories

The magnetic bubble memory device in its present form is a hybrid assembly of two major structural segments:

- a. A basic memory and control structure consisting of thin-film elements on a crystalline substrate, and
- b. A magnetic structure to provide a controlled magnetic field consisting of a magnet, magnetic coils and a housing.

These two major structural segments of the hybrid are interconnected by a mechanical substrate and lead frame. The interconnect substrate in present technology is normally a printed circuit board. The general form of the operating failure rate model is:

$$\lambda_p = \lambda_{n1} + \lambda_{n2}$$

where

λ_p = nonoperating failure rate in failures/10⁶ hrs.

λ_{n1} = nonoperating failure rate of the control structure

λ_{n2} = nonoperating failure rate of the magnetic memory structure.

Nonoperating Failure Rate of the Control Structure (λ_{n1})

$$\lambda_{n1} = \lambda_{nb1} \pi_{NT1} \pi_{NE} \text{ failures/10}^6 \text{ nonoperating hours}$$

where

λ_{nb1} = control structure nonoperating base failure rate, based on gate count (N_g)

MIL-HDBK-217
 MICROELECTRONIC DEVICES
 BUBBLE MEMORIES

$= .0015(N_g) \cdot 477$, where N_g is the number of transfer gates plus the number of dissipative control gates plus the number of major loops.

π_{NT1} = control structure nonoperating temperature factor, based upon NMOS technology for digital microcircuits (See Table 5.2.2.4-3 for NMOS)

$= \exp(-6159(\frac{1}{T} - \frac{1}{298}))$, where T is temperature ($^{\circ}\text{K}$)

π_{NE} = nonoperating environmental factor (See Table 5.2.2.4-7 for nonhermetic devices)

Nonoperating Failure Rate of the Magnetic Memory Structure (λ_{n2})

$\lambda_{n2} = .0089(N_L) \pi_{NT} \pi_{NE}$

where

N_L = number of loops, equal to the number of major loops plus the number of functional minor loops

π_{NT} = magnetic memory structure nonoperating temperature factor, based on technology (See Table 5.2.2.4-3)

π_{NE} = nonoperating environmental factor (See Table 5.2.2.4-8 for nonhermetic devices)

MIL-HDBK-217
MICROELECTRONIC DEVICES
BUBBLE MEMORIES

5.2.2.7-1 Example Nonoperating Failure Rate Calculation

Given: A 92K bit magnetic bubble memory with 10 connected pins, 1 major loop, 3 dissipative control elements (generate, replicate and detector bridge), 144 transfer gates, 640 bits per major loop, and 157 memory minor loops with 144 functional is installed in a ground benign nonoperating environment with a nonoperating ambient temperature of 25°C.

Step 1: From the example statement, N_g was equal to 148, found by adding the number of major loops (1) plus the number of dissipative control elements (3) plus the number of transfer gates (144).

Step 2: From Section 5.2.2.7, the control structure nonoperating base failure rate can be found by,

$$\begin{aligned}\lambda_{nb1} &= .0015 (N_g)^{.477} \\ &= .0015(148)^{.477} \\ &= .0163\end{aligned}$$

Step 3: From Table 5.2.2.4-3 for NMOS technology, a nonoperating temperature factor of 1 was found for 25°C.

Step 4: From Table 5.2.2.4-8, an appropriate nonoperating environmental factor of 1.0 was selected.

Step 5: The control structure nonoperating failure rate is

$$\begin{aligned}\lambda_{n1} &= \lambda_{nb1} \pi_{NT} \pi_{NE} \\ &= .0163 \times 1.0 \times 1.0 \\ &= .0163\end{aligned}$$

Step 6: From the example statement, the number of loops was found to be 145 equal to the number of major loops (1) plus the number of functional minor loops (144).

MIL-HDBK-217
 MICROELECTRONIC DEVICES
 BUBBLE MEMORIES

Step 7: From Table 5.2.2.4-3, the magnetic memory structure nonoperating temperature factor was determined to be 1.0 for 25°C.

Step 8: Since the nonoperating environmental factor was already determined, the magnetic memory structure can be found by the following expression

$$\begin{aligned}\lambda_p &= .0089(N_L) \pi_{NT} \pi_{NE} \\ &= .0089(145) \times (1.0) \times (1.0) \\ &= 1.29\end{aligned}$$

Step 9: From Section 5.2.2.7, the magnetic bubble memory nonoperating failure rate is equal the control structure nonoperating failure rate plus the magnetic memory structure

$$\begin{aligned}\lambda_p &= \lambda_{n1} + \lambda_{n2} \\ &= .0163 + 1.29 \\ &= 1.31 \text{ failures}/10^6 \text{ nonoperating hours}\end{aligned}$$

MIL-HDBK-217
DISCRETE SEMICONDUCTORS

5.2.3 Discrete Semiconductors

This section includes the nonoperating failure rate prediction models for discrete semiconductors.

5.2.3.1 Transistor and Diode Semiconductor Devices

The general nonoperating failure rate prediction model for transistors and diodes is as follows:

$$\lambda_p = \lambda_{nb} \pi_{NT} \pi_{NE} \pi_{NQ} \pi_{cyc} \quad \text{failures}/10^6 \text{ nonoperating hours}$$

where

- λ_p = predicted transistor or diode nonoperating failure rate
- λ_{nb} = nonoperating base failure rate (See Table 5.2.3-1)
- π_{NT} = nonoperating temperature factor, based on device style (see Table 5.2.3-2 for transistors, Table 5.2.3-3 for diodes and Table 5.2.3-4 for temperature factor parameter)
- π_{NE} = nonoperating environmental factor (See Table 5.2.3-5)
- π_{NQ} = nonoperating quality factor (See Table 5.2.3-6)
- π_{cyc} = equipment power on-off cycling factor (See Table 5.2.3-7 for transistors and Table 5.2.3-8 for diodes)

5.2.3.1.1 Example Nonoperating Failure Rate Calculation

Given: A Silicon, NPN general purpose JAN grade transistor is in a fixed ground installation at 30 degrees C ambient nonoperating temperature. The power is cycled "on" once every 1,000 nonoperating hours.

Step 1: The nonoperating failure rate model shown in Section 5.2.3.1 above is $\lambda_p = \lambda_{nb} \pi_{NT} \pi_{NE} \pi_{NQ} \pi_{cyc}$

MIL-HDBK-217
DISCRETE SEMICONDUCTORS

Step 2: Refer to Table 5.2.3-1 and find the appropriate λ_{nb} of .00027 failures per 10^6 hrs for a Group I Silicon, NPN type transistor.

Step 3: From Table 5.2.3-1 note that transistors, Silicon, NPN fall into the Group I category of discrete semiconductors.

Step 4: Next refer to Table 5.2.3-2 and find appropriate nonoperating temperature factor of 1.22 for a Group I Silicon, NPN transistor at 30°C ambient nonoperating temperature.

Step 5: Refer to Table 5.2.3-5 and find the correct nonoperating environmental factor (π_{NE}) of 5.8 for a Group I transistor in a ground fixed environment (GF).

Step 6: Refer to Table 5.2.3-6 and find correct nonoperating quality factor π_{NQ} of 3.6 for a JAN type transistor quality level.

Step 7: Next use Table 5.2.3-7 and find appropriate power on/off equipment cycling factor (π_{cyc}) of 1.05 for a transistor which has an equipment cycling rate of 1 per 1000 nonoperating hours.

Step 8: Determine the predicted transistor nonoperating failure rate (λ_p) in failures per million hours.

$$\lambda_p = \lambda_{nb} \pi_{NT} \pi_{NE} \pi_{NQ} \pi_{cyc}$$

$$\lambda_p = .00027 \times 1.22 \times 5.8 \times 3.6 \times 1.05$$

$$\lambda_p = 0.00722 \text{ failures per million hours}$$

5.2.3.2 Opto-Electronic Semiconductor Devices

The general nonoperating failure rate prediction model for opto-electronic semiconductor devices is as follows:

$$\lambda_p = \lambda_{nb} \pi_{NE} \pi_{NQ} \quad \text{failures}/10^6 \text{ nonoperating hours}$$

where

$$\lambda_p = \text{predicted nonoperating opto-electronic device failure rate}$$

MIL-HDBK-217
DISCRETE SEMICONDUCTORS

λ_{nb} = nonoperating base failure rate (See Table 5.2.3-1)

π_{NE} = nonoperating environmental factor (See Table 5.2.3-5)

π_{NQ} = nonoperating quality factor (See Table 5.2.3-6)

5.2.3.2.1 Example Nonoperating Failure Rate Calculation

Given: A commercial quality plastic-encapsulated single opto-isolator is being stored in a ground, benign application

Step 1: The nonoperating failure rate model shown in 5.2.3.2 above for opto-electronic devices is $\lambda_p = \lambda_{nb} \pi_{NE} \pi_{NQ}$

Step 2: From the example statement, the device is a single opto-isolator. Refer to Table 5.2.3-1 and find appropriate Group X, single isolator, nonoperating base failure rate of 0.00070 failures per million hours for this particular opto-electronic device.

Step 3: Next use Table 5.2.3-5 and select Ground Benign (G_b) factor of 1 for this group X device.

Step 4: Refer to Table 5.2.3-6 and select "plastic" quality level factor of 23 for this device,

Step 5: Determine the predicted single isolator nonoperating failure rate (λ_p) in failures per million hours.

$$\lambda_p = \lambda_{nb} \pi_{NE} \pi_{NQ}$$

$$\lambda_p = 0.00070 \times 1 \times 23$$

$$\lambda_p = 0.016 \text{ failures per million hours}$$

MIL-HDBK-217
DISCRETE SEMICONDUCTORS

TABLE 5.2.3-1: DISCRETE SEMICONDUCTOR NONOPERATING BASE FAILURE RATE (λ_{nb})

Part Class	Group	Part Type	λ_{nb} (Failures per 10^6 hrs)
A. Transistors	I	Si, NPN Si, PNP Ge, PNP Ge, NPN	.00027 .00027 .00040 .00040
	II	FET	.00039
	III	Unijunction	.0013
B. Diodes and Rectifiers	IV	Si, Gen. Purpose Ge, Gen. Purpose	.00017 .00042
	V	Zener/Avalanche	.00040
	VI	Thyristors	.00063
C. Microwave Semiconductors and Special Devices	VII	Detectors Mixers	.0027
	VIII	Varactors Step Recovery	.0027
	IX	Microwave Transistors	.041
D. Opto-Electronic Devices	X	LED	.00016
		Single Isolator	.00070
		Dual Isolator	.00089
		Phototransistor	.00038
		Photo Diode	.00028
		Alpha-Numeric Displays	.00025

MIL-HDBK-217
DISCRETE SEMICONDUCTORS

TABLE 5.2.3-2: TRANSISTOR NONOPERATING TEMPERATURE
FACTORS (Groups I, II, III, IX) (π_{NT})

T OC	GROUP						
	I		I		II	III	IX
	Si		Ge		FET	Unijunc- tion	Micro- wave
	NPN	PNP	PNP	NPN			
0	0.36	0.34	0.26	0.25	0.35	0.29	0.17
10	0.55	0.53	0.46	0.45	0.54	0.49	0.36
20	0.83	0.82	0.78	0.78	0.82	0.80	0.72
25	1.00	1.00	1.00	1.00	1.00	1.00	1.00
30	1.22	1.22	1.29	1.31	1.21	1.26	1.37
40	1.76	1.78	2.08	2.13	1.75	1.93	2.50
50	2.47	2.53	3.30	3.42	2.46	2.89	4.39
55	2.91	3.00	4.14	4.32	2.90	3.50	5.75
60	3.41	3.54	5.19	5.47	3.40	4.23	7.47
65	3.99	4.16	6.54	6.93	3.97	5.08	9.62
70	4.66	4.86	8.28	8.83	4.63	6.07	12.3
75	5.41	5.67	10.6	11.4	5.37	7.23	15.6
80	6.27	6.59	13.7	14.8	6.22	8.58	19.7
85	7.26	7.64	18.2	19.7	7.17	10.2	24.7
90	8.38	8.83	24.9	26.9	8.26	12.0	30.7
95	9.67	10.2			9.50	14.1	38.0
100	11.1	11.7			10.9	16.5	46.8
105	12.8	13.5			12.5	19.4	57.3
110	14.8	15.6			14.4	22.7	69.8
115	17.0	17.9			16.5	26.6	84.5
120	19.6	20.7			18.9	31.2	102
125	22.6	23.9			21.8	36.7	122
130	26.1	27.6			25.2	43.1	146
135	30.3	32.1				50.9	174
140	35.2	37.5				60.4	206
145	41.1	44.0				72.0	243
150	48.2	52.1				86.4	285
155	56.8	62.3				105	334
160	67.4	75.3				128	389

T = ambient nonoperating temperature (°C)

Temperature factor equation and parameter values are given in Table 5.2.3-4

MIL-HDBK-217
DISCRETE SEMICONDUCTORS

TABLE 5.2.3-3: DIODE NONOPERATING TEMPERATURE
FACTORS (Groups IV, V, VI, VII, VIII) (π_{NT})

T °C	GROUP					
	IV		V	VI	VII	VIII
	Gen. Purpose		Zener/ Av.	Thyristor	Microwave	Varactor, etc.
	Si	Ge				
0	0.26	0.17	0.39	0.27	0.43	0.35
10	0.46	0.36	0.58	0.47	0.62	0.54
20	0.78	0.72	0.84	0.79	0.86	0.82
25	1.00	1.00	1.00	1.00	1.00	1.00
30	1.28	1.39	1.19	1.30	1.17	1.21
40	2.03	2.60	1.65	2.07	1.56	1.75
50	3.14	4.73	2.24	3.20	2.06	2.46
55	3.87	6.32	2.59	3.95	2.35	2.90
60	4.74	8.45	2.99	4.85	2.68	3.40
65	5.78	11.3	3.44	5.92	3.04	3.97
70	7.00	15.2	3.94	7.21	3.44	4.63
75	8.43	20.5	4.50	8.73	3.89	5.37
80	10.1	28.1	5.13	10.5	4.40	6.22
85	12.1	39.5	5.84	12.7	4.97	7.17
90	14.4	57.1	6.63	15.2	5.61	8.26
95	17.1		7.52	18.2	6.34	9.50
100	20.2		8.52	21.8	7.18	10.9
105	23.9		9.65	26.0	8.16	12.5
110	28.2		10.9	31.0	9.31	14.4
115	33.2		12.4	36.9	10.7	16.5
120	39.1		14.1	43.9	12.4	18.9
125	46.2		16.0	52.2	14.5	21.8
130	54.6		18.2	62.3	17.1	25.2
135	64.8		20.9	74.3	20.6	29.1
140	77.3		24.1	88.8		33.9
145	92.9		27.9	106		39.7
150	113		32.6	128		46.9
155	138		38.4	154		55.8
160	172		45.8	187		67.1

T = ambient nonoperating temperature (°C)

Temperature factor equation and parameter values are given in Table 5.2.3-4

MIL-HDBK-217
DISCRETE SEMICONDUCTORS

TABLE 5.2.3-4: DISCRETE SEMICONDUCTOR NONOPERATING
TEMPERATURE FACTOR PARAMETERS

Group	Part Type	Temp. Constants			
		A _t	T _M	P	
Transistors I	Si, NPN	3356	448	10.5	
	Si, PNP	3541	448	14.2	
	Ge, PNP	4403	373	20.8	
	Ge, NPN	4482	373	19	
	II	FET	3423	448	13.8
	III	Unijunction	4040	448	13.8
Diodes IV	Si, Gen. Purpose	4399	448	17.7	
	Ge, Gen. Purpose	5829	373	22.5	
	V	Zener/Avalanche	3061	448	14
	VI	Thyristors	4311	448	9.6
	VII	Microwave	2738	423	16.6
	VIII	IMPATT, Gunn, Varactor, PIN, Step Recovery & Tunnel	3423	448	13.8
	Transistors IX	Microwave	5700	623	20

$$\pi_{NT} = \exp(-A_t(\frac{1}{T} - \frac{1}{298}) + (\frac{T}{T_M})^P)$$

where

$$T = \text{temperature } (^{\circ}\text{K}) = T(^{\circ}\text{C}) + 273$$

MIL-HDBK-217
DISCRETE SEMICONDUCTORS

TABLE 5.2.3-5: DISCRETE SEMICONDUCTOR NONOPERATING
ENVIRONMENTAL FACTOR (π_{NE})

Env.	GROUP									
	I	II	III	IV	V	VI	VII	VIII	IX	X
G _B	1	1	1	1	1	1	1	1	1	1
G _F	5.8	4.0	4.0	3.9	3.9	3.9	6.4	3.9	2.0	2.4
G _M	18	18	18	18	18	18	31	18	7.8	7.8
M _P	12	12	12	12	12	12	35	12	7.4	7.7
NS _B	9.8	6.0	9.3	4.8	5.8	5.8	8.0	5.8	3.6	3.7
NS	9.8	8.6	9.3	4.8	8.7	8.7	11	8.7	4.7	5.7
N _U	21	21	21	21	21	21	33	21	11	11
N _H	19	19	19	19	19	19	54	19	11	12
N _{UJ}	20	20	20	20	20	20	58	20	12	13
AR _W	27	27	27	27	27	27	78	27	16	17
A _I C	9.5	7.5	9.5	15	4.5	9.5	30	4.5	2.5	2.5
A _I T	15	9	15	20	6.5	15	40	6.5	3.5	3.5
A _I B	35	35	35	30	45	35	65	45	6.0	5.5
A _I A	20	30	20	25	25	20	50	25	3.5	3.5
A _I F	40	40	40	35	45	40	70	45	6.0	5.5
A _U C	15	10	15	25	7.5	15	50	7.5	5.0	3.0
A _U T	25	15	25	30	10	25	60	10	7.0	5.5
A _U B	60	55	60	50	70	60	105	70	10	8.0
A _U A	35	50	35	40	40	35	80	40	7.0	5.5
A _U F	65	65	65	50	70	65	110	70	10	10
S _F	1	1	1	1	1	1	1	1	1	1
M _F F	12	12	12	12	12	12	36	12	7.5	7.8
M _F A	17	17	17	17	17	17	50	17	11	11
U _S L	36	36	36	36	36	36	110	36	22	23
M _L	41	41	41	41	41	41	120	41	25	26
C _L	690	690	690	690	690	690	2000	690	250	450

MIL-HDBK-217
DISCRETE SEMICONDUCTORS

TABLE 5.2.3-6: DISCRETE SEMICONDUCTOR NONOPERATING
QUALITY FACTOR (π_{NQ})

Quality Level	π_{NQ}
JANTXV	0.57
JANTX	1.0
JAN	3.6
Lower, Hermetic*	13
Plastic**	23

* applies to all hermetic packaged discrete semiconductor devices and to Non-JAN hermetic packaged devices.

** applies to all discrete semiconductor devices encapsulated with organic material

TABLE 5.2.3-7: TRANSISTOR EQUIPMENT POWER ON-OFF
CYCLING FACTOR (π_{cyc}) (Groups I, II, III, IX)

Cycling Rate***(N_C) (Power Cycles/ 10^3 hrs.)	Mean-Time-Between Power Cycles	π_{cyc}
<1	>1000	
1	1000	1.05
2	500	1.10
3	333	1.15
4	250	1.20
5	200	1.25
10	100	1.50
20	50	2.00
50	20	3.50

$$\pi_{cyc} = 1 + .050(N_C)$$

N_C = number of equipment power on-off cycles per 1000 nonoperating hours

*** An equipment power on-off cycle is defined as the state during which an electronic equipment goes from zero electrical activation level to the normal design activation level plus the state during which it returns to zero.

MIL-HDBK-217
DISCRETE SEMICONDUCTORS

TABLE 5.2.3-8: DIODE EQUIPMENT POWER ON-OFF CYCLING
FACTOR (π_{cyc}) (Groups IV, V, VI, VII, VIII)

Cycling Rate***(N_c) (Power Cycles/ 10^3 hrs.)	Mean-Time-Between Power Cycles	π_{cyc}
<0.6	>1667	1.00
1	1000	1.08
2	500	1.17
3	333	1.25
4	250	1.33
5	200	1.42
10	100	1.83
20	50	2.66
50	20	5.15

$$\pi_{cyc} = 1 + .083(N_c)$$

N_c = number of equipment power on-off cycles per 1000 nonoperating hours

*** An equipment power on-off cycle is defined as the state during which an electronic equipment goes from zero electrical activation level to the normal design activation level plus the state during which it returns to zero.

MIL-HDBK-217
TUBES

5.2.4 Tubes

This section includes the nonoperating failure rate prediction model for electronic vacuum, microwave and other tube types.

The general model for tubes is as follows:

$$\lambda_p = \lambda_{nb} \pi_{NE} \quad \text{failures}/10^6 \text{ nonoperating hours}$$

where

λ_p = predicted tube nonoperating failure rate

λ_{nb} = nonoperating base failure rate (See Table 5.2.4-1)

π_{NE} = nonoperating environmental factor (See Table 5.2.4-2)

5.2.4.1 Example Nonoperating Failure Rate Calculation

Given: A pentode receiver type tube is being used in a Ground Mobile environment.

Step 1: The nonoperating failure rate model is shown in section 5.2.4 to be $\lambda_p = \lambda_{nb} \pi_{NE}$.

Step 2: Refer to Table 5.2.4-1 and select correct nonoperating base failure rate of 0.0040 for a pentode receiver tube

Step 3: Next select from Table 5.2.4-2 the nonoperating environmental factor of 31 for a ground mobile (G_M) environment.

Step 4: Determine the predicted tube nonoperating failure rate as follows:

$$\lambda_p = \lambda_{nb} \pi_{NE}$$

$$\lambda_p = 0.0040 \times 31$$

$$\lambda_p = 0.124 \text{ failures}/10^6 \text{ hours}$$

MIL-HDBK-217
TUBES

TABLE 5.2.4-1: TUBE NONOPERATING BASE FAILURE RATE (λ_{nb})

TYPE TYPE	λ_{nb} (failures/ 10^6 hrs)
RECEIVER Triode, Tetrode, Pentode Power Rectifier	0.0040 0.0090
CRT	0.013
THYRATRON	0.32
VIDICON	0.049
CROSSED FIELD AMPLIFIER (All types)	1.29
PULSED GRIDDED (All types)	1.03
TRANSMITTING Triode, Tetrode, Pentode Any Style with Peak Pwr. ≤ 200 kW, Freq. ≤ 200 MHz, or Average Pwr. ≤ 2 KW	0.56 1.61
TWYSTRON (All types)	2.60
MAGNETRON (All types)	1.02
KLYSTRON Continuous Wave Low Power Pulsed	1.20 0.19 1.15
TWT	0.69

MIL-HDBK-217
TUBES

TABLE 5.2.4-2: TUBE NONOPERATING ENVIRONMENTAL FACTORS (π_{NE})

Environment	π_{NE}
GB	1
GF	3.0
GM	31
Mp	31
NSB	15
NS	29
NU	47
NH	110
NUU	120
ARW	140
AIC	6.2
AIT	19
AIB	25
AIA	23
AIF	35
AUC	8.2
AUT	23
AUB	33
AUA	27
AUF	43
SF	1
MFF	63
MFA	91
USL	210
M _L	220
C _L	3600

MIL-HDBK-217
LASERS

5.2.5 Lasers

This section presents nonoperating failure rate models for laser peculiar items used in the following five major classes of laser equipment:

- o Helium/Neon
- o Argon Ion
- o CO₂ Sealed
- o CO₂ Flowing
- o Solid State

The models and failure rates presented in this section apply to the laser peculiar items only, i.e., those items wherein the lasing action is generated and controlled. In addition to the laser peculiar items, there are other assemblies used with lasers that contain electronic parts and mechanical devices (pumps, valves, hoses, etc.). The failure rates for these parts should be determined with the same procedures as used for other electronic and mechanical devices in the equipment or system of which the laser is a part. The electronic device failure rates are in other parts of this Handbook and the mechanical device failure rates are in Bibliography Item 47.

The laser failure rate models have been developed at the "functional," rather than "piece part," level because the available data were not sufficient for "piece part" model development. Nevertheless, the laser functional models are included in this Handbook in the interest of completeness. These laser models will be revised to include piece part models and other laser types when the data become available.

Because each laser family can be designed using a variety of approaches, the failure rate models have been structured on three basic

MIL-HDBK-217

LASERS

laser functions which are common to most laser families, but may differ in the hardware implementation of a given function. These functions are the lasing media, the laser pumping mechanism (or pump), and the coupling method.

Helium/Neon Lasers

The general nonoperating failure rate prediction model for helium/neon lasers is as follows:

$$\lambda_{\text{He/Ne}} = .11 \pi_{\text{NE}} \quad \text{failures}/10^6 \text{ nonoperating hours}$$

where

$\lambda_{\text{He/Ne}}$ = helium/neon laser nonoperating failure rate (includes the nonoperating failure rate contribution for the lasing media, the laser pumping mechanism and the coupling method)

π_{NE} = nonoperating environmental factor (See Table 5.2.5-1)

Argon Ion Lasers

The general nonoperating failure rate prediction model for Argon Ion lasers is as follows:

$$\lambda_{\text{AI}} = .61 \pi_{\text{NE}} \quad \text{failures}/10^6 \text{ nonoperating hours}$$

where

λ_{AI} = argon ion laser nonoperating failure rate (includes the nonoperating failure rate contribution for the lasing media, the laser pumping mechanism and the coupling method)

π_{NE} = nonoperating environmental factor (See Table 5.2.5-1)

MIL-HDBK-217
LASERS

Carbon Dioxide, Sealed Lasers

The general nonoperating failure rate prediction model for carbon dioxide sealed lasers is as follows:

$$\lambda_{\text{CO}_2 \text{ SEALED}} = (.65 + .013(N_{\text{op}})) \pi_{\text{NE}} \quad \text{failures}/10^6 \text{ nonoperating hours}$$

where

$\lambda_{\text{CO}_2 \text{ SEALED}}$ = carbon dioxide sealed nonoperating failure rate
(includes the nonoperating failure rate contribution for the lasing media, the laser pumping mechanism and the coupling method)

N_{op} = number of active optical surfaces (determine from Figure 5.1.5.7-4 in Section 5.1.5.7)

π_{NE} = nonoperating environmental factor (See Table 5.2.5-1)

Carbon Dioxide, Flowing Lasers

The general nonoperating failure rate prediction model for carbon dioxide flowing lasers is as follows:

$$\lambda_{\text{CO}_2 \text{ FLOWING}} = .039(N_{\text{op}}) \pi_{\text{NE}}$$

where

$\lambda_{\text{CO}_2 \text{ FLOWING}}$ = carbon dioxide sealed laser nonoperating failure rate
(includes the nonoperating failure rate contribution for the lasing media, the laser pumping mechanism and the coupling method).

N_{op} = number of active optical surfaces (determine from Figure 5.1.5.7-4 in Section 5.1.5.7)

π_{NE} = nonoperating environmental factor (See Table 5.2.5-1)

MIL-HDBK-217
LASERS

Solid State Lasers (Nd:YAG or Ruby Rod)

The general nonoperating failure rate prediction model for solid state lasers (either pumped by xenon or Krypton flashlamp) is as follows:

$$\lambda_{ss} = (.062 + .021(N_{op})) \pi_{NE}$$

where

λ_{ss} = solid state laser nonoperating failure rate (includes the nonoperating failure rate contribution for the lasing media, the laser pumping mechanism and the coupling method)

N_{op} = number of active optical surfaces (determined from Figure 5.1.5.7-4 in Section 5.1.5.7)

π_{NE} = nonoperating environmental factor (See Table 5.2.5-1)

TABLE 5.2.5-1: LASER NONOPERATING ENVIRONMENTAL FACTOR (π_{NE})

Environment	π_{NE}	Environment	π_{NE}
GB	1	AIA	44
GF	9.0	AI F	62
GM	44	AUC	35
MP	22	AUT	42
NSB	10	AUB	71
NS	49	AUA	57
NU	49	AUF	71
NH	35	SF	1
NUU	38	MFF	21
ARW	46	MFA	29
AIC	26	USL	69
AIT	35	ML	71
AIB	58	CL	-

MIL-HDBK-217
LASERS

5.2.5.1 Example Nonoperating Failure Rate Calculation

Given: Nd:YAG laser designator using a xenon flashlamp is being used in the A_{UF} nonoperating environment. The laser includes one totally reflective (TR) mirror, one prismatic "Q" switch, one partially reflective (PR) mirror and one exit lens.

Step 1: The nonoperating failure rate model for solid state lasers shown in Section 5.2.5 is $\lambda_{SS} = (.062 + .021(N_{Op}))\pi_{NE}$

Step 2: From Figure 5.1.5.7-1 in Section 5.1.5.7, determine the number of optical surfaces (N_{Op}) by,

- (1) One TR mirror = 1 optical surfaces
- (2) One "Q" switch = 2 optical surfaces
- (3) One PR mirror = 2 optical surfaces
- (4) One exit lens = 2 optical surfaces

Total active optical surfaces = 7

Step 3: Refer to Table 5.2.5-1 and find the correct nonoperating environmental factor (π_{NE}) of 71 for an A_{UF} environment.

Step 4: Determine the predicted nonoperating Nd:YAG nonoperating failure rate in failures per 10^6 nonoperating hours.

$$\lambda_{SS} = (.062 + .021(7)) \times 71 = 14.8 \text{ failures}/10^6 \text{ nonoperating hours}$$

MIL-HDBK-217
RESISTORS

5.2.6 Resistors

This section includes the nonoperating failure rate prediction model for resistors.

The general model for resistor devices is as follows:

$$\lambda_p = \lambda_{nb} \pi_{NE} \pi_{NQ} \pi_{cyc} \quad \text{failures}/10^6 \text{ nonoperating hours}$$

where

λ_p = predicted resistor nonoperating failure rate

λ_{nb} = nonoperating base failure rate (See Table 5.2.6-1)

π_{NE} = nonoperating environmental factor (See Table 5.2.6-2)

π_{NQ} = nonoperating quality factor (See Table 5.2.6-3)

π_{cyc} = equipment power on-off cycling factor (See Table 5.2.6-4)

5.2.6.1 Example Nonoperating Failure Rate Calculation

Given: Type RCR fixed composition 12,000 ohm resistor per MIL-R-39008, level M rated at 0.5 watts is being used in a trainer aircraft cockpit equipment. The power is cycled "on" twenty times every 1,000 nonoperating hours.

Step 1: The nonoperating failure rate model is shown in Section 5.2.6 to be $\lambda_p = \lambda_{nb} \pi_{NE} \pi_{NQ} \pi_{cyc}$.

Step 2: Refer to Table 5.2.6-1 and find RCR style and appropriate λ_{nb} of .00063 failures per million hours and find appropriate resistor type (Fixed Composition) for the specific resistor RCR style.

MIL-HDBK-217
RESISTORSTABLE 5.2.6-1: RESISTOR NONOPERATING BASE FAILURE RATE (λ_{nb})

Specification		Style	λ_{nb} (Failures per 10 ⁶ hrs)
Composition, Fixed			
MIL-R-11	Resistors, Fixed, Composition (Insulated)	RC	.000063
MIL-R-39008	Resistors, Fixed, Composition (Insulated) Established Reliability	RCR	.000063
Film, Fixed			
MIL-R-10509	Resistors, Fixed, Film (High Stability)	RN	.00010
MIL-R-11804	Resistors, Fixed, Film (Power Type)	RD	.00010
MIL-R-22684	Resistors, Fixed, Film, Insulated	RL	.00010
MIL-R-39017	Resistors, Fixed, Film, Insulated, Established Reliability	RLR	.00010
MIL-R-55182	Resistors, Fixed, Film, Established Reliability	RN(R, C or N)	.00010
Network, Film, Fixed			
MIL-R-83401	Resistor Network, Fixed, Film	RZ	.00043
Wirewound, Fixed			
MIL-R-26	Resistors, Fixed, Wirewound (Power Type)	RW	.00057
MIL-R-93	Resistors, Fixed, Wirewound (Accurate)	RB	.00057
MIL-R-18546	Resistors, Fixed, Wirewound (Power Type, Chassis Mounted)	RE	.00057
MIL-R-19005	Resistors, Fixed, Wirewound (Accurate), Established Reliability	RBR	.00057
MIL-R-39007	Resistors, Fixed, Wirewound (Power Type) Established Reliability	RWR	.00057
MIL-R-39009	Resistors, Fixed, Wirewound (Power Type Chassis Mounted) Established Reliability	RER	.00057
Thermistor			
MIL-T-23648	Thermistor (Thermally Sensitive Resistor) Insulated	RTH	.0027
Non-wirewound, Variable			
MIL-R-94	Resistors, Variable, Composition	RV	.0052
MIL-R-22097	Resistors, Variable, Non-wirewound (Lead Screw Actuated)	RJ	.0052
MIL-R-23285	Resistors, Variable, Film	RVC	.0052
MIL-R-39023	Resistors, Variable, Non-wirewound, Precision	RQ	.0052
MIL-R-39035	Resistors, Variable, Cermet, or Carbon Film (Lead Screw Actuated) Established Reliability	RJR	.0052
Wirewound, Variable			
MIL-R-19	Resistors, Variable, Wirewound (Low Operating Temperature)	RA	.0052
MIL-R-22	Resistors, Variable, Wirewound (Power Type)	RP	.0052
MIL-R-12934	Resistors, Variable, Wirewound, Precision	RR	.0052
MIL-R-27208	Resistors, Variable, Wirewound (Lead Screw Actuated)	RT	.00099
MIL-R-39002	Resistors, Variable, Wirewound, Semi-Precision	RK	.0052
MIL-R-39015	Resistors, Variable, Wirewound (Lead Screw Actuated), Established Reliability	RTR	.00099

MIL-HDBK-217
RESISTORSTABLE 5.2.6-2: RESISTOR NONOPERATING ENVIRONMENTAL FACTORS (π_{NE})

Env.	Fixed Comp.	Fixed Film	Film Network	Fixed WW	Therm.	Var. non-WW	Var. WW
GB	1	1	1	1	1	1	1
GF	2.9	2.4	2.4	2.1	4.8	2.5	2.5
GM	8.3	8.3	7.8	8.8	23	13	13
MP	8.5	9.9	8.8	11	17	19	18
NSB	4	4.7	4.2	5	7.9	7	7
NS	5.2	4.9	4.7	5	14	7	7
NU	12	15	14	15	17	17	14(2)
NH	13	16	14	17	25	29	29
NUU	14	17	15	18	27	31	31
ARW	19	22	19	24	33	41	41
AIC	3	3	2.5	4.3	4.3	12	5.5
AIT	3.5	4.5	3	7.3	7.7	16	6.6
AIB	5	6.8	6.5	12	19	24	9.5
AIA	3.5	5.8	6	9.7	15	22	8.6
AIF	6.5	9.5	9	13	38	33	14
AUC	5	7.5	6	10	4.6	19	6.5(2)
AUT	7	11	6.5	13	8.6	25	9(2)
AUB	10	18	15	23	21	37	18(2)
AUA	7	13	15	18	17	32	13(2)
AUF	15	23	20	28	42	52	20(2)
SF	(1)	(1)	(1)	(1)	(1)	1	1
MFF	8.6	10	8.9	11	15	19	20(2)
MFA	13	14	12	16	21	26	28(2)
USL	25	30	26	33	49	56	58(2)
ML	29	35	30	38	51	64	66(2)
CL	490	590	510	610	950	1100	1100(2)

NOTES: 1) Env. = Environment, Comp. = Composition, WW = Wirewound, Therm. = Thermistor, Var. = Variable

2) Semiprecision wirewound or high power wirewound variable resistors shall not be used in these environments.

MIL-HDBK-217
RESISTORS

TABLE 5.2.6-3: RESISTOR NONOPERATING QUALITY FACTOR

Quality Level	π_{NQ}
S	0.15
R	0.28
P	0.52
M	1.0
MIL-SPEC	2.4
Lower	4.4

TABLE 5.2.6-4: RESISTOR EQUIPMENT POWER ON-OFF CYCLING FACTOR

Cycling Rate* (Power Cycles/10 ³ hrs.)	Mean-Time-Between Power Cycles (Hours)	π_{cyc}
< 0.8	>1250	1
1	1000	1.06
2	500	1.13
3	333	1.19
4	250	1.25
5	200	1.32
10	100	1.63
20	50	2.26
50	20	4.15

$$\pi_{cyc} = 1 + .063(N_C)$$

N_C = Number of power on-off cycles per 1000 nonoperating hours

*An equipment power on-off cycle is defined as the state during which an electronic equipment goes from zero electrical activation level to the normal design activation level plus the state during which it returns to zero.

MIL-HDBK-217
RESISTORS

Step 3: Refer to Table 5.2.6-2 and select appropriate π_{NE} factor of 3.5 for Fixed Composition type resistor and in an AIT environment.

Step 4: Refer to Table 5.2.6-3 and select appropriate π_{NQ} factor of 1.0 for a level M quality part.

Step 5: Refer to Table 5.2.6-4 and select appropriate π_{cyc} factor of 2.26 for a cycling rate of 20 per 1000 nonoperating hours.

Step 6: $\lambda_p = \lambda_{nb} \times \pi_{NE} \times \pi_{NQ} \times \pi_{cyc}$
 $= .000063 \times (3.5) \times (1) \times (2.26)$
 $\lambda_p = .000498 \text{ failures}/10^6 \text{ hours}$

MIL-HDBK-217
CAPACITORS

5.2.7 Capacitors

This section includes the nonoperating failure rate prediction model for capacitors.

The general model for capacitor devices is as follows:

$$\lambda_p = \lambda_{nb} \pi_{NE} \pi_{NQ} \pi_{cyc}$$

where

- λ_p = predicted capacitor nonoperating failure rate
- λ_{nb} = nonoperating base failure rate (See Table 5.2.7-1)
- π_{NE} = nonoperating environmental factor (See Table 5.2.7-2)
- π_{NQ} = nonoperating quality factor (See Table 5.2.7-3)
- π_{cyc} = equipment power on-off cycling factor (See Table 5.2.7-4)

5.2.7.1 Example Nonoperating Failure Rate Calculation

- Given: Style CSR solid tantalum capacitor MIL-C-39003, level R, rated at 40 Vdc is being used in a ground fixed environment. The power is cycled "on" twice every 1,000 nonoperating hours.
- Step 1: The nonoperating failure rate model is shown in Section 5.2.7 to be $\lambda_p = \lambda_{nb} \pi_{NE} \pi_{NQ} \pi_{cyc}$.
- Step 2: Refer to Table 5.2.7-1 and find CSR style and appropriate λ_{nb} of .00018 failures per million hours.
- Step 3: Refer to Table 5.2.7-1 and find appropriate capacitor type (Electrolytic-Tantulum Solid) for the specific capacitor CSR style.

MIL-HDBK-217
CAPACITORSTABLE 5.2.7-1: CAPACITOR NONOPERATING BASE FAILURE RATE (λ_{nb})

Specification		Style	λ_{nb} (Failures per 10 ⁶ hrs)
Paper/Plastic Film			
MIL-C-25	Capacitors, Fixed, Paper	CP	.0011
MIL-C-11693	Capacitors, Fixed, Paper, Metallized Paper, Metallized Plastic, RFI Feed-Thru, Established Reliability and Non-Established Reliability	CZ	.0011
MIL-C-12889	Capacitors, Fixed, Paper, RFI Bypass	CA	.0011
MIL-C-14157	Capacitors, Fixed, Paper-Plastic, Established Reliability	CPV	.0011
MIL-C-18312	Capacitors, Metallized Paper, Paper-Plastic, Plastic	CH	.0011
MIL-C-19978	Capacitors, Fixed, Plastic (or Paper-Plastic), Established and Non-Established Reliability	CQ/CQR	.0011
MIL-C-39022	Capacitors, Fixed, Metallized, Paper-Plastic Film or Plastic Film Dielectric, Established Reliability	CHR	.0011
MIL-C-55514	Capacitors, Plastic, Metallized Plastic, Established Reliability	CFR	.0011
MIL-C-83421	Capacitors, Super-Metallized Plastic, Established Reliability	CRH	.0011
Mica			
MIL-C-5	Capacitors, Fixed, Mica	CM	.00075
MIL-C-10950	Capacitors, Fixed, Mica, Button Style	CB	.00075
MIL-C-39001	Capacitors, Fixed, Mica, Established Reliability	CMR	.00075
Glass			
MIL-C-11272	Capacitors, Glass	CY	.00045
MIL-C-23269	Capacitors, Fixed, Glass, Established Reliability	CYR	.00045
Ceramic			
MIL-C-20	Capacitors, Fixed, Ceramic (Temperature Compensating)	CC/CCR	.00039
MIL-C-11015	Capacitors, Fixed, Ceramic (General Purpose)	CK	.00039
MIL-C-39014	Capacitors, Fixed, Ceramic (General Purpose), Established Reliability	CKR	.00039
Electrolytic			
MIL-C-62	Capacitors, Fixed, Electrolytic (DC, Aluminum, Dry Electrolyte, Polarized)	CE	.0064
MIL-C-3965	Capacitors, Fixed, Electrolytic (Non-solid Electrolyte), Tantalum	CL	.0064
MIL-C-39003	Capacitors, Fixed, Electrolytic, Tantalum, Solid Electrolyte, Established Reliability	CSR	.00018
MIL-C-39006	Capacitors, Fixed, Electrolytic, Tantalum, Non-solid Electrolyte, Established Reliability	CLR	.0064
MIL-C-39018	Capacitors, Fixed, Electrolytic, Aluminum Oxide	CU	.0064
Variable Capacitors			
MIL-C-81	Capacitors, Variable, Ceramic	CV	.012
MIL-C-92	Capacitors, Air, Trimmer	CT	.015
MIL-C-14409	Capacitors, Variable, Piston Type, Tubular Trimmer	PC	.0038
MIL-C-23183	Capacitors, Vacuum or Gas, Fixed and Variable	CG	.046

MIL-HDBK-217
CAPACITORSTABLE 5.2.7-2: CAPACITOR NONOPERATING ENVIRONMENTAL FACTORS (π_{NE})

Env.	Paper/ Plas. Film	Mica/ Glass	Cer.	Electrolytic			Var.
				Tant. Solid	Tant. Non-Solid	Al.	
GB	1.0	1.0	1.0	1.0	1.0	1.0	1.0
GF	2.2	2.1	2.0	2.4	1.4	2.0	3.3
GM	8.3	8.8	8.3	7.8	10	12	9.6
MP	9.9	11	11	9.2	11	12	17
NSB	4.7	5.0	5.0	4.4	5.0	5.8	7.7
NS	6.3	5.9	5.2	4.9	6.7	6.7	8.2
NU	14	15	15	13	15	13	18
NH	15	16	16	14	16	19	25
NUU	16	17	18	15	17	20	27
ARW	21	23	24	20	23	27	36
AIC	3.2	3.5	2.7	2.5	2.5	9.5	5.0
AIT	4.3	4.0	3.3	2.5	4.0	10	5.3
AIB	7.0	8.0	6.2	7.0	6.5	10	7.8
AIA	4.9	4.0	5.0	3.0	6.0	10	7.7
AIF	9.8	10	8.0	7.5	10	15	13
AUC	7.6	15	6.0	4.5	8.5	28	20
AUT	13	15	12	6.0	15	30	38
AUB	23	35	15	25	20	30	57
AUA	17	15	17	10	20	30	50
AUF	33	40	30	30	40	40	85
SF	1.0	1.0	1.0	1.0	1.0	1.0	1.0
MFF	9.9	11	11	9.3	11	12	16(1)
MFA	13	15	15	13	15	17	22(1)
USL	23	31	32	27	31	36	47(1)
ML	33	36	36	31	36	41	54(1)
CL	560	610	610	510	610	690	930

NOTES: 1) Vacuum or Gas, fixed and variable (CG) style capacitors shall not be used in these environments.
 2) Plas. = Plastic, Tant. = Tantalum, Al. = Aluminum, Env. = Environment.

MIL-HDBK-217
CAPACITORS

TABLE 5.2.7-3: CAPACITOR NONOPERATING QUALITY FACTOR

Quality Level	π_{NQ}
T	0.05
S	0.10
R	0.23
P	0.46
M	1.0
L	1.7
MIL-SPEC	2.5
Lower	5.3

TABLE 5.2.7-4: CAPACITOR EQUIPMENT POWER ON-OFF CYCLING FACTOR

Cycling Rate* (Power Cycles/10 ³ hrs.)	Mean-Time-Between Power Cycles (Hours)	π_{cyc}
< 0.3	>3333	1
0.5	2000	1.08
1	1000	1.16
2	500	1.32
3	333	1.48
4	250	1.64
5	200	1.80
10	100	2.60
20	50	4.20
50	20	9.00

$$\pi_{cyc} = 1 + 0.16(N_C)$$

N_C = Number of equipment power on-off cycles per 1000
nonoperating hours

*An equipment power on-off cycle is defined as the state during which an electronic equipment goes from zero electrical activation level to the normal design activation level plus the state during which it returns to zero.

MIL-HDBK-217
CAPACITORS

Step 4: Refer to Table 5.2.7-2 and select appropriate π_{NE} factor of 2.4 for Electrolytic-Tantalum Solid type resistor in a Gf environment.

Step 5: Refer to Table 5.2.7-3 and select appropriate π_{NQ} factor of 0.23 for a level R quality part.

Step 6: Refer to Table 5.2.7-4 and select appropriate π_{cyc} factor of 1.32 for a cycling rate of 2 per 1000 nonoperating hours.

Step 7: $\lambda_p = \lambda_{nb} \times \pi_{NE} \times \pi_{NQ} \times \pi_{cyc}$
 $= .00018 \times (2.4) \times (0.23) \times (1.32)$
 $\lambda_p = .0001312 \text{ failures}/10^6 \text{ hours}$

MIL-HDBK-217
INDUCTIVE DEVICES

5.2.8 Inductive Devices

This section presents the nonoperating failure rate prediction model for inductive devices. The inductive devices included in this section are transformers and coils.

The general model for inductive devices is as follows:

$$\lambda_p = \lambda_{nb} \pi_{NQ} \pi_{NE} \pi_{cyc} \quad \text{failures/10}^6 \text{ nonoperating hours}$$

where

- λ_p = predicted transformer or coil nonoperating failure rate
- λ_{nb} = nonoperating base failure rate (See Table 5.2.8-1)
- π_{NQ} = nonoperating quality factor (See Table 5.2.8-2)
- π_{NE} = nonoperating environmental factor (See Table 5.2.8-3)
- π_{cyc} = equipment power on-off cycling factor (See Table 5.2.8-4 for transformers and 5.2.8-5 for coils)

5.2.8.1 Example Nonoperating Failure Rate Calculation

Given: Power transformer with type designation TF5SX03GA203 procured per the requirements of MIL-T-27. The power is cycled "on" ten times every 1000 nonoperating hours, and is in a ground fixed environment.

Step 1: The nonoperating failure rate model is shown in Section 5.2.8 to be $\lambda_p = \lambda_{nb} \pi_{NQ} \pi_{NE} \pi_{cyc}$

Step 2: Refer to Table 5.2.8-1 and find MIL-T-27 power transformer part class, and appropriate λ_{nb} of .00028.

Step 3: Refer to Table 5.2.8-2 and select appropriate π_{NQ} of 3.1 for a MIL-SPEC quality part.

MIL-HDBK-217
INDUCTIVE DEVICES

Step 4: Refer to Table 5.2.8-3 and select appropriate π_{NE} of 5.7 for a ground fixed environment.

Step 5: Refer to Table 5.2.8-4 and select appropriate π_{cyc} of 8.5 for an equipment power cycling rate of 10 cycles per 1000 hours.

Step 6: $\lambda_p = \lambda_{nb} \times \pi_{NQ} \times \pi_{NE} \times \pi_{cyc}$
 $= (.00028) \times (3.1) \times (5.7) \times (8.5)$
 $= .042 \text{ failures}/10^6 \text{ nonoperating hours}$

MIL-HDBK-217
INDUCTIVE DEVICES

TABLE 5.2.8-1: INDUCTIVE DEVICE NONOPERATING BASE FAILURE RATE (λ_{nb})

Part Class	λ_{nb}
Transformers	
MIL-T-27 Transformers and Inductors, Audio	.000055
MIL-T-27 Transformers and Inductors, Power	.00028
MIL-T-27 Transformers and Inductors, High Power Pulse	.00028
MIL-T-21038 Transformers, Low Power Pulse	.000055
MIL-T-55631 Transformers, IF, RF, and Discriminator	.00028
Coils	
MIL-C-15305 Coils, Fixed and Variable, RF	.00015
MIL-C-39010 Coils, Molded, RF, ER	.00015

TABLE 5.2.8-2: INDUCTIVE DEVICE NONOPERATING QUALITY FACTOR (π_{NQ})

Quality Level *	π_{NQ}
S	.06
R	.15
P	.38
M	1.0
MIL-SPEC	3.1
Lower	11

* S,R,P and M levels refer to coils only.

MIL-HDBK-217
INDUCTIVE DEVICES

TABLE 5.2.8-3: INDUCTIVE DEVICE NONOPERATING ENVIRONMENTAL FACTORS (π NE)

Environment	Transformers	Coils
GB	1	1
GF	5.7	3.6
GM	12	12
Mp	11	11
NSB	5.1	5.1
NS	5.7	5.7
NU	14	14
NH	16	16
NUU	18	18
ARW	24	24
AIC	4.5	4
AIT	6	4.5
AIB	6	5.5
AIA	6	4.5
AIF	9	9
AUC	6.5	5
AUT	6.5	6.5
AUB	7.5	7.5
AUA	7.5	6.5
AUF	10	10
SF	1	1
MFF	11	11
MFA	15	15
USL	32	32
ML	36	36
CL	310	610

MIL-HDBK-217
INDUCTIVE DEVICES

TABLE 5.2.8-4: TRANSFORMER EQUIPMENT POWER ON-OFF
CYCLING FACTOR (π_{cyc})

Cycling Rate* (Power Cycles/ 10 ³ hrs.)	Mean-Time-Between Power Cycles	π_{cyc}
$\leq .05$	$\geq 20,000$	1.00
.1	10,000	1.08
.2	5,000	1.15
.5	2,000	1.38
1	1,000	1.75
2	500	2.50
5	200	4.75
10	100	8.50
20	50	16.0
50	20	38.5

$$\pi_{cyc} = 1 + .75(N_c)$$

N_c = number of equipment power on-off cycles per 1000 nonoperating hours

TABLE 5.2.8-5: COIL EQUIPMENT POWER ON-OFF
CYCLING FACTOR (π_{cyc})

Cycling Rate* (Power Cycles/ 10 ³ hrs.)	Mean-Time-Between Power Cycles	π_{cyc}
$\leq .1$	$\geq 10,000$	1.00
.2	5,000	1.08
.5	2,000	1.19
1	1,000	1.38
2	500	1.76
5	200	2.90
10	100	4.80
20	50	8.60
50	20	20.0

$$\pi_{cyc} = 1 + .38(N_c)$$

N_c = number of equipment power on-off cycles per 1000 nonoperating hours

* An equipment power on-off cycle is defined as the state during which an electronic equipment goes from zero electrical activation level to the normal design activation level plus the state during which it returns to zero.

MIL-HDBK-217
ROTATING DEVICES

5.2.9 Rotating Devices

This section presents the method to be used for estimating the nonoperating failure rate for motors with power ratings below one horsepower, synchros and resolvers, and elapsed time meters.

Average nonoperating failure rates for rotating devices are presented in Table 5.2.9-1.

TABLE 5.2.9-1: NONOPERATING FAILURE RATES FOR ROTATING DEVICES
(failures/ 10^6 nonoperating hours)

Part Type	Nonoperating Failure Rate (failures/ 10^6 nonoperating hours)
Motors (ac or dc)	.045
Synchros	.14
Resolvers	.14
Elapsed Time Meters	1.2

MIL-HDBK-217
RELAYS

5.2.10 Relays

This section includes the nonoperating failure rate prediction model for relays:

The general model for relays is as follows:

$$\lambda_p = \lambda_{nb} \pi_{NQ} \pi_{NE} \quad \text{failures}/10^6 \text{ nonoperating hours}$$

where

λ_p = predicted relay nonoperating failure rate

λ_{nb} = nonoperating base failure rate (See Table 5.2.10-1)

π_{NQ} = nonoperating quality factor (See Table 5.2.10-2)

π_{NE} = nonoperating environmental factor (See Table 5.2.10-3)

TABLE 5.2.10-1: RELAY NONOPERATING BASE FAILURE RATE (λ_{nb})

Package Type	Contact Voltage (when operated)	Nonoperating Base Failure Rate (failures/ 10^6 nonoperating hrs)
Nonhermetic	<50 millivolts	.010
Nonhermetic	>50 millivolts	.002
Hermetic	any	.0004

TABLE 5.2.10-2: RELAY NONOPERATING QUALITY FACTOR (π_{NQ})

Quality Level	π_{NQ}
Established Reliability	0.46
MIL-SPEC	1.0
Lower	4.2

MIL-HDBK-217
RELAYS

TABLE 5.2.5-1: RELAY NONOPERATING ENVIRONMENTAL FACTOR (π_{NE})

Environment	π_{NE}	Environment	π_{NE}
GB	1	AIA	7.5
GF	2.3	AIF	10
GM	8.2	AUC	8.0
MP	21	AUT	9.0
NSB	8.0	AUB	15
NS	8.0	AUA	10
NU	14	AUF	15
NH	32	SF	1
NUU	34	MFF	21
ARW	46	MFA	29
AIC	5.5	USL	62
AIT	6	ML	71
AIB	10	CL	N/A

5.2.10.1 Example Nonoperating Failure Rate Calculation

Given: A MIL-SPEC double-pole, double-throw armature relay is being used in a nonoperating ground fixed environment. The design operating contact voltage is 0.5 volts.

Step 1: The nonoperating failure rate model is shown in Section 5.2.10 to be $\lambda_p = \lambda_{nb} \pi_{NQ} \pi_{NE}$

Step 2: Since armature relays are nonhermetic, refer to Table 5.2.10-1 and find appropriate λ_{nb} of .002 for nonhermetic relays with a contact voltage greater than 50 millivolts when operated.

Step 3: Refer to Table 5.2.10-2 and find appropriate π_{NQ} of 1.0 for MIL-SPEC parts.

Step 4: Refer to Table 5.2.10-3 and select π_{NE} of 2.3 for a ground fixed environment.

Step 5: $\lambda_p = \lambda_{nb} \pi_{NQ} \pi_{NE}$
 $= (.002) \times (1.0) \times (2.3)$
 $= .0046 \text{ failures}/10^6 \text{ nonoperating hours}$

MIL-HDBK-217
SWITCHES

5.2.11 Switches

This section includes the nonoperating failure rate prediction model for switches.

The general model for switches is as follows:

$$\lambda_p = \lambda_{nb} \pi_{NQ} \pi_{NE} \quad \text{failures}/10^6 \text{ nonoperating hours}$$

where

λ_p = predicted switch nonoperating failure rate

λ_{nb} = nonoperating base failure rate (See Table 5.2.11-1)

π_{NQ} = nonoperating quality factor (See Table 5.2.11-2)

π_{NE} = nonoperating environmental factor (See Table 5.2.11-3)

TABLE 5.2.11-1: SWITCH NONOPERATING BASE FAILURE RATE (λ_{nb})

Contact Voltage (when operated)	Nonoperating Base Failure Rate
≤ 50 millivolts	0.030
> 50 millivolts	0.006

TABLE 5.2.11-2: SWITCH NONOPERATING QUALITY FACTOR (π_{NQ})

Quality Level	π_{NQ}
Established Reliability	0.46
MIL-SPEC	1.0
Lower	4.2

MIL-HDBK-217
SWITCHESTABLE 5.2.11-3: SWITCH NONOPERATING ENVIRONMENTAL FACTOR (π_{NE})

Environment	π_{NE}	Environment	π_{NE}
GB	1	AIA	14
GF	2.9	AIF	18
GM	13	AUC	9
MP	21	AUT	9
NSB	7.9	AUB	18
NS	7.9	AUA	18
NU	18	AUF	23
NH	32	SF	1
NUU	34	MFF	19
ARW	41	MFA	26
AIC	7.2	USL	63
AIT	7.2	ML	64
AIB	14	CL	1200

5.2.11.1 Example Nonoperating Failure Rate Calculation

Given: A MIL-SPEC rotary switch is installed in an airborne inhabited, cargo nonoperating environment. The switch, when operated, is used to transfer digital circuits with less than 50 millivolts.

Step 1: The nonoperating failure rate model is shown in Section 5.2.11 to be $\lambda_p = \lambda_{nb} \pi_{NQ} \pi_{NE}$.

Step 2: Refer to Table 5.2.11-1 and select nonoperating base failure rate of 0.030 for contact voltage less than 50 millivolts

Step 3: Refer to Table 5.2.11-2 and select appropriate nonoperating quality factor of 1.0 for MIL-SPEC devices.

Step 4: Refer to Table 5.2.11-3 and select π_{NE} of 7.2 for airborne, inhabited environment.

Step 5: $\lambda_p = \lambda_{nb} \pi_{NQ} \pi_{NE}$

$$= (.030) \times (1.0) \times (7.2)$$

$$= .216 \text{ failures}/10^6 \text{ nonoperating hours}$$

MIL-HDBK-217
CONNECTORS

5.2.12 Connectors

This section includes the nonoperating failure rate prediction model for connectors:

The general model for connectors is as follows:

$$\lambda_p = \lambda_{nb} \pi_{NE} \text{ failures}/10^6 \text{ nonoperating hours}$$

where

λ_p = predicted connector nonoperating failure rate

λ_{nb} = nonoperating base failure rate (See Table 5.2.12-1)

π_{NE} = nonoperating environmental factor (See Table 5.2.12-2)

TABLE 5.2.12-1: CONNECTOR NONOPERATING BASE FAILURE
RATE (λ_{nb})

Connector Type	Nonoperating Base Failure Rate (failures/ 10^6 nonoperating hrs)
Circular	.00044
Coaxial	.00044
Power	.00044
Rack and Panel	.0029
Printed Wiring Board	.0029

MIL-HDBK-217
CONNECTORS

TABLE 5.2.12-2: CONNECTOR NONOPERATING ENVIRONMENTAL FACTOR (π_{NE})

Environment	π_{NE}	Environment	π_{NE}
G _B	1	A _{IA}	5.3
G _F	2.3	A _{IF}	11
G _M	8.3	A _{UC}	4.3
M _P	8.5	A _{UT}	15
N _{SB}	4.1	A _{UB}	9.8
N _S	5.5	A _{UA}	8.0
N _U	13	A _{UF}	15
N _H	13	S _F	1
N _{UU}	14	M _{FF}	8.5
A _{RW}	19	M _{FA}	12
A _{IC}	2.8	U _{SL}	25
A _{IT}	4.8	M _L	29
A _{IB}	7.0	C _L	490

5.2.12.1 Example Nonoperating Failure Rate Calculation

Given: A MIL-SPEC circular connector with 20 pins is installed in a ground fixed environment.

Step 1: The nonoperating failure rate model is shown in Section 5.2.12 to be $\lambda_p = \lambda_{nb} \pi_{NE}$

Step 2: Refer to Table 5.2.12-1 and select appropriate λ_{nb} of .00044.

Step 3: Refer to Table 5.2.12-2 and select π_{NE} of 2.3 for a ground fixed environment.

Step 4: $\lambda_p = \lambda_{nb} \pi_{NE}$
 $= (.00044) \times (2.3)$
 $= .00101 \text{ failures}/10^6 \text{ nonoperating hours}$

MIL-HDBK-217
INTERCONNECTION ASSEMBLIES

5.2.13 Interconnection Assemblies with Plated Through Holes (PTHs)

This section includes the nonoperating failure rate prediction model for interconnection assemblies with PTHs. The interconnection assembly model predicts the nonoperating failure rate for both the interconnection board and the solder connections used to connect the components to the interconnection board. For interconnection assemblies without PTHs, use Section 5.2.14, Connections.

The general model for interconnection assemblies is as follows:

$$\lambda_p = \lambda_{nb} \times N_{pth} \times \pi_{NE} \text{ failures / } 10^6 \text{ hours}$$

where

λ_p = predicted interconnection assembly nonoperating failure rate

λ_{nb} = nonoperating base failure rate (See Table 5.2.13-1)

N_{pth} = number of functional plated through holes (includes nonsoldered functional via holes)

π_{NE} = nonoperating environmental factor (See Table 5.2.13-2)

TABLE 5.2.13-1: INTERCONNECTION ASSEMBLY NONOPERATING BASE FAILURE RATE (λ_{nb})

Interconnection Technology	λ_{nb}
Double-Sided Soldered Printed Wiring	.0000014
Multilayer Soldered Printed Wiring	.0000028
Discrete Wiring w/Electroless Deposited PTH	.0000089

MIL-HDBK-217
INTERCONNECTION ASSEMBLIES

TABLE 5.2.13-2: INTERCONNECTION NONOPERATING ENVIRONMENTAL
FACTOR (π_{NE})

Environment	π_{NE}	Environment	π_{NE}
GB	1	AIA	5.0
GF	2.3	AIF	9.0
GM	6.9	AUC	5.4
Mp	6.9	AUT	11
NSB	4.1	AUB	18
NS	5.3	AUA	14
NU	11	AUF	25
NH	13	SF	1
NUU	14	MFF	7.8
ARW	17	MFA	11
AIC	2.3	USL	25
AIT	4.1	ML	26
AIB	7.2	CL	500

5.2.13.1 Example Nonoperating Failure Rate Calculation

Given: A plated through hole printed wiring assembly having 6 circuit planes and 700 PTHs is installed in an airborne, uninhabited fighter nonoperating environment.

Step 1: The nonoperating failure rate model is shown in Section 5.2.13 to be $\lambda_p = \lambda_{nb} \times N_{pth} \times \pi_{NE}$

Step 2: Refer to Table 5.2.13-1 and select λ_{nb} of .0000028 for multilayer soldered printed wiring assemblies.

Step 3: From the example statement, $N_{pth} = 700$

Step 4: Refer to Table 5.2.13-2 and select π_{NE} of 25 for airborne, uninhabited fighter.

Step 5: $\lambda_p = \lambda_{nb} \times N_{pth} \times \pi_{NE}$
 $= .0000028 \times 700 \times 25$
 $= .049 \text{ failures}/10^6 \text{ nonoperating hours}$

MIL-HDBK-217
CONNECTIONS

5.2.14 Connections

This section presents the nonoperating failure rate model for connections including interconnection assemblies without plated through holes. The nonoperating failure rate of the structure which supports the connections and parts should be considered zero.

The general model for connections is as follows:

$$\lambda_p = \pi_{NE} \sum_{i=1}^n (N_i \lambda_{nbi})$$

where

λ_p = predicted connections nonoperating failure rate

π_{NE} = nonoperating environmental factor (See Table 5.2.14-2)

N_i = number of connections of the i th type

λ_{nbi} = nonoperating base failure rate of the i th type connection (See Table 5.2.14-1)

TABLE 5.2.14-1: CONNECTIONS NONOPERATING BASE FAILURE
RATE (λ_{nb})

Connection Type	λ_{nbi}
Hand Solder	.000089
Crimp	.000013
Weld	.0000017
Solderless Wrap	.00000012
Wrapped and Soldered	.0000048
Clip Termination	.0000041
Reflow Solder	.0000024

MIL-HDBK-217
CONNECTIONSTABLE 5.2.14-2: CONNECTIONS NONOPERATING ENVIRONMENTAL
FACTOR (π_{NE})

Environment	π_{NE}	Environment	π_{NE}
GB	1	AIA	4.5
GF	2.1	AIF	6.8
GM	6.6	AUC	2.7
MP	7.3	AUT	5.4
NSB	3.5	AUB	6.8
NS	4.4	AUA	6.3
NU	8.9	AUF	8.6
NH	11	SF	1
NUU	12	MFF	6.6
ARW	14	MFA	9.0
AIC	2.3	USL	22
AIT	4.1	ML	23
AIB	5.0	CL	420

5.2.14.1 Example Nonoperating Failure Rate Calculation

Given: A solderless wrap discrete wiring assembly is to be used in an inhabited cargo airborne nonoperating environment. The assembly consists of 1560 wraps and 156 of the posts are connected to either the ground or voltage planes with reflow solder.

Step 1: The expanded nonoperating failure rate expression from Section 5.2.14 is:

$$\lambda_p = \pi_{NE} (N_1 \lambda_{nb1} + N_2 \lambda_{nb2})$$

Step 2: From the example statement, $N_1 = 1560$ wraps and $N_2 = 156$ reflow solder connections.

MIL-HDBK-217
CONNECTIONS

Step 3: Refer to Table 5.2.14-1 and select a λ_{nb1} value of .00000012 for solder wrap and .0000024 for reflow solder.

Step 4: Refer to Table 5.2.14-2 and select a π_{NE} value of 2.3 for AIC

Step 5: $\lambda_p = \pi_{NE} (N_1 \lambda_{nb1} + N_2 \lambda_{nb2})$
= $2.3((1560 \times .00000012) + (156 \times .0000024))$
= .00129 failures/ 10^6 nonoperating hours

MIL-HDBK-217
MISCELLANEOUS PARTS

5.2.15 Miscellaneous Parts

This section includes average nonoperating failure rates for miscellaneous parts.

Table 5.2.15 includes average nonoperating failure rates for miscellaneous parts.

TABLE 5.2.15-1: NONOPERATING FAILURE RATES FOR MISCELLANEOUS PARTS
(failures/10⁶ nonoperating hours)

Part Type	Specification	Nonoperating Failure Rate
Vibrators	MIL-V-95	3.3
Quartz Crystals	MIL-C-3098	.039
Fuses		.0014
Lamps		
Neon		.029
Incandescent		.11
Fiber Optic Cables per fiber km (single fiber types only)		.014
Single Fiber Optic Connectors		.014
Meters	MIL-M-10304	1.4
Circuit Breakers		.29
Microwave Elements (coaxial and waveguide)		
Attenuators		*
Fixed Elements (directional couplers, fixed studs and cavities)		negligible
Variable Elements (tuned stubs and tuned cavities)		.014
Microwave Ferrite Devices		.043
Dummy Loads		.011
Terminations (thin or thick film loads used in strip-line and thin film circuits)		.010

* The nonoperating failure rate of attenuators should be calculated the same as for Style RD resistors in Section 5.2.6.

